UCLouvain

Institute of Experimental and Clinical Research (IREC)

Pharmacology and Therapeutics (FATH)

Pierre Sonveaux Laboratory

Mitochondrial Protein COX7b Is Responsible for Brain-Specific Metastasis of Human Breast Cancer Cells

Marine Blackman

2022

Thesis Promoter: Pierre Sonveaux

Thesis submitted in fulfilment of the requirements for a PhD degree

in Biomedical and Pharmaceutical Sciences

REMERCIEMENTS

À l'issue de cette longue aventure, je souhaiterais remercier tous ceux qui m'ont accompagnée sur ce chemin doctoral et ont permis son accomplissement. Merci déjà au Télévie et à la Fondation Louvain pour le financement de ce fabuleux projet.

Tout d'abord, merci à mon chef, le professeur Pierre Sonveaux. Tout cela n'aurait pas pu être possible sans vous, sans votre haut niveau d'exigence et votre profonde humanité. J'ai du mal à trouver les mots justes pour vous exprimer toute ma reconnaissance, merci de m'avoir épaulée et permis de croire à nouveau en ce rêve. Merci de m'avoir accueilli au sein de votre laboratoire et de vous être battu à mes côtés pour que je puisse avoir une deuxième chance de réaliser mon doctorat. Merci de m'avoir challengée et guidée dans ce chapitre important de ma vie. Merci d'avoir cru en moi, même lorsque je n'y croyais plus moi-même. Merci d'avoir été plus qu'un chef, mais un mentor et une inspiration.

Je tiens à remercier les membres de mon comité de thèse qui m'ont accompagnée durant toutes ces années, les professeurs Patrice Cani, Laure Bindels et François Duhoux. Merci pour le temps dédié à l'encadrement de ma thèse. Merci de m'avoir accompagnée avec rigueur scientifique et bienveillance, merci pour les questions et remarques pertinentes, pour les discussions enrichissantes, et pour les encouragements et félicitations qui m'ont redonné confiance et donné la force de poursuivre après une période difficile. Merci aux membres externes, les professeurs Nor Eddine Sounni (ULiège) et Monica Montopoli (Italie), d'être venus compléter ce jury de thèse, merci pour l'intérêt porté à mon travail et à l'amélioration de mon manuscrit.

Merci à toute mon équipe pour l'aide, les conseils et les discussions. Merci aussi pour toutes les réjouissances, les verres et les moments partagés. Merci à ma chère post-doc Tania, qui a commencé presque en même temps que moi et avec qui j'ai partagé toutes ces années conjointement, en science et en amitié. Merci pour ton dynamisme et ton petit brin de folie. Merci aux doctorants Luca, Debora et ensuite Justine et Justin, avec qui j'ai partagé l'aventure doctorale. Merci Luca pour tous ces moments partagés, ces discussions interminables, scientifiques ou non, merci pour le simple plaisir d'avoir partagé le quotidien avec toi. Justine et Justin, nous n'avons partagé que la moitié de nos doctorats mais quel plaisir de vous avoir eu pour ces années. Merci Justine pour les échanges profonds, et plus légers, pour ta présence et ton écoute, pour ton amitié. Merci Justin, mon binôme canadien, d'avoir ramené un peu de mon autre 'chez-moi', merci pour les échanges dynamiques, la présence vivante et le soutien. Merci aux techniciens Marie, Thibaut et Loïc pour l'assistance technique précieuse et pour l'agréable camaraderie que j'ai ressenti avec chacun de vous. Merci plus particulièrement à Marie avec qui j'ai majoritairement collaboré pour

ce projet, pour ton investissement dans le projet, pour ta proactivité à proposer de meilleurs anticorps, de trouver d'autres solutions pour les injections, etc. Merci aussi pour ton sourire communicatif. Merci à Claude, pour le début de cette aventure commencée avec toi et pour cette belle amitié qui est restée malgré les années. Merci à tous les membres présents et passés, Emmanuel, Zohra, Sara, et aux membres nouvellement arrivés, Ilaria, Mauricio, Alan, je vous souhaite une aussi belle aventure au sein de l'équipe PSO. Merci aux membres de l'équipe PSO large, Arthur, Chiara, Léopold, Perrine, Maxime, Quentin, Ferran, Françoise, d'avoir encore davantage sublimé les moments scientifiques et les team buildings.

Merci encore à toute l'équipe d'avoir partagé le quotidien de cette épopée doctorale, je suis émue à l'idée de quitter cette seconde famille. Merci aussi pour votre compréhension et votre bienveillance qui m'ont donnée espoir et courage dans l'épreuve que j'ai traversée.

Merci aux professeurs Jean-Luc Balligand, Olivier Feron, Chantal Dessy et Cyril Corbet. Merci à tous les collègues FATH pour la collaboration et pour cette belle convivialité, pour les discussions au détour du couloir, pour les partages de moments plus complexes et pour les moments festifs. Merci à tous les doctorants, post-docs, et techniciens, passés et présents. Merci à Catherine et Emeline pour votre enthousiasme et votre bonne humeur tout au long de ce périple ensemble, et votre engouement à découvrir le sexe de bébé, merci à Laurenne et Céline pour les papotes et les rires, merci à Roxane et Charline pour toutes les conversations chevaux (et autre), merci à Valentin pour les petits partages de jeunes parents, et merci à tous ceux que je n'aurais pas nommé pour les sourires et les échanges.

Merci aux voisins MORF/MIRO, aux plateformes IREC (IREC2IP, NEST, FACS, CTMA, ANIM) et aux autres pôles voisins. Merci à Caroline Bouzin, Nicolas Joudiou, Aurélie Daumerie, Michèle De Beukelaer, Marc de Bournonville, Davide Brusa, Jérôme Ambroise, Bertrand Bearzatto, Solveig Mouterde, Rachid El Kaddouri, Jean-Paul Dehoux, d'avoir été d'importantes personnes ressources lors de cette thèse. Merci à tous les chercheurs ayant permis de faire avancer la science conjointement entre nos laboratoires (dont les pôles GYNE, CARD, UNamur). Merci pour ces précieuses collaborations.

Merci à mes amis doctorants d'avant et de maintenant. Merci à Charlotte, Sara, Fanny, Lucie, Elisabeth, Thomas, Edith pour vos amitiés précieuses. Merci aussi à Jonathan, Violette, Matias, Manuel, et bien d'autres pour toutes ces aventures doctorales vécues avec vous, merci pour des weekends docs de folie et pour l'ambiance festive qui régnait dans les labos. Merci à Mélissa et Stéphanie, quelle joie de vous avoir retrouvées sur le campus, merci de faire partie de ma vie. La

première partie de mon aventure doctorale m'aura apportée toutes ces personnes merveilleuses que je suis heureuse de compter dans ma vie.

Merci aussi à mes amis hors doctorat et ma famille d'avoir été sources de joie, de soutien et de motivation. Merci à ma gang du Canada, aux louvanistes d'origine, aux futures pierres de Walhain, aux bonhommes, aux louvanistes estudiantins, aux cousin.e.s, et bien d'autres.

Merci à ma famille proche, ma maman Nathalie, mon beau-père Jean, mes sœurs Florence et Amandine, mes semi-demi-frères et ma super belle-famille. Merci pour un soutien constant, pour tous vos encouragements lors des périodes plus compliquées, et pour cette proximité rare que nous entretenons. Merci Flo pour ces appels constants depuis le Canada et pour ton attention toute particulière à ma santé mentale. Merci Amandine d'être quotidiennement dans ma vie et dans celle de mon fils. Merci Maman et Jean de nous avoir en plus accueilli, nous et notre tribu, pour me permettre de finir ma thèse. Avoir une famille unie et pétillante à mes côtés est une vraie force dans ma vie doctorale et personnelle, merci d'être là.

Merci à Rudy, mon mari. Merci d'être à mes côtés, de toujours respecter mes choix, merci de m'aider à me réaliser, merci d'avoir pris la charge à la maison pour que je puisse dédier toute l'énergie que j'avais à l'avancée de mon doctorat, d'avoir été (et d'être) un si merveilleux papa pour notre petit garçon lorsque j'étais accaparée par la thèse, et de n'avoir pas hésité à me soutenir (et souper) au labo les nombreux soirs qui finissaient tard.

Merci à Samuel, mon fils, de m'apporter autant de joie et, par son sourire, d'avoir illuminé cette dernière année doctorale. Merci de m'avoir encouragée de tes petits coups de pieds intérieurs avant ton arrivée.

Merci à mes grands-parents, Anne et Yves Stassin, qui se sont toujours enquis de l'avancée de mes recherches et qui avaient toujours le mot pour me redonner courage les fois où je débarquais avec le moral dans les chaussettes.

J'aimerais finir par une pensée toute particulière pour mon papy Yves, qui a été mon plus grand fan jusqu'à son dernier jour il y a 4 mois. Merci pour ton soutien et pour ta si grande fierté pour mon parcours académique et mon travail de recherche. Tu as tenu à suivre tout mon parcours en détail, jusqu'à ce dernier jour où tu es parti en nous aimant toujours aussi fort. Merci d'avoir été une source de ressourcement et de motivation, et un exemple de persévérance et d'optimisme. Ta fierté a été source de beaucoup de joie et résonne encore en moi, j'espère que de là-haut tu as pu suivre la dernière ligne droite avec l'intérêt qui te caractérisait. La tristesse de ne pas t'avoir avec moi pour la dernière étape doctorale n'a d'égale que la fierté que tu avais de me savoir bientôt docteure.

Acknowledgements

Merci à tous ceux qui de près ou de loin ont contribué à la réussite de ce rêve de longue date. Merci du fond du cœur à tous.

List of Abbreviations

2DG	2-deoxyglucose
2-HG	2-hydroxyglutarate
AA/Rot	antimycin A/Rotenone
ABAT	GABA transaminase
ABC	ATP-binding cassette
ACC	acetylCoA carboxylase
ACLY	ATP-citrate lyase
ACSS2	acetylCoA synthetase 2
ADP	adenosine diphosphate
AJCC	American Joint Committee on Cancer
ALDH	aldehyde dehydrogenase
AMP	adenosine monophosphate
Ang-2	angiopoietin-2
AQP-1	aquaporin-1
AR	androgen receptor
ASCT2	alanine serine cysteine transporter 2
ATP	adenosine triphosphate
BBB	blood brain barrier
BCAA	branched-chain amino acid
BCL2L1	B-cell lymphoma 2-like 1
BL1	basal-like 1
BLIA	basal-like immunoactivated
BLIS	basal-like immunosuppressed
BMDC	bone marrow-derived cells

Abbreviations

BMEC	brain microvascular endothelial cells
BRCA1	tumor suppressor gene breast cancer 1
CAT	carnitine-acylcarnitine translocase
CCL	chemokine C-C motif ligand
CCR	chemokine C-C motif receptor
CD	cluster of differentiation
CDK	cyclin-dependent kinase
cGAMP	cyclic GMP-AMP
CiC	citrate carrier
CK	cytokeratins
c-Myc	cellular myelocytomatosis oncogene
CNS	central nervous system
COX	cytochrome c oxidase
COX2	cyclooxygenase-2
CPT1	carnitine palmitoyltransferase-1
CRISPR	clustered regularly interspaced short palindromic repeats
CSC	cancer stem cell
CSF	cerebrospinal fluid
CTC	circulating cancer cell
Cx43	connexin-43
CXCL	chemokine C-X-C motif ligand
CXCR	chemokine C-X-C motif receptor
DCIS	ductal carcinoma in situ
DNA	deoxyribonucleic acid
DR3	death receptor 3
DRP1	dynamin-related protein 1

Abbreviations

ECM	extracellular matrix
EGFR	epidermal growth factor receptor
EMT	epithelial-to-mesenchymal transition
ER	estrogen receptor
ESL-1	E-selectin-ligand-1
ETC	electron transport chain
F1,6BP	fructose-1,6-bisphosphate
F6P	fructose-6-phosphate
FA	fatty acid
FABP7	fatty acid binding protein 7
FAK	focal adhesion kinase
FAO	fatty acid oxidation
FASN	fatty acid synthase
FBP2	fructose-1,6-bisphosphatase 2
FCCP	trifluoromethoxy carbonylcyanide phenylhydrazone
FDG	[^{18}F]-fluorodeoxyglucose
FH	fumarate hydratase
FUSCC	Fudan University Shanghai Cancer Center
G3P	glyceraldehyde 3-phosphate
G6P	glucose-6-P
GABA	gamma-aminobutyric acid
GAT	GABA transporter
GCL	glutamate-cysteine ligase
G-CSF	granulocyte colony-stimulating factor
GDH	glutamate dehydrogenase
GES	gene expression signature

Abbreviations

GFP	green fluorescent protein
GLOBOCAN	Global Cancer Statistics
GLS	glutaminase
GLUT	glucose transporter
GnRH	gonadotropin-releasing hormone
GOT	glutamate-oxaloacetate transaminase
GSH	glutathione
GSSG	glutathione disulfide
GST	glutathione transferase
HBEGF	heparin-binding EGF-like growth factor
HER2	human epidermal growth factor receptor 2
HIF-1	hypoxia-inducible factor-1
HK	hexokinase
ICAM	intercellular adhesion molecule
IFNα	interferon α
IL-1β	interleukin-1β
ILC	invasive lobular carcinoma
IM	immunomodulatory
IMM	inner mitochondrial membrane
iPSC	induced pluripotent stem cell
ISF	(brain) interstitial fluid
ISS	(brain) interstitial system
JAM	junctional adhesion molecule
Ki67	cell proliferation marker Kiel67
KISS1	kisspeptin 1
KLF4	Krüppel-like factor 4

Abbreviations

KO	knock-out
L1CAM	cell adhesion molecule L1
LAR	luminal androgen receptor
LCIS	lobular carcinoma *in situ*
LDH	lactate dehydrogenase
lncRNA	long non-coding RNAs
LOX	lysyl oxidase
MCT	monocarboxylate transporter
MES	mesenchymal-like
MET	mesenchymal-to-epithelial transition
MFN	mitofusin
miRNA	micro-RNA
MIS	mitochondrial intermembrane space
MLS	microphthalmia with linear skin lesions
MMP	matrix metalloproteinase
MPC	mitochondrial pyruvate carrier
MRI	magnetic resonance imaging
MSL	mesenchymal/stem-like
mtDNA	mitochondrial DNA
mtOCR	mitochondrial OCR
mtROS	mitochondrial ROS
nDNA	nuclear DNA
NDUFB	NADH ubiquinone oxidoreductase
NF-κB	nuclear factor kappa B
NK	natural killer (cell)
NMDAR	N-methyl-D-aspartate receptors

Abbreviations

NRF2	p38 nuclear factor-like 2
NST	invasive carcinoma of no special type
O_2	oxygen
OAA	oxaloacetate
OCR	oxygen consumption rates
OCT4	octamer-binding transcription factor 4
Oligo	oligomycin
Opa1	optic atrophy 1
OS	overall survival
OXPHOS	oxidative phosphorylation
PA	plasminogen activators
PARP	poly ADP-ribose polymerase
PCDH7	protocadherin-7
pCR	pathological complete response
PDH	pyruvate dehydrogenase
PD-L1	programmed death-ligand 1
PEP	phosphoenolpyruvate
PET	positron emission tomography
PFA	paraformaldehyde
PFK	phosphofructokinase
PG	prostaglandin
PGM	phosphoglucomutase
P-gp	P-glycoprotein
PHGDH	phosphoglycerate dehydrogenase
Pi	inorganic phosphate molecule
PKM	pyruvate kinase

Abbreviations

PLGF	placental growth factor
PMN	pre-metastatic niche
PPARγ	peroxisome proliferator-activated receptor γ
PPP	pentose phosphate pathway
PR	progesterone receptor
PSGL-1	P-selectin glycoprotein ligand-1
PTEN	phosphatase and tensin homolog
PTGS2	prostaglandin-endoperoxide synthase 2
PUFA	polyunsaturated fatty acids
RB1	retinoblastoma 1
RNA	ribonucleic acid
ROS	reactive oxygen species
RT-qPCR	real-time quantitative polymerase chain reaction
SALL4	Sal-like transcription factor 4
SCD	stearoylCoA desaturase 1
SDH	succinate dehydrogenase
SEMA4D	semaphorin-4D
sFasL	soluble Fas ligand
SHMT2	serine hydroxymethyltransferase 2
SLC1A5_var	solute carrier family 1 member 5 variant
SOD	superoxide dismutase
SOX2	SRY-Box transcription factor 2
SREBP1	sterol regulatory element-binding protein-1
ST6GALNAC5	brain-specific sialyltransferase
STAT1	signal transducer and activator of transcription 1
STR	short tandem repeat (profiling)

Abbreviations

TCA	tricarboxylic acid (cycle)
T-DM1	trastuzumab-emtansin/DM1
T-DXd	trastuzumab-deruxtecan
TEER	transendothelial electrical resistance
Tf	tissue factor
TGFβ	transforming growth factor β
TIMP1	tissue inhibitor of metalloproteinase-1
TJ	tight junction
TNBC	triple negative breast cancer
TNF	tumor necrosis factor
TNM	tumor-nodes-metastasis (system)
TP53	tumor protein 53
TPP^+	triphenylphosphonium
UICC	Union for International Cancer Control
uPA	urokinase plasminogen activator
VCAM	vascular cell adhesion molecule
VDAC	voltage-dependent anion carrier
VEGF	vascular endothelial growth factor
WBRT	whole brain radiation therapy
xCT	cystine-glutamate transporter
ZO-1	zona occludens protein-1
αKG	α-ketoglutarate
ΔΨm	mitochondrial membrane potential

TABLE OF CONTENTS

I. INTRODUCTION……p.19

1 Cancer Metastasis……p.21

1.1 Context

1.2 The Metastatic Cascade

1.2.1 Detachment

1.2.2 Intravasation

1.2.3 Survival in the circulation

1.2.4 Extravasation

1.2.5 Colonization

1.3 Organotropism

1.4 Pre-metastatic niche

2 Cancer Metabolism……...p.31

2.1 The Warburg Effect

2.2 Beyond the Warburg Effect

2.3 Mitochondria

2.4 Mitochondria in Cancer

2.5 Glycolysis

2.6 TCA cycle

2.7 Oxidative phosphorylation

2.8 Fatty acid oxidation

2.9 mtROS

2.10 Metabolic rewiring

2.10.1 Glucose

2.10.2 Glutamine

2.10.3 Lipids

2.10.4 Other carbon/nitrogen sources

2.11 Factors influencing fuel choice

2.12 mtROS unification hypothesis

Table of contents

2.13 Metabolism and (organ-specific) Metastasis
2.13.1 Metabolism & Metastasis
2.13.2 Metabolism & Organotropism

3 Cancer Stemness……p.55
3.1 Stem Cells
3.2 Cancer Stem Cells (CSC)
3.3 Identification of CSC
3.4 CSC metabolism
3.5 CSC mitochondria

4 Breast Cancer……p.61
4.1 Prevalence
4.2 Classification
4.2.1 BC Stages
4.2.2 BC Histologic subtypes
4.2.3 BC Molecular subtypes
4.2.4 BC Prognosis
4.2.5 Concordance between TNBC and Basal-like subtypes
4.2.6 HER2-enriched subtype and HER2- tumors
4.2.7 Claudin-low status
4.3 Treatment
4.4 Triple-Negative Breast Cancer (TNBC)
4.5 Breast Cancer Brain Metastasis (BCBM)
4.5.1 BCBM prevalence in TNBC
4.5.2 BCBM prognosis in TNBC
4.5.3 Increased incidence of BCBM

5 The Brain……p.77
5.1 Brain anatomy, parenchyma and anatomical barriers
5.1.1 Meninges
5.1.2 Brain cells

Table of contents

5.1.3 Interstitial system

5.1.4 Interstitial fluid composition

5.1.5 Blood-brain barrier (BBB)

5.1.5.1 Specialized endothelium

5.1.5.2 Pericytes and astrocytes

5.2 Invasion of the brain microenvironment

5.2.1 Breaching the BBB

5.2.1.1 BBB disruption

5.2.1.2 BBB infiltration

5.2.2 Interactions with brain cells

5.2.3 Neuronal phenotype

5.3 Brain metastasis treatment

6 Brain Metastases Metabolism……p.91

6.1 Glucose oxidation, TCA, PPP and folate cycle

6.2 Acetate metabolism

6.3 Lipid metabolism

6.4 Amino Acid metabolism

6.5 GABA metabolism

II. AIM OF THE THESIS……..p.97

III. RESULTS…….p.99

IV. DISCUSSION…….p.129

V. GENERAL CONCLUSION……p.147

VI. PERSONAL CONTRIBUTIONS…….p.149

VII. REFERENCES…….p.151

I. INTRODUCTION

Foreword

Dear reader,

My doctoral work focused on cancer and its most dreaded form, metastasis. Cancer is a major health issue, with millions of patients around the world being diagnosed every year. Unfortunately, as a cancer lesion progresses, cancer cells progressively acquire the capacity to leave the primary tumor and colonize new organs in a process called ‘metastasis’. Despite treatment advances, metastatic dissemination still worsens the prognosis of patients, as it often marks the transition from curative to palliative care and causes millions of deaths every year. Therefore, preventing metastasis is a priority in cancer research. More specifically, brain metastasis is a particularly feared outcome, remaining highly difficult to treat and rapidly affecting patients’ quality of life.

Recent advances in cancer research have shown that metastatic cells display preferences for which organ to colonize, a concept known as ‘organotropism’. My thesis addresses the question of **metabolism as a possible driver of metastatic organotropism**, following the idea that circulating cancer cells possess certain metabolic preferences and search for an organ of destination that meets desired criteria. Metabolism refers to the processes by which cells utilize nutrients and obtain their energy, and it has been established that cancer cells rewire their metabolism during cancer development. At the beginning of my thesis work, whether metabolic properties could be responsible for organotropism was still an open question.

During about four years, I investigated the metastatic process from a metabolic point of view, with a special focus on **breast cancer brain metastasis** as an example for metastatic organ selectivity. This model was chosen because most breast cancer patients are diagnosed at a premetastatic stage, providing an opportunity for metastasis prevention. I focused on triple-negative breast cancer based on the morbidly high frequency of metastases and on the severity of brain colonization observed in this subtype of breast cancer, as well as on the availability of two independently generated cellular models/assets. Our approach was intended to design and establish a strategy for the study of organotropism, while aiming for a possible treatment clue for this life-threatening outcome. We further hoped to generalize our findings to brain metastases associated to other cancer types, and to broaden the experimental strategy for the study of organ-specific metastasis in general.

Introduction

In the introductory section, I will first address the general cancer notions of **metastasis**, **metabolism** and **stemness**, required to understand my work. Metastasis and metabolism are core concepts of this thesis, since they are at the basis of our working hypothesis. Then, we will dive further into the **breast cancer** subtype used as a model, and subsequently discover the **brain environment** - the specific destination of the metastatic cells under focus. Finally, we will discuss the existing knowledge on **metabolic traits of brain metastatic progenitor cells**.

CHAPTER 1 – CANCER METASTASIS

To understand the major health issue related to the cancer disease, we will first address the concept of 'metastatic dissemination', when cancer cells acquire the capacity to colonize distant organs.

1.1 Metastatic dissemination of cancer cells is the main cause of cancer-related fatalities. Clinically, it is estimated that about 90% of cancer-related deaths are due to a metastatic disease (Chaffer and Weinberg 2011, Lambert 2017). Indeed, once cancer cells leave the tumor of origin and start invading remote tissues and organs, it becomes much more complex – sometimes even impossible – to cure the patient. Understanding the precise mechanisms controlling the metastatic process is a key determinant in developing more efficient anticancer therapies and a priority for improved patient outcome. Indeed, preventing metastatic dissemination would allow to keep cancers localized and more easily curable. In that case, cancers could also be managed as chronic diseases, being under control for long-term survival, with patients still carrying the disease.

1.2 The metastatic cascade, through which cancer cells develop the ability to colonize distant sites, is a multi-step process requiring specific skills (Chaffer and Weinberg 2011, Obenauf 2015, Steeg 2016, Lambert 2017, Singh 2017) (**Figure 1**). Due to its complexity, the metastatic cascade, which will be detailed below, is a very inefficient process. Every single step must be completed for a secondary tumor to establish and develop, and only a tiny percentage of circulating cancer cells (CTCs) eventually succeed to colonize a secondary organ among the millions that exit the primary site every day (Fidler 1970, Chambers 2002, Vanharanta 2013). This minority of cells are called **metastatic progenitor cells** (Patrawala 2006).

The acquisition of necessary traits for successful metastasis is consensually believed to be the result of harsh environmental conditions in the primary tumor, including inflammation, hypoxia (low level of oxygen), nutrient scarcity, and local acidosis (Jang 1997, Vaupel 2004, Lunt 2009, DeClerck 2010, Gilkes 2014, Rankin

2016, Payen 2016, Porporato 2016). These hostile areas, the distribution of which may fluctuate in time and space, promote the metastatic switch by forcing the cancer cells to adapt and to develop strategies to overcome unprecedented challenges (Pietila 2016). For instance, that a high expression of cathepsin S (a specific protease required for brain invasion) at the primary site correlates with increased brain metastasis incidence supports the concept of a subset of cancer cells acquiring metastatic prerequisites to colonize specific organs rather than a later adaptation during metastatic dissemination (Sevenich 2014).

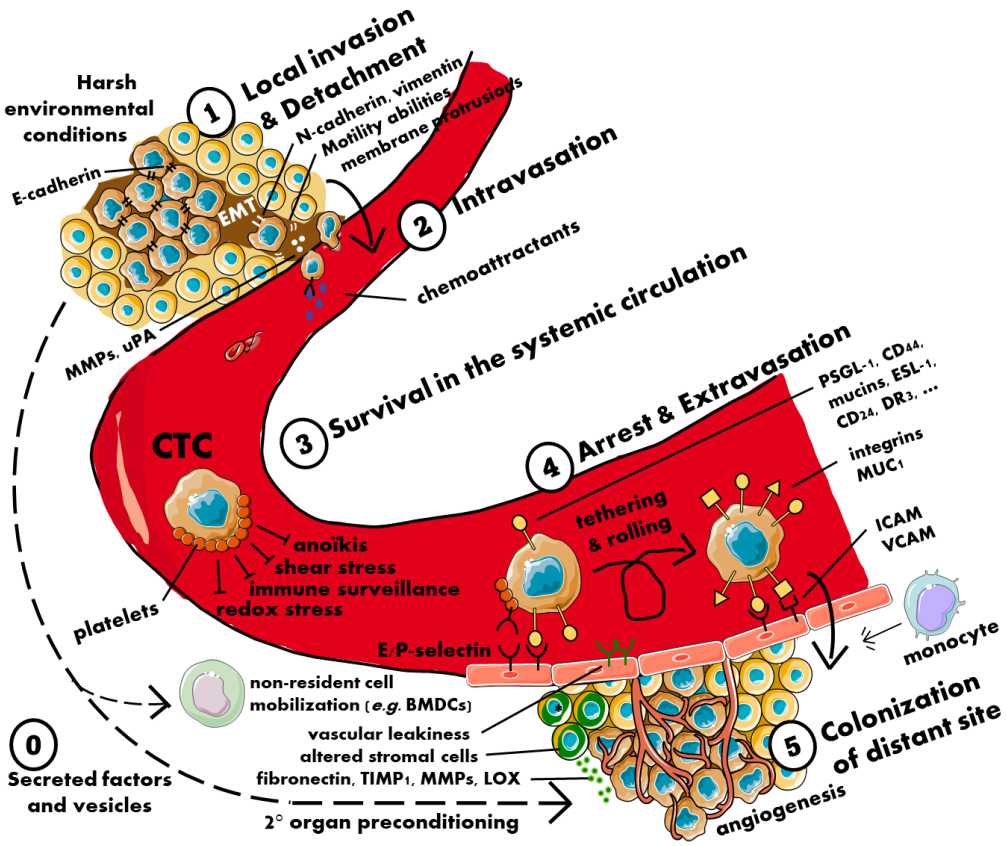


Figure 1. The metastatic cascade consists of five sequential steps and is preceded by the establishment of pre-metastatic niches (Step 0). Cancer cells leave the primary tumor through local

invasion and detachment (Step 1). Harsh environmental conditions promote the development of metastatic progenitor cells through a loss of epithelial markers (black bars) and a gain of mesenchymal markers, motility properties and proteolytic enzyme secretion (all represented in white). Intravasation into blood or lymphatic vessels requires invasive properties and the action of chemoattractants (Step 2). Circulating cancer cells (CTCs) must then resist to several stresses to survive in the systemic circulation, and platelets can be used as a protective shield (Step 3). The expression of selectin ligands allows the initial tethering and rolling of cancer cells on the endothelium, and the expression of additional ligands by cancer cells (integrins, MUC1) and additional receptors by endothelial cells (ICAM, VCAM) are important for subsequent arrest and CTC extravasation (Step 4). Metastatic progenitor cells colonize a distant organ and develop micrometastases then macrometastases, triggering angiogenesis for adequate blood supply (Step 5). Secondary organ preconditioning includes non-resident cell mobilization, vascular leakiness, altered stromal cells, a modified extracellular matrix (ECM) and released homing molecules (Step 0). Other abbreviations: BMDC – bone marrow-derived cells, TIMP1 – tissue inhibitor of metalloproteinase 1, MMPs – matrix metalloproteinases, LOX – lysyl oxidase, uPA – urokinase plasminogen activator, PSGL-1 – P-selectin glycoprotein ligand-1, CD – cluster of differentiation, ESL-1 – E-selectin-ligand-1, DR3 – death receptor 3, MUC1 – mucin 1, ICAM – intercellular adhesion molecule, VCAM – vascular cell adhesion molecule.

1.2.1 Detachment from the primary tumor. First, cancer cells at the primary tumor site must escape the organ of origin, starting with local invasion (**Figure 1** *Step 1*). To acquire a metastatic phenotype and start to invade the tissue, cells must (1) detach from the neighboring cells in the primary tissue, (2) degrade the surrounding tissues to make their way towards the bloodstream, and (3) acquire migration and invasion properties. The epithelial-to-mesenchymal transition (EMT) is a biological phenomenon occurring naturally during embryonic development, which is hijacked by cancer cells to lose their epithelial features and gain mesenchymal ones for migration and metastasis (Chaffer and Weinberg 2011, Savagner 2015). Losing epithelial features mainly translates in losing cell-cell adhesion by downregulating the expression of intercellular junction proteins, such as E-cadherin, occludin and claudins (Lu and Kang 2019). Gaining mesenchymal characteristics provides cells with motility abilities and proteolytic enzymes to digest the extracellular matrix (ECM) and the basal membrane, which includes matrix metalloproteinases (MMPs) and urokinase plasminogen activator (uPA) (Lu and Kang 2019, Kessenbrock 2010). EMT occurs through the activation of EMT transcription factors (like Snail, Slug, Zeb1 and Twist), subsequently inducing a downregulation of the expression of the epithelial markers listed above and an upregulation of the expression of

mesenchymal markers like N-cadherin, vimentin and fibronectin. EMT is a recognized facilitator of the early stages of metastasis; however, it has been challenged as an absolute necessity for cancer cells, arguing that it may act more as a catalyst than as a driver of metastasis (reviewed by Jolly in 2017). Alternative mechanisms to EMT-mediated single cell dissemination have been suggested, since collectively migrating cancer cells with intact cell-cell contacts, *ea.* preserved E-cadherin expression, were observed (Clark and Vignjevic 2015). Despite the possibility of other pathways than EMT to alter invasion properties, the answer to the necessity or not of EMT for cancer metastasis may reside in a hybrid state or spectrum view of EMT, or in the idea that leading cancer cells of collective migration groups may harbor EMT traits (Westcott 2015). With these considerations arises the concept of the non-binary nature of EMT: a hybrid epithelial/mesenchymal state, which nuances a strict and total transition, or a spectrum of phenotypes along different axes (including motility, cell-cell adhesion, etc.) that cumulatively define EMT (Nieto 2016, Jolly 2017). Partial transitions, or positions along the spectrum, allow to retain epithelial traits that may yield a maximal efficiency for the tumor-initiating potential (Grosse- Wilde 2015, Ruscetti 2015).

1.2.2 Intravasation. Cancer cells must next undergo intravasation to enter the vasculature, either directly or *via* the lymphatic system (**Figure 1** *Step 2*). The same proteolysis and motility abilities acquired earlier are employed, as well as chemotactic abilities. Chemotaxis is defined as directed migration in response to an external gradient of chemoattractants. It is mediated by the expression of adequate sensors (Roussos 2011). For example, it has been reported that chemotactic migration and intravasation of gastric cancer cells was enhanced by the upregulation of chemokine (C-X-C motif) receptors 1 and 2 (CXCR1/2) (Lin 2007), that chemokine (C-C motif) receptor 7 (CCR7)-expressing cells responded to the chemokine (C-C motif) ligand 21 (CCL21) (Hayasaka 2022), and that neutralizing the interaction between CXCR4 and chemokine (C-X-C motif) ligand 12 (CXCL12) impaired breast cancer metastasis (Müller 2001). The authors also showed that the chemotactic and invasive responses upon ligand-receptor interaction was mediated by actin polymerization and pseudopodia formation.

1.2.3 Survival in the systemic circulation. Once in the bloodstream, cancer cells need to survive to a multitude of lethal challenges, including anoïkis (death by detachment), reoxygenation/redox stress, host's immune response, and mechanical destruction due to hemodynamic shearing forces within vessels (Joyce 2009) (**Figure 1** *Step 3*). This particularly severe transition forces CTCs to develop defense mechanisms. A well-recognized strategy is to use platelets as a protective layer, both to evade immune surveillance (particularly natural killer [NK] cell-mediated lysis) and to reduce shear stress (Palumbo 2007, Joyce 2009, Goubran 2014). For this process, the expression of tissue factor (Tf) and the subsequent expression of thrombin by cancer cells trigger platelet activation and coagulation, leading to platelet aggregation around the CTCs. The binding between platelets and CTCs is achieved *via* fibrin filaments and specific integrins, or trough P-selectin on activated platelets binding to P-selectin ligands expressed on the surface of CTCs (Goubran 2014). For collectively migrating cancer cells, less prevalent but more efficient CTC clusters provide similar protection as platelet shields in addition to offering anoïkis resistance (Aceto 2014, Jolly 2017).

Cancer cells are faced with high levels of oxygen in the bloodstream as compared to hypoxic areas in the primary tumor. Redox homeostasis mechanisms are required for CTCs to survive to the elevated oxidative stress induced by reoxygenation as well as loss of matrix adhesion and nutrient deprivation upon entry in blood vessels (Schafer 2009, Jeon 2012, Piskounova 2015, Zheng 2017, Tasdogan 2020, Bartkowiak 2020). They activate antioxidant mechanisms to counteract oxidative damage, mainly the glutathione (GSH) system, a tripeptide comprising cysteine, glutamate and glycine. GSH serves as a redox buffer: its reduced form reacts with oxidizing substances to neutralize them, which generates glutathione disulfide (GSSG) (Wu 2004). GSH can be regenerated from its oxidized form by glutathione reductase, with reducing equivalents from NADPH-generating pathways (Fan 2014). Cancer cells increase GSH synthesis and regeneration, including by increasing the uptake of the rate-limiting precursor cysteine mediated by cystine-glutamate transporter xCT (Lewerenz 2013), by increasing the expression of the rate-limiting enzyme glutamate-cysteine ligase (GCL) (Lu 2013), and by increasing the activity of

NADPH-generating pathways (Fan 2014, Tasdogan 2020). They were also reported to hijack the specialized blood-restricted β-chain of hemoglobin (β-globin), a molecule naturally designed to interact with oxygen (Zheng 2017).

1.2.4 Arrest & extravasation. The virtual inexistence of intravascular metastases (Tilkorn 2010) indicates that CTCs must extravasate to colonize the organ of destination (**Figure 1** *Step 4*). Cancer cells arrest at the site of metastasis through homing mechanisms and physical restraints, and they employ similar mechanisms than leucocytes for adhesion and extravasation (Ramakrishna 2013, Labelle 2012, Reymond 2013) using selectins, *i.e.*, transmembrane glycoproteins involved in vascular cell adhesion between leucocytes (L-selectin), activated platelets (P-selectin) and endothelial cells (P-selectin and activated E-selectin). Accordingly, CTCs reroute vascular adhesion mechanisms and express carbohydrate selectin ligands, such as P-selectin glycoprotein ligand-1 (PSGL-1), CD44, E-selectin-ligand-1 (ESL-1), mucins, CD24 and death-receptor 3 (DR3), to interact with E-selectin on endothelial cells (Aigner 1997, Kim 1997, Hollingsworth 2004, Dimitroff 2005, Burdick 2006, Gout 2006, Kang 2015). Selectin-mediated tethering events induce cancer cell rolling along the endothelium, followed by cell arrest and adhesion (Vestweber 2002, Ley 2007, Läubli 2010). In addition, the vascular endothelium is activated by proinflammatory stimuli that increase the expression of tethering proteins, and thus plays an active role in cancer cell transendothelial migration (Miles 2008). CTCs breach the endothelial barrier at the site of adhesion, still employing ligands typically expressed by leucocytes (McEver 1997, Kannagi 1997, Läubli 2010). Cell adhesion molecules, like mucin 1 (MUC1) and intercellular adhesion molecule (ICAM)-1, or integrin α4β1 and vascular cell adhesion molecule (VCAM)-1, establish further cell-cell contacts, and thus strengthens the adhesion between cancer and endothelial cells (Geng 2012, Soto 2014). Moreover, cells in the bloodstream modulate the efficiency of CTC extravasation. For example, monocytes can increase CTC transendothelial migration *via* L-selectin-dependent recruitment (Qian 2009, Läubli 2009). Platelets are also more than physical shields against immune cells and shear stress, as they aid endothelial attachment and extravasation *via* platelet P-selectin, induction of endothelial P-selectin expression and secretion

of molecules inducing endothelial cells opening (Erpenbeck 2010, Reymond 2013, Goubran 2014),

1.2.5 Colonization of distant sites. Once in the organ of destination, cancer cells must survive in the new microenvironment, interact with resident cells, and initiate tumor growth to create a secondary tumor (**Figure 1** *Step 5*). Just as EMT enables dissemination, cancer cells undergo a process of differentiation (MET) to regain epithelial properties and form pre-angiogenic micrometastases (Gunasinghe 2012, Banyard 2015, Lu and Kang 2019). Adequate blood supply, resulting from the development of a tumor-associated vascular network (neoangiogenesis) and the recruitment of a supporting stroma, is required for the successful transformation of micrometastases in macrometastases (Chambers 2002, Chaffer and Weinberg 2011).

1.3 Metastatic cells display distinct preferences in organ colonization, a concept named 'organotropism', at the basis of the seed and soil hypothesis. The last two stages of the metastatic cascade (entry and survival in a secondary organ, **Figure 1** *Steps 4&5*) are non-random phenomena, owing to differences in organ targeting (Paget 1889, Nguyen 2009, Obenauf and Massague 2015). Indeed, different types of cancers preferentially metastasize to specific secondary sites, creating distinct metastatic patterns and distribution frequencies. For example, prostate cancers preferentially spread to the bones, pancreatic cancers to the liver and malignant melanomas to the lungs (Obenauf and Massague 2015, Tas 2012). Distinctly, luminal breast cancers mainly colonize the bones whereas triple negative breast cancer (TNBC) has increased incidence of lung and brain metastases (Lin 2008, Smid 2008, Kennecke 2010, Sihto 2011, Harell 2012, Wu 2017, Darlix 2019).

The concept of the organ specificity of metastases, also called 'metastatic organotropism', was introduced in 1889 by the English surgeon *Stephen Paget* with the **Seed-and-Soil theory** (Paget 1889). He postulated that the 'seed' (the metastatic progenitor cell) must find its appropriate 'soil' (the microenvironment of a secondary site) to successfully establish a metastasis. This theory was challenged by Ewing in the 1930s, who believed that metastasis was solely dependent on the

dynamics of hematogenous flow (Ewing 1928). Later, the importance of both the mechanical properties of the vasculature and the compatibility of the "seed" with the "soil" in the new organ were recognized (Fidler 1976, Azevedo 2015). Revisited several times since then (Fidler 2003, Langley 2011, Liu 2017), the seed and soil hypothesis brings forward the notion that the formation of metastases is finely tuned by features of the metastatic progenitor cells, features of the microenvironment at destination and, more importantly, interactions between the two. For example, compared to exiting the peripheral vasculature, CTC extravasation into the brain requires the expression of specific proteins to process the specialized brain vasculature (see 5.2.1 Crossing the blood brain barrier). An additional interpretation of Paget's postulate proposes that different primary cancer types may develop common mechanisms to colonize the same (distant) metastatic site (Mashimo 2014, Gao 2019). It further suggests the existence of concomitant populations of metastatic progenitor cells in the same primary tumor, with different organotropisms.

1.4 Prior to the metastatic cascade arises the paradigm of the pre-metastatic niche. Before the onset of metastases, soluble factors and extracellular vesicles are secreted and released in the blood stream by the primary tumor, which modify distant organs towards a permissive environment for future metastatic cells (extensively covered in Peinado 2017) (**Figure 1** *Step 0*). Tumor-derived factors, like pro-angiogenic factors and inflammatory cytokines (*e.g.* VEGF-A, PLGF, G-CSF, CCL2, TGFβ, TNF), drive the preconditioning of the microenvironment by acting on endothelial cells to increase vascular leakiness, by altering resident cells such as fibroblasts and macrophages, and by mobilizing non-resident cells. As such, soluble factors including VEGF were shown to upregulate the expression of E-selectin in a focal adhesion kinase (FAK)-dependent manner on endothelial cells to create hyperpermeability regions and to promote CTC adhesion (Hiratsuka 2011).

The first proof-of-principle study regarding the pre-metastatic niche (PMN) demonstrated that soluble factors produced by a primary tumor activate resident fibroblasts, which stimulate fibronectin deposition in the ECM and mobilize bone marrow-derived cells (BMDCs). BDMCs are recruited to the PMN by high levels of fibronectin, and they express MMP9 to further alter the ECM, as well as CXCL12 to

attract CXCR4-expressing CTCs (Kaplan 2005). In a general manner, ECM remodeling is mediated by altered host cells producing new ECM components and expressing and/or secreting specific enzymes to modulate the existing ECM (such as tissue inhibitor of metalloproteinase-1 [TIMP1], MMPs and lysyl oxidase [LOX]). Subsequently, vascular leakiness, a modified ECM and resident cell-derived attractants collectively help the recruitment of activated non-resident cells (such as BMDCs and neutrophils) to further shape the PMN in a pro-inflammatory and immunosuppressive milieu supporting tumor growth. Not only is a pro-tumorigenic environment created, but the remodeling of PMN blood vessels and the release of attracting molecules during PMN formation also facilitate the homing of metastatic progenitor cells. For example, collagen IV-derived peptides released by the MMP2 activity of BMDCs were shown to promote the homing of additional BMDCs, and later CTCs, to lung PMNs (Erler 2009). This phenomenon exemplifies the fact that proteolytic remodeling, such as collagen IV degradation, does not only remove a physical matrix barrier with collagen IV being the main component of the vascular basement membrane (Hudson 1993), but it also releases previously sequestered (cryptic) factors and signals. For example, aside from homing factors, Davis and his team demonstrated that MMP-mediated proteolysis of collagen IV in the basement membrane exposes a normally hidden cryptic epitope (Xu 2001). Epitope exposure induces novel integrin interactions (loss of integrin α1β1 binding and gain of integrin αvβ3 binding), which activates endothelial cell adhesion and migration (Xu 2001). This matrix-immobilized epitope within collagen IV thus functions as a cryptic regulatory signal that initiates an integrin-mediated signaling cascade resulting in altered cellular migratory behaviors.

Beside tumor-derived factors, exosomes were also evidenced to drive PMN formation. For example, it was reported that pancreatic cancer exosomes can target macrophages in the liver to produce transforming growth factor β (TGFβ), which induces hepatic stellate cells to produce fibronectin, subsequently recruiting bone marrow-derived macrophages (Costa-Silva 2015). In addition, breast cancer cells were found to produce microRNA-122-containing vesicles that suppressed glucose metabolism in stromal cells of lung and brain PMNs, allowing enhanced glucose

availability in the tissue (Fong 2015). Furthermore, PMN formation has been proposed as a driver of organotropism, due to the precise targeting of exosomes to specific host cells. Kaplan *et al.* (Kaplan 2005) showed that melanoma-conditioned medium is capable of redirecting lung cancer cells to organs usually associated with melanoma metastasis. In line with this notion, a recent landmark study reported that exosomes could dictate organotrophic behaviors by distinct integrin expression patterns: integrin α6β4 promotes exosome uptake in lung PMNs, whereas αvβ5 promotes homing to liver PMNs (Hoshino 2015).

The rationale of this work starts with the concept that **organ-specific metastases** may possess specific **metabolic properties adapted to the distant metabolic microenvironment.** We will therefore address the concept of cancer metabolism in the next chapter.

CHAPTER 2 - CANCER METABOLISM

To unite the vast complexity of neoplastic diseases, cancer was conceptualized using common biological traits, or hallmarks, of cancer phenotypes. Six original **cancer hallmarks** defined the acquired characteristics supporting tumor development (**Figure 2**). In the last two decades, two enabling characteristics and two **emerging hallmarks** were added due to research progress. As their names indicate, these emerging hallmarks have gained tremendous momentum in their fields. One of them, termed **'deregulating cellular energetics'**, consists in the reprogramming of energy metabolism in cancer cells. This chapter covers what lies behind this major concept in cellular functions; what cancer cells consume and how they transform nutrients in energy. Metabolic reprogramming is indeed a key feature of tumor development, being crucial for cancer cells due to their increased bioenergetic and biosynthetic demands. As such, further in-depth understanding of cancer metabolism is paramount to develop new therapeutic strategies targeting deregulated metabolic pathways specific to cancer cells.

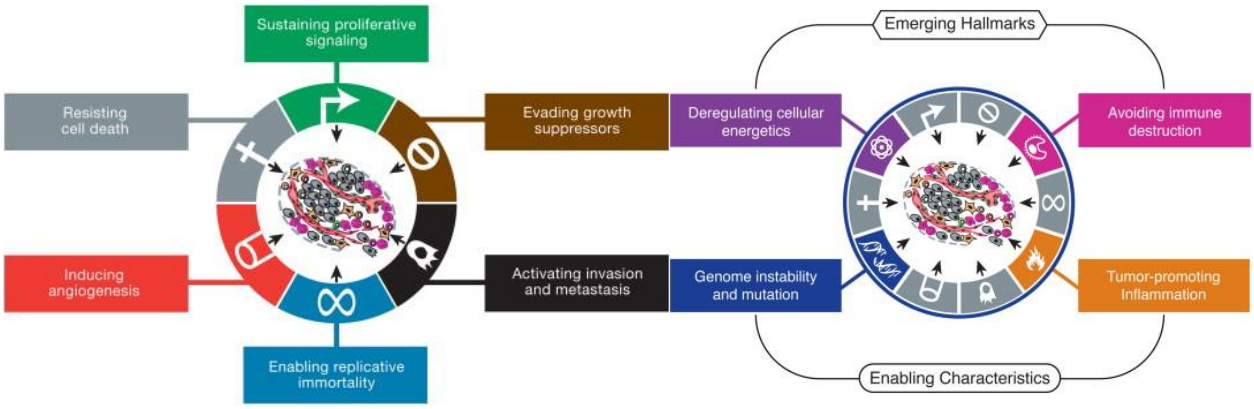


Figure 2. Cancer hallmarks. On the left, the six original hallmarks of cancer (figure from Hanahan and Weinberg 2000). On the right, emerging hallmarks and enabling characteristics (figure from Hanahan 2011).

2.1 Metabolic reprogramming was first thought to merely reflect the ability of cancer cells to use aerobic glycolysis, the so-called "Warburg effect". In 1925, Otto Warburg observed that cancer cells could ferment glucose to lactate at a high rate even in the presence of oxygen (Warburg 1925, 1956). This medical

breakthrough allowed the development of a widely used imaging technique for the detection and monitoring of tumors: FDG-PET scanning. By exploiting the high avidity of tumors for glucose, [^{18}F]-fluorodeoxyglucose (FDG) positron emission tomography (PET) can highlight areas of elevated glucose uptake (Vander Heiden 2009, Almuhaideb 2011, Zhu 2011). However, Warburg also formulated the hypothesis that mitochondria were not functional in tumors, which has wrongly let mitochondria apart from core tumor metabolism for a long time.

2.2 In the recent years, extensive research has shown that cancer metabolism cannot be summarized by the Warburg effect and that the situation is much more complex. Our understanding of tumor metabolism has radically evolved as new metabolic characteristics of cancer cells were discovered (Pavlova 2016, Pavlova 2022). Not only are some tumors more oxidative than others, but intercellular heterogeneity can also arise both in space and time due to the progressive acquisition of additional mutations, and to the incredible metabolic flexibility and plasticity of cancer cells (Danhier 2017). The new vision of cancer metabolism is beyond the Warburg Effect and the strict view of dependance on aerobic glycolysis. Although cancer cells can rely on increased aerobic glycolysis to maintain sufficient energy production during biosynthesis, portraying tumor metabolism as this sole phenomenon is reductive and incorrect. Most often, cancer cell mitochondria are functional and play a pivotal role in tumor development and progression (Porporato 2014, Zong 2016). Mitochondria first regained focus through their role in regulated cell death, and their subsequent targeting in chemo- and radio-sensitization (Fulda 2010). From a metabolic standpoint, the production of oncogenic metabolites and the remarkable adaptability of mitochondrial pathways for metabolic plasticity (Dang 2009, Fendt 2013, Wise 2011) supported a critical role of mitochondrial metabolism in cancer, which was eventually given proper recognition (Wallace 2012, Vyas 2016).

2.3 Mitochondria are subcellular organelles with multiple essential functions: providing energy, supporting biosynthesis, producing reactive oxygen species, and regulating apoptosis. According to the well-established endosymbiotic theory of mitochondrial evolution (Margulis 1975, Zimorski 2014,

Degli Esposti 2014), these organelles originate from the symbiotic relationship of an aerobic probacteria engulfed by eukaryotic cells approximately 1.5 billion years ago. Mitochondria are best known for their role as powerhouses of the cells. Indeed, their central bioenergetic function is to produce energy in the form of adenosine triphosphate (ATP), for which they are the main source in normal cells, and by hosting important metabolic pathways like the tricarboxylic acid (TCA) cycle (detailed in 2.6 - 2.8) (Mitchell 1961) (**Figures 3 & 6**). TCA cycle metabolites also provide building blocks for anabolic reactions and the biosynthesis of nucleotides, amino acids, lipids, heme, and others. Furthermore, mitochondria are a major site of reactive oxygen species (ROS) production, and they are key to many crucial biological processes in the cells: regulated cell death (by hosting regulators of the apoptotic pathway like cytochrome c), signaling pathways, stress sensing, redox and calcium homeostasis (Gaude and Frezza 2014, Sabharwal 2014, Porporato 2018, Vyas 2016, Payen 2019). A specific autophagy process, termed mitophagy, ensures mitochondrial fitness by recycling damaged and inefficient mitochondria for a continuous, proper functioning of the organelles (Galluzzi 2017).

2.4 Due to their roles in bioenergetics and biosynthesis as well as in the control of cell death and oxidative stress, mitochondria are now considered to be key players in cancer pathophysiology. Mitochondrial involvement can start early during tumorigenesis, with a contribution to malignant transformation *via* mitochondrial ROS (mtROS)-generated DNA defects, oncometabolites (fumarate, succinate and 2-hydroxyglutarate [2-HG]) acting on DNA methylation and gene expression, and/or deficits in senescence mechanisms (Gaude & Frezza 2014, Sciacovelli &Frezza 2016). The importance of mitochondria is highlighted by the phenomenon of mitochondrial transfer, where mtDNA-depleted cancer cells recover the ability to form tumors by importing mitochondria from the host (Dong 2017, Tan 2015). The impact of mitochondrial bioenergetics is further underlined by mitochondria-targeting therapies used to target cancer cells (Weinberg 2015, Denisenko 2019, Huang 2021). Mitochondria inhibitors, like electron transport chain (ETC) Complex I inhibitors metformin and phenformin (Wheaton 2014, Birsoy 2014, Griss 2015, Weinberg 2015), and specific antioxidant drugs aiming at the

mitochondria, like MitoQ and MitoTEMPO (Kalvanaraman 2017, Porporato 2014, Capeloa 2022a/b/c), can efficiently inhibit tumor growth and progression. Note that mitochondria-targeted drugs often consist of a bioactive molecule attached to a lipophilic and positively charged moiety, generally triphenylphosphonium (TPP^+), to direct the agent to the strongly negative potential of tumor mitochondria (Forrest 2015, Zielonka 2017).

2.5 Glycolysis breaks down glucose (six carbons) in 2 molecules of pyruvate (three carbons) that can subsequently be converted to lactate or enter into the TCA cycle. In the preparatory phase of glycolysis (5 steps), glucose is phosphorylated by hexokinase (HK), which traps glucose in the cells in the form of glucose-6-P (G6P), isomerized to fructose-6-phosphate (F6P) and phosphorylated again by the rate-limiting enzyme phosphofructokinase (PFK) to generate fructose-1,6-bisphosphate (F1,6BP) (**Figure 3**). This molecule is cleaved to obtain two 3-carbon fragments, yielding two glyceraldehyde 3-phosphate (G3P) molecules by the concerted action of two enzymes. In the payoff phase (5 steps), G3P is oxidized/dehydrogenated and dephosphorylated, generating energy in the form of both NADH and ATP. The last step is performed by pyruvate kinase (PKM) that converts phosphoenolpyruvate (PEP) to pyruvate. **Pyruvate** is a key metabolite, as it is the branch point between glycolysis and mitochondrial respiration (**Figure 6**): it can be further oxidized in the mitochondria or reduced to lactate by NADH-dependent enzyme lactate dehydrogenase 5 (LDH5; NADH itself being generated by glycolysis), a process known as '**lactic fermentation**'.

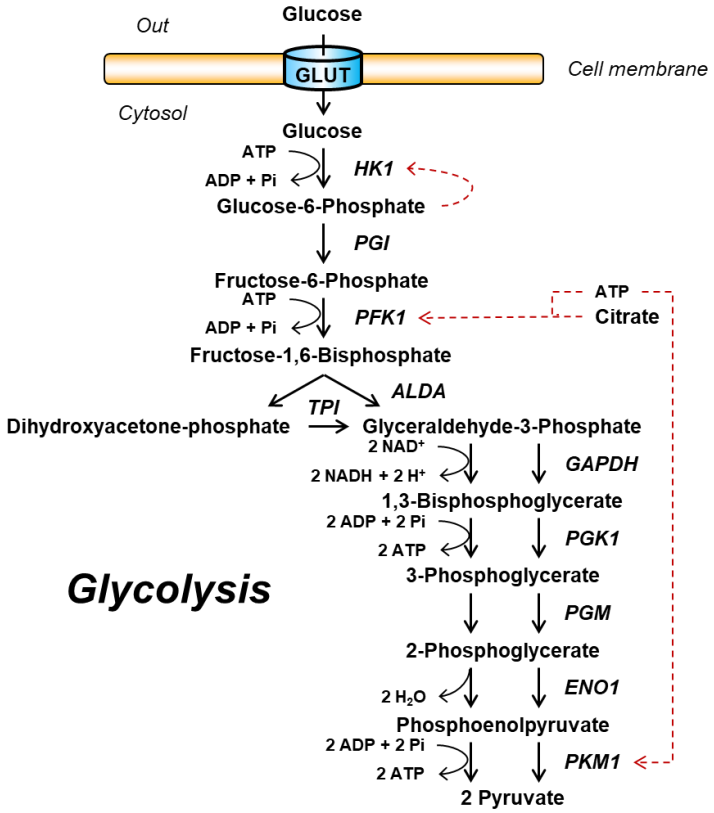


Figure 3. Canonical glycolysis. Allosterically regulated glycolytic enzymes are shown with red arrows. Abbreviations: ADP, adenosine diphosphate; ALDA, aldolase A; ATP, adenosine triphosphate; ENO1, enolase 1; GAPDH, G3P dehydrogenase; GLUT, glucose transporter; HK1, hexokinase; PFK1, phosphofructokinase 1; PGI, phosphoglucose isomerase; PGK1, phosphoglycerate kinase 1; PGM, phosphoglycerate mutase; PKM1, pyruvate kinase 1; Pi, inorganic phosphate molecule; TPI, triosephosphate isomerase. Figure from Payen 2015.

Glycolysis is faster but less efficient than mitochondrial respiration in generating energy from glucose, as it yields 2 ATP molecules per glucose, as compared to 36 through mitochondrial respiration (Yetkin-Arik 2019). The pathway is regulated by the three enzymes catalyzing irreversible reactions: HK, PFK and PKM. High energy metabolites exert a negative feedback loop on these enzymes: HK is inhibited by G6P (its product); PFK is allosterically inhibited by ATP, citrate and F2,6BP; and PKM is inhibited by ATP. This is called 'the Pasteur effect' (Wu 1959), and it is

alleviated when low energy compounds (adenosine diphosphate [ADP], adenosine monophosphate [AMP], and inorganic phosphate [Pi]) activate glycolytic regulatory enzymes. PKM is also allosterically activated by upstream F1,6BP, through the stabilization of its active tetrameric conformation.

Glycolytic intermediates can be diverted from glycolysis to fuel alternate/branched pathways, like the pentose-phosphate pathway (PPP), the biosynthesis of phospholipids and the serine biosynthesis pathway feeding the folate/one-cycle pathway (see section 2.10). PKM is a crucial enzyme to orient the fate of glucose derivatives: it opens the glycolytic flow when active and shunts glycolytic intermediates to the branching pathways when inactive (Mazurek 2011).

2.6 The TCA cycle is an important metabolic hub occurring in the matrix of mitochondria. Pyruvate entry in the mitochondria is mediated by mitochondrial pyruvate carriers (MPCs) (McCommis 2015) (**Figure 6**). Once inside mitochondria, the gatekeeper enzyme pyruvate dehydrogenase (PDH) transforms and traps pyruvate in acetylCoA. The fate of acetylCoA can be dual. On the one hand, the TCA cycle can serve as an oxidizing wheel to break down pyruvate into CO_2 and produce reducing equivalents used later for ATP/energy production (see 2.7). Sequentially, **acetylCoA** (*e.g.* derived from pyruvate) is added to oxaloacetate to form citrate, citrate is converted to isocitrate, which is decarboxylated twice to successively form **α-ketoglutarate** and succinyl-CoA, and succinyl-CoA is then further reduced to yield succinate, fumarate, malate and finally oxaloacetate, closing the circle. During this process, **reducing equivalents** are produced in the form of 3 molecules of NADH, 1 molecule of $FADH_2$ and 1 molecule of GTP. On the other hand, several TCA cycle intermediates can serve as precursors for the biosynthetic processes required for cell maintenance, division and during cell growth, such as lipogenesis for membrane construction. The TCA cycle can also be fueled by acetylCoA derived from other sources than pyruvate, *e.g.* fatty acid oxidation, and by metabolites entering into the circle at different entry points by means of anaplerotic pathways, *e.g.* glutamine *via* glutamate and α-ketoglutarate (Owen 2002, DeBerardinis 2010).

2.7 Oxidative phosphorylation uses the reducing equivalents generated in the TCA cycle to fuel the electron transport chain located in the mitochondrial inner membrane, generating a transmembrane proton gradient, and finally producing ATP. Oxidative phosphorylation (OXPHOS) consists in sequential redox reactions in specific ETC complexes that release energy to pump protons from the mitochondrial matrix into the mitochondrial intermembrane space (MIS) (**Figure 4**). This proton gradient is subsequently used for ATP synthesis. Electrons derived from reduced cofactors NADH and $FADH_2$ are fed into the ETC through Complex I (NADH dehydrogenase) and II (succinate dehydrogenase [SDH]), respectively. Both complexes shuttle their electrons to Complex III *via* ubiquinone (coenzyme Q10), but, of Complexes I and II, only Complex I pumps protons into the MIS. Complex III (ubiquinone-cytochrome c reductase) pumps proton as well and reduces 2 molecules of cytochrome c to shuttle the electrons to **Complex IV (cytochrome c oxidase [COX])**, where O_2 serves as the final electron acceptor to produce water. Like Complexes I and III, Complex IV pumps protons into the MIS. The proton-motive force resulting from the gradient generated by ETC Complexes I, II and IV is at the basis of ATP production by Complex V (ATP synthase). There, protons (H^+) follow their gradient and pass through the ATP synthase, which acts as a windmill harvesting the mitochondrial membrane potential ($\Delta\Psi m$) (Nicholls 2001). This rotational energy is converted in chemical energy when an inorganic phosphate molecule (Pi) is combined with ADP and a proton to produce ATP (Stock 1999).

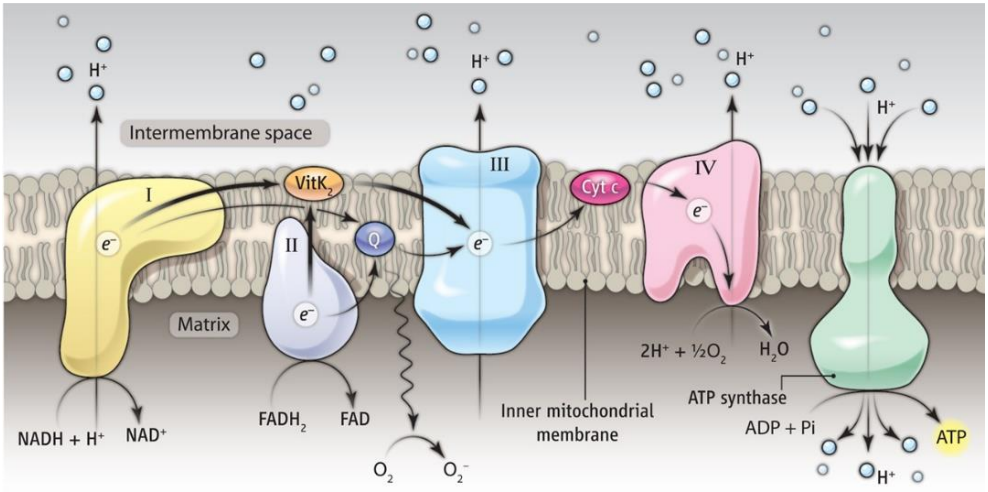


Figure 4. The electron transport chain. Located in the inner mitochondrial membrane, Complexes I-IV of the electron transport chain (ETC) shuttle electrons from reduced cofactors NADH and $FADH_2$ to molecular oxygen (O_2), and Complexes I, II and IV pump protons (H^+) from the mitochondrial matrix into the mitochondrial intermembrane space. Complex V (ATP synthase) converts the energy of the proton gradient into ATP production. Superoxide ($O_2^{\bullet-}$) is produced when a single electron leaking from the ETC reacts with O_2. Figure from Dirty Medicine 2019[a].

2.8 Fatty acids are processed in mitochondria through fatty acid β-oxidation. Fatty acid (FA) shuttling into mitochondria depends on the carnitine system (Melone 2018) (**Figure 6**). In the process, carnitine palmitoyltransferase-1 (CPT1) links the acyl groups of FAs to carnitine for their transport across mitochondrial membranes facilitated by carnitine-acylcarnitine translocase (CAT). Then, once inside the mitochondrial matrix, CPT2 releases FAs from carnitine. FAs are subsequently oxidized in a cyclic metabolic pathway where acyl-CoAs are shortened by 2 carbon atoms to produce 1 acetylCoA unit at each round (Houten and Wanders 2010). Each cycle also yields 1 NADH and 1 $FADH_2$ reducing equivalents. AcetylCoA can then fuel the TCA cycle, whereas NADH can fuel the ETC.

2.9 By shuttling electrons, mitochondria generate ROS. Physiologically, mitochondrial α-ketoglutarate dehydrogenase, pyruvate dehydrogenase and glycerol-3-phosphate dehydrogenase, as well as the ETC, can produce mtROS

[a] Available at https://www.youtube.com/@DirtyMedicine (Accessed last on 13/02/2023)

(Payen 2019). While oxygen is usually fully reduced by Complex IV to form water at the ETC, Complexes I and II can prematurely shunt single electrons to molecular oxygen, which creates superoxide ($O_2^{\bullet-}$) (Murphy 2009, Zhao 2019). This happens mostly through electron leakage under normal conditions (**Figure 4**). It can, however, also occur *via* bottlenecks in the respiration chain (limited respiration rate but high NADH/NAD^+ ratio fueling the ETC), reverse electron transfer from ubiquinone to Complex I (high H^+ gradient and abundant reduced ubiquinone) and under hypoxia (paradoxical increase in ROS production at Complex III due to a yet poorly understood altered flux of electrons) (Murphy 2009, Selivanov 2011, Sabharwal 2014). Highly reactive $O_2^{\bullet-}$ can be detoxified to hydrogen peroxide (H_2O_2) by superoxide dismutases (SODs), a reaction mainly rate-limited by the diffusion speed of superoxide (Zhao 2019, Hsu 1996). At lethal (high) ROS levels, if the protective antioxidant machinery is overwhelmed, cytochrome c is oxidized, which inhibits the binding of cytochrome c to the IMM, triggering its release, apoptosome formation in the cytosol and, subsequently, cell apoptosis (Zamzami 1995, Ott 2002) (**Figure 5**). Apart from apoptosis, mtROS generation is also involved in redox signaling at non-lethal levels, including induction of autophagy, mitochondrial biogenesis, hypoxia response and **mitohormesis** (Brunelle 2005, St-Pierre 2006, Dewaele 2010, Sena 2012). Mitohormesis designates the process by which moderate levels of mtROS activate antioxidant cell defenses, paradoxically enhancing oxidative stress resistance (Yun 2014, Ristow 2014, Barcena 2018). For instance, mtROS activate p38 nuclear factor-like 2 (NRF2), which induces the transcription of several antioxidant proteins (DeNicola 2011, Zarse 2012, DeNicola 2015, Ye 2014).

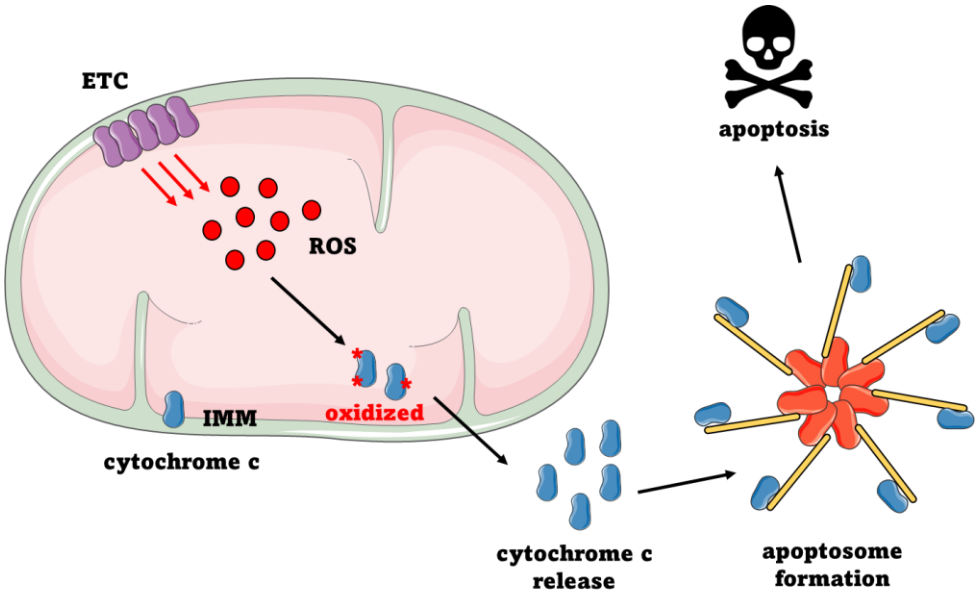


Figure 5. Cytochrome c mediates cellular apoptosis at high mtROS levels. When not efficiently counterbalanced by antioxidant mechanisms, mtROS (mainly produced by the ETC) trigger cytochrome c oxidation, inhibiting its binding to the inner mitochondrial membrane (IMM), causing its subsequent release and the formation of the apoptosome.

2.10 Cancer cells display extensive rewiring of cellular metabolism, characterized by a high degree of plasticity. Cancer cells often possess the capacity to interchangeably use glycolysis coupled to lactic fermentation, glycolysis coupled to the TCA cycle and to OXPHOS, fatty acid oxidation (FAO) and glutaminolysis for energy production (metabolic plasticity), in adaptation to fluctuating environmental conditions encompassing hypoxia, local acidosis, and nutrient deprivation (DeNicola 2015, DeBerardinis 2016) (**Figure 6**). Cancer cells also exhibit a remarkable metabolic flexibility in their use of nutrients. They can further reprogram their metabolism to fulfill their aberrantly elevated bioenergetic and biosynthetic needs.

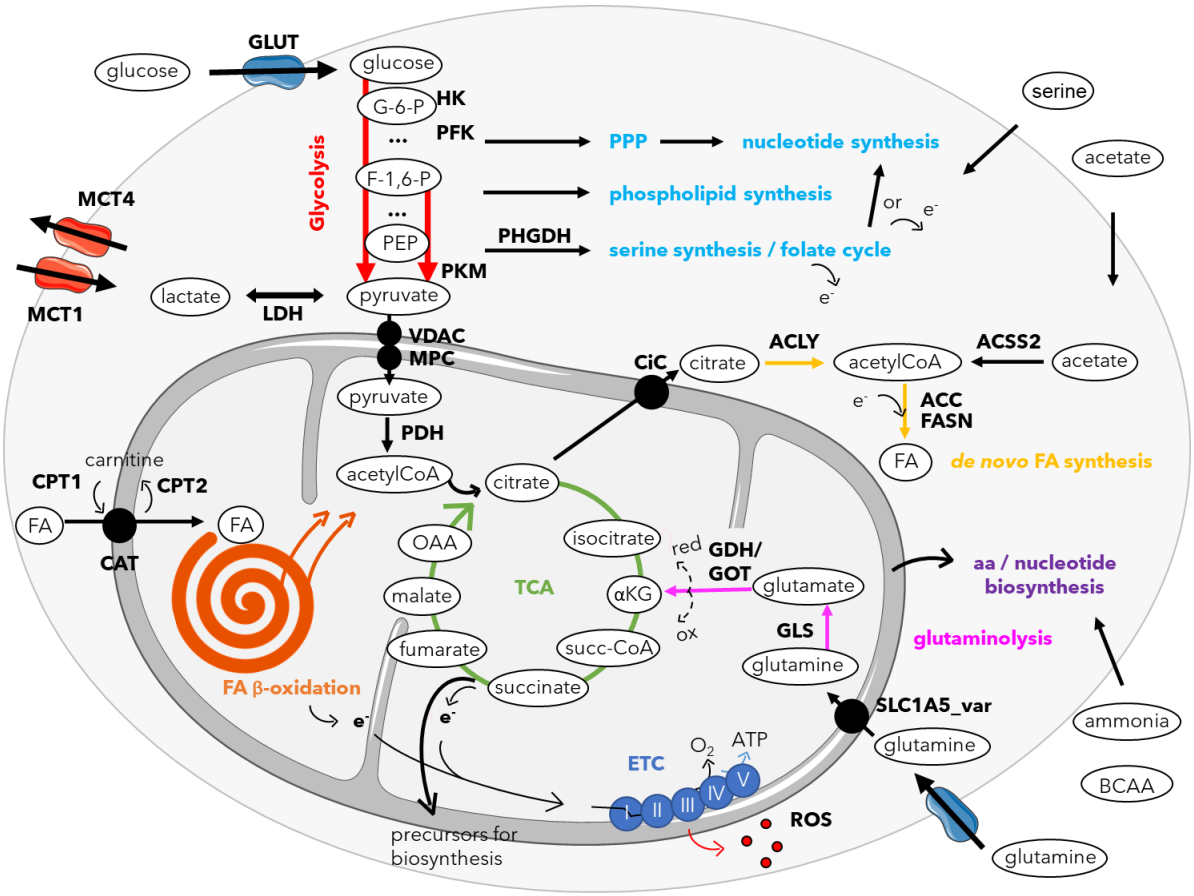


Figure 6. Cancer cell metabolic pathways. Glycolysis (in red) breaks down glucose to glycolytic intermediates for branching pathways (in light blue) or to pyruvate, which is converted to lactate in the cytosol (for fermentation) or acetylCoA inside the mitochondrion. The tricarboxylic acid (TCA) cycle generates reducing equivalents and/or biosynthesis precursors. The electron transport chain (ETC) composed of 5 complexes (I to V) produces ATP and is a major source of reactive oxygen species (ROS). Fatty acid (FA) oxidation produces acetylCoA for the TCA cycle. New FAs are generated from citrate (or from imported acetate) by *de novo* FA synthesis. Glutaminolysis allows the use of glutamine to fuel biosynthesis or the TCA cycle. Cancer cells can use alternate carbon and nitrogen sources. Other abbreviations: GLUT – glucose transporter, G-6-P – glucose-6-phosphate, F-1,6-P – fructose-1,6-bisphosphate, PEP – phosphoenolpyruvate, HK – hexokinase, PFK – phosphofructokinase, PKM – pyruvate kinase, PPP – pentose phosphate pathway, PHGDH – phosphoglycerate dehydrogenase, e^- – electrons/reducing equivalents, LDH – lactate dehydrogenase, MCT – monocarboxylate transporter, VDAC – voltage-dependent anion channel, MPC – mitochondrial pyruvate carrier, PDH – pyruvate

dehydrogenase, OAA – oxaloacetate, αKG – α-ketoglutarate, succ-CoA – succinyl-CoA, ATP – adenosine triphosphate, CAT – carnitine-acylcarnitine translocase, CPT - carnitine palmitoyltransferase, CiC – citrate carrier, ACLY – ATP-citrate lyase, ACC – acetylCoA carboxylase, FASN – fatty acid synthase, ACSS2 – acetylCoA synthetase 2, SLC1A5_var – solute carrier family 1 member 5 variant, GLS – glutaminase, GDH – glutamate dehydrogenase, GOT – glutamate-oxaloacetate transaminase, red – reductive carboxylation, ox – oxidative decarboxylation, BCAA – branched-chain amino acid..

2.10.1 **High rate glucose uptake** enhances glucose-dependent OXPHOS, high-rate lactic fermentation, or an increased activity of side-branch pathways of glycolysis, like the pentose phosphate pathway (PPP) and the serine pathway (**Figure 6**). Coupling glycolysis to lactic fermentation is essential for cancer cells to survive in a low oxygen environment (hypoxia) or when they experience mitochondrial defects. In tumors *in vivo*, many cancer cells reside in hypoxic areas. Short-term survival is ensured by alleviation of the Pasteur effect, as less allosteric feedback inhibition is exerted by high energy metabolites and more allosteric activation is exerted by low energy compounds on key glycolytic enzymes, thus accelerating the glycolytic flux (**Figure 7** *left*). Cancer cells adapt to long-term hypoxia by further activating hypoxia-inducible factors-1 and -2 (HIF-1 and HIF-2), *i.e.*, transcription factors increasing the expression of glycolytic enzymes and transporters, as well as lactate dehydrogenase-1 (LDH-1) converting pyruvate to lactate (Papandreou 2006, Payen 2015, Lee 2020) (**Figure** 7 *right*). However, cancer cells can also employ a pleiotropy of mechanisms to constitutively activate HIF-1 under normoxic conditions (Kaelin 2008) and increase glucose uptake (the Warburg effect). Multiple oncogenic signaling pathways indeed facilitate glucose entry and metabolism by upregulating the expression of glucose transporter, especially GLUT1 and GLUT3, and glycolytic enzymes (Murakami 1992), or triggering the re-expression of embryonic enzymes HK2 (trapping glucose inside cells) and/or PKM2 (controlling pyruvate production), which, compared to adult isoforms, have higher catalytic activities and are resistant to feedback Pasteur inhibition due to the absence of allosteric sites (Lee 2019, Christofk 2008).

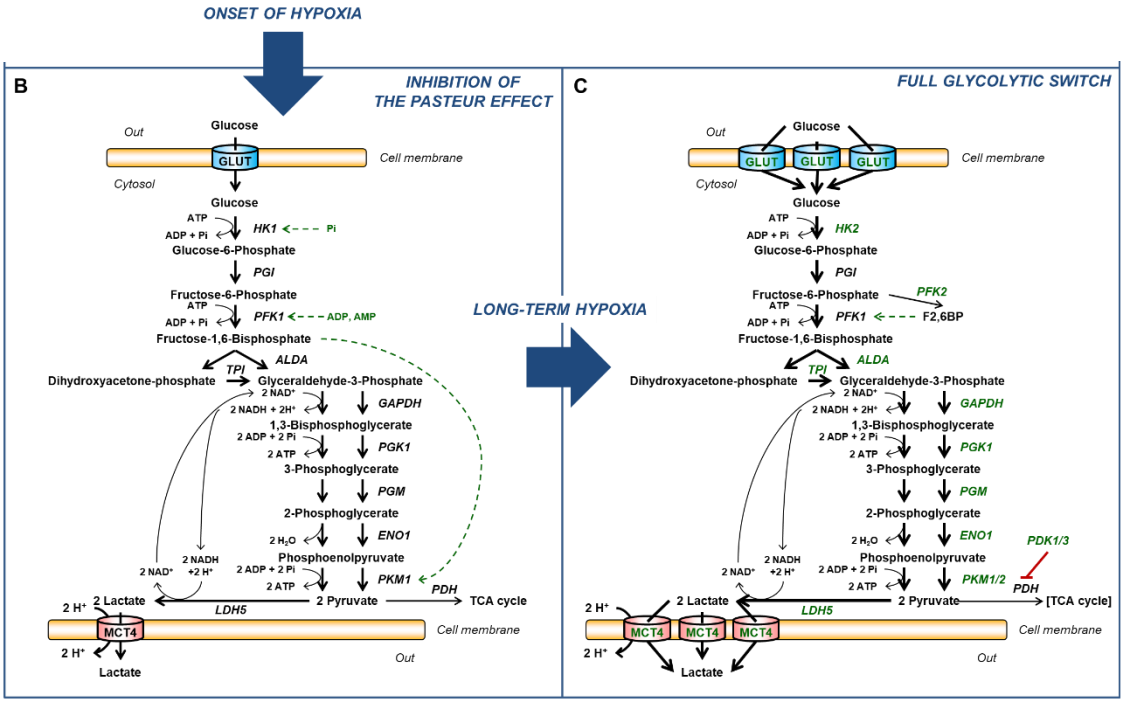


Figure 7. Metabolic adaptations to hypoxia. The early cellular response to hypoxia is the inhibition of the Pasteur effect by low energy metabolites that activate glycolytic regulatory enzymes (*left*). Long-term hypoxia further triggers the upregulation of hypoxia-inducible factor-1 and -2 (HIF-1 and HIF-2), which increase the expression of glucose transporters (GLUTs) and promote the expression of glycolytic enzyme isoforms (such as hexokinase 2 [HK2] and pyruvate kinase 2 [PKM2]) that are resistant to the Pasteur effect. HIF-induced glycolytic enzymes and transporters are represented in green (*right*). Other abbreviations: ALDA, aldolase A; ANT, adenine nucleotide transporter; CiC, citrate carrier; CS, citrate synthase; CytC, cytochrome c; ENO1, enolase 1; F2,6BP, fructose-2,6-bisphosphate; FH, fumarate hydratase; GAPDH, G3P dehydrogenase; GLUT, glucose transporter; IDH, isocitrate dehydrogenase; LDH5, lactate-dehydrogenase 5; MCT4, monocarboxylate transporter 4; MDH2, malate dehydrogenase 2; MPC, mitochondrial pyruvate carrier; OGDC, oxoglutarate dehydrogenase; PGI, phosphoglucose isomerase; PGK1, phosphoglycerate kinase 1; PGM, phosphoglycerate mutase; PFK2, phosphofructokinase 2; SCS, succinyl-CoA synthetase; SDH, succinate dehydrogenase; TPI, triosephosphate isomerase. Figure from Payen 2015.

In addition to the bioenergetic contribution of glucose to lactic fermentation and to OXPHOS, an increased glycolytic flux further provides glycolytic intermediates for subsidiary pathways (like one-carbon metabolism), as well as carbon precursors (*via*

the TCA cycle) and nucleic acids (*via* the PPP) to meet the biosynthetic needs of proliferating cells (Lunt 2011, Ahn 2015, Pavlova 2016, Shukla 2017, Pavlova 2022). Under the control of PKM2 that can switch on an off through alternating from an active tetrameric to an inactive dimeric state (Keller 2012, Keller 2014), glycolytic intermediates can serve to fuel branching pathways for biosynthesis purposes: the **pentose phosphate pathway (PPP)** involved in nucleic acid synthesis for RNA production and DNA replication, the generation of glycerol-3-phosphate for phospholipid biosynthesis (a major cell membrane component), and **serine biosynthesis** fueling the one-carbon folate cycle, which can redirect as much as 50% of glucose-derived carbons in cancer cells (Locasale 2011, Possemato 2011). The folate cycle creates one-carbon species used for nucleotide synthesis, methylation reactions, and/or further oxidation to produce reducing equivalents, sometimes up to 50% of all cellular NADPH (Tibbetts and Appling 2010, Locasale 2013, Fan 2014, Ye 2014). These branched pathways to glycolysis are particularly important in cancer, as evidenced by PPP enzymes being frequently overexpressed (Wang 2011, Xu 2009), and the one-carbon pathway enzyme methylenetetrahydrofolate dehydrogenase (MTHFD2) being one of the top three overexpressed metabolic enzymes in cancer (Nilsson 2014).

2.10.2 The ability to process **glutamine** provides a glucose-independent route for energy production and biosynthesis (**Figure 6**), especially if pyruvate oxidation is compromised by hypoxia or defective mitochondria (DeBerardinis 2010). Glutamine is a building block for amino acid and nucleotide synthesis. Cancer cells not only accelerate glutamine uptake for this purpose, but they also engage in glutamine metabolism as alternate source of acetylCoA to fuel the TCA cycle and/or as a biosynthetic precursor (DeBerardinis 2007). The oxidative metabolism of glutamine is rather employed by cells for harnessing the energy contained in the molecule, whereas reductive glutamine metabolism aims to generate **citrate**, the branch point between mitochondrial metabolism and *de novo* fatty acid synthesis (see 2.10.3).

Glutaminolysis starts with glutamine uptake facilitated by alanine-serine-cysteine transporter 2 (ASCT2), followed by glutamine deamination by glutaminases (GLSs) to yield **glutamate**. Glutamate can then fuel the TCA cycle through its conversion to

TCA intermediate **α-ketoglutarate**, a reaction catalyzed by glutamate dehydrogenase (GDH) or by glutamate-oxaloacetate transaminase (GOT). Glutamine-derived citrate is generated when acetylCoA is added to glutamine-derived oxaloacetate at the last step of the TCA cycle. However, glutamine also provides citrate through reverse canonical TCA reactions, with the carboxylation of α-ketoglutarate in citrate (reductive carboxylation of glutamine) (Yang 2017, Metallo 2011, Mullen 2012, Wise 2011). The reductive metabolism of glutamine was reported to be particularly important in the cases of TCA cycle defects (Mullen 2012), hypoxia (Wise 2011, Metallo 2012) and in the presence of ETC inhibitors (Fendt 2013). Of note, reductive carboxylation still requires oxidative decarboxylation occurring in parallel to create the reducing equivalents needed for synthesis (Mullen 2014). Of further note, similarly to labelled glucose imaging techniques, several studies have shown that labelled glutamine imaging is efficient for detecting cancers, based on the existence in most solid tumors of areas of elevated glutamine uptake (Lieberman 2011, Venneti 2015).

2.10.3 The ability to exploit **lipid** metabolism is a crucial metabolic feature of cancer cells, which can upregulate FAO and/or lipogenesis (**Figure 6**). Increased energy demands can thus be fueled by FAO. FAs are highly energetic molecules that provide acetylCoA and reducing equivalents. Rapidly proliferating cells need building blocks for membrane production, which are mainly constituted of FAs. They therefore rely on a high FA bioavailability to survive and proliferate (Mashima 2009, Maan 2018, Broadfield 2021). While normal cells typically use dietary lipids and display low levels of ***de novo* lipogenesis**, cancer cells preferentially make their own lipids to fulfill their needs and, therefore, exhibit a dramatic increase in lipid production (Li and Cheng 2014, Menendez and Lupu 2007). *De novo* lipogenesis converts acetylCoA to fatty acids, which is mediated by acetylCoA carboxylase (ACC) and fatty acid synthase (FASN) (**Figure 6**). In the cytosol, the acetylCoA pool for *de novo* lipogenesis can be fueled by ATP-citrate lyase (ACLY) converting citrate (exiting the TCA or produced through reductive carboxylation of glutamine) to acetylCoA (Bauer 2005). Reducing equivalents used for FA synthesis are suggested to come primarily from the PPP (Fan 2014, Lewis 2014). Overall, FA metabolism has

been closely linked to the growth of primary cancer lesions (German 2016, Svensson 2016), cellular reprogramming in acidic microenvironment (Corbet 2016), and metastasis (detailed in 2.13 Metabolism and Metastasis). The expression of the three key enzymes of FA synthesis (ACLY, ACC and FASN) is commonly upregulated in cancers, and their inhibition retards tumor growth and progression (Milgraum 1997, Hatzivassiliou 2005, Migita 2008, Chajes 2006, Flavin 2010, Icard 2019, Fhu 2020).

2.10.4 The flexibility to use a variety of carbon and nitrogen sources including **acetate**, **lactate**, **serine**, **ammonia** and **branched-chain amino acids** allows cancer cells to efficiently fuel upregulated bioenergetic and biosynthetic pathways, and to deal with nutrient depletion using substitute resources (Figure 6).

Acetate (derived exogenously from the diet, mainly from gut microbiome metabolism, or endogenously through hydrolytic reactions of protein/histone deacetylases and acetylCoA hydrolase [Knowles 1974]) can serve as an alternate carbon source for the mitochondrial acetylCoA pool through the action of acetylCoA synthetase 2 (ACSS2). Acetate-derived acetylCoA can subsequently fuel the TCA cycle for energy production (breakdown pathway), *de novo* FA synthesis (biosynthesis pathway), as well as for acetylation reactions that regulate processes like transcription and autophagy (Wellen 2009, Marino 2014, Comerford 2014, Mashimo 2014, Schug 2015).

Long considered as a mere metabolic waste, lactate, produced by glycolytic cancer and host cells, can serve as a main nutrient for oxidative cancer cells (Sonveaux 2008, Kennedy 2013, Goodwin 2015, Sharma 2022). Our team demonstrated that lactate fuels OXPHOS in cancer cells, resulting from monocarboxylate transporter 1 (MCT1)-mediated uptake and the subsequent conversion of lactate to pyruvate by LDH-1 (Sonveaux 2008). A lactate tracer is now under development to improve cancer imaging techniques (Van Hée 2017).

As aforementioned, serine has a key role as major substrate of the highly upregulated one-carbon/folate cycle (Nilsson 2014), supporting the anabolic needs

of cancer cells. Extracellular serine can be employed by cancer cells, and serine starvation was shown to impair tumor growth (Maddocks 2013).

Ammonia, originating mostly from the catabolism/deamination of amino acids and other nitrogen-containing compounds like purine and pyrimidine (Mohiuddin & Khattar 2022), can be recycled in cancer cells by glutamate dehydrogenase for amino acid synthesis to support cancer cell proliferation (Spinelli 2017).

Branched-chain amino acids (BCAAs) leucine, isoleucine and valine can be converted to *e.g.* acetylCoA to be oxidized in the TCA cycle (Ananieva 2018).

2.11 Fuel choice is influenced by cell-intrinsic and cell-extrinsic factors. Intrinsically, epigenetics and the tissue of origin affect cancer cell bioenergetics but, more importantly, oncogenic and tumor suppressor alterations are the major events triggering metabolic reprogramming (Ward 2012). Changes in cellular energetics can occur through a deregulation of master regulators, alterations of transcription factors and metabolic enzymes (such as c-Myc mutations), mitochondrial alterations, and a modification of non-coding RNA production (DeNicola 2015). Cancer metabolism is also regulated by external factors, since it must fit environmental cues and limitations, like the presence of surrounding cells and the availability of specific nutrients. Oxygen availability greatly impacts metabolism, as hypoxia induces the expression of a multitude of proteins, including glycolysis-related enzymes (Payen 2015, Lee 2020), ACSS2 for acetate metabolism (Schug 2015) and serine hydroxymethyltransferase 2 (SHMT2) for serine metabolism (Ye 2014). Hypoxia affects cancer cells that are located beyond the diffusion distance of oxygen (> 100-200µm from blood vessels), which can be on the lower end due to a high oxygen consumption rate, to the proliferation rate exceeding angiogenesis rate, and/or to abnormal, disorganized and less functional blood vessels compared to normal tissues (Thomlinson 1955, Tannock 1972, Olive 1993, Jain 2002, Vaupel 2004, Sorg 2008, Grimes 2014a/b). Neighboring cells can also compete for nutrients or, on the contrary, be rerouted by cancer cells to supply them with nutrients (*e.g.* cancer-associated fibroblasts and adipocytes) (Nieman 2011). Furthermore, a metabolic symbiosis can occur with other cancer cells present in the tissue, as unraveled by

our team in 2008. Indeed, Sonveaux *et al.* (Sonveaux 2008) identified a lactate-based metabolic symbiosis, where cancer cells in normoxic areas use lactate to fuel OXPHOS and spare glucose for lactate-producing, hypoxic cancer cells. The importance of the local microenvironment is further highlighted by cancer cells displaying different *in vivo* and *in vitro* metabolic phenotypes (Davidson 2016), and by gliomas and brain metastases of different origins exhibiting similar metabolic patterns (Mashimo 2014). Following the Seed and Soil hypothesis, a match should exist between intrinsic and extrinsic factors for successful metastasis.

2.12 The apparent dichotomy of carbon utilization can be unified through a mtROS hypothesis. It is still controversial whether increased or decreased mitochondrial activities are required for cancer cells, since there is a considerable heterogeneity in the reliance on fermentative *versus* respiratory metabolisms. Aside from metabolic plasticity and different temporal necessities for lactic fermentation and OXPHOS, a hypothesis has been raised to unify the findings of both increased and decreased OXPHOS impeding (or promoting) cancer progression: both have protumoral consequences explained by mtROS overproduction. Indeed, a moderate increase in mtROS levels, kept under control by efficient antioxidant defenses, is beneficial for cancer cells by contributing to transformation, survival and growth (Payen 2019, Sabharwal 2014) (**Figure 8**). In these circumstances, increased OXPHOS promotes the production of subcytotoxic levels of mtROS owing to increased electron leak, just as malfunctioning mitochondria pathologically generate mtROS (Sabharwal 2014, Hsu 2016, Poporato 2014) (see 2.9 mtROS). ROS can support cancer growth and survival through a variety of mechanisms, including cysteine residue oxidation leading to inactivation of tumor-suppressor PTEN (Lee 2002), activation of the MAPK/ERK pathway (Gorrini 2013), possible cytoskeleton remodeling (Jiang 2017), degradation of ECM components (Galadari 2017), and HIF-1 stabilization (Comito 2011) acting on EMT-inducing transcription factors (Jiang 2017).

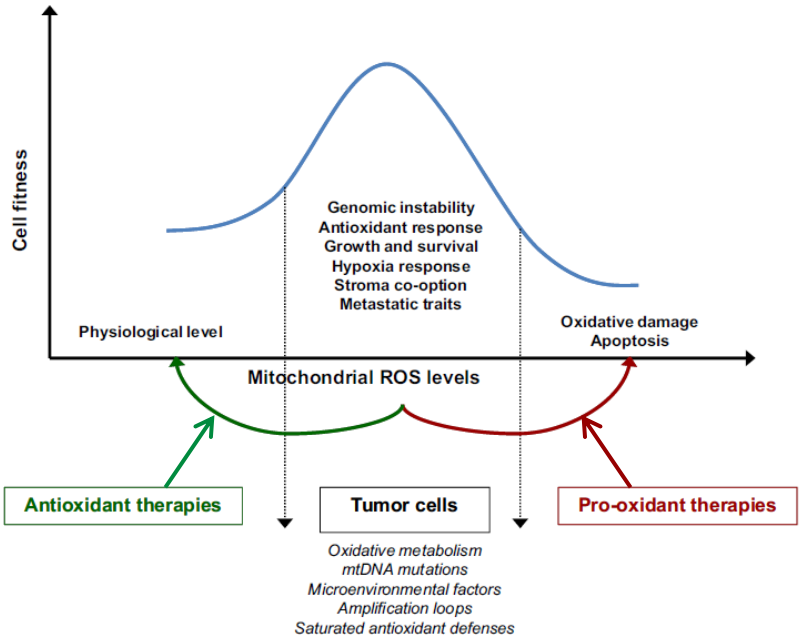


Figure 8. mtROS unification hypothesis. A moderate increase in mtROS levels kept under control by efficient antioxidant defenses is beneficial for cancer cells. Physiological levels of ROS are involved in numerous signaling pathways. Increased levels of ROS induce several pro-tumorigenic features. High levels of ROS are detrimental as they cause oxidative damage and cellular apoptosis (Figure from Payen 2019).

Tumors maintain a definite and adequate ROS level, enough to sustain tumor growth and survival but below cytotoxicity, by a right balance between ROS production and antioxidant mechanisms (Denisenko 2019, Vyas 2016, Payen 2019). Local ROS overproduction needs to be buffered to prevent lethal ROS concentrations. A slight elevation of ROS levels primes the antioxidant machinery, consequently increasing cellular resistance to oxidative stress through the aforementioned process of mitohormesis. Above a lethal threshold, ROS however inhibit cancer progression by inducing cellular damage and senescence. Anticancer approaches thus attempt to take advantage of this distinct mtROS production, by either using mitochondria-targeted antioxidants like MitoQ and MitoTEMPO (Porporato 2014, Kalvanaraman 2017, Capeloa 2022a/b/c) or, on the opposite, pro-oxidant molecules inducing more oxidative damage (Berndtsson 2007, Townsend 2008, Sassi 2014, and reviewed in

Huang 2021). Of note, compared to mitochondria-targeted antioxidants, the use of general antioxidants can be inefficient or even detrimental for cancer patients, for instance by reducing p53 activation (Klein 2011, Sayin 2014), which is argued to be due to a lack of specificity for mtROS (Sullivan and Chandel 2014). In contrast, mitochondria-targeted antioxidants have proven beneficial effects (Porporato 2014, Capeloa 2022a/b/c).

2.13 Metabolism & (organ-specific) metastasis

2.13.1 Research has shown that metabolism is associated to, or could even drive, metastasis. Metastasis requires the activation of the glycolytic program and the PPP (Smallbone 2007, Sottnik 2011, Santidrian 2013, Payen 2016). However, optimal mitochondrial metabolism and biogenesis have been reported to be equally important for metastatic dissemination (LeBleu 2014, Porporato 2016, Porporato 2018). Our team has indeed reported that a mitochondrial switch to elevated OXPHOS activity is linked to a high metastatic potential (Porporato 2014). A high (sublethal) mtROS production in highly oxidative cancer cells indeed activates the TGFβ pathway and triggers prometastatic behaviors (Porporato 2014). In a hostile microenvironment, mitochondria thus act as a metabolic sensor to activate metastasis. In addition, the seminal work of Ishikawa *et al.* (Ishikawa 2008) showed that the transfer of ROS-producing mitochondria from metastatic to nonmetastatic cancer cells also transferred the metastatic phenotype, thereby transforming recipient cells in metastatic progenitor cells. Hence, in their study, specific mtDNA mutations inducing mtROS production were sufficient to trigger metastasis. Similarly, mitochondria null cancer cells can recover mtDNA from host cells to support metastasis, with a concomitant elevation of mtROS production (Tan 2015). Furthermore, targeting mtROS with mitochondria-targeting agents MitoTEMPO and MitoQ inhibited cancer metastasis as a whole in preclinical models of human breast cancers in mice (Porporato 2014, Capeloa 2022a/b/c).

Taken together, these studies demonstrate that the ambivalent effects of mitochondrial respiration regarding metastasis can also be rationalized under the mtROS unification hypothesis (see 2.12) (**Figure 8**), with mtROS as a common

mediator of metastasis for highly glycolytic and highly oxidative cancer cells. Moderate mtROS levels can activate signaling transduction cascades corelated to the metastatic process, including at the level of the proto-oncogene SRC and focal adhesion kinase Pyk2 (Porporato 2014, Park 2016). Hence, two opposite metabolic phenotypes (elevated or dysfunctional mitochondrial activities) equally promote an invasive phenotype (Ishikawa 2008, Porporato 2014). On the one hand, overloading the ETC by enhanced rate of TCA cycling results in electron leak and elevated sublethal mtROS production, promoting tumor metastasis. On the other hand, several types of partial mitochondrial dysfunction, mitophagy defects and/or partial ETC inhibition can also promote metastasis by favoring mild mtROS overproduction due to ETC bottlenecking. In this context, the work of our team (Porporato 2014) demonstrated that targeting mtROS production, by experimentally inducing a complete loss of mitochondrial functions or by the use of mitochondria-targeted antioxidants, abolished metastatic progression. *A contrario*, severe oxidative stress (excessive ROS production and/or a saturated/dysfunctional antioxidant machinery) oversteps the lethal threshold and inhibits metastatic dissemination by impeding cellular fitness and survival (Piskounova 2015; see 2.12) (**Figure 8**). Besides mtROS production, mtDNA mutations are also associated with invasiveness through the accumulation of mitochondrial oncometabolites that promote EMT and metastasis (Frezza 2017, Sciacovelli 2016).

Metastatic cells also need lipid metabolism, with mitochondrial β-oxidation supporting the high energy needs of metastatic progenitor cells (Park 2016). Park *et al.* (Park 2016) further showed that FAO activates SRC kinase in the TGFβ pathway. In patients, FA uptake and metabolism have been strongly correlated to metastatic progression and poor prognosis in multiple cancer types (Nath and Chan 2016, Pascual 2017, Ladanyi 2018, Pan 2019). An intricate relationship between FA oxidation and ROS production has been suggested in these studies. Indeed, besides providing energy, FAO promotes ROS and NADH production, pointing at mtROS as potential mediators of the prometastatic effects of FAO.

On the biosynthetic part of lipid metabolism, silencing experiments of *ACLY* (Wen 2019) and *FASN* (De Piano 2020) demonstrated the requirement of *de novo* lipogenesis for metastasis. Cancer cells can store lipids in vesicles, called 'lipid droplets', to constitute energy reserves to be summoned during the metastatic course (Corbet 2016). This discovery further underlines the importance of *de novo* lipogenesis for cancer cells, as well as it explains this requirement by linking it to the high FA demand for oxidation in metastatic cancer cells. Anti-metastatic strategies targeting lipid metabolism are emerging, with the objective to inhibit lipid utilization or synthesis (Pascual 2018).

2.13.2 Metabolism and Organotropism. During my PhD thesis, we aimed to go a step further and investigated the emerging concept of a metabolic control of metastatic organotropism. We initially hypothesized that the metabolic preferences of metastatic progenitor cells would drive the organ specificity of metastasis. Metabolism is essential for cell survival and stress resistance, but each secondary organ has a distinct metabolic composition and presents distinct metabolic challenges to overcome, which may impose unique metabolic states for CTC colonization. Metabolic differences amongst metastatic sites include *e.g.* nutrient availability, oxygen concentration and oxidative stress. Metastatic cell fitness in given organs could therefore be dictated by compatible metabolic profiles. This concept proposes a deeper connection between cancer metabolism and metastasis, and entails the idea that subsets of metastatic progenitor cells have a specific metabolic signature, or some kind of metabolic sensor, driving them to colonize a given organ. For instance, Dupuy *et al.* (Dupuy 2015) reported that bone and lung metastases of breast cancer cells displayed OXPHOS reliance, whereas liver metastases showed a fermentative metabolism. Other metabolic pathways for organ colonization have been reported (Schild 2018, Pascual 2018, Wang 2021), with specific metabolic phenotypes promoting brain tropism being covered later in Chapter 6. Understanding the ability to establish tissue tropism profiles has an

important therapeutic potential, especially since CTCs are directly accessible to pharmacological agents.

The existence of a metabolic control of metastatic organotropism would signify that the metabolic state of metastatic progenitor cells needs to be compatible with the metabolic microenvironment of distant organs to ensure cancer survival and growth. In line with this notion, gaining a deeper understanding of cancer metabolism at secondary sites is crucial to unveil new therapeutic strategies aiming at disrupting the metabolic concordance between metastatic progenitor cells and secondary sites, thus preventing the metastatic colonization of specific organs. In this work, we focused our attention on the brain tropism of breast cancer cells. Chapters 4 and 5 first introduce breast cancers and the brain environment, respectively. We then address the precise topic of metabolic phenotypes in brain-trophic cancer cells in the last chapter. Chapter 3 will address one last cancer concept proposed to be involved in metastasis, the new and evolving cancer stem cell model.

Introduction

CHAPTER 3 - CANCER STEMNESS

Stemness, or possessing stem cell characteristics, is a relatively recent notion in the cancer field. Cancer stem cells are associated with numerous traits of cancer pathophysiology, including tumorigenesis, chemoresistance and - more importantly for the scope of this study - metastasis.

3.1 Stem cells are undifferentiated cells at the origin of all cell lineages; they possess the ability to generate differentiated daughter cells and to maintain the stem cell pool through self-renewal. Possessing stemness characteristics implies possessing the underlying mechanisms conferring stem cell properties, notably through the expression of stemness transcription factors, such as cellular myelocytomatosis oncogene **(c-Myc)**, SRY-Box transcription factor 2 **(SOX2)**, Krüppel-like factor 4 **(KLF4)**, octamer-binding transcription factor 4 **(OCT4)**, homeobox protein Nanog **(Nanog)**, and sal-like transcription factor 4 **(SALL4)** (Zhao 2017). The importance of these factors is demonstrated by their use to generate induced pluripotent stem cells (iPSCs). The expression of the first 4 factors (known as the Yamanaka factors) can convert differentiated somatic cells to an embryonic undifferentiated state, with similar gene expression profiles and epigenetic properties as embryonic stem cells (Takahashi 2006).

3.2 The concept of cancer stem cells is a new and evolving model of tumor evolution. The cancer stem cell (CSC) concept proposes that a subpopulation of cancer cells possesses a stemness phenotype with self-renewal abilities and a multilineage differentiation potential, and that these cells are imputable for tumor growth, metastasis, resistance to therapy and recurrence (Zhao 2017, Peitzsch 2017, Shen 2021) (Figure 9). Just like stem cells generating daughter cells to populate an organ, they generate the bulk of cancer cells and are able to generate secondary tumors. In addition, their ability to shift to a quiescent phenotype renders them generally resistant to conventional anticancer therapies targeting rapidly dividing cells or metabolically active cells (Phillips 2006, Diehn 2009, Touil 2014, Kumar 2020). After dormancy, CSC reactivation can cause cancer recurrence (Freedland 2007, Li 2015, Wang 2021, Xi 2022). CSCs can also actively counteract

anticancer treatments by expelling drugs through ATP-binding cassette (ABC) transporters and/or by maintaining low levels of ROS (Hadnagy 2006, Shen 2021). Efficient targeting of CSCs is considered to be a top priority for anticancer therapy by many research groups (Shen 2021).

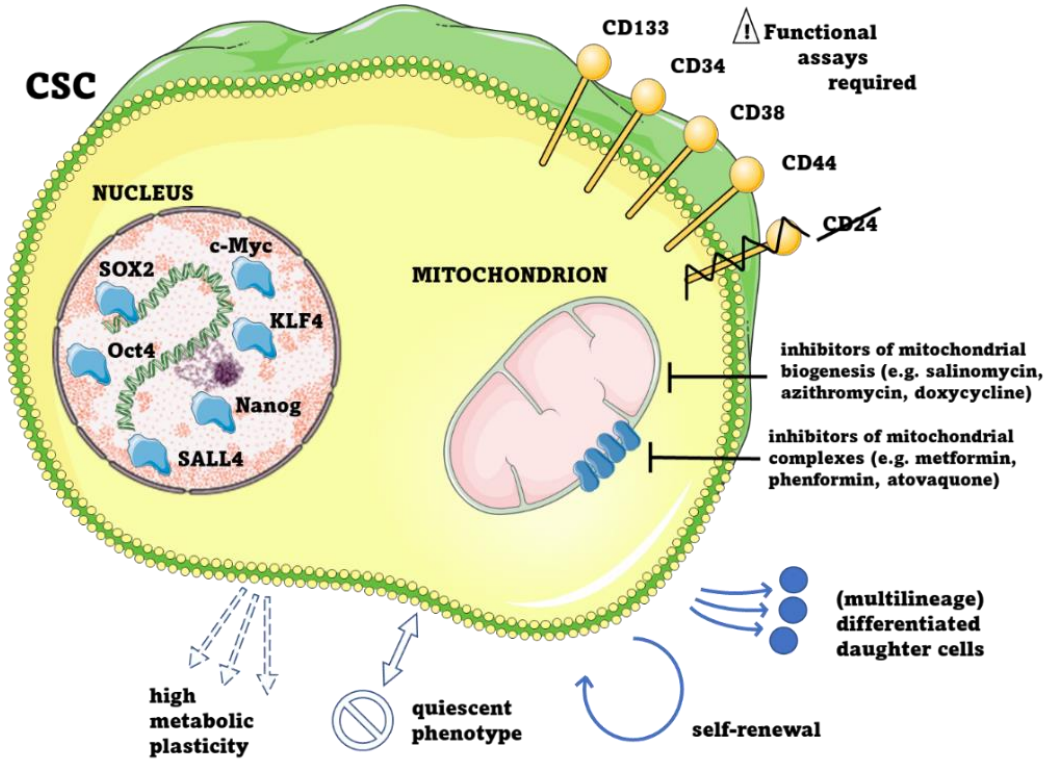


Figure 9. The cancer stem cells concept and mitochondria-targeting drugs negatively affecting CSC fitness. CSC features, transcription factors and major biomarkers are indicated.

Recently, a discovery has reinforced the idea that cancer is a disease arising through the formation of CSCs, described as ‘stemness gone wrong’ (Tomasetti and Vogelstein, 2015). The authors stated that cancers are mainly driven by accumulated somatic mutations in tissue stem cells. While some tissue types develop cancer a million times more often than others (called the ‘cancer lifetime risk’), they showed

that differences in tissue-specific cancer risks cannot be fully explained by genetic and environmental factors, but by a third one: the lifetime number of divisions of tissue-specific stem cells. The strong correlation of 0.8 indicates that about 65% of cancers would be due to random mutations arising in stem cells, whereas only about one third would be attributed to inherited genetic predispositions or well-known factors (smoking, alcohol, UV exposure, etc.), making of stem cell divisions within a tissue the major contributor to human cancers (Tomasetti and Vogelstein, 2015). The conclusion of this correlative study is, however, still an open debate.

3.3 CSC research is complexified by the lack of consensually accepted surface biomarkers for their identification and isolation, and by their possible differentiation in culture. CSC isolation is generally based on the expression of surface markers CD34, CD38, CD133, CD44 and CD24 (Zhao 2017, Shen 2021). Many studies rely on the representative CD133 biomarker, while others use the documented high CD44/CD24 ratio indicating both the tumorigenicity and cancer cell proliferation status (Dou 2010, Li 2017, Shen 2021). In breast cancer, the most common use of CSC biomarkers relies on the $CD44^{+}/CD24^{-}$ and aldehyde dehydrogenase 1 $(ALDH1)^{+}$ phenotype (Li 2017, Zhang 2020) first described in 2003 (Al-Hajj 2003) and in 2007 (Ginestier 2007), respectively. Additional biomarkers used for characterizing breast CSCs include CD133, CD49f, CD61, PROCR, CD90, CD70, ABCG2, LGR5, SSEA-3, and ESA (Zhang 2020). **Figure 10** shows the important findings related to breast CSC identification. However, the expression of CSC surface markers may fluctuate, and functional assays are thus necessary to assess stemness properties. Tumorigenicity can be assessed through sphere-formation assays in non-adherent and serum-free culture conditions to maintain the stemness status (Bahmad 2018). Transplantation assays in animal models can assess self-renewal capacities (Rycaj 2015).

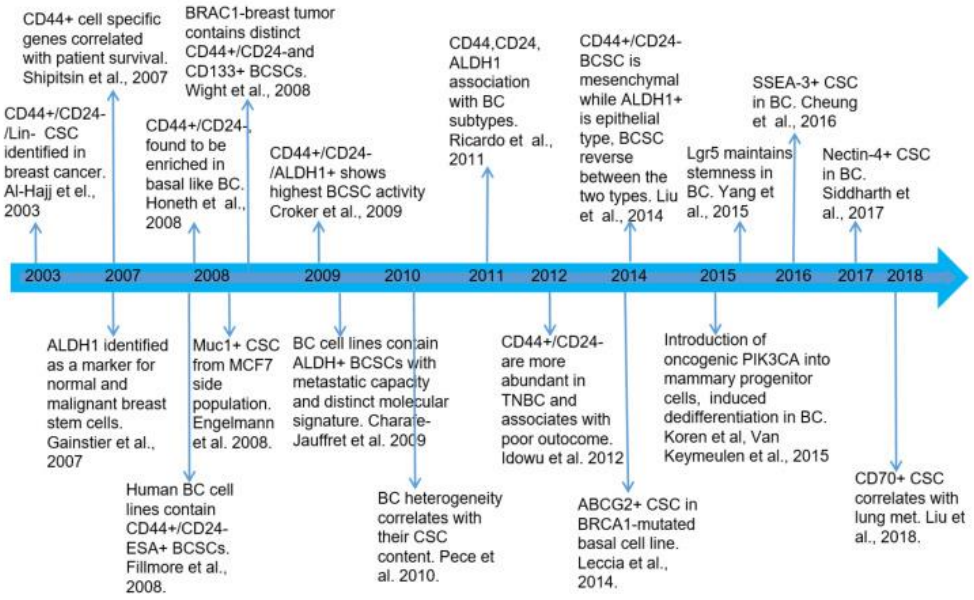


Figure 10. Timeline of major findings regarding breast cancer stem cells (CSCs) since they were initially identified in 2003. Figure from Zhang 2020. BC – breast cancer

3.4 CSC metabolism is characterized by a quiescent phenotype and a high metabolic plasticity inherent to their stemness status. Some studies have shown a predominant glycolytic metabolism in osteosarcoma, glioblastoma, lung cancer, colon cancer and breast cancer CSCs, in line with the glycolytic switch in the reprogramming process of iPSCs; whereas others have reported a predominant OXPHOS metabolism in ovarian, lung and pancreatic cancer CSCs (reviewed in Porporato 2018 and Shen 2021). Furthermore, distinct CSCs from the same cancer were observed to have different preferences in their use of glucose, which further highlights their metabolic plasticity and heterogeneity (Gammon 2013).

3.5 Despite metabolic heterogeneity and plasticity, mitochondrial functions and biogenesis appear as key players of CSC fitness, and several mitochondria-targeting drugs negatively impact CSCs. Inhibitors of mitochondrial complexes have been used experimentally to selectively target pancreatic, breast and ovarian CSCs through inducing mitochondrial dysfunctions (Hirsh 2009, Alvero 2011, Jung 2011, Rattan 2012, Yeh 2013, Janzer 2014, Fiorillo

2016, Ozsvari 2017, Fiorillo 2020, reviewed in Shen 2021 and Suárez-Rivero 2021) (**Figure 9**). Mitochondria-inhibiting molecules being tested in clinical trials (Hadad 2011, Bonanni 2012, Niraula 2012, Janku 2021) are yet mainly under the scope of targeting cancer cell metabolism, rarely as anti-CSC strategies specifically (DeVito 2014). Lisanti and his team (Lamb 2014, De Luca 2015) further aimed to identify global phenotypic characteristic of CSCs, and they pinpointed mitochondrial biogenesis at the basis of CSC maintenance, driving both their anchorage-independent survival and propagation. The same group later reported that FDA-approved antibiotics impairing mitochondrial biogenesis as an "off-target" effect (caused by the evolutionary relationship between bacteria and mitochondria) could be repurposed to target CSCs in several tumor models (Lamb 2015, Fiorillo 2019). In addition, clinical trials for the treatment of cancer-associated infections showed that these antibiotics, albeit not intending to aim at cancer cells, compromised mitochondrial biogenesis and displayed antitumor potential, with up to 1.7-fold increase in 1-year patient survival (Han 2015, Chu 2014). Recent advances provided *in vivo* functional evidence of the selective inhibitory effects of mitochondrial inhibitors on cancer metastasis (Ózsvári 2020). The authors also reported that both a CSC-based mitochondrial 4-gene signature and a mitochondrial ribosomal gene signature predicted distant metastasis and tumor recurrence in breast cancer patients, further supporting a role of mitochondria and, more specifically, mitochondrial biogenesis, in the maintenance of the CSC phenotype (Ózsvári 2020).

CSCs may well be at the basis of cancer development and metastasis. Stemness transcription factors profoundly rewire cellular metabolism. Even if metabolic changes are still odd-described and may vary in function of the cancer type, mitochondrial biogenesis and function are reported to play a crucial role in CSC maintenance.

CHAPTER 4 - BREAST CANCER

Our work focuses on breast cancer as a model, due to its high prevalence and early diagnosis. Hence, patients with cancers detected at the premetastatic stage could potentially benefit from metastatic prevention therapy. The high frequency of breast cancer brain metastasis and the availability of two breast cancer brain-specific cell lines further directed our study to this specific cancer type.

4.1 Breast cancer is the most frequent malignant tumor diagnosed worldwide. Breast cancer has been the leading malignancy amongst women (24.5%) and the leading cause of cancer-associated mortality in women (15.5%) worldwide for many years (Siegel 2016, Siegel 2017, Ferlay 2018, Bray 2018). It now has become the most prevalent cancer all genders combined, as uncovered by a study of 36 cancer types over 185 countries (GLOBOCAN 2020, Sung 2020). In this study, breast cancer (11.7%; 2.3 million of new cases per year) surpassed lung cancer in incidence rate (11.4%) and represented the leading cause of cancer deaths in 110 countries. The highest rates were observed in Australia/New Zealand, Northern America, and Europe. Importantly, Belgium – our country – is displaying the highest global rate of breast cancer worldwide (GLOBOCAN 2020).

4.2 CLASSIFICATION

4.2.1 Breast cancer is diagnosed using five stages (0-I-II-III-IV). Staging combines information about the tumor size at the primary site (the largest diameter measured, T), the nodal involvement (extent of cancer at the regional lymph nodes, N) and the spread to distant metastatic sites (M) (**Table 1**). This system, called the TNM system, was jointly published by the American Joint Committee on Cancer (AJCC) and the Union for International Cancer Control (UICC) (Brierley 2017, Giuliano 2017, Harbeck 2019). It summarizes the extent of regional and distant disease, with stage IV corresponding to metastatic breast cancer.

Table 1. The 5-stage classification of breast cancer using the TNM system.

STAGES		T (1° tumor)	N (regional LNs)	M (metastasis)
0	*in situ*	Tis	Absence (N0)	Absence (M0)
I	Localized limited	T1 < 2cm T2 < 5cm T3 > 5cm	Absence (N0)	Absence (M0)
II	Localized advanced	**T4 invasion of chest wall and/or skin**	Absence (N0)	Absence (M0)
III	Regional limited / extensive		**Presence*** N1 < 3 LNs N2 > 3 LNs N3 > 10 LNs or level III involvement	Absence (M0)
IV	Metastatic/ distant			**Presence** (M1)

T: extent of primary (1°) tumor, the greatest diameter is measured. N: absence/presence and extent of regional lymph node involvement/metastasis. M: presence or absence of distant metastasis, including distant lymph nodes. Bold underlines the defining characteristics for higher stage classification. LNs – Lymph nodes. *Broadly summarized here, for more details see Giuliano 2017.

4.2.2 Breast cancers can be categorized according to their degrees of invasion and histopathologic appearances (histologic subtypes). Breast cancers can be confined to the epithelial compartment *(in situ*) or invading the stroma (invasive); *in situ* carcinomas are not life-threatening, but are precursors of invasive carcinomas. Breast cancers were originally classified as ductal or lobular, considered to originate from cells lining the milk ducts or in the lobules producing the milk. However, cytoarchitectural features (histologic subtype) or specific biomarkers like E-cadherin (Singhai 2011, Pai 2013) now dictate their placement in ductal/lobular category (Rosai 2011, Sinn 2013, Makki 2015). Lobular carcinoma *in situ* (LCIS) is a benign condition and is not considered to be a true breast cancer, but it can lead to both ductal and lobular invasive carcinomas. Ductal carcinoma *in situ* (DCIS) is a potentially malignant intraductal proliferation of epithelial cells diagnosed in about

16% of all breast cancers. Invasive carcinoma is a heterogenous group comprising many histological subtypes (tubular, cribiform, mucinous, etc.) with distinctive features, and a main one called invasive carcinoma of no special type (NST) for invasive carcinomas lacking characteristic features (about 75%). Invasive lobular carcinoma (ILC), comprising variants such as solid, alveolar and tubulolobular, accounts for around 10% of invasive carcinomas and are characterized by E-cadherin loss (Singhai 2011, Pai 2013).

4.2.3 Breast cancer is a heterogenous disease that can be subcategorized according to molecular features. Biological markers are used to classify breast cancers in molecular subtypes, but different markers and classifications exist (**Figure 11**). Breast cancer was first classified using the expression levels of 50 cancer-related genes (prediction analysis of a microarray of 50-gene set, PAM50) in 5 intrinsic subtypes: Luminal A, Luminal B, HER2-enriched, Basal-like and Normal-like breast cancer (Perou 2000). To note, studies have considered this last subtype as an artefact due to low cancer cellularity and, thus, a high presence of normal breast cells (Parker 2009, Peddi 2012, Harbeck 2019).

Clinical practice does not routinely use microarray-based gene expression profiling, but rather a surrogate classification based on histological and molecular characteristics. Breast cancer can feature an activation of hormone receptors (estrogen receptor [ER] and progesterone receptor [PR]) and/or of the human epidermal growth factor receptor 2 (HER2/ERBB2). Theses molecular features allow to categorize breast cancers in surrogate intrinsic subtypes and are viewed as biomarkers for prognosis and treatment choice (**Figure 11**). On the molecular level, the disease can therefore be divided in 5 main subtypes: **Luminal A-like** (50-70%), **Luminal B-like(HER2-)** (10-20%), **Luminal B-like/HER2+** (11-13%), **HER2-enriched non-luminal** (5-6%), and **Triple Negative** (surrogate for basal-like, 10-15%) tumors (Harbeck 2019, Acheampong 2020, Morra 2021). Luminal tumors are characterized by the expression of ER and/or PR, whereas HER2+ and HER2-enriched tumors are distinguished by the expression of HER2, and the TNBC subtype by the absence of all three receptors. It is important to note that different groups (3 to 5) can also arise in the literature from this classification: Luminal A-like

and B-like tumors can be grouped in “luminal tumors” (hormone receptor-positive tumors) and/or luminal&HER2+ and HER2-enriched (non-luminal) can be grouped in “HER2-positive tumors”. Cell proliferation marker Ki67 is an additional biomarker of breast cancer prognosis, used mainly to distinguish between luminal A-like and B-like (HER2-) tumors (Cheang 2009). Some studies simplify the luminal B tumor definition as ER+/HER2-/Ki67high or ER+/PR+/HER2+ (Sperduto 2013, Acheampong 2020). It is however important to note that luminal B tumors can be HER2+ (hence the subtype luminal&HER2+) or not, or have a low expression of hormone receptors (Prat and Perou 2011). Trying to bring a consensus between the different subtype definitions, the 2013 St. Gallen International Breast Cancer Conference issued a new definition based on clear percentages of immunohistochemical staining results: luminal A (ER/PR+, HER2−, Ki67 < 20%), luminal B (ER+, HER2−, PR < 20% and/or Ki67 ≥ 20%); HER2+ luminal B (ER+, HER2 overexpression, any PR and Ki67), HER2 overexpression (ER−, PR−, HER2 overexpression), basal-like TNBC (ER−, PR−, HER2−), and other special histological subtypes (Goldhirsch 2013).

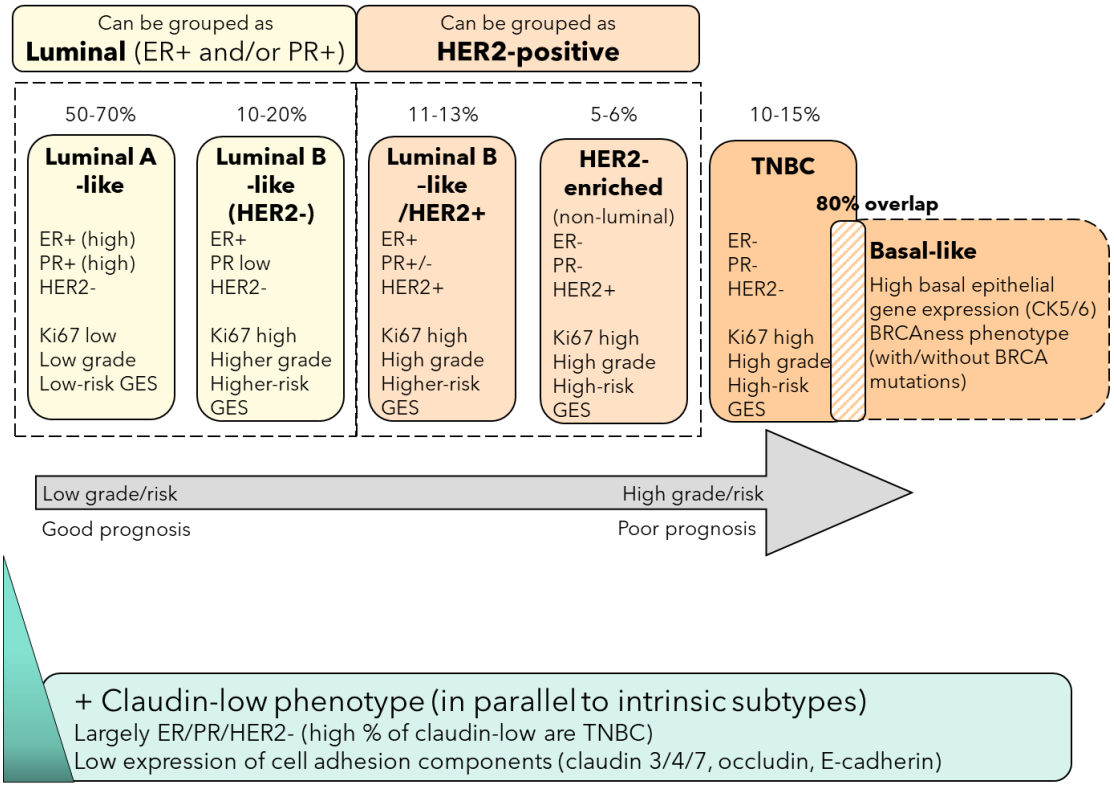


Figure 11. Molecular classification of breast cancers. The five (surrogate) intrinsic subtypes and the claudin-low phenotype, as well as their molecular features and incidence (in percentages), are represented. The different ways of grouping the categories are indicated by dashed rectangles. The great majority (about 80%) of TNBC present basal-like features and vice-versa. Ki67 is a cell proliferation marker. ER – estrogen receptor, PR – progesterone receptor, HER2 – Human epidermal growth factor receptor 2, GES – gene expression signature, CK – cytokeratin, BRCA – tumor suppressor gene breast cancer, TNBC – triple negative breast cancer.

4.2.4 Prognosis is closely associated with breast cancer subtype, rationalizing the need for classification. Luminal A-like tumors are at the low-risk end of the prognosis spectrum (**Figure 11**), with features such as low grade, low proliferation (low Ki67 index), a low-risk gene expression signature (GES) and a high expression of ER and PR (Harbeck 2019). The luminal B-like group can be distinguished from the luminal A-like subtype by its higher grade/proliferation/GES and potential lower expression of ER and PR. These luminal types (hormone receptor-positive) can be

treated with endocrine (hormonal) therapies, due to their dependency on pathways downstream of ER and PR. However, Luminal B-like tumors display a poorer prognosis due to higher-risk features, a lower sensitivity to endocrine therapy and possible chemoresistance. HER2-enriched tumors display high grade and high proliferation features, but an intermediate prognosis: these tumors are aggressive but can respond to anti-HER2 therapy (Harbeck 2019). By contrast, TNBC does not show expression of ER, PR and HER2 and display aggressive features (high grade, high proliferation) and a poor prognosis due, in part, to the inefficacy of endocrine and targeted therapies (Harbeck 2019).

4.2.5 TNBC is used as a surrogate for the PAM50 basal-like subtype, even if these groups do not exactly superimpose each other. Not all basal-like breast cancers are triple-negative, and not all TNBC tumors display a basal-like phenotype (Bertucci 2008, Parker 2009, de Ronde 2010, Bastein 2012, Marra 2020). Nevertheless, both subgroups share many clinical and molecular features, and overlap for approximately 80% (Lin 2008, Prat and Perou 2011, Chen 2018, Garrido-Castro 2019). The use of the common pathological markers is thus considered to be a reasonable surrogate for the basal-like classification, and they are often used interchangeably in the literature and in the Clinics. Aside low expression of ER, PR and HER2, the basal-like phenotype includes a high expression of basal epithelial genes (like cytokeratins [CKs] 5, 6 and 17) (Perou 2000, Nielsen 2004, Rosai 2011), and inactivating mutations of the tumor suppressor genes breast cancer 1 (*BRCA1*) and 2 (*BRCA2*) (Turner 2006, Jung 2016, Lim 2009), or a BRCAness phenotype characterized by homologous recombination deficiency without *BRCA* mutations (reviewed in Turner 2004). Some studies use additional surrogate markers (epidermal growth factor receptor [EGFR] and CK5/6) to distinguish TNBC-non basal (Voduc 2010).

4.2.6 HER2-enriched intrinsic subtype includes HER2- tumors. ER, PR and the HER2 status, although useful in the Clinics, have their limitations as surrogate markers for the HER2-enriched subtype, since using the ER-/HER2+ definition does not fully recapitulate the intrinsic classification (Prat & Perou 2011). HER2-enriched tumors that are clinically HER2- could be explained by mutational events of the

HER2 pathway phenocopying HER2 amplification, hence the name of 'HER2-enriched' and not 'HER2-positive'. The question remains about the benefit of anti-HER2 therapies for these tumor subtypes.

4.2.7 Breast tumors can carry a claudin-low status as an added phenotype to the intrinsic subtype while these tumors were previously categorized in a sixth intrinsic subtype or later as a subcategory of the TNBC group (Fougner 2020). This claudin-low phenotype (**Figure 11**) first emerged in 2007 after the onset of intrinsic subtyping. Studies reported 'claudin-low' tumors, for which the PAM50-based assignation was overwritten for a new 'claudin-low' category (Herschkowitz 2007, Prat 2010, Sabatier 2014, Dias 2017). Tumors with a claudin-low status are aggressive and present a low expression of critical cell adhesion components (including claudins 3, 4 and 7, occludin and E-cadherin), hence their name. They show enrichment in mesenchymal and stemness features (Taube 2010, Lim 2009). They are also characterized by genomic stability, a low mutational burden, and a high immune and stromal cell infiltration (Prat 2010, Dias 2017). This last characteristic has led to the misidentification of tumors in the claudin-low group due to their pronounced stromal infiltration (Fougner 2020). Claudin-low tumors are typically negative for ER, PR and HER2, which is why they were later considered as a subgroup of the TNBC group (Dias 2017, Prat 2010). However, Fougner *et al.* (Fougner 2020) recently uncovered a more complex phenotype, where the claudin-low status is a parallel feature to the intrinsic subtype. When claudin-low tumors were stratified by intrinsic subtypes, their genomic, transcriptomic and clinical features reflected their intrinsic subtype. This included gene expression patterns, proliferation levels and survival. Indeed, the poor prognosis initially associated to the claudin-low group was dissolved once claudin-low tumors were subdivided into their intrinsic subtypes. The survival patterns were similar for patients with claudin-low and non-claudin-low tumors for each intrinsic subtype, indicating that the claudin-low status does not affect patient survival. Nevertheless, it could still be clinically relevant for EMT-targeted therapies, chemotherapy resistance and/or immunotherapy efficacy due to their high immune infiltration, low mutational burden and high programmed

death-ligand 1 (PD-L1) expression (Prat 2010, Sabatier 2014, Nieto 2016, Morel 2017, Fougner 2019).

As a distinct group of claudin-low tumors, they were originally thought to originate from mammary epithelial stem cells due to their stem cell properties (Prat 2010, Prat & Perou, 2011). However, Pommier *et al.* (Pommier 2020) reported that claudin-low tumors could be divided in 3 main subgroups according to their tumorigenesis: two groups seem to originate from luminal and basal-like tumors *via* an EMT activation process, and one group is associated to mammary stem cells with low genomic alterations and *tumor protein 53 (TP53)* mutations. This is consistent with the perspective of Fougner *et al.* (Fougner 2020) that the claudin-low status is a phenotype that breast cancers can carry in addition to their intrinsic subtype.

4.3 Breast cancer treatment is based on multimodal therapies. The molecular subtype of breast cancers is currently the most important criterium for prognosis and, consequently, for therapy choices (**Table 2**). Following the emergence of molecular markers, the clinical management of the disease indeed changed from a tumor burden approach to a biology-centered strategy. It is important to note that advanced breast cancer is not considered to be curable but is treatable. Therapies thus aim to prolong patient's survival and quality of life (palliative care).

*For premenopausal women, an aromatase inhibitor has to be combined with ovarian function suppression by ovariectomy or a GnRH analogue (in the cases of high-risk early BC or advanced BC). Bone-modifying agents bisphosphonates can be added to improve the outcome in (true or induced) postmenopausal women with early BC. **High risk of recurrence is defined as >10% over 10 years (mammaprint genetic test), or as tumor size > 2 cm and/or positive lymph nodes, or as $LN^+ > 4$ or $LN^+ =$ 1-3 combined with tumor size > 5 cm, grade 3 or Ki67 > 20% (for CDK4/6 use). ***Use of anthracycline or taxane (if no prior use or if rechallenge possible), or the following compounds. ET – endocrine therapy, ABC – advanced breast cancer, ER – estrogen receptor, HER2 – human epidermal growth factor receptor 2, (TN)BC – (triple negative) breast cancer, Neo – Neoadjuvant, Adj – Adjuvant, GnRH – gonadotropin-releasing hormone, T-DM1 – trastuzumab emtansine, pCR – pathological complete response, CDK – cyclin-dependent kinase, PARP – poly ADP-ribose polymerase, BRCA – tumor suppressor gene breast cancer, T-DXd – trastuzumab deruxtecan, PD-L1 – programmed death-ligand 1, AR – androgen receptor, LAR – luminal androgen subtype. Main references: Harbeck 2019, Derouane 2021, Gennari 2021, ESMO Metastatic Breast Cancer Living Guidelines, v1.0.0 May 2022 [b]. There is no worldwide consensus; this table is based on European Guidelines.

[b] Available at https://www.esmo.org/living-guidelines/esmo-metastatic-breast-cancer-living-guideline (accessed last on 13/02/2023)

Table 2. Breast cancer treatment according to molecular subtype and disease progression

<table>
<tr><th>Subtype</th><th>Surgery / radiation</th><th>Endocrine Therapy (ET)</th><th>Anti-HER2 therapy</th><th>Chemotherapy Early BC</th><th>Chemotherapy Advanced BC (ABC)</th></tr>
<tr><td>Luminal A-like</td><td rowspan="6">Cornerstone for Early BC (upfront for low risk cancers or if neoadjuvant therapy not possible, otherwise neoadjuvant therapies preferred prior to surgery and radiation, followed by adjuvant therapies)</td><td rowspan="3">Neo/Adj/ABC
- ER inhibitor (Tamoxifen) or ER degrader (fulvestrant)
- Estrogen synthesis inhibitor (aromatase) inhibitor) + ovarian function suppression in premenopausal women*</td><td></td><td rowspan="2">+ Adj CDK4/6 inhibitor (abemaciclib) for non-pCR patients / high risk of recurrence**

If high risk of recurrence**: switch to adjuvant anthracycline and a taxane, or docetaxel and cyclophosphamide (for low tumor burden or cardiac complications risk)</td><td rowspan="2">First lines with endocrine therapy + CDK4/6 inhibitors (abemaciclib) or mTOR inhibitors (everolimus) to target endocrine resistance

If progression despite several lines of endocrine therapy or visceral crisis : sequential monotherapy*** of anthracycline, taxane, capecitabine, vinorelbine, eribulin, gemcitabine, carboplatine

- if BRCA mutations: PARP inhibitors after endocrine therapy (in trials for BRCAness)
- if PIK3CA mutations: PIK3 inhibitor (alpelisib) under trials</td></tr>
<tr><td>Luminal B-like</td><td></td></tr>
<tr><td>Luminal/ HER2</td><td>Neo/Adj/ABC
Dual blockade by antibodies targeting HER2 (trastuzumab & pertuzumab)

[Adj treatment de-escalation of early BC with low tumor burden, or for later lines of advanced BC: trastuzumab only]</td><td>Anthracycline and a taxane, or docetaxel and carboplatin

[Adj paclitaxel if low tumor burden]</td><td rowspan="3">Sequential monotherapy

First line with docetaxel (with anti-HER2 + ET if luminal)

Second/later line(s) with T-DM1, T-DXd, tucatinib, taxane, vinorelbine, capecitabine, eribulin, or platinum agent</td></tr>
<tr><td>HER2-enriched</td><td rowspan="2"></td><td>[Adj treatment escalation of non-pCR patients: T-DM1]</td></tr>
<tr><td>TNBC</td><td></td><td>Anthracycline and a taxane, or docetaxel and cyclophosphamide + platinum agent (carboplatine) + immunotherapy (pembrolizumab) if PD-L1+
[Adjuvant capecitabine for non-pCR patients]</td><td>Platinum agent preferred (carboplatine)
Sequential monotherapy of anthracycline, taxane, capecitabine, vinorelbine, or eribulin***
- if BRCA mutations: PARP inhibitors in first line (in trials for BRCAness)
- immunotherapy (pembrolizumab) added to chemotherapy if PD-L1+
- AR inhibitor for LAR subtype in trials</td></tr>
</table>

Breast cancer treatment consists in locoregional and systemic approaches. Locoregional strategies include surgical removal and postoperative radiation therapy targeting the primary tumor and/or proximal lymph nodes. Surgery remains the cornerstone of early BC treatment. Radiation therapy is prescribed with an individualized approach depending on multiple factors, including the severity of the cancer. Systemic therapies can be administered preoperatively (neoadjuvant) and/or postoperatively (adjuvant), and mainly include endocrine therapy, anti-HER2 therapy, chemotherapy, cyclin-dependent kinase (CDK)4/6 inhibitors, immunotherapy and poly ADP-ribose polymerase (PARP) inhibitors (Gennari 2021). In early HER2+ and TNBC subtypes, the neoadjuvant setting is the standard of care, but adjuvant therapy can also be administered. Endocrine therapies targeting ER+ and/or PR+ luminal tumors encompass the standard use of tamoxifen (ER inhibitor) or fulvestrant (ER degrader), and in the case of high risk early BC or advanced BC, an aromatase inhibitor (estrogen synthesis inhibitor), used alone in post-menopausal women or combined with ovarian function suppression (ovariectomy or gonadotropin-releasing hormone [GnRH] analogue) in premenopausal women (Cardoso 2018, Rugo 2016, Harbeck 2019). Bone-modifying agents bisphosphonates can be added in adjuvant therapy to improve the outcomes of (true or induced) postmenopausal women with early BC. Chemotherapy can be added to the endocrine therapy in luminal tumors, whereas it is the standard of care for HER2+ and TNBC patients. Chemotherapeutic drugs include agents that damage DNA (anthracyclines, cyclophosphamide, platinum agents) or the microtubules required for mitosis (taxanes). The chemotherapy regimen in early breast cancer is typically a sequence of an anthracycline and a taxane, but other options may be used, like docetaxel and cyclophosphamide (as effective in TNBC), or a platinum agent such as carboplatin may be added (Mackey 2016, Harbeck 2019). In advanced BC, the preferred first line treatment consists of anthracyclines, taxanes, capecitabine, vinorelbine or eribulin (if the first two have already been used to treat early BC, then there is the option of an anthracycline and/or taxane rechallenge or of the use of the other three compounds). Only systemic chemotherapy, but no targeted therapy, is available for TNBC, and a platinum agent is preferred to treat advanced TNBC. In HER2+ breast cancers, a dual HER2 blockade using the HER2-targeting antibodies

trastuzumab and pertuzumab, in parallel to chemotherapy, is standard. Treatment de-escalation at the adjuvant setting (early BC with low tumor burden) or in later/heavier lines of treatment (advanced BC) can be applied by using only trastuzumab. On the contrary, treatment escalation for non-pathological complete response (pCR) patients is implemented with the trastuzumab-emtansin agent, where the HER2-targeting antibody is linked to the cytotoxic agent DM1 (T-DM1) (Barok 2014, Conte 2020). PARP inhibitors can be employed for BRCA mutation carriers, and are in trials for BRCAness phenotypes, using the principle of synthetic lethality with homologous recombination deficiency (Lord 2016, Geenen 2018). Immunotherapy through immune checkpoint blockade inhibitors has provided encouraging responses for some patients (Schmid 2018, Garrido-Castro 2019, Heeke 2021), anti-PD-L1 immunotherapy is now used against PD-L1-expressing tumors (Cortes 2020, Schmid 2020). Resistance to treatment can arise. For example, tamoxifen needs the metabolic enzyme CYP2D6 to be active, and resistance occurs in CYP2D6-low cells (Jin 2005). CDK4/6 inhibitors (to block the cell cycle downstream of ER signaling), mTOR inhibitors (to block another pathway upstream of CDK4/6) and PIK3 inhibitors (under trials for bearers of PIK3CA mutations) are used to target endocrine resistance (Johnston 2020, Derouane 2021). In luminal advanced BC, the preferred first lines of treatment are thus a combination of endocrine therapy and CDK4/6 inhibitors, with chemotherapy used only after several lines of treatment or in case of visceral crisis. The strategy relies on the sequential use of different endocrine therapies or chemotherapies. Many options exist for second/later lines of treatments in advanced BC (if not used previously): anthracyclines, taxanes, capecitabine, vinorelbine, eribulin, as well as platinum agents, the novel anti-HER2 tyrosine kinase inhibitor tucatinib (Curigliano 2022) and new antibody-drug conjugates (HER-targeting antibody and cytotoxic agent) like T-DM1 (Diéras 2017) and trastuzumab deruxtecan (T-DXd) (Modi 2020, Cortés 2022). The optimal sequence is unknown, and the choice thus depends on the toxicity and efficacy of the previous agent(s) used (Harbeck 2019, Gennari 2021).

4.4 TNBC is characterized by the absence of ER, PR and HER2. Despite this common characteristic, tumors belonging to the TNBC subtype still have marked

heterogeneity and can further be subcategorized for prognosis and therapy (reviewed in Marra 2020 and Yin 2020) (**Figure 12** *top*). Lehmann's initial classification identified six clusters: basal-like 1 (BL1), basal-like 2 (BL2), immunomodulatory (IM), mesenchymal-like (MES), mesenchymal/stem-like (MSL), and luminal androgen receptor (LAR) (Lehmann 2011). However, it was later recognized that Lehmann's IM and MSL subtypes were due to the presence of infiltrating lymphocytes and tumor-associated stromal cells (Lehmann 2016). This classification was refined in 4 TNBC molecular clusters: BL1, BL2, MES and LAR (Lehmann 2016, Bareche 2018, Wang 2019) (**Figure 12** *left*). BL1 has alterations of cell cycle genes and DNA repair mechanism genes (*BRCA1*, *BRCA2*, *TP53* and *retinoblastoma 1* [*RB1*]). BL2 also has alterations of cell cycle genes, added to an overexpression of growth factor signaling pathways, like AKT1, and myoepithelial/basal markers. MES shows enrichment for genes involved in cell motility, invasion and EMT. LAR displays overexpression of luminal differentiation genes and an overactivation of the androgen receptor (AR) signaling pathway, combined with a higher mutational burden. Subsequently, other research groups have also categorized TNBCs in 4 molecular clusters (Marra 2020): BLIA (basal-like immunoactivated), BLIS (basal-like immunosuppressed), MES and LAR (Burstein 2015); or IM (immunomodulatory), BLIS, MES and LAR (Liu 2016, Jiang 2019) (**Figure 12** *right*). Each subtype displays discrete gene expression profiles and, importantly, distinct prognoses (*e.g.* BLIS has a worse prognosis than BLIA) and response rates to therapies (*e.g.* AR could be targeted in the LAR subtype). However, these different classifications do not exactly superimpose each other (Yin 2020, **Figure 12** *bottom*), according to a detailed comparison of the classification provided by Ahn in 2016.

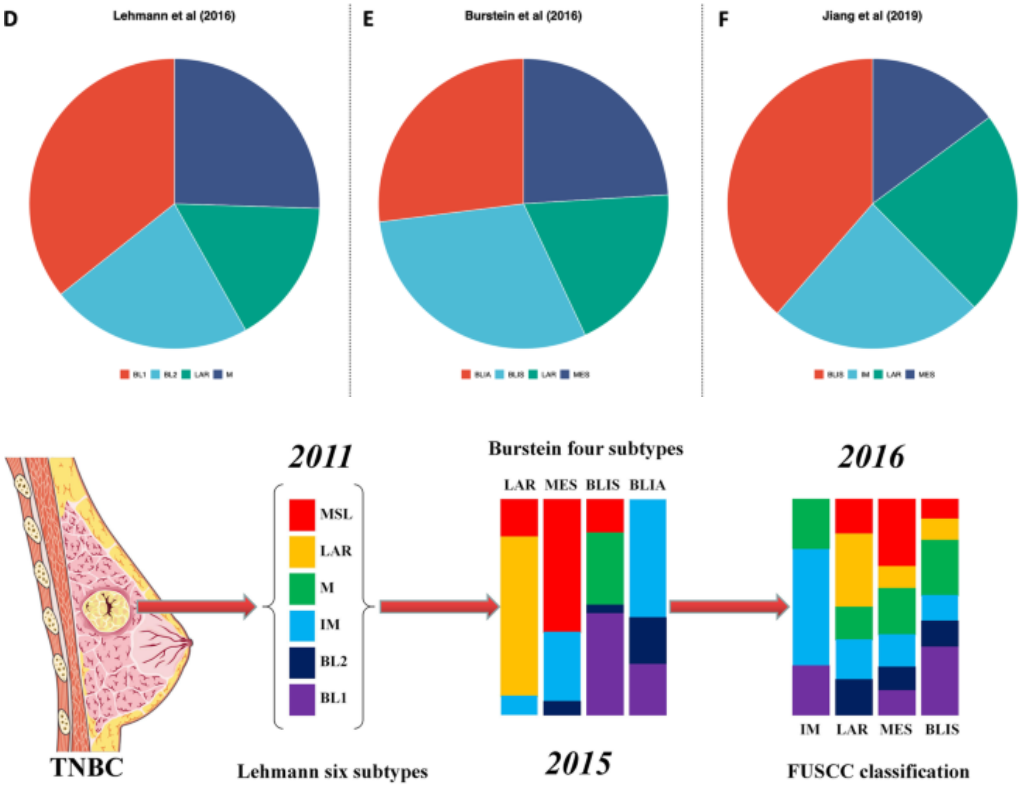


Figure 12. TNBC molecular subclassification. According to Lehmann (2011, 2016), Burstein (2015) and the Fudan University Shanghai Cancer Center (FUSCC) classification (Liu 2016, Jiang 2018). On top, the comparison provided by Marra *et al.* (Marra 2020). On the bottom, the comparison provided by Yin *et al.* (Yin 2020).

4.5 Breast cancer brain metastasis is a devastating diagnosis for patients. Metastatic breast cancer can spread to multiple organs: mainly bones, lungs, liver, and brain (Lin 2008, Smid 2008, Kennecke 2010, Sihto 2011, Harell 2012, Wu 2017, Darlix 2019) (**Figure 13** *left*). The breast cancer subtype influences the propensity to invade these organs: luminal tumors have the highest rate of bone metastases, HER2+ tumors are prone to liver and brain metastases, and TNBCs are associated with increased lung and brain metastases. This latter metastatic site, however less frequent in breast cancer overall, is a dreaded prognosis, as it rapidly decreases life expectancy and life quality due to neurological defects (Klos and O'Neill 2004, Witzel 2016). Despite the existence of various therapeutic strategies, most patients rapidly

face a palliative situation, with a median survival time ranging from 8 to 14 months (see 4.5.2). The risk to develop a brain metastasis and the prognosis after brain metastasis occurrence have both been shown to correlate with the breast cancer subtype (**Figure 13**).

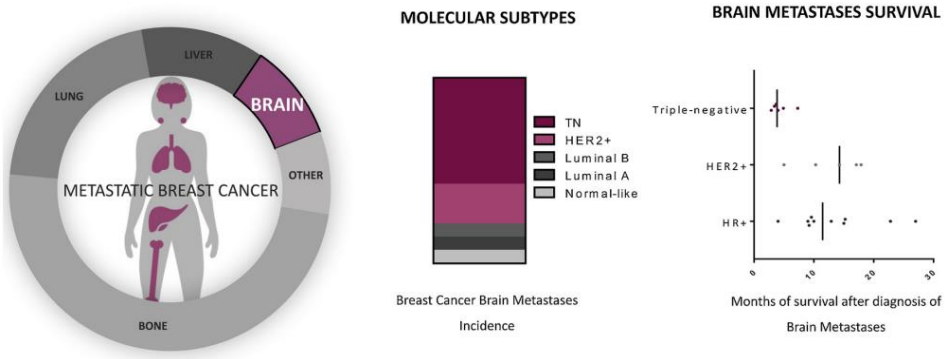


Figure 13. Increased risk and poorer prognosis of brain metastatic breast cancer for the TNBC subtype. HR – hormone receptor, HER2 – human epidermal growth factor receptor 2, TN(BC) – triple negative (breast cancer). Figure from Carvalho 2020.

4.5.1 The TNBC subtype displays the highest probability of breast cancer brain metastasis. TNBC has an incidence of 25% to 46% for patients to eventually develop brain metastasis, whereas 5-18% of luminal and 12-40% of HER2+ tumors develop brain metastasis, despite their main tropism for bones (Bendell 2003, Smid 2008, Lin 2008, Kennecke 2010, Jin 2018, Darlix 2019, Lin 2020). A higher incidence in HER2-enriched tumors is sometimes documented, which may be due to increased survival rates resulting from progresses with anti-HER2 therapies. Compared to other breast cancer subtypes, TNBC also presents a reduced time for the occurrence of brain metastases (Hines 2008, Sperduto 2013, Niikura 2014).

4.5.2 The TNBC subtype exhibits the poorer prognosis in the presence of brain metastases, with a median patient survival time of only 4 to 7 months. Focusing solely on TNBC brain metastasis patients, median survival times of 4.9 months (53 patients, Lin 2008) and 7.3 months (433 patients, Jin 2018) have been reported. The divergent survival times reported in distinct studies are due to different inclusion criteria and treatment strategies, which include the impact of cancer therapy

improvement. Comparing TNBC brain metastasis with breast cancer brain metastasis (other subtypes and overall) helps to put in perspective the divergent numbers, and reveals a reduced survival time following brain metastasis diagnosis for TNBC-bearing patients. As such, the survival expectancy of patients with breast cancer brain metastasis is in the order of months and further decreased for the TNBC subtype. Niwinska *et al.* (Niwinska 2010b) reported a median overall survival time after brain metastasis diagnosis of 10 months among all subtypes, 12 to 15 months for the other subtypes and only 4 months for the TNBC subtype (420 patients). Sperduto *et al.* (Sperduto 2013) reported higher median survival times of 14.4 months (breast cancer brain metastasis overall), 10 to 23 months (other subtypes) and only 7.3 months for TNBC (383 patients). Higher numbers may be explained by the fact that all patients included in the second study received radiotherapy, as data came from a radiation oncology department. A same overall breast cancer brain metastasis survival of 14 months was observed in a subset of patients who underwent craniotomy (140 patients; Shen 2015). Despite some variability, the median survival time of TNBC patients was decreased by half in both studies when compared to the overall survival time of patients with breast cancer brain metastasis.

Two larger studies including 1,256 and 4,033 breast cancer brain metastasis patients support the previous data (Niikura 2014, Darlix 2019). They reported a median survival time of ~ 8 months for breast cancer brain metastasis in general, and only 4.4-4.9 months in the case of TNBC brain metastasis, as compared to 7-9 months (luminal), 11-13 months (HER2-enriched) and 16-19 months (luminal-HER2) for the other subtypes (Niikura 2014, Darlix 2019). To note, a rare case described a median survival of 1.15 year for TNBC brain metastasis as compared to 2.11 years for breast cancer brain metastasis (McKee 2015). Albeit patients survived strikingly longer, the numbers, however, followed the same trend as the other clinical reports: the median survival time was decreased by half in the case of TNBC brain metastasis, as compared to all breast cancer brain metastasis patients. Niwinska *et al.* (Niwinska 2010b) also reported that systemic therapy could prolong the survival of breast cancer brain metastasis patients with luminal and HER2-enriched tumors (to 14 and 11 months, respectively), but could barely extend the survival (to 4

months) of TNBC-bearing patients. Collectively, these studies illustrate that survival times and rates after brain metastasis diagnosis are dramatically shorter for TNBC patients.

4.5.3 The incidence of breast cancer brain metastasis has increased over the years with advances in neuroimaging (increased detection of brain lesions) and anticancer therapy (longer patient survival). Clinical numbers were shown to be underestimated due to inadequate detection: brain metastases were diagnosed in up to 16% of metastatic breast cancers, while autopsy studies revealed an incidence as high as 34% (Lee 1983, Tsukada 1983, Boogerd 1993, Lin 2004, Kirsh 2005). Before biomarker-based therapy and at the beginning of neuroimaging, the incidence of breast cancer brain metastasis had been estimated to be around 10% (DiStefano 1979), increasing to 16% in the following decades, and reaching 24% to 34% in later retrospective studies (Niikura 2014, Rostami 2016, Genre 2017). The increased occurrence is attributable to progress in cancer therapies prolonging patient survival, thus granting more time for the development of brain metastases, as well as to improvements in detection methods, including the more frequent use of magnetic resonance imaging (MRI) (Crivellari 2001, Dawood 2008, Brufsky 2011, Pestalozzi 2013).

In conclusion, the TNBC subtype has a tropism for the brain microenvironment and is associated with a poorer prognosis than any other breast cancer subtype developing brain metastases. TNBC is already difficult to treat due to the absence of ER, PR and HER2 (rendering mostly futile the use of endocrine and anti-HER2 therapies), and is in addition more prone to develop a very lethal form of metastasis with a very short survival prognosis for patients. Due to the general treatment unresponsiveness of TNBC, no adequate strategy exists to date to prevent and manage TNBC brain metastasis.

CHAPTER 5 – THE BRAIN ENVIRONMENT

The destination of the metastatic progenitor cells of interest in this work is the **brain**. It embodies the control tower of our body and mind. As such, unlike any other parts of the human body, it displays exclusive features, including a **specialized barrier** to ensure its protection. Brain colonization is a life-threatening outcome, as it compromises this delicate and crucial machinery.

5.1 Brain anatomy, parenchyma & anatomical barriers

5.1.1 The central nervous system, composed of the brain and spine, is encapsulated in three layers of membranes, the meninges, or leptomeninges when focusing on the two inner layers. The dura mater is the thick and strong outer layer. It is followed by the arachnoid mater with its spiderweb-like structure of connective tissue. The pia mater is the thin and nourishing innermost layer, which supplies the brain tissue with blood. Underneath the arachnoid mater is the subarachnoid space filled with cerebrospinal fluid (CSF) that flows from the ventricles (Lei 2017, Chatterjee 2019, Shetty and Zanirati 2020). This vital liquid cushions both brain and spine, being however mainly hypoxic and nutrient-deficient (Boire 2020).

5.1.2 The brain parenchyma is composed of different types of neural cells and contains mainly astrocytes. Neurons (5-10 µm in body diameter) are the cells responsible for the fundamental neurocognitive functions of the brain, through the transmission of nerve impulses (**Figure 14**). Their projections, called 'axons', can extend up to 1 m to form intricate networks of connections (synapses) with other neurons. Neurons are mainly classified in glutamatergic and γ-aminobutyric according to the neurotransmitters released: glutamate (excitatory) or γ-aminobutyric acid (GABA, inhibitory), respectively. Even if fundamental, neural cells are greatly outnumbered by glial cells (Thorne 2006, Pelvig 2008, Azevedo 2009), among which astrocytes (10 µm in diameter and significantly more when activated) are the most abundant, outnumbering the neurons by over 5-fold (Sofroniew 2010). Their star-shaped morphology, hence their name, is due to the massive number of arborescent protrusions necessary for their important functional and structural roles as carers of

neurons (Wolak and Thorne 2013). Oligodendrocytes (1-3 µm in body diameter) are the cells forming the myelin sheath around the axons, accelerating the propagation of electrical nerve impulses (El Waly 2014). The microglia ensures immunosurveillance, as immune cells from the body are not allowed inside the central nervous system (CNS). The brain is thus considered to be a safe haven from circulatory immune cells.

5.1.3 Brain cells are surrounded by an extracellular matrix and a brain-specific fluid called 'the brain interstitial fluid', together forming the brain interstitial system. Long thought to be an inert structural space, the brain interstitial system (ISS) is, instead, a dynamic space connecting the vasculature to neural networks. Notably, it accounts for a large fraction of the brain: 15-20% of its total volume (Lei 2017, Chatterjee 2019). The importance and function of the ISS has been detailed in a recent review paper (Shetty and Zanitari 2020). The interstitial fluid, in which brain cells are soaked, is believed to originate from the CSF, the vasculature and brain cell metabolism (Abbott 2004, Iliff 2012, Brinker 2014, Magdoom 2019). By providing the necessary nutrients from the vasculature to brain cells, as well as eliminating cellular waste products, its role is essential in maintaining a stable environment for the CNS. The appropriate composition of the brain interstitial fluid (ISF) is of utmost importance for brain homeostasis and optimal functioning of the neurons.

5.1.4 Different molecules are found in the brain interstitial fluid, *e.g.*, neurotransmitters, nutrients, metabolic by-products and signaling molecules (cytokines, growth factors). As aforementioned, GABA and glutamate are the common neurotransmitters released by neurons at synapses to activate GABAergic and glutamatergic receptors, respectively. After their release, they are rapidly absorbed by (other) neurons and astrocytes to ensure precise, time-wise effects of synaptic conduction and to avoid any toxicity that would arise at high concentrations (Danbolt 2001). Because of its neurotransmitter role, glutamate is the most abundant amino acid in the brain. Apart from glutamate, the brain interstitial space displays high levels of glutamine (Yudkoff 1993) and BCAA (Yudkoff 1997, Daikhin 2000), but

lower levels of glucose than in the blood due to its rapid consumption by brain cells (Gruetter 1992, Shestov 2011).

Glucose is the major energy source for brain cells and is massively imported by GLUTs, mainly GLUT1 and GLUT3 (Vannucci 1997). This energy source is mostly used to restore the electric potential of neural cells, discharged during the conduction of nerve impulses. Blood flow is crucial to sustain the brain with its needs of glucose and oxygen, in order to insure the continuous oxidative metabolism of glucose in neurons. Permanent brain damage would occur rapidly if blood would stop flowing to the brain. Conversely, the time to reach irreversible damage is longer in the case of hypoglycemia. Indeed, upon glucose restriction, neurons metabolize other fuels to maintain energy generation for proper brain activities: ketone bodies, like acetoacetate and β-hydroxybutyrate (formed by FA catabolism in the liver), and metabolic by-products of glycolysis, like pyruvate and lactate, building up after intense exercise or prolonged starvation (Gjedde 1975, Nybo 2004, Pierre 2005, Hawkins 2005). Like FAs, ketone bodies can be used to fuel the TCA cycle *via* their transformation in acyl-CoA.

Lipids constitutes around 50% of the brain, making it the highest FA-rich organ of the body (Katz 2007). However, metabolite profiling of mouse brain tissue and mass spectrometry analyses of the brain extracellular fluid showed lower levels of triacylglycerols and other storage lipids (Jain 2014, Jin 2020, Ferraro 2021). The lipid-rich brain microenvironment seems to accumulate specialized lipids instead of storing FAs as triacylglycerols (O'Brien &Sampson 1965). The brain FA compartment is particularly enriched in polyunsaturated fatty acids (PUFA), essentially derived from FAs obtained from the environment (Benatti 2004, Katz 2007, Liu 2014).

5.1.5 The unique brain environment is separated from the blood circulation by a highly specialized barrier located at brain capillaries: the blood-brain barrier.
The BBB maintains intact brain lipid bilayers and a well-controlled composition of the ISF, despite physiological fluctuations in plasma composition and possible contacts with harmful blood-borne substances and pathogens (Eichler 2011, Wilhelm 2013) (**Figure 14**). The BBB is a dynamic tissue with a highly selective permeability: it

impedes the free diffusion of molecules between the blood and the brain, but still allows the passage of a limited number of molecules (*e.g.* O_2 and CO_2). Alongside, it provides adequate carrier-mediated transcellular transport for required nutrients, signaling molecules and metabolic waste products (Redzic 2011). It includes an active efflux of lipophilic molecules, metabolic by-products and toxins, which helps to protect the lipid bilayers of brain cells. In addition, enzymes like peptidases and nucleotidases metabolize substances to counteract their entry into the brain environment (Abbott 2006). The BBB therefore physically and metabolically restrains the passage of molecules that could interfere with brain homeostasis, hence protecting the delicate neural tissue and providing a stable environment for neurotransmission. Consequently, the integrity of the BBB is crucial for brain function. The BBB is formed by a specialized endothelium composed of brain microvascular endothelial cells (BMECs), and supported by pericytes and end-foot processes of astrocytes (Redzic 2011, Fidler 2011, Wilhelm 2013) (**Figure 14**).

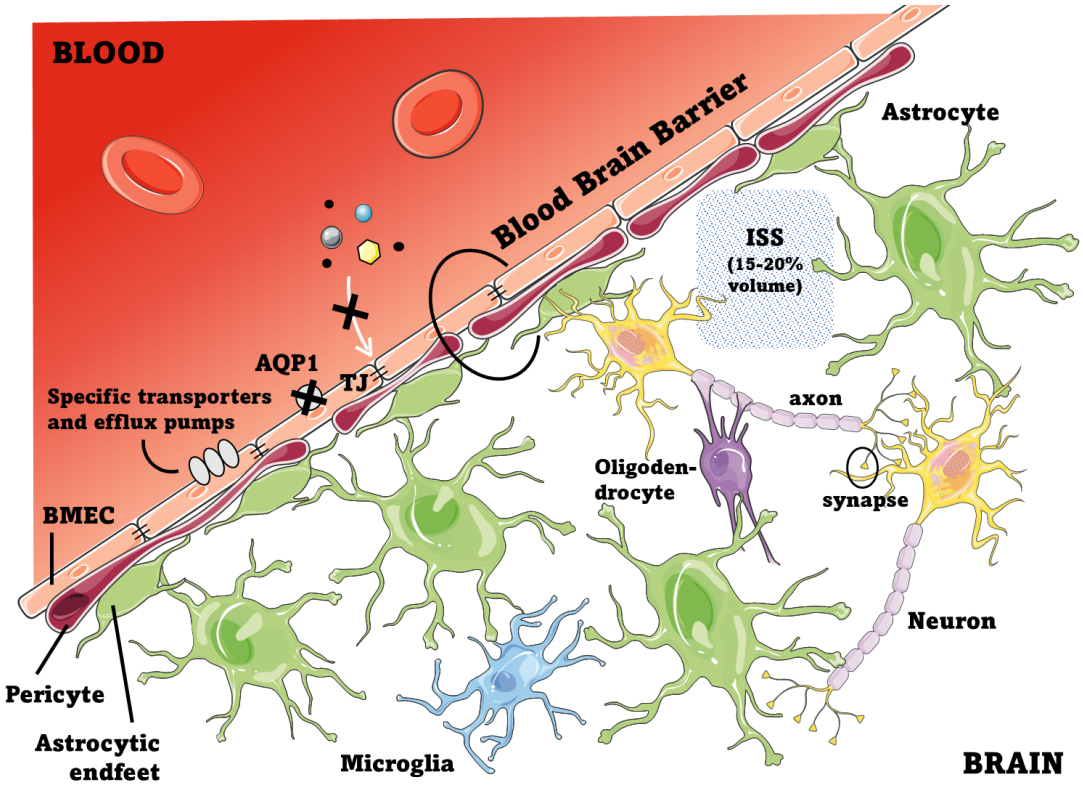


Figure 14. The brain parenchyma and anatomical barrier. The brain is composed of different types of neural cells, including neurons, astrocytes, oligodendrocyte and microglia, and of the interstitial system (ISS). The blood-brain barrier is a highly specialized structure at the interface of brain capillaries and the brain parenchyma, and is formed by brain microvascular endothelial cells (BMECs) displaying unique features, pericytes and the end-foot processes of astrocytes. TJ – tight junction, AQP1 – aquaporin 1.

5.1.5.1 The unique features of the BBB are primarily due to the **specialized endothelium** of brain capillaries, which are structurally and functionally different from capillaries of the peripheral vasculature (Brightman 1969, Brightman 1992, Hawkins 2005, Weiss 2009). Common capillaries have a leaky structure due to their fenestrated membranes, whereas brain capillaries lack fenestrations. In addition, brain microvascular endothelial cells (BMECs) are sealed together by tight junctions (TJs) that render them impermeable to the vast majority of substances (including water). They, express a wide variety of specific transporters and efflux pumps and display a reduced rate of endocytosis. To pass across the endothelial layer (*i.e.*, to enter or leave the brain), substances need to translocate through the cells, whether through membrane permeability or specific transport mechanisms. Small hydrophobic molecules, like oxygen and CO_2, can diffuse through the plasma membrane of the endothelial cells. Most molecules are, however, transferred by dedicated transporters located on both basal and apical sides of the cells. This allows for a highly selective transport (Gloor 2001, Brasnjevic 2009, Filey & Stroman 2011). In addition, some efflux transporters can reverse the entry of unwanted lipophilic molecules permeating the membranes.

A low rate of endocytosis restricts the transcellular route. The reduced pinocytic activity of BMECs limits the transcellular passage of macromolecules (Rubin 1991).

Tight junctions interconnecting BMECs restrict the paracellular route. TJs seal the brain vascular endothelium and block the intercellular passage of macromolecules, including water (Begley 2003). As a core structure of the BBB, they are responsible for the extremely high transendothelial electrical resistance (TEER) of 1,500 – 2,000 Ωcm^2 (Gloor 2001, Petty 2002, Pereira & Furlan 2010). Besides

their sealing role, TJs also maintain the structural integrity of the BBB, albeit in a very fluidic manner described as 'bending without breaking' (Huber 2001, Dalvi 2014). TJ complexes consist of both transmembrane proteins (claudins, occludin and junctional adhesion molecules-A/B/C) and cytoplasmic adapter proteins for linkage to the actin cytoskeleton, like zona occludens proteins (ZO)-1/3 (Redzic 2011, Dalvi 2014, Wrobel 2016). These complexes are arranged in multiple bands for higher efficiency. Their positions on the cell surface shapes the polarity of BMECs (Lippoldt 2000, Gloor 2001).

Specific transporters and efflux pumps regulate the transcellular route. Water channel aquaporin-1 (AQP-1) is absent from the endothelium of brain capillaries, whereas it is abundant on peripheral capillaries (Nielsen 1993, Dolman 2005). The BBB is thus essentially impermeable to water. Lipid-soluble non-polar molecules can easily diffuse through lipid bilayers; however, these molecules can represent toxic substances for the brain and can disturb the lipid bilayers of brain cells. Their abundance in the brain is lower than what might be expected from their lipophilicity, which is explained by the active efflux of lipophilic molecules to preserve lipid bilayers in the brain and avoid a detrimental impact on brain functions (Dean 2001). Enhanced levels of ABC efflux transporters, like P-glycoprotein (P-gp) and ABCG2 (also known as 'breast cancer resistance protein'), counteract the entry of harmful substances into the brain (reviewed in Dalvi 2014). Due to different substrate specificities, their combined expression allows a synergistic effect and further efflux efficiency: P-gp transports hydrophobic compounds, and ABCG2 transports both hydrophobic and hydrophilic-conjugated organic anions.

5.1.5.2 The permeability of the BBB is further restricted by **pericytes and astrocytes** in the brain parenchyma. Both are closely associated with BMECs, with astrocytic foot processes even ensheathing 99% of the surface of BMECs (Haseloff 2005, Lai 2005). In addition, pericytes are involved in BBB differentiation and in the maintenance of TJs (Lai 2005). Astrocytes can modulate BMEC properties, since coculture experiments with astrocytes have shown elevated BBB-related enzymatic

activities, glucose transporter expression, TJ abundance, TEER and BBB tightening (Janzer 1987, Haseloff 2005),

5.2 Invasion of the brain microenvironment

To establish in the brain parenchyma, metastatic progenitor cells must breach the BBB and interact with brain cells. For the rarer case of leptomeningeal metastasis (in the subarachnoid space), they rather infiltrate the CFS and travel in the meninges (Achrol 2019). Numerous research groups have therefore focused their investigations on mediators of cancer cell passage through the BBB and on interactions between invading cancer cells and host cells, especially astrocytes (**Figure 15**).

5.2.1 Metastatic cells must overcome an additional challenge for their extravasation in the brain: they must migrate through the BBB. The absence of a classic lymphatic drainage system renders the vascular circulation the only entry route for metastatic progenitor cells into the brain (Wilhelm 2013). Several mechanisms and adhesion molecules controlling this process have been identified, classified here in two main categories: BBB disruption and infiltration (**Figure 15** *left*).

5.2.1.1 BBB disruption. To cross the BBB, metastatic progenitor cells disrupt endothelial TJs and migrate between adjacent endothelial cells. Most cancer cells use the paracellular route for transendothelial migration (Wrobel 2016). Various factors secreted by cancer cells can stimulate TJ opening. Integrin $\alpha_v\beta_3$ activation, which occurs subsequently to cancer cells binding to the BBB, was shown to induce elevated levels of VEGF and to promote the recruitment of supporting blood vessels within the brain microenvironment (Lorger 2009). A close association with cerebral microvessels is indeed essential for colonization (Kienast 2010, Valiente 2014). Apart from its role in angiogenesis, VEGF can also enhance vascular permeability by disrupting TJs and adherent junctions of the endothelium (Li 2013, Fan 2011). Angiopoietin-2 (Ang-2) impairs the structure of TJ proteins ZO-1 and claudin-5 for brain colonization by metastatic breast cancer cells (Avraham 2014). Neuropeptide substance P secreted by breast metastatic progenitor cells enhances this process

by inducing BMEC-mediated Ang-2 secretion (Rodriguez 2014). MMPs, which can be expressed on the cancer cell membrane or secreted in the extracellular space, can degrade TJ proteins by proteolytic processing (Yang 2007). MMP-1, 2 and 9 were reported to be overexpressed in breast cancer brain metastatic cells (Mendes 2005, Xie 2006, Mendes 2007, Stark 2007, Hu 2010, Liu 2012, Momeny 2015, Wu 2015, Wang 2013, Conrad 2018). Among MMPs, cathepsin S was shown to mediate the BBB transmigration of breast cancer cells *via* the degradation of junctional adhesion molecule (JAM)-B (Sevenich 2014). Interestingly, both cancer cells and macrophages produce cathepsin S, and depletion of both production is necessary to reduce brain metastasis *in vivo* (Sevenich 2014).

Besides secreted factors, cancer cells can also produce vesicles carrying, *e.g.*, non-coding RNAs, such as micro-RNAs (miRNAs) and long non-coding RNAs (lncRNAs) that conspire to destroy the endothelial integrity of the BBB. Tumor-derived exosomes were shown to enhance BBB permeability: miR-105 disrupts ZO-1 (Zhou 2014), lncRNA GS1–600G8.5 downregulates ZO-1, claudin-5 and N-cadherin expression in the brain endothelium (Lu 2020), and miR-181c impairs the dynamics of intracellular actin in endothelial cells (Tominaga 2015). These BBB-disrupting vesicles can be secreted by the cancer cells in the context of PMN formation.

5.2.1.2 BBB infiltration. Metastatic progenitor cells express general mediators of extravasation across non-fenestrated capillaries, supplemented by specialized enhancers of BBB penetration. The seminal work of Bos *et al.* (Bos 2009) identified a breast cancer brain metastasis signature including brain-specific sialyltransferase ST6GALNAC5, cyclooxygenase-2 (COX2, also known as prostaglandin-endoperoxide synthase 2 [PTGS2]), and EGFR ligand heparin-binding EGF-like growth factor (HBEGF). Interestingly, COX2 and HBEGF were previously shown to be linked to breast cancer infiltration into the lungs, and one can therefore propose that they are needed for extravasation through the non-fenestrated and tight capillaries of both the brain and the lungs (Minn 2005, Bos 2009). Apart from COX2 and HBEGF, gene expression analyses of cancer cells with a high brain metastatic activity and *in vitro* BBB infiltration studies identified ST6GALNAC5 as a specific

mediator of BBB crossing (Bos 2009). Functional validation of ST6GALNAC5 demonstrated that it facilitates the passage of breast cancer metastatic progenitor cells through the BBB to promote brain metastasis (Bos 2009). Normally restricted to the brain, ST6GALNAC5 is suggested to act by enhancing cancer cell adhesion to brain endothelial cells (Okajima 1999). In addition, other molecules have been associated with increased metastatic progenitor cell infiltration through the BBB, even if they may not be specific for brain metastasis: CXCL12 receptor CXCR4 enhances MDA-MB-231 penetration through BMECs (Lee 2004), molecular chaperone αB-crystallin has been associated with an increased $\alpha_3\beta_1$ integrin-mediated adhesion of breast cancer cells onto the brain endothelium (Malin 2014), and semaphorin-4D (SEMA4D) was shown to be overexpressed on cancer cells to promote interactions with plexin-B1 on brain endothelial cells (Klotzs 2020).

5.2.2 After crossing the BBB to penetrate the tissue, metastatic progenitor cells closely interact with brain residential cells, including neurons and astrocytes. Interactions trigger host cells to inadvertently support cancer growth. Brain metastatic cells can indeed hijack the neuro-protective and neuro-caring functions of astrocytes. They can induce astrocyte activation through gap junctions and/or secreted molecules, in order to support both cancer growth and chemotherapy protection as explained below (**Figure** 15 *right*).

First, brain metastatic cells need to evade the defensive mechanisms developed by reactive astrocytes. The seminal work of Valiente *et al.* (Valiente 2014) revealed that naturally expressed plasminogen activators (PAs) in the brain trigger the production of plasmin, an enzyme that releases the pro-apoptotic cytokine soluble Fas Ligand (sFasL) by cleaving it from astrocytic membranes to induce Fas-mediated cancer cell death. However, just as neuroserpin is inherently expressed by neurons to avoid the action of plasmin (Yepes 2000), brain metastatic cells were shown to express serpins (including neuroserpin) to inhibit the otherwise lethal astrocytic PA-plasmin system (Valiente 2014).

Secondly, brain metastatic cells can establish gap junctions with astrocytes to diffuse intracellular mediators of apoptotic signals and gain pro-survival signals. Gap junctions were shown to prevent the chemotherapy-mediated accumulation of

cytoplasmic calcium and to promote chemotherapy resistance in melanoma cell lines, however not restricted to brain-trophic ones (Lin 2010). The same team showed that the establishment of gap junctions upregulated the expression of survival genes *glutathione s-transferase α5 (GST5A)* (for oxidative stress response), *B-cell lymphoma 2-like 1* (*BCL2L1)* and *TWIST1*, which consequently conferred chemotherapy resistance, however again not specifically in brain-trophic cell lines (Kim 2011). Chen *et al.* (Chen 2016) further demonstrated that gap junctions also function to deliver second messenger cyclic GMP-AMP (cGAMP) to astrocytes, inducing the production of inflammatory factors interferon α (IFNα) and TNF. This resulted in triggering signal transducer and activator of transcription 1 (STAT1) and nuclear factor κB (NF-κB) survival signals in cancer cells, promoting tumor growth and chemotherapy resistance. These authors then found that connexin-43 (Cx43)-composed gap junctions were formed between cancer cells and astrocytes together with protocadherin-7 (PCDH7) to specifically target astrocytes (and not microglia nor endothelial cells) (Chen 2016). Cx43 or PCDH7 silencing, as well as inhibitors of gap junction activity or elements of the involved pathways, inhibited brain metastasis.

Thirdly, as exemplified in the latter study, metastatic progenitor cells can activate astrocytes to generate the production of factors promoting cancer cell survival, proliferation, and migration. Such pro-tumoral signals include TGFβ, IFNα, TNF, interleukins, cytokines and chemokines (Sierra 1997, Termini 2014, Chen 2016, Fares 2021). For instance, breast cancer-derived brain metastatic cells secrete interleukin-1 β (IL-1β) to stimulate astrocytes, and astrocytes then produce Notch-1 signaling activator jagged-1 (Xing 2013). Notch signaling was also shown to be upregulated in brain-trophic melanoma cells, although *erroneously classified as breast cancer cells* in the study (Nam 2008, Lacroix 2008), and inhibition of tumoral Notch signaling reduced the occurrence of breast cancer brain metastasis in mice (McGowan 2011). Another example arises from cancer cells secreting COX2-induced prostaglandins (PG) and triggering astrocytes to release the chemokine CCL7, which promotes the survival and proliferation of stem-like breast cancer brain metastatic cells (Wu 2015). The interaction between brain-specific cell lines and astrocytes was also shown to upregulate the expression of CXCL1, CCL2 and CXCL12 in astrocytes, and to downregulate the expression of Kisspeptin 1 (KISS1)

in brain metastatic cancer cells (Kaverina 2017). Of note, astrocytes were also found to release miRNA19a-containing exosomes to induce a loss of PTEN in brain cancer cells and to increase the secretion of chemokine CCL2, consequently recruiting pro-tumoral myeloid cells in the brain (Zhang 2015).

Besides contacts with astrocytes, brain metastatic cancer cells can also mimic astrocytes to interact with neurons (Zeng 2019). A study indeed reported that they can form pseudo-synapses with glutamatergic neurons in order to capture glutamate and activate glutamate transporter N-methyl-D-aspartate receptors (NMDAR) and their downstream proliferation signals (Zeng 2019). Furthermore, brain metastatic cells require close interactions with endothelial cells, even after transendothelial migration, for co-opting brain capillaries (Carbonell 2009, Kienast 2010, Lorger &Felding-Habermann 2010, Valiente 2014). Valiente *et al.* (Valiente 2014) identified cell adhesion molecule L1 (L1CAM) as a mediator of the interaction between metastatic cancer cells and the endothelium. This axon pathfinding molecule was expressed by cancer cells to spread along brain capillaries. They further demonstrated that the aforementioned serpins, which are upregulated in brain metastatic cell lines, protected L1CAM from plasmin cleavage, thus supporting L1CAM-mediated vascular co-option in the brain (Valiente 2014). The same group also reported that a subpopulation of STAT3-expressing astrocytes promoted brain cancer breast metastasis. Conversely, a genetic targeting or pharmacological inhibition of astrocytic STAT3 impaired the viability of brain metastases (Priego 2018). This was particularly striking, as a same observation was also made in human brain metastasis patients (Priego 2018). STAT3 had previously been shown to orchestrate cancer and endothelial cells interactions (Lee 2015).

5.2.3 To establish in the brain, cancer cells can mimic brain cells and adopt a neuronal phenotype. Several upregulated genes detected in brain metastases, when compared to bone metastases, are also genes that are upregulated in the normal brain tissue compared to other tissues (Klein 2009). Additionally, brain tumors of different cell lines were shown to cluster together along with normal brain tissue, whereas all tumors of the other organs clustered by cell line and not by organ (Park 2011). This observation reflects inherent cell line-specific gene expression

signatures that are nevertheless overwritten by the acquisition of neuronal characteristics for development in the brain, and similarly in astrocyte co-cultures (Park 2011). Cancer cells can upregulate the expression of neurological signaling genes, like neuropathic pain signaling, synaptic potentiation, axonal guidance signaling and glutamate receptor signaling (Park 2011). Another study revealed GABAergic characteristics in clinical samples of brain metastatic cancer cells (Neman 2014, detailed in section 6.5). Furthermore, the innovative work on organ-specific metastasis by Burnett *et al.* (Burnett 2015) unveiled genes upregulated solely in brain metastasis compared to both parental cells and other metastatic sites (breast, lungs, bones, adrenal glands). In the top 25 differentially expressed genes, 11 were linked to neuronal activity, suggesting that brain metastatic cells possess a neuronal phenotype to grow in the brain and to exploit neuronal signaling networks for their own purpose (Burnett 2015). To note, GSH-mediated detoxification, NRF2-mediated oxidative stress response and semaphorin signaling pathways were found to be activated in brain-seeking metastatic progenitor cells, paralleled with elevated NF-κB survival signaling (Burnett 2015). As exemplified by the findings of Neman *et al.* (see section 6.5; Neman 2014), acquiring neuronal cell characteristics may represent an approach to copy brain cell metabolism (see Chapter 6).

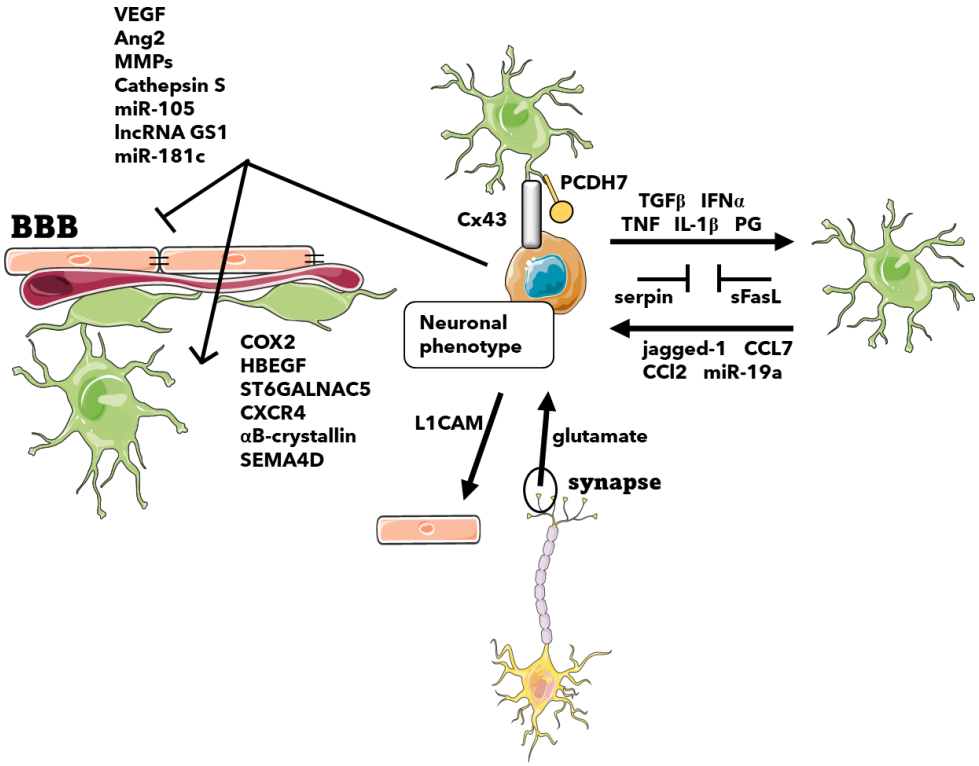


Figure 15. Mechanisms of brain microenvironment invasion. Brain metastatic cancer cells express different factors to disrupt tight junctions (TJs) and invade the blood brain barrier (BBB), interact with neural cells (astrocytes in green, neurons in yellow and endothelial cells in pink), and exhibit a neuronal phenotype. Cx43-composed gap junctions allow the passage of several apoptotic signals, pro-survival signals and secondary messengers. Other abbreviations: VEGF – vascular endothelial growth factor, Ang2 – angiopoietin 2, MMP – matrix metalloproteinase, miR – miRNA, lncRNA – long non-coding RNA, COX2 – cyclooxygenase-2, HBEGF, heparin binding EGF-like growth factor, ST6GALNAC5 – brain-specific sialyltransferase, CXCR – chemokine (C-X-C motif) receptor, SEMA4D – semaphoring-4D, Cx43 – connexin-43, PCDH7 – protocadherin-7, TGFβ - transforming growth factor β, IFNα – interferon-alpha, TNF – tumor necrosis factor, IL-1β – interleukin-1β, PG – prostaglandins, sFasL – soluble Fas Ligand, CCL – chemokine (C-C motif) ligand, L1CAM – cell adhesion molecule L1.

5.3 Brain metastasis treatment is mainly impaired by the BBB and protective behaviors of host cells. Even if BBB integrity can be compromised in some tumor areas, permeability is still very limited, and most anticancer compounds do not penetrate the brain (Huber 2001, Lockman 2010, Wilhelm 2013, Achrol 2019). The

brain is thus considered to be a sanctuary site for metastatic cancer cells, beyond the reach of many chemotherapeutic agents and immune surveillance. Additionally, host brain cells can protect cancer cells from chemotherapy-induced cytotoxicity (section 5.2.2). This phenomenon added to the scarcity of treatments capable of penetrating the BBB, makes of brain metastasis a major clinical issue. Surgical resection can be part of the treatment strategy if metastases are accessible and in limited numbers. Radiation can be delivered to the whole brain (WBRT) or to specific areas (stereotactic radiotherapy), where a large dose is deliver to the metastatic area (Mahajan 2017, Brown 2017). Due to its larger field of action, WBRT provides a better control but poorer neuro-cognitive outcomes. Systemic therapies used to treat breast cancer brain metastases, including chemotherapies and immunotherapies, are not specific and usually follow the treatment scheme of the primary breast tumor (*e.g.,* anti-HER2 therapy for HER2+ tumors) (Groves 2010, Ahluwalia 2014, Singh 2017). However, they are usually futile, due to poor drug distribution in the brain and/or to acquired resistance due to previous chemotherapeutic treatment(s) of the primary tumor (Stricker 2015). There is, therefore, an urgent need for the discovery of new therapeutic drugs capable of penetrating the BBB.

Metastatic invasion of the brain is a dramatic outcome for cancer patients. Major studies on the topic usually address the BBB crossing capacities of metastatic progenitor cells and their interactions with host brain cells. Indeed, the establishment of brain metastases depends on **activators of BBB extravasation** and on **favorable cellular interplays** between invading cancer cells and brain cells (mainly astrocytes). Many parameters have been described, such as ST6GALNAC5, PCDH7, neuroserpin, and **neuronal cell characteristics**. The investigation of **metabolic factors** facilitating brain metastasis (Chapter 6) may help to find ways of impinging brain metastasis. As most therapeutic drugs are restrained from accessing the brain by the BBB, new therapeutic strategies attacking CTC metabolic properties could circumvent the need for BBB-penetrating compounds.

CHAPTER 6 – METABOLISM OF BRAIN METASTASES

This chapter describes **metabolic components** expressed by cancer cells for efficient **brain colonization**. To fit in the unique brain microenvironment, brain metastatic cells display **remarkable metabolic adaptations** in both glycolysis and oxidative glucose metabolism; acetate, lipid, amino acid and GABA metabolism; as well as in the pentose phosphate pathway for enhanced redox homeostasis mechanisms (**Figure 16**). These changes relate to brain-specific metabolites and brain host cells, both of which cancer cells must cope with.

6.1 Glucose oxidation, TCA, PPP and folate cycle.

Chen *et al.* (Chen 2007) collected breast CTCs from a patient and established brain-seeking variants (breast cancer cells invading the brain with a higher incidence and increased tumor burden) through two rounds of selection in mice. They reported that 50% of differentially expressed proteins identified in brain-seeking metastatic progenitor cells belonged to cell metabolism. Brain metastatic cells displayed increased expression of enzymes involved in glycolysis, the TCA cycle, OXPHOS, fatty acid β-oxidation, the PPP and the GSH system when compared to parental cells. This observation pointed towards the dependency of these cells on the oxidation of glucose and FAs for energy purposes, in parallel with an elevated PPP flux for oxidative stress response (Chen 2007). Fischer *et al.* (Fischer 2019) further reported that mitochondrial respiration was upregulated in melanoma brain metastases as well, with an enrichment in the gene expression of the OXPHOS pathway and increased OXPHOS activity revealed by metabolomics. In this study, OXPHOS inhibitors reduced the occurrence of brain metastasis and/or improved the survival rates of brain metastases-bearing mice. Upregulated cellular redox-active proteins concorded with increased mitochondrial respiration, as they support the detoxification of OXPHOS-induced mtROS to maintain cell redox homeostasis. The authors also reported that brain-trophic metastatic progenitor cells were less sensitive to glycolysis inhibitor 2-deoxyglucose (2DG) and to Bortezomib, a proteasome inhibitor used as an oxidative stress inducer, that the parental cancer cells. One can propose that all these overactivated pathways (and the reducing equivalents thus generated) concur to mtROS detoxification, using pathways like

GSH synthesis to counteract the oxidative stress encountered by cancer cells and not just to balance increased respiration.

Glucose oxidation by cancer cells residing in the brain was also demonstrated by ^{13}C-labelled glucose and ^{13}C NMR spectroscopy, where lactate was shown not to be the only end-product (Maher 2012). Glucose was also used to produce energy in the TCA cycle and to supply pools of intermediates for nucleotide and amino acid synthesis, which included fueling the serine biosynthesis and folate cycle pathways (which can be used as a NADPH production site for biosynthesis and redox homeostasis). Accordingly, brain-seeking metastatic progenitor cells were shown to upregulate the expression of serine synthesis genes, including *PHGDH*, encoding an enzyme which genetic silencing or pharmacological inhibition attenuated brain metastasis (Ngo 2020). Albeit glucose oxidation was occurring, less than 50% of the acetyl-CoA pool was derived from the labeled blood-borne glucose, thus indicating that other fuels were oxidized in the TCA cycle (Maher 2012; see next section).

6.2 Acetate metabolism

Acetate is heavily used by the normal brain tissue, particularly as a glial fuel (Waniewski 1998, Zielke 2009, Wyss 2011, Salzillo 2016). Following the previous observation that glucose was not the sole fuel for the acetyl-CoA pool (Maher 2012), Mashimo *et al.* (Mashimo 2014) made the riveting discovery that both primary brain cancers (gliomas) and brain metastases of various origins can metabolize acetate *via* the TCA cycle to meet their high bioenergetic and biosynthetic requirements. Acetate was shown to label the mitochondrial acetyl-CoA pool (used as a TCA substrate) of cancer cells in the brain (Mashimo 2014). This constituted a striking observation that the same environment was associated with different cancers converging towards a same phenotype, and that cancer cells must have a metabolic complementarity to the host organ. This conclusion is particularly intriguing since metastatic cancer cells, themselves capable of oxidizing acetate, came from organs that did not demonstrate acetate uptake. For acetate oxidation, cancer cells expressed ACSS2 to convert acetate in acetyl-CoA, and ACSS2 expression directly

correlated with the rate of entry of acetate into the TCA cycle (Mashimo 2014). Of note, gliomas and brain metastases oxidized glucose and acetate, but not glutamine, in this study.

6.3 Lipid metabolism

Klein *et al.* (Klein 2009) identified numerous metabolism-related genes among the differentially expressed genes between clinical brain metastases and bone metastases. Fatty acid binding protein 7 (*FABP7*) was identified as a top upregulated gene, along with translation initiation factor EIF2S3. Upregulated in the normal brain tissue compared to other organs, FABP7 belongs to a family of proteins involved in FA metabolism and transport (Feng 1994, Hauenerland 2004). FABP7 overexpression was validated in a later study where it was additionally shown to promote breast cancer brain metastasis (Cordero 2019). FABP7 was reported to promote the glycolytic phenotype and lipid droplet storage of brain-trophic metastatic progenitor cells, to drive the survival of cancer cells injected in the brain (as compared to FABP7-knockdown cells) and to increase the incidence of breast cancer brain metastasis when experimentally overexpressed in parental cells injected in the circulation (Cordero 2019). In clinical samples, FABP7 expression was associated with poor prognosis and a high breast cancer brain metastasis prevalence (Cordero 2019). In parallel, Zou *et al.* (Zou 2019) suggested that brain metastatic cells could take advantage of the high PUFA brain microenvironment by activating PUFA secretion by astrocytes, since inflammation-activated astrocytes were previously shown to increase PUFA release (Aizawa 2016). They further reported that astrocytic PUFAs activate pro-proliferative peroxisome proliferator-activated receptor γ (PPARγ) signaling in invaded brain metastatic cells (Zou 2019). PPARγ blockade reduced astrocyte-induced tumor growth and *in vivo* brain metastatic burden.

Other studies, on the contrary, argued for a limited access of lipids from the bloodstream to the brain and for the requirement of FA synthesis by cancer cells in the brain. For instance, Ferraro *et al.* (Ferraro 2021) demonstrated that breast cancer cells established in the brain had elevated FA synthesis and an increased expression of FASN compared to other metastatic sites. They further showed that cancer cells

in the brain depend on the lipids produced by FASN for survival, since FASN inhibition selectively reduced breast cancer brain metastasis *in vivo*. Similarly, breast cancer brain metastatic cells were described to possess a lipogenic phenotype and to *de novo* upregulate a lipogenesis transcription factor named 'sterol regulatory element-binding protein (SREBP1)', which triggers FASN, ACC and stearoyl-CoA desaturase 1 (SCD1) expression (Santa-Codina 2019, Jin 2020; Ricoult 2016). The genetic ablation of SREBP1, SCD1, and other FA-related elements hindered the development of intracranial-injected brain metastatic cancer cells (Jin 2020). In the study of Santa-Codina *et al.* (Santa-Codina 2019), increased FA synthesis was accompanied by a high ability of cancer cells to oxidize FA and a high hypoglycemic resistance. They also identified the stress chaperone GRP94 as a modulator of SREBP-1-dependent FA accumulation, as *GRP94* silencing decreased SREBP-1 expression and tumor growth *in vivo.* However, brain metastatic cells were oddly grown in the mammary fat pad, not in the brain, for these *in vivo* experiments (Santa-Codina 2019).

Brain-trophic metastatic progenitor cells seem to use different strategies in the brain, being thus reported to reprogram lipid metabolism by altering lipid transport, synthesis and oxidation. An important observation to underline is that the extracranial SREBP1-dependent phenotype (increased FA synthesis) could predict brain colonization, proving that pre-existent metabolic properties promoting brain metastasis were displayed prior to intracranial selection (Jin 2020).

6.4 Amino acid metabolism

To thrive in the low glucose concentrations of the brain interstitial space, breast cancer brain metastatic cells were found to increase the oxidation of glutamine and BCAAs, as well as gluconeogenesis to support their own survival and growth (Chen 2015). Breast cancer cells in the brain exhibited resistance to glucose starvation by synergistically elevating glutamine and BCAA oxidation, paralleled with a glucose-independent production of lactate (Chen 2015). In addition, cancer cells displayed an overexpression of enzymes involved in amino acid oxidation (like glutamate dehydrogenase [GDH] 1 and 2) and of the gluconeogenesis enzyme fructose-1,6-bisphosphatase 2 (FBP2), which was also upregulated in clinical specimens of brain

metastasis compared to primary breast cancers (Chen 2015). Silencing *FBP1/2* inhibited the survival and growth of the parental cancer cells injected in the brain (Chen 2015). The authors further showed that amino acid oxidation and FBP-based gluconeogenesis sustained PPP and purine synthesis in cancer cells. A high uptake of BCAAs in breast cancer brain metastatic cells was confirmed by the fact that labelled BCAAs have a higher sensitivity than glucose analogue tracer [^{18}F]-FDG for brain metastasis imaging (Bochev 2012, Chen 2007b, Kitajima 2008, Manohar 2013, Ishiwata 1993a/b, Kirikae 1989, Wong 2002).

6.5 GABA metabolism

Breast cancer cells in the brain can hack the neuronal communication system consisting of neurotransmitter exchanges, in order to redirect neurotransmitters GABA (described here) and glutamate (see 5.2.2) for their own use. Indeed, because GABAergic communication occurs in approximately 40% of brain synapses, GABA abundance is higher in the brain environment than in the breast tissue. Harnessing its energy can thus confer a growth advantage to cancer cells (Roberts 1986, Ferraro 2021). Neman *et al.* (Neman 2014) investigated GABA-related variables in clinical samples of breast cancer brain metastasis, and found GABAergic characteristics in brain metastatic cells, with increased expression of GABA receptor, GABA transporter (GAT) and GABA transaminase (ABAT), as well as activated GABA catabolism. The neuron-like properties that were acquired granted cancer cells with the unique metabolic ability of importing GABA and converting it to succinate to fuel the TCA cycle and, ultimately, the NADH pool (Neman 2014).

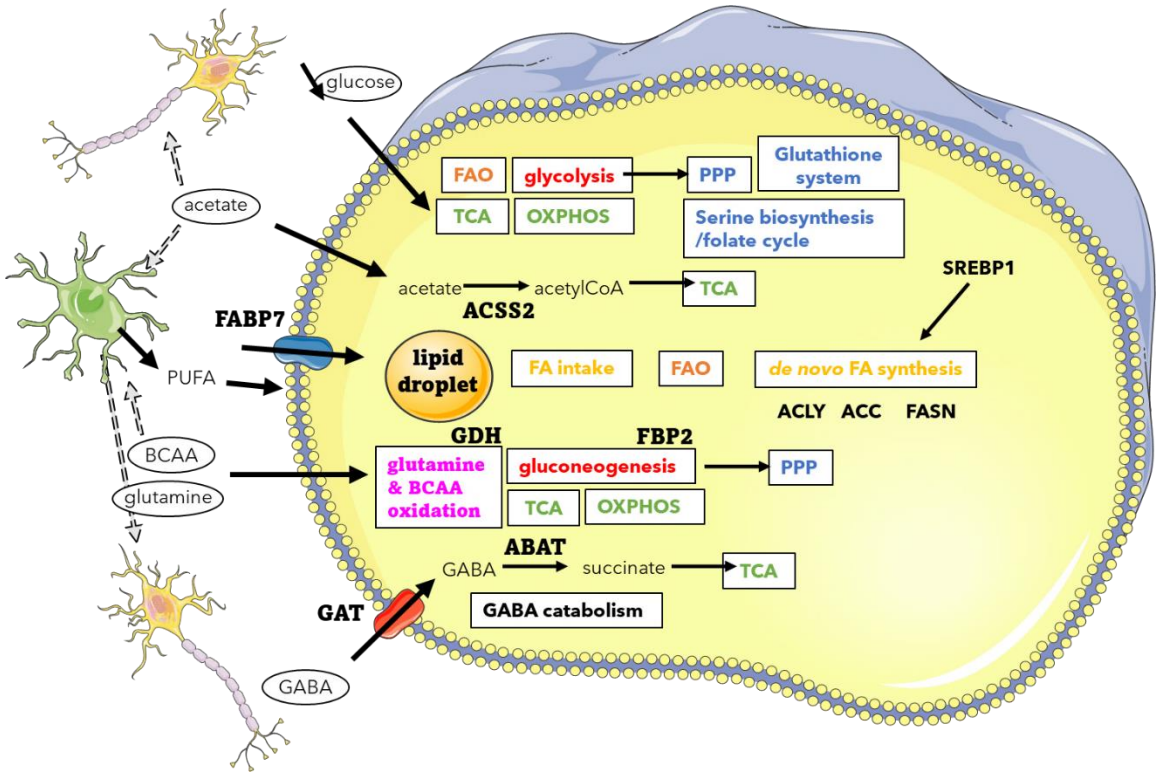


Figure 16. Metabolic adaptations of brain metastasis. Brain metastatic cancer cells display remarkable metabolic adaptations in the metabolism of glucose, acetate, lipids, amino acids and γ aminobutyric acid (GABA), as well as in the pentose phosphate pathway (PPP), serine biosynthesis / folate cycle pathway and in the glutathione system for enhanced redox homeostasis mechanisms. FA(O) – fatty acid (oxidation), TCA – tricarboxylic acid cycle, OXPHOS – oxidative phosphorylation, BCAA – branched-chain amino acid, ACSS2 – acetylCoA synthetase 2, FABP7 – fatty acid binding protein 7, PUFA – polyunsaturated fatty acids, ACLY – ATP-citrate lyase, ACC – acetyl-CoA carboxylase, FASN – fatty acid synthase, SREBP1 – sterol regulatory element-binding protein 1, BCAA – branched-chain amino acid, GDH – glutamate dehydrogenase, FBP2 – fructose-1,6-bisphosphatase 2, GAT – GABA transporter, ABAT – GABA transaminase

Metastatic progenitor cells with the ability to exploit endogenous brain substrates and/or substrates secreted by host cells thrive in the **brain microenvironment**. Acquiring neuron-like properties may be associated to **metabolic adaptations** facilitating growth in the brain.

II. AIM OF THE THESIS

My thesis work focused on identifying metabolic characteristics of metastatic breast cancer cells responsible for selective homing into the brain. More specifically, we addressed the question of **metabolism as a possible driver of metastatic organotropism**, following the seed and soil theory. The objective of the study was therefore **to identify metabolic protein(s), enzyme(s) or transporter(s), responsible for the brain tropism of metastatic progenitor cells** derived from human metastatic TNBCs.

The models used were the parental MDA-MB-231 human metastatic TNBC cell line and its two brain-specific metastatic variants 231-BR and 231-BR-2 that were generated independently of each other. MDA-MB-231 is a highly aggressive, invasive and poorly differentiated cell line (Liu 2003, Chavez 2010) exhibiting a claudin-low phenotype, a CSC phenotype (CD44+/CD24-), and an endothelial-like morphology with invasive stellate projections (Kenny 2007, Holiday 2011, Harrell 2014). It originates from a pleural effusion of a mammary adenocarcinoma-bearing 51-year-old patient (Cailleau 1978). Brain-trophic cell lines were generated by serial cycles of *in vivo* selection in female nude mice (**Figure 17**), involving consecutive intracardiac (left ventricle) injections of the parental cancer cells, retrieval of cells that had metastasized to the brain, *in vitro* expansion of collected metastatic cancer cells and reinjection of these cells in next animals for several rounds of selection, until metastatic dissemination was only observed in the brain. These cells are thus considered to be brain-specific metastatic variants (Yoneda 2001, Patel 2011, Burnett 2015). 231-BR was obtained from the laboratory of P. Steeg and had already been extensively used in literature (Yoneda 2001, Patel 2011, Burnett 2015). 231-BR-2 was not yet published, but was generated by the same group than Burnett *et al.*, totally independently of 231-BR, to obtain a brain-specific variant of their own in parallel to the lung/adrenal gland/bone/liver-specific variants that they had previously generated (Burnett 2015).

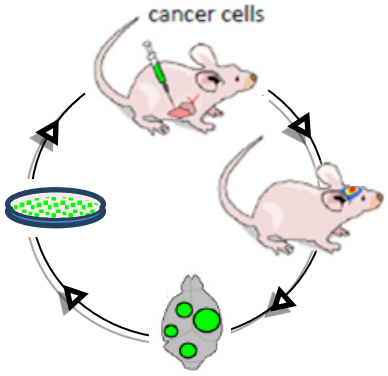


Figure 17. Cycles of *in vivo* selection for the generation of brain-specific metastatic variants. Intracardiac injections of the parental cancer cells, retrieval of cells that had metastasized to the brain, *in vitro* expansion of collected metastatic cancer cells and reinjection of these cells in next animals for serial rounds of selection. Adapted from Valiente 2018.

Our **general aim** was to identify differentially expressed metabolic enzyme(s) and/or transporter(s) controlling brain-specific breast cancer metastasis in our cell models, as potential target(s) for anticancer therapy.

Specific Aim 1: comparative metabolic analyses,

Specific Aim 2: comparative genetic analyses,

Specific Aim 3: identification of differentially expressed metabolic enzyme(s) and/or transporter(s),

Specific Aim 4: functional *in vivo* validation of metabolic enzymes/transporters that control the brain-specific metastasis of MDA-MB-231 variants.

Clinical perspective: to impede brain colonization by metastatic cancer cells.

Long-term perspective: extension to human cervix and pancreatic cancer models.

III. RESULTS

cancers

MDPI

Article

Mitochondrial Protein Cox7b Is a Metabolic Sensor Driving Brain-Specific Metastasis of Human Breast Cancer Cells

Marine C. N. M. Blackman [1], Tania Capeloa [1], Justin D. Rondeau [1], Luca X. Zampieri [1], Zohra Benyahia [1], Justine A. Van de Velde [1], Maude Fransolet [2], Evangelos P. Daskalopoulos [3], Carine Michiels [2], Christophe Beauloye [3] and Pierre Sonveaux [1,4,*]

[1] Pole of Pharmacology and Therapeutics, Institut de Recherche Expérimentale et Clinique (IREC), Walloon Excellence in Life Sciences and Biotechnology (WELBIO), Université Catholique de Louvain (UCLouvain), Avenue Hippocrate 57 Box B1.53.09, 1200 Brussels, Belgium
[2] URBC-NARILIS, University of Namur, 5000 Namur, Belgium
[3] Pole of Cardiology, Institut de Recherche Expérimentale et Clinique (IREC), Université Catholique de Louvain (UCLouvain), Avenue Hippocrate 55 Box B1.55.05, 1200 Brussels, Belgium
[4] Walloon Excellence in Life Sciences and Biotechnology (WELBIO) Research Institute, 1300 Wavre, Belgium
* Correspondence: pierre.sonveaux@uclouvain.be

Simple Summary: What controls organotropism during cancer metastasis is still largely unknown. The "seed-and-soil hypothesis" of Stephen Paget (1889) proposes that metastatic onset strictly depends on a match between the needs of a given metastatic progenitor cell (the seed) and the resources provided by a given organ (the soil). Here, we decided to challenge this old theory in the context of cancer metabolism. Considering that metastasis can be prevented, we focused on triple-negative breast cancer brain metastasis. Comparing RNAseq data from wild-type human cancer cells and two independent brain-seeking variants, we identified cyclooxygenase 7b (Cox7b) in Complex IV of the mitochondrial electron transport chain as a driver of triple-negative breast cancer brain metastasis. Cox7b is not an easy therapeutic target and is most probably not unique in driving brain metastasis. Therefore, our general approach could be used to identify other metabolic proteins responsible for organotropism and amenable for metastasis-prevention therapy.

Abstract: Distant metastases are detrimental for cancer patients, but the increasingly early detection of tumors offers a chance for metastasis prevention. Importantly, cancers do not metastasize randomly: depending on the type of cancer, metastatic progenitor cells have a predilection for well-defined organs. This has been theorized by Stephen Paget, who proposed the "seed-and-soil hypothesis", according to which metastatic colonization occurs only when the needs of a given metastatic progenitor cell (the seed) match with the resources provided by a given organ (the soil). Here, we propose to explore the seed-and-soil hypothesis in the context of cancer metabolism, thus hypothesizing that metastatic progenitor cells must be capable of detecting the availability of metabolic resources in order to home in a secondary organ. If true, it would imply the existence of metabolic sensors. Using human triple-negative MDA-MB-231 breast cancer cells and two independent brain-seeking variants as models, we report that cyclooxygenase 7b (Cox7b), a structural component of Complex IV of the mitochondrial electron transport chain, belongs to a probably larger family of proteins responsible for breast cancer brain tropism in mice. For metastasis prevention therapy, this proof-of-principle study opens a quest for the identification of therapeutically targetable metabolic sensors that drive cancer organotropism.

Keywords: breast cancer; brain metastasis; tissue-specific metastasis; organotropism; cancer metabolism; oxidative phosphorylation (OXPHOS); mitochondria; cyclooxygenase 7b (Cox7b)

check for updates

Citation: Blackman, M.C.N.M.; Capeloa, T.; Rondeau, J.D.; Zampieri, L.X.; Benyahia, Z.; Van de Velde, J.A.; Fransolet, M.; Daskalopoulos, E.P.; Michiels, C.; Beauloye, C.; et al. Mitochondrial Protein Cox7b Is a Metabolic Sensor Driving Brain-Specific Metastasis of Human Breast Cancer Cells. *Cancers* **2022**, *14*, 4371. https://doi.org/10.3390/cancers14184371

Received: 8 August 2022
Accepted: 5 September 2022
Published: 8 September 2022

Publisher's Note: MDPI stays neutral with regard to jurisdictional claims in published maps and institutional affiliations.

Copyright: © 2022 by the authors. Licensee MDPI, Basel, Switzerland. This article is an open access article distributed under the terms and conditions of the Creative Commons Attribution (CC BY) license (https://creativecommons.org/licenses/by/4.0/).

1. Introduction

Entry in the metastatic phase often represents a point of no return for cancer patients, as it is associated with a transition from curative to palliative care. This is mainly due to a limitation of therapeutic options, as local treatments are not always an option for (poly)metastatic patients, and secondary tumors are generally more resistant to treatments than primary tumors [1]. Treating brain metastasis offers the additional challenge of blood–brain barrier (BBB) protection in an initially immunopreserved environment [2]. Consequently, poorly symptomatic cancers that are often detected at an advanced, post-metastatic stage are associated with poor 5-year overall survival rates, while slowly evolutive cancers that are commonly detected at the premetastatic stage are, in contrast, associated with much longer patient survival rates. Between these two extremes, improvements of detection methodologies and their systematic use in individuals at risk allow an early detection of some aggressive types of cancers. This is typically the case of triple-negative breast cancer (TNBC), which is most often detected at the premetastatic stage [3]. However, these cancers usually evolve quite rapidly despite early treatment delivery, and distant metastases have a high prediction to occur. About 35% of TNBC patients develop metastases in the course of the disease, despite surgery, chemotherapy, and radiotherapy [4]. Furthermore, immunotherapy with checkpoint inhibitors has only shown modest efficacy in a subset of patients [5]. Overall, polymetastatic TNBC is currently still regarded as a largely incurable disease [6].

While the vast majority of solid tumors primarily colonize regional lymph nodes, distant metastases do not occur randomly: different cancer types present different metastatic patterns, with different frequencies. For example, malignant melanomas preferentially metastasize to the lungs (frequency of 85%, including micrometastases), the liver (54–77%), the gastrointestinal tract (~60%), the brain (36–54%), the bones (23–49%), and distant skin and subcutis (~18%) [7–9]. In the case of TNBC, metastases occur in the central nervous system (~46% of patients), lungs (~41%), liver (~29%), bones (~24%), and breast or chest wall (~22%) [10]. Brain metastasis is particularly detrimental, with a median patient survival time of 4 to 7 months [10,11]. These numbers further highlight that several organs can be colonized at the same time. Thus, in both cases, a large proportion of patients that were metastasis-free at diagnosis become polymetastatic over the course of the diseases.

Among circulating tumor cells (CTCs), only a minority, termed "metastatic progenitor cells" [12,13], possess all the characteristics that are mandatory to successfully establish a metastasis. The preference of these cells for a limited panel of secondary organs has been theorized by Stephen Paget [14] in 1889 and revisited several times since then (see reference [15] for a recent review). In the "seed and soil" hypothesis, Paget proposed that metastases do not occur randomly in secondary organs but, rather, colonize a given organ based on a match between the needs of a (sub)population of metastatic progenitor cells ("the seed") and the resources provided by the secondary organ ("the soil"). His proposition highlighted the importance of the tumor microenvironment at both primary and secondary tumor locations. Further interpretation also suggests the possible coexistence of several different populations of metastatic progenitor cells with different tropisms for secondary organs in the same patient.

So, what does the seed-and-soil hypothesis implicate? On the one hand, the capabilities of metastatic progenitor cells would depend on the genetic and epigenetic characteristics inherited from their tissue of origin as well as from genetic and epigenetic changes acquired over time, from the onset of malignancy until dissemination. Indeed, metastatic progenitor cells are, nowadays, consensually believed to originate from metabolically hostile cancer areas characterized by a combination of hypoxia, nutrient deprivation, and metabolic waste accumulation causing, e.g., microenvironmental acidification [16–23]. Each parameter, per se, contributes to the metastatic switch, defined as a discrete event converting non-metastatic cancer cells to their metastatic version [24]. However, it is the coexistence of these parameters and their fluctuation over time and space that constitutes an ideal situation for cancer cell adaptation and evolution, which both necessitate environmental changes

to operate [25]. The outcome of these processes is the generation of subsets of cancer cells that simultaneously possess mesenchymal characteristics, resist anoïkis, migrate and invade directionally, resist redox and shear stresses in the systemic circulation, and possess stem cell characteristics [26]. On the other hand, resources available at the secondary site would depend not only on the basal composition and mode of function of the organ to be colonized but also on the organ's "education" by the primary tumor, a paradigm formulated as "premetastatic niche" formation [27]. In the process, cancer cells at the initial site produce and secrete soluble factors (including, e.g., VEGF-A, PLGF, G-CSF, CCL2, TGFβ, TNF, and enzymes such as lysyl oxidase that remodel the extracellular matrix) and exosomes that modify the composition and integrity of the secondary site (see reference [28] for a detailed review). As a result, vascular leakiness is increased; resident cells, such as fibroblasts, modify their behavior; non-resident cells, such as bone-marrow-derived cells and neutrophils, are recruited; a proinflammatory milieu offering immunoprotection is formed; and the structure of the extracellular matrix is remodeled to yield a provisional matrix promoting cell migration, invasion, and, hence, colonization [28].

The homing of metastatic progenitor cells at the secondary site is facilitated by the enhanced permeability of blood vessels lining premetastatic niches. In an active process, CTCs expressing E-selectin ligands (that may include CD44, PSGL-1, ESL-1, β2-integrins, and L-selectin [29]) roll on and adhere on endothelial cells expressing E-selectin at their luminal surface, extravasate (which may require proteolytic activities by CTCs, especially to cross the BBB during brain metastasis [30]), and invade the niche. There, they anchor to host cells and undergo a process of differentiation to generate a secondary tumor. Intravascular metastasis is a rare event.

In the general context of metastasis, we previously observed that mitochondria act as metabolic sensors of the primary tumor microenvironment, producing superoxide and activating the prometastatic transforming growth factor β (TGFβ) pathway in metabolically hostile tumor microenvironments [31]. Inactivating mitochondrial superoxide with specific drugs MitoTEMPO or MitoQ blocked the metastatic process as a whole [13,31,32]. Others showed that transferring superoxide-producing mitochondria from metastatic to nonmetastatic cancer cells was sufficient to turn recipient cells into metastatic progenitor cells [33]. In the context of the seed-and-soil hypothesis, we, therefore, hypothesized that a successful metastatic process would require a match between the metabolic needs of a given subset of metastatic progenitor cells and the availability of specific metabolites at a given secondary site. In other words, we propose that the metabolic preferences of a metastatic progenitor cell would participate in, and perhaps drive, organotropism. Thus, metabolic pairing between different "seeds" and different "soils" would be responsible for the existence of a restricted panel of secondary sites for a given tumor type.

This study on brain tropism is the first of a series addressing this general hypothesis. Using the human TNBC MDA-MB-231 cell line as a working model, we report a cause–effect relationship between the expression of cyclooxygenase 7b (Cox7b) in Complex IV of the electron transport chain (ETC) of metastatic progenitor cells and the brain tropism of these cells. In brain-seeking variants, Cox7b expression enhances oxidative phosphorylation (OXPHOS), while, compared to other organs, the brain is well-known to be enriched in OXPHOS substrates glucose, lipids, and lactate. Cox7b most probably belongs to a larger family of proteins driving brain metastasis, and other organs would offer other substrates to other subsets of metastatic progenitor cells, which could lead to the potential identification of several targets for the therapeutic prevention of tissue-specific metastasis.

2. Materials and Methods

2.1. Chemicals and Reagents

Unless stated otherwise, all chemicals and reagents were from Sigma-Aldrich (Overijse, Belgium).

2.2. Cells and Cell Culture

Parental MDA-MB-231 human triple-negative breast adenocarcinoma cancer cells were from Caliper (Mechelen, Belgium; catalogue #119369). MDA-MB-231-derived brain-seeking variants 231-BR [34] and 231-BR-2 [35,36] were kind gifts from Patricia Steeg (National Cancer Institute, Bethesda, MD, USA) and Harikrishna Nakshatri (Indiana University School of Medicine, Indianapolis, IN, USA), respectively. Cells were routinely cultured in DMEM containing glutaMAX and 4.5 g/L glucose (Thermo Fisher, Erembodegem, Belgium; catalogue #61965026) supplemented with 10% FBS and maintained at 37 °C in a 5% CO_2 humidified atmosphere. Cells were authenticated using short tandem repeat (STR) profiling (Eurofins Genomics, Ebersberg, Germany).

Human astrocytes (T0281, expressing hTERT), mouse astrocytes (T0289, expressing the SV40 large T antigen), human hepatocytes (T0063, expressing HPV E6/E7, hTERT and MycT58A), and human bronchial epithelial cells (T0753, expressing hTERT and Cdk4) used in migration assays were immortalized cells from Applied Biological Materials Inc. (ABM, Richmond, BC, Canada). Astrocytes were routinely cultured in DMEM with glutaMAX and 4.5 g/L glucose (Thermo Fisher; catalogue #61965026) supplemented with 10% FBS and 5% astrocyte growth supplement (Sanbio, Uden, The Netherlands; catalogue #1852; for human astrocytes only). Hepatocytes were maintained in PriGrow IX medium (ABM; catalogue #TM019) supplemented with 10% FBS and then were progressively transferred to the same medium as cancer cells. Bronchial cells were maintained in Prigrow X medium (ABM; catalogue #TM0753), and then were progressively transferred to bronchial epithelial cell growth medium (BEGM; Lonza, Verviers, Belgium; catalogue #CC-3170).

2.3. Genetic Manipulations

For constitutive luciferase and GFP expression, cells were infected with lentiviruses carrying the luciferase and GFP sequences along with puromycin resistance gene (Amsbio, Alkmaar, The Netherlands; catalogue #LPV020), as detailed in Appendix A.1.

COX7B gene silencing was performed using a CRISPR-Cas9 strategy following Zhang's lab protocol [37], and Cox7b overexpression using the pCMV3 expression vector (Bio-Connect, Te Huissen, The Netherlands; catalogue #HG20762-UT), as detailed in Appendix A.2. and Appendix A.3. pSpCas9(BB)-2A-Puro (PX459) V2.0 and pU6-(BbsI) CBh-Cas9-T2A-mCherry were kind gifts from Feng Zhang (Addgene, Watertown, MA, USA; plasmid #62988) and Ralf Kuehn (Addgene; plasmid #64324), respectively.

2.4. Metastatic Take in Mice

On day 0, 6-week-old female NMRI nude mice (Janvier, Le Genest-Saint-Isle, France) received image-guided intraventricular injections of 100,000 cancer cells, using a Vevo 2100 imaging system (FUJIFILM VisualSonics, Toronto, ON, Canada) equipped with a 30 MHz transducer. Briefly, mice were anesthetized (80 mg/Kg ketamine and 8 mg/Kg xylazine) and secured on the animal platform in supine position, and their thoraxes were shaved. Two-dimensional (2D) parasternal long-axis ultrasound images of the left ventricle were acquired, in order to ascertain the optimal point in the apex of the heart for the intraventricular injection. A microinjector system with a 26G hypodermic needle was used to perform a precise echocardiography-guided intraventricular injection of 100,000 cancer cells constitutively expressing luciferase and GFP. Following injection, the blood flow within the left ventricle was closely observed (and images were recorded), confirming that the cancer cells were successfully injected intraventricularly. All mice were followed-up for a few minutes with echography, to ascertain that the injection did not lead to any injury, and were closely monitored until recovery.

Metastasis development was monitored using a Xenogen IVIS 50 bioluminescence imaging system (PerkinElmer, Seer Green, UK) and quantified with Living Image software (PerkinElmer). Every week, mice were injected i.p with 0.15 mg/g bodyweight of luciferin (PerkinElmer) and were anesthetized using isoflurane after a 10-min incubation. Chemiluminescence was detected with a 1–12 s acquisition time. Mice were sacrificed after

4 weeks by cervical dislocation under terminal anesthesia, and organ chemiluminescence was acquired ex vivo before fixation in 4% paraformaldehyde (PFA).

2.5. Cell Migration and Invasion

Corning transwell inserts (Avantor, Leuven, Belgium; catalogue #62406-198) were used to measure cell migration and invasion capacities, as detailed in Appendix A.4. FBS 1% (general migration/invasion) or confluent nonmalignant cells (astrocytes, hepatocytes, bronchial cells) seeded in the lower chamber were used as chemoattractants.

2.6. Cell Numbers

Cell numbers were determined over time on a SpectraMax i3 spectrophotometer equipped with a MiniMax imaging cytometer (Molecular Devices, Munich, Germany), after seeding 5000 cells per well in a 96-well plate. Results were normalized to initial cell numbers.

2.7. Metabolic Assays

Oxygen consumption rates (OCRs) were measured on a Seahorse XF96 bioenergetics analyzer using the XF Cell Mito Stress Test Kit and the Fuel Flex test kit, in accordance with the instructions of the manufacturer (Agilent, Machelen, Belgium). Details are provided in Appendix A.5. Glucose and lactate concentrations were measured using an enzymatic CMA600 analyzer (Aurora Borealis, Schoonebeek, The Netherlands), in accordance with the instructions of the manufacturer, in the supernatant of 150,000 (for 24 h assays) and 250,000 (for 48 h assays) cells seeded in exactly 1 mL of culture medium. Wells containing medium only were used as controls for the calculation of glucose consumption and lactate production. The ATP content of 10,000 cells per well (96-well plate) was measured using the Cell titer Glo assay of Promega (Leiden, The Netherlands; catalogue #G7570). All metabolic measurements were normalized to total protein content determined after overnight incubation with 0.5 M NaOH using the Bio-Rad protein assay (Temse, Belgium; catalogue #5000006) on a SpectraMax i3 spectrophotometer equipped with a MiniMax imaging cytometer.

2.8. Electron Microscopy

Cells were collected and resuspended in 400 µL of a 2.5% glutaraldehyde solution containing 0.1 M of sodium cacodylate at pH 7.4 in a pyramidal BEEM capsule (Agar Scientific, Stansted, UK; catalogue #G360). Samples were then processed as previously described [38]. Images were acquired on a TECNAI G^2 20 LaB6 transmission microscope (Field Electron and Ion Company, Hillsboro, OR, USA).

2.9. Mitochondrial Abundance and Mitochondrial DNA Content

Mitochondrial DNA (mtDNA) content was measured using RT-qPCR as previously described [39]. Briefly, total DNA was isolated with a QIAmp DNA kit (Qiagen, Antwerp, Belgium). The 12S-rRNAA mitochondrial gene (forward primer: 5′-GTA CCC ACG TAA AGA CGT TAG G-3′; reverse primer: 3′-TAC TGC TAA ATC CAC CTT CG-5′; labeled probe: 5′-CCC ATG AGG TGG CAA GAA AT-3′ FAM), in parallel with nuclear gene RNAseP (RNAseP VIC-labeled probe; Thermo Fisher Scientific; catalogue #4401631), were then analyzed by RT-qPCR (50 ng of sample and 1 µL of each primer pair [10µM]), with TaqMan universal master mix II with UNG (Thermo Fisher). For presentation, mtDNA content was normalized to nuclear DNA (nDNA) content [40].

2.10. Microarray Database Analysis

According to Gene Expression Omnibus (GEO) and reference [36], database #GSE66495 reports on the whole genome expression, determined using Illumina Human HT-12 V4 expression beadchips, of MDA-MB-231 parental cells and tissue-specific metastatic variants derived thereof (including 231-BR), which were maintained in MEM with 10% FBS. For

database reanalysis, we first extracted metabolic genes related to glycolysis, OXPHOS, and the TCA cycle. We next retained only genes that were differentially expressed ($p < 0.05$, using one-way ANOVA) in brain (231-BR), adrenal (ADMD-231), bone (BMD-231) and/or lung (LMD-231) metastatic variants, compared to parental MDA-MB-231 cells. They are displayed in Table 1. We then identified the genes that were differently expressed ($p < 0.05$, using one-way ANOVA) in 231-BR versus ADMD-231, BMD-231, and LMD-231 cells. Expression changes were independently confirmed by RT-qPCR using fresh lysates from brain-seeking variants 231-BR and 231-BR-2 and MDA-MB-231 parental cells.

Table 1. Metabolic genes differentially expressed in 231-BR versus other tissue-specific variants of parental MDA-MB-231 human breast cancer cells.

Gene ID	231-BR (Brain-Seeking)	ADMD-231 (Adrenal-Glands-Seeking)	BMD-231 (Bone-Seeking)	LMD-231 (Lung-Seeking)	p [4]	p [5]
HK2 [1]	**1.62** [2,3]	**1.83**	**1.66**	**1.70**	>0.05	>0.05
ALDH1A3	1.18	**1.53**	**1.43**	**1.48**	<0.05	>0.05
ALDH9A1	**1.55**	1.04	1.07	1.09	>0.05	<0.05
ALDH3A1	**1.18**	1.03	1.21	1.16	>0.05	>0.05
PCK2	1.08	−1.43	**−1.21**	**−1.33**	<0.05	<0.05
IDH1	−1.18	**−1.31**	−1.13	−1.14	>0.05	>0.05
FH	**1.54**	1.08	1.04	1.11	>0.05	<0.05
MDH2	−1.10	**−1.19**	**−1.17**	−1.27	>0.05	>0.05
ATP5I	1.25	**1.36**	**1.33**	1.33	>0.05	>0.05
ATP5G2	−1.06	**−1.21**	−1.07	−1.11	>0.05	>0.05
ATP6V0E2	**1.62**	1.43	1.41	1.34	>0.05	>0.05
ATP6V1D	1.69	**2.45**	1.83	1.96	>0.05	>0.05
ATP6V0D1	−1.02	**−1.23**	−1.14	−1.11	>0.05	>0.05
ATP6V0D2	**1.21**	1.08	1.03	1.20	>0.05	>0.05
ATP6V1B1	**1.25**	−1.09	−1.07	1.03	<0.05	<0.05
COX17	−1.47	−1.46	**−1.50**	−1.52	>0.05	>0.05
COX7B	**2.02**	1.06	−1.06	−1.20	<0.05	<0.05
NDUFB7	1.45	**1.54**	1.27	1.21	>0.05	>0.05
NDUFB8	**−1.43**	**1.46**	**1.45**	**1.54**	<0.05	<0.05
NDUFV3	1.10	**1.51**	1.42	1.37	>0.05	>0.05
UQCRB	**1.31**	1.05	1.27	1.30	>0.05	>0.05
PGM5	−1.11	**6.42**	**4.32**	**4.51**	<0.05	<0.05

[1] From the GEO #GSE66495 microarray database ($n = 3$ per cell line), including only those genes involved in glycolysis, the TCA cycle, and oxidative phosphorylation. [2] Numbers report on fold changes, compared to parental MDA-MB-231 cells used as control. [3] Bold numbers are fold changes with $p < 0.05$ compared to parental MDA-MB-231 cells using one-way ANOVA. [4] p value for 231-BR compared to all other tissue-seeking variants using one-way ANOVA. [5] p value for 231-BR compared to all other tissue-seeking variants and parental cells using one-way ANOVA. Genes of interest ($p < 0.05$) are highlighted in gray.

2.11. Real-Time Quantitative PCR

Total RNA was collected using the NucleoSpin RNA kit (Filter Service, Eupen, Belgium; catalogue #740955.50), quantified with a NanoDrop 1000 Spectrophotometer (Thermo Fisher), and reverse-transcribed in cDNA with the RevertAid First Strand cDNA synthesis kit (Thermo Fisher; catalogue #K1621), using the same quantity (500–1000 ng) for all RNA samples and a 90-min incubation time. cDNAs were diluted 1:10 in DNase/RNase-free distilled water (Thermo Fisher), and 2 µL were used with 5 µL of 2X Takyon qPCR Master Mix and 0.2 µL of each primer (10 µM) and completed to 10 µL with water for RT-qPCR analysis (ViiA 7417 Real-Time instrument, Thermo Fisher). Primers were: *ALDH9A1* Forward 5′-AAG GAG CAG GGT GCT AAA GT-3′ and Reverse 5′-TCG TCT CTG CAA TTA GTT AAT ACA C-3′; *FH* Forward 5′-TGC CAA CCC CAG TTA TTA AAG C-3′ and Reverse 5′-CTT CAG CTA CCT CAT CTG CTG-3′; *NDUFB8* Forward 5′-CGG ATG ATG GCA TGG GGT A-3′ and Reverse 5′-GGT GCC AGT GCA TCG GTT-3′; *COX7B* Forward 5′-TAC CTG AAG CGA ATT GGC AC-3′ and Reverse 5′-GCT TCG AAC TTG GAG ACG

AT-3′; and *β-actin* Forward 5′-CCC GCG AGC ACA GAG C-3′ and Reverse 5′-TCA TCA TCC ATG GTG AGC TGG- 3′. All gene expression data were normalized to *β-actin* gene expression.

2.12. Western Blotting

Western blotting was performed, as previously described [41], after protein collection in RIPA buffer containing phosphatase (PhosSTOP) and protease (proteases inhibitor cocktail) inhibitors. Membranes were incubated overnight with primary rabbit antibodies against ALDH9A1 (Proteintech; catalogue #26621), FH (BIOKE, Leiden, The Netherlands; catalogue #4567S), NDUFB8 (Proteintech, Manchester, UK; catalogue #14794), COX7b (Abcam, Cambridge, UK; catalogue #ab137094), and Vinculin (BIOKE; catalogue #4650S), or mouse antibodies against β-actin (Sigma-Aldrich; catalogue #A5441). Staining was revealed with an Amersham Imager 600 (Diegem, Belgium). All data are normalized to vinculin or β-actin expression.

2.13. Immunohistochemistry

Brains were collected, cut along the separation between right and left hemispheres, and embedded in paraffin. Sections (5 µm thick) were performed from the center of each hemisphere, to produce 10 slides for each sample. For each hemisphere, 3 slides from the beginning, the middle, and the end were used for immunostaining, and the process was repeated up to 3 times in order to analyze slices representative of the whole brain.

Brain sections were immunostained for GFP (Bio-Techne, Abingdon, UK; catalogue #600-308; BIOKE; catalogue #2956), with a secondary Envision anti-rabbit antibody coupled to HRP (Agilent; catalogue #K4003), and hematoxylin and eosin counterstained. Slides were scanned at 20x magnification with a SCN400 bright field Slide Scanner (Leica Biosystems, Diegem, Belgium). Metastasis number and surface area were determined using cytomine (Liège, Belgium; cytomine.org; accessed on 1 December 2021) and QuPath software version 0.1.2 (Belfast, UK) [42].

2.14. Clinical Database Analysis

Overall Survival (OS) curves were generated on Kaplan–Meier plotter (kmplot.com) with the auto select best cutoff for the 202110 Affy ID (*COX7B*) on the RNA-seq mRNA dataset (breast cancer and renal clear cell carcinoma in pan-cancer) and on gene chip mRNA datasets for lung cancers [43]. Sources for the databases include GEO, EGA, and TCGA.

2.15. Statistics

Data are shown as means ± SEM (error bars are sometimes smaller than symbols) or as individual values with the median. n indicates the total number of replicates per group/condition. Graphpad Prism version 9.2.0. (San Diego, CA, USA) was used for statistical analyses. Mann–Whitney U test, Student's t-test, one-way ANOVA, and two-ways ANOVA were used where indicated. $p < 0.05$ was considered to be statistically significant.

3. Results

3.1. Validation of Brain-Seeking Variant Models Derived from Human MDA-MB-231 Triple-Negative Breast Cancer Cells

The objective of our study was to identify metabolic protein(s) responsible for the brain tropism of human metastatic breast cancer. As models, we used MDA-MB-231 triple-negative breast cancer (TNBC) cells and two independently derived brain-seeking variant cell lines, 231-BR and 231-BR-2 [34–36], which were generated by serial cycles of in vivo selection in mice. The selection protocol involved intracardiac cancer cell injection in the left ventricle of female nude mice, surgical isolation, expansion of metastatic cancer cells retrieved from the brain, and intracardiac injection of these cells sequentially in additional animals for several rounds, until metastatic dissemination became restricted to the brain [34–36]. To identify metabolic drivers of brain-specific metastasis, we first ascertained

the validity of the two model cell lines in vitro and in vivo. Short tandem repeat (STR) profiling confirmed that all variants were genomically similar to the parental MDA-MB-231 cells (Table S1). For in vivo assays, cells were infected with lentiviruses to constitutively express luciferase and green fluorescent protein (GFP). An intracardiac injection of 100,000 MDA-MB-231 parental cells (Figure 1a) did not generate brain metastases in female nude mice, whereas the use of either the 231-BR or 231-BR-2 variants yielded metastases in most animals (4/5 for 231-BR and 6/9 for 231-BR-2) 4 weeks after injection, which were detected by ex vivo bioluminescence imaging on isolated brains (Figure 1b).

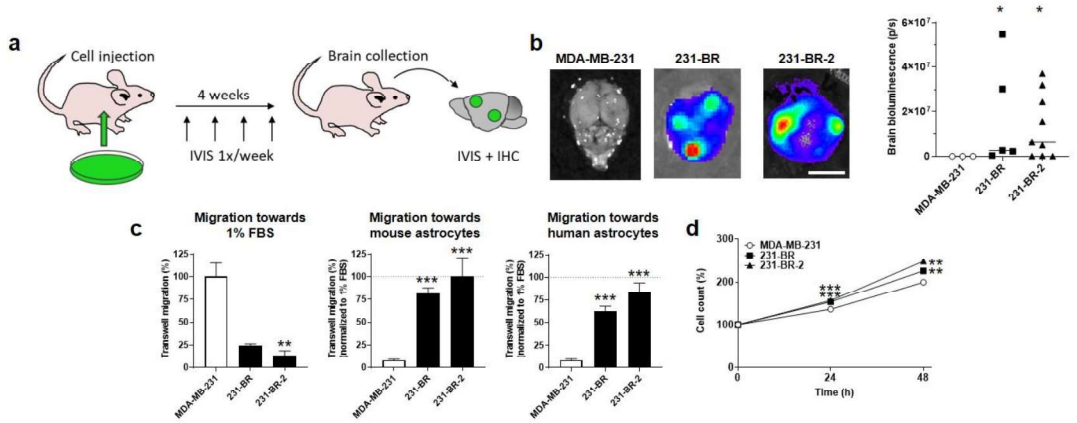


Figure 1. Validation of the brain tropism of MDA-MB-231-derived brain-seeking variants. (**a**) Schematic representation of in vivo experiments, where 6-week-old female mice were injected intracardially with 100,000 luciferase- and green fluorescent protein (GFP)-expressing cancer cells on Day 0, imaged once a week to track metastases, and sacrificed at Week 4 for organ collection, followed by ex vivo bioluminescence imaging and immunohistochemistry. (**b**) Ex vivo bioluminescence imaging of mouse brains at the end of the protocol illustrated in (**a**). Pictures on the left are representative of mouse brains in luciferin-containing medium captured using a Xenogen IVIS 50 bioluminescence imaging system. The right graph shows brain bioluminescence intensity in mice having received parental MDA-MB-231 cancer cells or 231-BR or 231-BR-2 brain-seeking variants (n = 3–9). Bar = 5 mm. (**c**) Migration of MDA-MB-231, 231-BR, and 231-BR-2 cells was assayed in transwells towards 1% FBS (n = 2–3), towards mouse astrocytes (n = 6) or towards human astrocytes (n = 6). (**d**) Cell count (%) over time on a SpectraMax i3 spectrophotometer equipped with a MiniMax imaging cytometer, after seeding 5000 cells per well in a 96-well plate (n = 18–19). Data are shown as individual values and medians (**b**) or as means ± SEM (**c**,**d**). * $p < 0.05$, ** $p < 0.01$, *** $p < 0.005$; compared to MDA-MB-231; using Mann–Whitney test (**b**), one-way ANOVA with Dunnett's post hoc test (**c**), or two-way ANOVA with Dunnett's post hoc test (**d**).

For in vitro model validation, we developed a transwell assay aimed to test the general and organotropic migration of the human breast cancer cells in the upper well towards 1% FBS or towards living immortalized nonmalignant astrocytes in the lower well, respectively. Since the selection of the brain-seeking variants was made in mice, we tested both mouse and human astrocytes as attractants. While parental MDA-MB-231 cells had a higher capacity to migrate towards 1% FBS compared to the two brain-seeking variants, conversely, 231-BR and 231-BR-2 cells migrated much more efficiently towards mouse or human astrocytes (Figure 1c), thus validating their preferential tropism for the brain. Of note, both brain-seeking variants were slightly, yet significantly, more proliferative than the parental cells, as determined by direct cell counting over time (Figure 1d).

3.2. Brain-Seeking Variants of MDA-MB-231 Cells Undergo an Oxidative Switch

Using Seahorse oximetry and the dedicated Fuel Flex test kit of Agilent, we next determine the oxidative metabolic preferences of the parental and brain-seeking variant cells. The assay involves sequential inhibition of glucose-fueled (using 2 μM of mitochondrial pyruvate carrier inhibitor UK5099), glutamine-fueled (using 3 μM of glutaminase 1 inhibitor BPTES), and lipid-fueled (using 4 μM of carnitine palmitoyl-transferase 1A inhibitor Etomoxir) OXPHOS. The results show that OXPHOS in MDA-MB-231 cells was supported almost equally by glutamine (52%) and fatty acids (48%), but not at all by glucose, whereas OPXHOS in the two brain-seeking variants was supported not only by glutamine and fatty acids but also by glucose (5.1 ± 0.6 % for 231-BR and 8.4 ± 1.4% for 231-BR-2 cells) (Figure 2a). Glucose uptake, lactate release, and, hence, the glycolytic ratio ([glucose]/[lactate]) were unchanged in full medium (DMEM containing glutaMAX, 4.5g/L glucose, and 10% FBS) (Figure 2b). Therefore, changes in the capacity to use OXPHOS fuels reflected an increased oxidative flexibility of brain-seeking variants compared to parental cells, rather than an increased dependency on glucose. Accordingly, both 231-BR and 231-BR-2 cell lines presented improved basal and maximal respiration activities as well as an improved oxidative ATP production, compared to parental cells (Figure 2c).

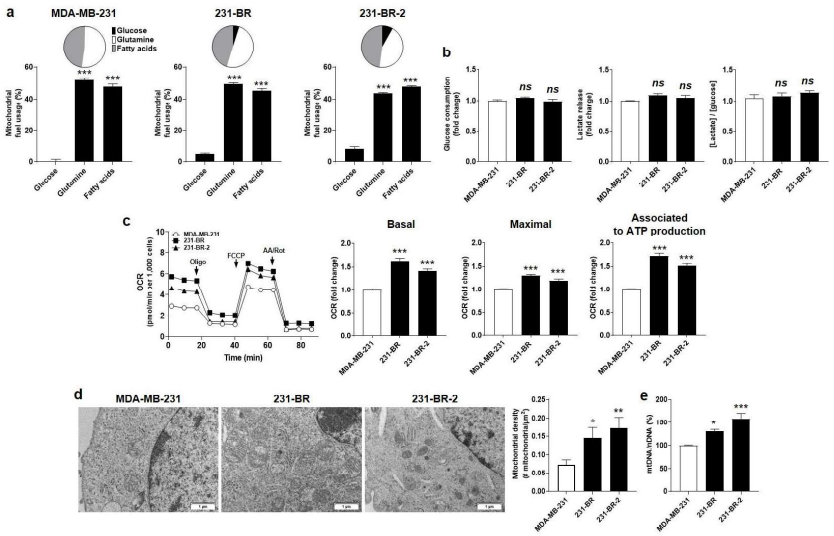


Figure 2. Brain-seeking variants are more oxidative than parental MDA-MB-231 human breast cancer cells. (**a**) Mitochondrial fuel usage of MDA-MB-231 (**left**, n = 14), 231-BR (**middle**, n = 14–16), and 231-BR-2 (**right**, n = 14–15) cancer cells was determined using the Fuel Flex test kit (Agilent) on a Seahorse XF96 bioenergetics analyzer. Data are presented as pie and column graphs, where total fuel usage = 100%. (**b**) Glucose consumption (**left**, n = 11–16), lactate production (middle, n = 16–17), and the lactate/glucose ratio (**right**, n = 13–16) were determined from measurements in deproteinized cell supernatants using an enzymatic CMA600 analyzer. (**c**) Basal (**left**, n = 29–32) and maximal (**middle**, n = 28–32) oxygen consumption rates (mtOCRs), as well as the OCR of the cells associated to mitochondrial ATP production (**right**, n = 29–32), were measured using a XF Cell Mito Stress Test kit (Agilent) on a Seahorse XF96 bioenergetics analyzer. Representative Seahorse traces are shown on far left. (**d**) Transmission electron microscopy pictures of the cells are shown on the left (bars = 1 μm), and the mitochondrial density is quantified on the right graph (n = 6–12). (**e**) Mitochondrial DNA/nuclear DNA (mtDNA/nDNA) cell content determined using RT-qPCR (n = 5). All data are shown as means ± SEM. * $p < 0.05$, ** $p < 0.01$, *** $p < 0.005$, ns: $p > 0.05$; compared to first column; using one-way ANOVA with Dunnett's post hoc test (**a–c**,**e**).

The oxidative switch evidenced in brain-seeking variants was linked to qualitative and quantitative changes affecting mitochondria. Qualitatively, electron microscopy revealed enlarged mitochondria in 231-BR compared to the parental cells, whereas they were smaller but more abundant in 231-BR-2 compared to MDA-MB-231 cells (Figure 2d). The mitochondrial to nuclear DNA ratio (mtDNA/nDNA) was determined using RT-qPCR, revealing a significantly increased mtDNA abundance in both 231-BR and 231-BR-2 compared to the parental cells (Figure 2e). Collectively, we concluded that the oxidative efficiency of mitochondria was increased in the brain-seeking variants of MDA-MB-231 cells.

3.3. Identification of Four Candidate Metabolic Genes That Could Account for the Brain Tropism of Human Breast Cancer Cells

Based on our working hypothesis of a metabolic preference of brain-seeking variants for metabolites present in the brain and on the above evidence of metabolic differences in the filiation, we next aimed to identify metabolic genes/proteins associated to the brain tropism of 231-BR and 231-BR-2 cells. We first analyzed the publicly available microarray database GEO #GSE66495, reporting on the whole genome expression of not only MDA-MB-231 and 231-BR cells but also MDA-MD-231-derived adrenal (ADMD-231), bone (BMD-231), and lung (LMD-231) metastatic variants [36]. We focused on genes involved in glycolysis, the TCA cycle, and OXPHOS.

Using the two-step methodology described in the materials and methods, we identified 22 metabolic genes differentially expressed in at least one metastatic variant compared to parental MDA-MB-231 cells, among which 6 were further differentially expressed in 231-BR cells compared to any other metastatic variant (Table 1). Significantly upregulated genes were *ALDH9A1* (Genbank ID 223, on chromosome 1) encoding aldehyde dehydrogenase 9 family member A1, *FH* (Genbank ID 2271, on chromosome 1) encoding fumarate hydratase, and *COX7B* (Genbank ID 1349, on chromosome X) encoding cytochrome c oxidase subunit 7B. Significantly downregulated genes were *ALDH1A3* (Genbank ID 220, on chromosome 15) encoding aldehyde dehydrogenase 1 family member A3, *NDUFB8* (Genbank ID 4714, on chromosome 10) encoding NADH:ubiquinone oxidoreductase subunit B8, and *PGM5* (Genbank ID 5239, on chromosome 9) encoding phosphoglucomutase 5.

Among the six genes, *ALDH1A3* and *PGM5* expression was not significantly different ($p > 0.05$) between 231-BR and parental MDA-MB-231 cells (Table 1). They were, therefore, excluded from further analysis.

3.4. Cytochrome c Oxidase Subunit 7b in Mitochondrial Complex IV Is a Candidate Protein Supporting the Brain Tropism of Human Breast Cancer Cells

We next aimed to validate our short list of four genes: *ALDH9A1*, *FH*, *NDUFB8*, and *COX7B*. To avoid idiosyncrasies that would have been associated to 231-BR cells, changes in gene expression were independently tested using RT-qPCR in both 231-BR and 231-BR-2 brain-seeking variants. We further verified that the changes in protein matched the changes in mRNA expression. Uncropped western blots are displayed in Figure S1.

ALDH9A1 encodes a cytosolic aldehyde dehydrogenase that catalyzes the oxidation of γ-aminobutyraldehyde and aminoaldehydes derived from polyamines. It is involved in carnitine biosynthesis [44], which facilitates the transport of fatty acids across the inner mitochondrial membrane for β-oxidation and, potentially, in a marginal pathway for the biosynthesis of neurotransmitter γ-aminobutyric acid (GABA) [45] (Figure 3a, left). Compared to parental MDA-MB-231 cells, *ALDH9A1* mRNA expression was significantly increased in 231-BR, but it was slightly decreased in 231-BR-2 cells (Figure 3a, middle). The corresponding protein was overexpressed in 231-BR but not in 231-BR-2 cells (Figure 3a, right), which disqualified it as a shared metabolic sensor for brain tropism in our model cell lines.

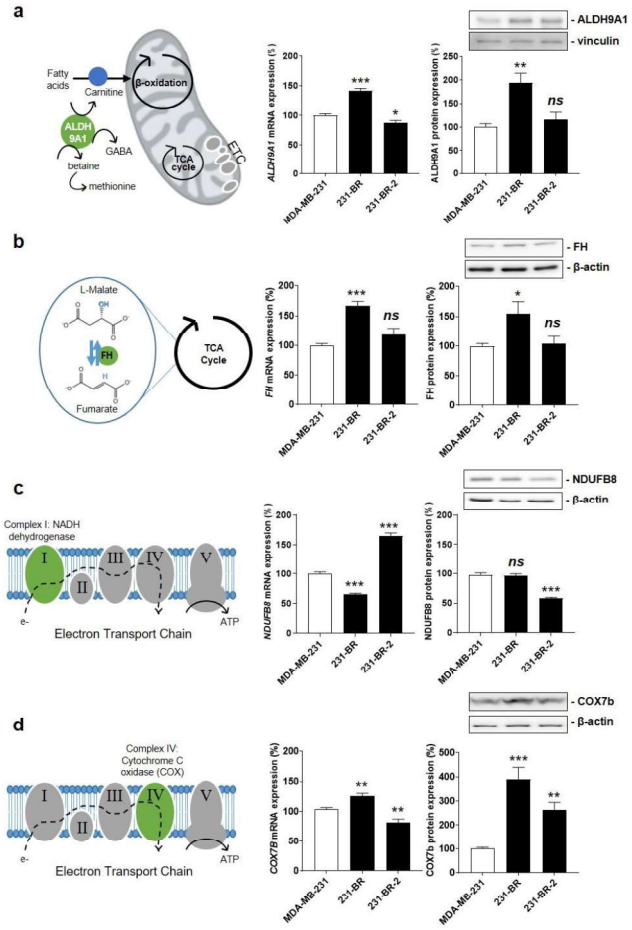


Figure 3. Identification of Cox7b as a candidate protein for the brain tropism of human breast cancer. (**a**) The left drawing depicts the three main functions of aldehyde hydrogenase 9A1 (ALDH9A1) that catalyzes the biosynthesis of γ-aminobutyric acid (GABA) in the cytosol, the biosynthesis of carnitine to facilitate the transport of fatty acids across the inner mitochondrial membrane, and the oxidation of γ-aminobutyraldehyde and aminoaldehydes derived from polyamines in the mitochondrial matrix. The middle graph shows *ALDH9A1* mRNA expression normalized to *β-actin* (n = 5–6), and the right graph shows ALDH9A1 protein expression normalized to vinculin (n = 6), in MDA-MB-231, 231-BR, and 231-BR-2 cancer cells. (**b**) The left drawing depicts fumarate hydratase (FH) activity, which catalyzes the reversible hydration of fumarate to malate in the TCA cycle. The middle graph shows *FH* mRNA expression normalized to *β-actin* (n = 5–6), and the right graph shows FH protein expression normalized to β-actin (n = 9). (**c**) The left drawing localizes NDUFB8 as a component of electron transport chain (ETC) Complex I (green). The middle graph shows *NDUFB8* mRNA expression normalized to *β-actin* (n = 6), and the right graph shows NDUFB8 protein expression normalized to β-actin (n = 3). (**d**) The left drawing depicts cyclooxygenase 7b (COX7b) as a component of ETC Complex IV (green). The middle graph shows *COX7B* mRNA expression normalized to *β-actin* (n = 5–6), and the right graph shows Cox7b protein expression normalized to β-actin (n = 9). All data are shown as means ± SEM. * $p < 0.05$, ** $p < 0.01$, *** $p < 0.005$, ns: $p > 0.05$; compared to MDA-MB-231 cells; using one-way ANOVA with Dunnett's post hoc test (**a–d**).

FH encodes fumarate hydratase, the seventh enzyme of the TCA cycle that catalyzes the hydration of fumarate to *L*-malate (Figure 3b, left). When mutated/inactivated, FH can cause various diseases, including hereditary and sporadic forms of cancer [46]. In the context of brain-specific breast cancer metastasis, FH mRNA and protein expression was increased in 231-BR but not in 231-BR-2 cells (Figure 3b, middle and right), thus disqualifying this enzyme as a shared metabolic sensor for brain tropism.

NDUFB8 encodes an accessory subunit of NADH ubiquinone oxidoreductase, a large protein complex known as ETC Complex I at the inner mitochondrial membrane (Figure 3c, left). The subunit is bound to NADH dehydrogenase 5 (ND5) in the proton-pumping module of Complex I [47]. Similar to microarray data analysis, RT-qPCR showed significantly reduced *NDUFB8* mRNA expression in 231-BR compared to MDA-MB-231 cells (Figure 3c, middle). However, it was significantly increased in 231-BR-2 cells, and the changes in protein expression did not match the changes in mRNA expression (Figure 3c, middle and right). Overall, this disqualified NDUFB8 as a metabolic sensor for brain-selective metastasis.

COX7B encodes subunit 7b of cytochrome c oxidase (Cox), a large protein complex known as ETC Complex IV that catalyzes the transfer of electrons from reduced cytochrome c to molecular oxygen at the inner mitochondrial membrane (Figure 3d, left) [48]. Cox7b is a short 80 amino acid protein that stabilizes the complex and modulates Cox activity [49]. *COX7B* mRNA expression was increased in 231-BR but decreased in 231-BR-2 cells (Figure 3d, middle). However, the expression of the corresponding protein was increased in both variants (Figure 3d, right). Considering that among the four candidate proteins only Cox7b expression showed a similar change in both brain-seeking variants, we retained Cox7b for further investigation.

3.5. Cox7b Expression Drives Human Breast Cancer Cell Migration towards Astrocytes

Transwell migration assays were used to establish a causal link between Cox7b expression and MDA-MB-231 brain chemoattraction, mimicked by cell migration towards immortalized human and mouse astrocytes. Chemoattraction at other important metastatic sites [34] was mimicked by immortalized human hepatocytes (T0063) and human bronchial epithelial cells (T0763). All four cell lines were nonmalignant.

As expected, *COX7b* silencing in brain-seeking variant cells, using a CRISPR-Cas9 strategy (Figure S2a), significantly decreased 231-BR cell migration towards human and mouse astrocytes but not towards human hepatocytes and human bronchial cells (Figure 4a). The general migratory phenotype towards serum (1% FBS, used as a control) was unaffected. Similarly, *COX7B* silencing significantly reduced 231-BR-2 migration towards human and mouse astrocytes but not towards human hepatocytes, human bronchial cells, or serum (Figure 4b). Conversely, experimental Cox7b protein overexpression in parental MDA-MB-231 cells (Figure S2b) increased their migration towards human and mouse astrocytes, while migration towards human hepatocytes, human bronchial cells, or serum was not changed (Figure 4c).

Together, these in vitro results supported a cause–effect relationship between Cox7b protein expression and the brain tropism of human metastatic breast cancer cells. In particular, Cox7b protein overexpression was sufficient to trigger a selective brain tropism of otherwise pan-metastatic, wild-type MDA-MB-231 cells. This finding does not exclude that other proteins could have a similar function in other cancer cell lines.

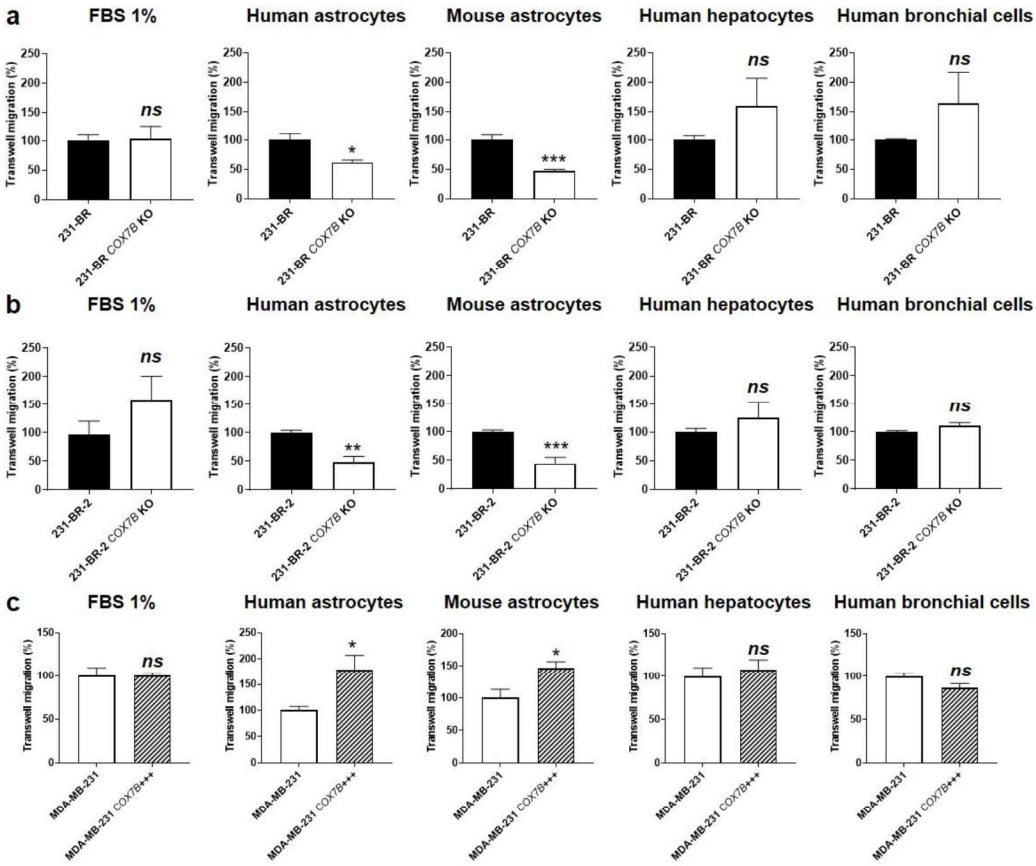


Figure 4. Cause–effect relationship between Cox7b expression and the selective migration of human breast cancer cells towards astrocytes. (**a**) Migration assayed in transwells of 231-BR brain-seeking variants, expressing or not expressing (KO using a CRISP-Cas9 strategy) Cox7b, towards 1% FBS (n = 9), human astrocytes (n = 3), mouse astrocytes (n = 5), human hepatocytes (n = 6), or human bronchial cells (n = 6). (**b**) Migration of 231-BR-2 brain-seeking variants, expressing or not expressing Cox7b, towards 1% FBS (n = 9), human astrocytes (n = 5–6), mouse astrocytes (n = 7), human hepatocytes (n = 6), or human bronchial cells (n = 6). (**c**) Migration of MDA-MB-231 parental cancer cells, overexpressing Cox7b or expressing basal levels of Cox7b, towards 1% FBS (n = 7), human astrocytes (n = 9), mouse astrocytes (n = 6), human hepatocytes (n = 6), or human bronchial cells (n = 6). All data are normalized to control (first columns) and are shown as means ± SEM. * $p < 0.05$, ** $p < 0.01$, *** $p < 0.005$, ns: $p > 0.05$; using Student's t-test (**a–c**).

3.6. Cox7b Expression Promotes the Oxidative Phenotype of Human Metastatic Breast Cancer Cells

The data displayed in Figure 2 showed that increased OXPHOS is a major metabolic characteristic of 231-BR and 231-BR-2 brain-seeking variants compared to parental cells. Since Cox7b resides in the ETC [49], we reasoned that its expression might modulate the OCR of the cells, which was measured using Seahorse oximetry.

COX7B silencing reduced 231-BR basal OCR and OCR associated to ATP production, but maximal OCR, reflecting the respiration spare capacity, was unchanged (Figure 5a). Comparatively, *COX7B* silencing reduced all basal OCR, maximal OCR, and OCR associated to ATP production in 231-BR-2 cells (Figure 5b), demonstrating that loss of *COX7B* represses

OXPHOS in brain-seeking variants of metastatic breast cancer. Of note, *COX7B* silencing did not decrease cell numbers (Figure S3), suggesting the existence of rescue metabolic pathways preventing cell death. Cox7b overexpression in wild-type MDA-MB-231 cells induced the opposite effect, i.e., an oxidative switch characterized by a rise in all basal OCR, maximal OCR, and OCR associated to ATP production (Figure 5c).

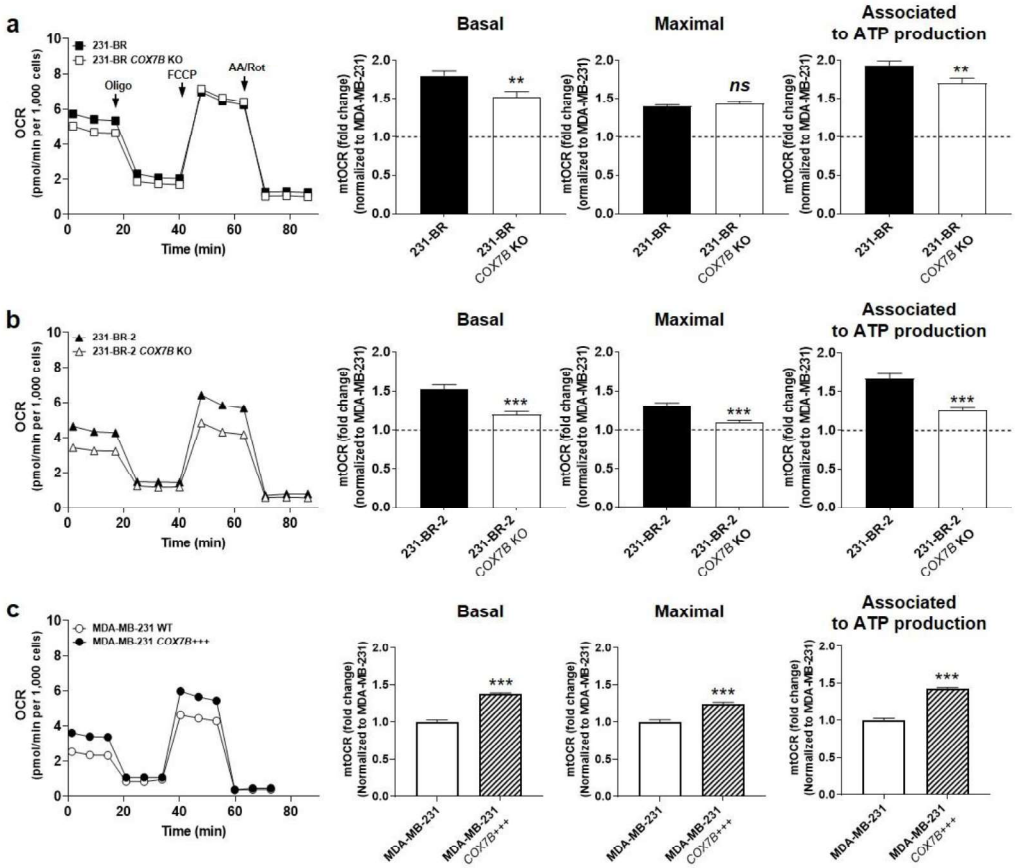


Figure 5. Cox7b expression drives the oxidative switch of brain-seeking variants. (**a**) 231-BR brain-seeking variants expressing or not expressing (KO using a CRISP-Cas9 strategy) Cox7b. Basal (**left**) and maximal (**middle**) oxygen consumption rates (mtOCRs), as well as the OCR of the cells associated to mitochondrial ATP production (**right**), were measured using a XF Cell Mito Stress Test Kit (Agilent) on a Seahorse XF96 bioenergetics analyzer (n = 20 all). Representative Seahorse traces are shown on far left. (**b**) As in (**a**), but using 231-BR-2 brain-seeking variants expressing or not expressing Cox7b (n = 15–20). (**c**) As in (**a**), but using MDA-MD-231 parental cancer cells overexpressing or expressing basal levels of Cox7b (n = 23–32). All data are normalized to control (dotted lines) and are shown as means ± SEM. ** $p < 0.01$, *** $p < 0.005$, ns: $p > 0.05$; using Student's t-test (**a–c**).

Together, these experiments demonstrated that Cox7b is an OXPHOS inducer. They further established a positive correlation between the oxidative activities of human metastatic breast cancer cells and their preferential migration towards astrocytes. Of note, Cox7b expression did not modulate the OXPHOS substrate preference of the brain-seeking variants (Figure S4).

3.7. Cox7b Expression Is Responsible for the Brain Tropism of Metastatic Human Breast Cancer Cells in Mice

To experimentally establish a cause–effect relationship between Cox7b expression and breast cancer brain metastasis, we ran a series of in vivo experiments in nude mice, as depicted in Figure 1a. Briefly, because our investigation interrogated metastatic tropism linked to metastatic take (a late metastatic event) but not metastatic cell dissemination from a primary tumor (an early metastatic event), breast cancer cells were injected in the left cardiac ventricle, which is known to generate systemic metastatic lesions to the bones, brain, ovary, and adrenal glands using MDA-MB-231 cells [34,35]. The constitutive and concurrent expression of luciferase and GFP by our model cell lines allowed for a confirmation of bioluminescence data with immunohistochemistry.

Following the protocol depicted in Figure 1a, *COX7B* silencing with a CRISPR-cas9 strategy in 231-BR and 231-BR-2 brain-seeking variants resulted in an almost total loss of brain tropism following intracardiac injection (Figure 6a). This was evidenced using ex vivo luciferase bioluminescence imaging on brains isolated at the time of mouse sacrifice. Conversely, parental MDA-MB-231 cells, which did not generate detectable brain metastasis for 4 weeks, gained a strong increase in the occurrence of brain metastases upon Cox7b overexpression (Figure 6a). For validation, brains were collected at the end of the experiments, sliced, stained with an antibody against GFP, and counterstained with hematoxylin and eosin. Figure 6b shows representative pictures of the brains, with insets representing typical metastasis-positive areas. Analyses revealed a strong decrease in the number of metastases per mouse and in the metastasis-positive tumor area per slice in mice injected with 231-BR and 231-BR-2 cells lacking *COX7B*, compared to wild-type 231-BR and 231-BR-2 cells (Figure 6b, left and middle graphs). The opposite effects were seen in mice that received parental MDA-MB-231 cells overexpressing Cox7b compared to wild-type MDA-MB-231 cells (Figure 6b, right graphs). Collectively, these in vivo data established a cause–effect relationship between Cox7b expression and the brain tropism of human TNBC in mice.

We concluded our study by analyzing publicly available gene chip and RNA-seq mRNA expression databases [43] reporting on clinical human breast and lung cancers, as wells as on renal clear cell carcinoma, all subtypes included. High Cox7B expression was identified as an independent poor prognosis factor for overall patient survival in all three cancer types (Figure 6c).

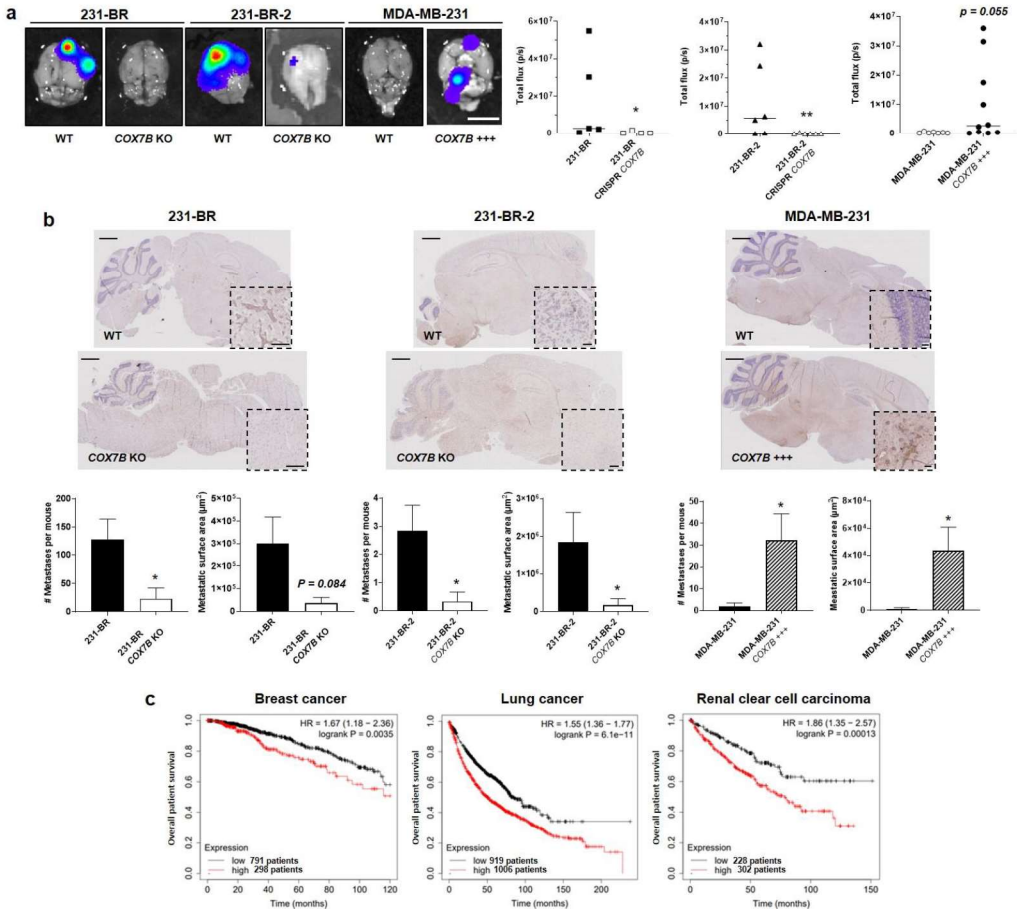


Figure 6. Cox7b drives the tropism of metastatic human breast cancer cells to the brain. (**a**,**b**) The brain tropism of 231-BR and 231-BR-2 brain-seeking variants, expressing or not Cox7b (KO using a CRISP-Cas9 strategy), and of parental MDA-MB-231 human breast cancer cells, overexpressing or not overexpressing Cox7b, was assessed using the protocol depicted in Figure 1a. The cells constitutively expressed luciferase and GFP. (**a**) Ex vivo bioluminescence imaging of mouse brains 4 weeks after the intracardiac injection of cancer cells. Pictures on the **left** are representative of mouse brains in luciferin-containing medium captured using a Xenogen IVIS 50 bioluminescence imaging system. Graphs on the right show brain bioluminescence intensity (n = 4–10). (**b**) Central sections of the brains were immunostained for GFP and counterstained for hematoxylin and eosin. Representative pictures are shown on top (bars = 1 mm). Insets represent typical GFP-positive metastatic lesions (bars = 100 µm). On the bottom, the left graphs represent the number of detected metastases (**left**) and the metastasis-positive surface area per mouse (n = 4–10). Representative images of the brains are shown. (**c**) Overall survival of patients with breast cancer (**left**, all types combined, 1090 patients), lung cancer (**middle**, all types combined, 1925 patients) and renal clear cell carcinoma (RCC, **right**, 530 patients). Data are shown as individual values and medians (**a**), means ± SEM (**b**), or individual values (**c**). * $p < 0.05$, ** $p < 0.01$, using Mann–Whitney test (**a**), Student's t-test (**b**), or log rank test (**c**).

4. Discussion

In the context of the seed-and-soil hypothesis proposing that secondary organs should fulfill the specific needs of metastatic progenitor cells [14], this study aimed to investigate the existence of a metabolic control of tissue-specific metastasis. We used breast cancer brain metastasis as an example, and we selected the human MDA-MB-231 TNBC cancer cell line as a working model for the generally high propensity of this breast cancer subtype to metastasize in humans [50] and because two brain-seeking variants derived from the same parental cell line were already available from two independent laboratories [34–36]. It allowed us to validate characteristics identified in one variant by those of the other. In this model, we report that Cox7b, a structural subunit of ETC Complex IV [51,52], drives metastatic breast cancer cell homing to the brain: repression of Cox7b expression selectively blocked the migration of brain-seeking variants towards astrocytes and their capacity to generate brain metastases in mice; conversely, pan-metastatic parental cells manipulated to gain Cox7b expression increased their selective migration towards astrocytes and their capability to generate brain metastases. This series of experiments established a cause–consequence relationship between Cox7b expression and metastatic brain tropism in the MDA-MB-231 model. Other proteins could exert a similar function in other cancer cell lines and models.

Mammalian Cox, also known as Complex IV, is a 13-subunit multiheteromeric enzyme that catalyzes the oxidation of cytochrome c and the reduction of molecular oxygen to water at the terminal step of OXPHOS in the mitochondrial ETC [48]. Complex IV is located at the inner mitochondrial membrane. In the complex, Cox7b is a short 80 amino acid nuclear-encoded transmembrane protein that associates with mitochondria-encoded subunits Cox1, Cox2, and Cox3, which contain the four catalytic redox centers of the enzyme [49]. Cox7b is ubiquitously expressed. It has no enzymatic activity but stabilizes the complex and positively modulates Cox activity. Its expression is increased in several degenerative pathologies characterized by high OXPHOS activities (see reference [53] for a recent review), and inactivating mutations have been associated with the development of microphthalmia with linear skin lesions (MLS) [54]. The fact that Cox7b stabilizes Complex IV is in line with our observation that high Cox7b expression triggers OXPHOS, whereas *COX7B* silencing has the opposite effect. To date, nothing is known about the regulation of Cox7b expression in mammalian cells.

Interestingly, high Cox7b expression was enhanced through rounds of in vivo selection using intracardiac delivery in mice, thus bypassing adaptation and selection in a primary tumor. This highlights a key characteristic of metastatic cancer cells: selective homing. Homing is an active process involving cancer cell interactions with vascular endothelial cells at given body locations; transvascular diapedesis; nesting in the premetastatic niche; the establishment of molecular relationships with host cells at the new location; and a phenotypic reversion from a stem to a proliferative phenotype for most post-metastatic cancer cells [26,55]. This succession of events would be incomplete without answering to the question: how do metastatic progenitor cells sense that they have arrived at the metastatic location, while they are still in the blood stream? If they exist, sensor systems should be sensitive enough to discriminate changes in the composition of the blood between different organs.

For homing, physical interactions between metastatic progenitor cells and host cells in the metastatic niche can be excluded as a triggering event, because they occur after extravasation. Theses interactions would rather primarily retain and re-educate/redifferentiate cancer cells at the metastatic site. Similarly, physical interactions between metastatic progenitor cells and endothelial cells lining blood vessels along premetastatic niches might not be the primary event for homing. Indeed, our in vitro experiments demonstrate that selective cancer cell migration towards host cells, seen as feeder cells, can be manipulated in the absence of vascular cells in vitro. In other words, metastatic progenitor cells would sense soluble molecules produced by host cells that act as chemoattractants. These molecules are expected to reach the blood stream in concentrations high enough to be sensed and with a

concentration gradient steep enough to be followed by metastatic progenitors. Our data suggest that Cox7b could be such a sensor in human TNBC cells, but the exact nature of the metabolic signal(s) recognized by Cox7b is still unknown. Based on the observation that Cox7b expression increases OXPHOS activity, candidate chemoattractants should be primarily sought among TCA cycle substrates and intermediates. These chemoattractants would be produced by human and mouse astrocytes in culture and in vivo, but not by human bronchial cells nor by human hepatocytes. Lactate, which is produced and secreted by astrocytes to feed neurons [56], pyruvate, acetate, and glutamate are attractive candidates [57,58]. Of note, brain-seeking variants also gained metabolic flexibility to fuel OXPHOS, but this was not linked to Cox7b expression.

Our study was primarily aimed at proving the concept of a metabolic control of organotropism, and our data support that idea, even if additional experiments are still warranted to demonstrate our initial hypothesis. Cox7b was identified using the MDA-MB-231 model solely. This TNBC cell line was used because it represents a cancer type that is often detected in patients before entry in the metastatic phase, but that evolves to this phase despite treatments in a significant number of patients. Hence, in a cohort study where 25,362 TNBC patients were included, only 6% were at the metastatic stage and only 0.68% had brain metastases at the time of diagnosis; however, even for those with localized disease, approximately 25% of patients relapsed with distant metastasis [59,60]. Overall, brain metastasis affected up to 50% of TNBC patients in the course of the disease [10]. Our choice of the model was, thus, driven by the possibility to identify a suitable target for the prevention of brain metastasis. At the end of the study, one must recognize that Cox7b is not a suitable pharmacological target, as this structural protein has no enzymatic activity and is buried within Complex IV at the mitochondrial inner membrane. However, we believe that the use of the same selection approach for in vivo organotropism starting from different types of cancer cells (e.g., other breast cancer cells, prostate cancer, cervix cancer, melanoma) will reveal additional metabolic proteins controlling tissue-specific homing. Candidates have already been proposed [61] that must still be validated as being causal in organotropism. Among these, some could be amenable for therapy, with the ultimate intention of interfering with the metabolic sensing of different subtypes of metastatic progenitor cells at different secondary sites. Some of these targets could further be shared by different types of tumors (as illustrated here, with high Cox7b expression in primary tumors being a poor predictive factor of overall survival not only in breast cancer but also in lung cancer and in renal clear cell carcinoma), and others could be specific for a particular cancer type metastasizing to a particular secondary organ. Furthermore, a metabolic sensor could have additional effects unrelated to metastasis. This is the case of Cox7b, which sensitizes cancers to cisplatin chemotherapy, with high Cox7b expression in primary tumors being a favorable factor for overall patient survival upon cisplatin treatment [62].

5. Conclusions

This study is the first of a series investigating the existence of metabolic sensors for tissue-specific metastasis in the context of the seed-and-soil hypothesis and the premetastatic niche theory. Using parental human MDA-MB-231 TNBC cells and two independent brain-seeking variants selected in mice as models, we identified mitochondrial protein Cox7b in ETC Complex IV as a selective regulator of brain metastasis. Silencing and overexpression experiments established a causal link between Cox7b expression and metastatic brain tropism in vivo, where metabolically active astrocytes were sufficient to chemoattract brain-seeking metastatic variants expressing high levels of Cox7b. While Cox7b is not adapted as a direct target for the therapeutic prevention of brain metastasis, we believe that our general strategy, applied to other cancer types and/or different secondary sites, has the potential to unravel other, unprecedented target candidates.

6. Patent

M.C.N.M.B. and P.S. are inventors of patent application EP22191920, entitled "Stem Cells with Brain Tropism", which is related to the work reported in this manuscript.

Supplementary Materials: The following supporting information can be downloaded at: https://www.mdpi.com/article/10.3390/cancers14184371/s1. Figure S1: uncropped western blots; Figure S2: Validation of *COX7B* silencing and overexpression; Figure S3: *COX7B* silencing does not alter brain-seeking variant cell numbers in vitro; Figure S4: *COX7B* silencing does not alter the metabolic plasticity of brain-seeking variant cells; Table S1: Short tandem repeat profiles.

Author Contributions: Conceptualization, M.C.N.M.B., C.B. and P.S.; methodology, M.C.N.M.B., T.C. and P.S.; investigation, M.C.N.M.B., T.C., L.X.Z., J.D.R., Z.B., J.A.V.d.V., M.F. and E.P.D.; formal analysis, M.C.N.M.B., T.C. and P.S.; validation, C.M., C.B., and P.S.; resources, C.B. and P.S.; data curation, P.S.; writing—original draft preparation, M.C.N.M.B. and P.S.; writing—review and editing, M.C.N.M.B., T.C., J.D.R., L.X.Z., Z.B., J.A.V.d.V., M.F., E.P.D., C.M., C.B. and P.S.; visualization, M.C.N.M.B. and P.S.; supervision, P.S.; project administration, P.S.; funding acquisition, P.S. All authors have read and agreed to the published version of the manuscript.

Funding: This work was supported by the FRFS-WELBIO strategic axis of the Walloon Region of Belgium (WELBIO-CR-2022A-13), the Belgian Fonds National de la Recherche Scientifique (F.R.S.-FNRS, CDR J.0135.18, CDR J.0177.22), the Belgian Télévie (project n° 7.4529.17), the European Union's Horizon 2020 research innovation program under the Marie Skłodowska–Curie grant agreements No. 722605 TRANSMIT, and the Louvain Foundation. M.C.N.M.B. is a Ph.D. Fellow of the Télévie; L.X.Z. is a Ph.D. Fellow of Marie Skłodowska–Curie grant No 722605 TRANSMIT.; P.S. is a F.R.S.-FNRS Research Director and a WELBIO Investigator.

Institutional Review Board Statement: Mouse experiments were performed with the approval of UCLouvain Comité d'Ethique pour l'Expérimentation Animale (approval IDs: 2016/UCL/MD/018 and 2020/UCL/MD/033), according to national and European animal care regulations.

Informed Consent Statement: Not applicable.

Data Availability Statement: All data are contained within the article and the Supplementary Materials.

Acknowledgments: The authors thank François P. Duhoux (Department of Medical Oncology, Institut Roi Albert II, Cliniques Universitaires Saint-Luc, Brussels, Belgium) for sharing his medical expertise; Thibaut Vazeille, Loïc Hamelin, and Marie Bedin for excellent technical assistance; the Morph-Im technological platform and electron microscopy services of UNamur; and Davide Bruza, Caroline Bouzin, Michèle De Beukelaer, Aurélie Daumerie, and Marc De Burnonville at UCLouvain IREC's core facilities. The authors further thank Patricia Steeg (NIH) and Harikrishna Nakshatri (Indiana University School of Medicine) for the kind gift of MDA-MB-231-derived brain-seeking variants 231-BR and 231-BR-2, respectively. The plasmids used in this study were provided by the laboratories of Feng Zhang and Ralf Kuehn, via Addgene.

Conflicts of Interest: M.C.N.M.B. and P.S. are inventors of a patent application entitled "Stem Cells with Brain Tropism". The authors declare no other conflicts of interest related to the present study. The funders had no role in the design of the study; in the collection, analyses, or interpretation of data; in the writing of the manuscript; or in the decision to publish the results.

Appendix A

Appendix A.1 Cell Infection for Constitutive Luciferase and GFP Expression

For constitutive luciferase and GFP expression, cells were infected with lentiviruses carrying the luciferase and GFP sequences along with a puromycin resistance gene (Amsbio; catalogue #LPV020). Briefly, 70%–80% of the confluent cells in a 24-well plate were transduced with 2 µL per well of the lentivirus solution in 1mL medium with 10 µL/mL polybrene. Cells were selected by a 48–72 h incubation with 1 µg/mL puromycin (InvivoGen, Toulouse, France) and FACS-sorted for GFP expression on a Becton Dickinson FACSAriaIII system (Erembodegem, Belgium).

Appendix A.2 COX7B Gene Silencing

CRISPR plasmids were constructed following Zhang's laboratory protocol [37] with pX459 (Addgene; catalogue #62988, puromycin selection) or pU6-(BbsI)_CBh-Cas9-T2A-mCherry (Addgene; catalogue #64324, red fluorescence selection) plasmids [37,63,64]. These plasmids contain both Cas9 and guide RNA (gRNA) expression cassettes, with BbsI restriction sites for the insertion of gRNA sequences. Prevalidated gRNA sequences were chosen in the GenScript genome-wide database [65] for a non-overlapping duo of gRNAs: 5′-AGCGCACTAAATCGTCTCCA-3′ and 5′-GAGTTACCCCAAAGGAATGG-3′. Sticky ends were created for insertion in the vector plasmids, with CACCG at the 5′ of the gRNA sense sequence and AAAC at the 5′ and C at the 3′ of the gRNA antisense sequence.

gRNA oligonucleotides (Eurogentec, Seraing, Belgium) were annealed into double-stranded DNA, with 1 µL of stock solutions containing 100 µM of each sense and antisense oligonucleotides in 2 µL of 5X T4 ligase buffer (Thermo Fisher; catalogue #46300018), 0.5 µL of T4 PNK (BIOKE; catalogue #M0201) and 5.5 µL of DNase/RNase-free distilled water. Incubation times were 37 °C for 30 min, followed by 95°C for 5 min, and then the temperature was decreased at a rate of 5 °C/min until reaching 25 °C.

The Golden Gate DNA Assembly protocol [66] was then used for inserting 1 µL of annealed gRNA at 1 µM into 100 ng of vector plasmid, in a solution containing 5 µL of 10x Fast Digest buffer (Thermo Fisher; catalogue #B64), 0.5 µL of ATP 0.1 M (Thermo Fisher; catalogue #R1441), 0.5 µL of BSA 10 mg/mL (Promega; catalogue #R396D), 1 µL of restriction enzyme BpiI (Thermo Fisher; catalogue #FD1014), and 2 µL of T4 ligase 5 U/µL (Thermo Fisher; catalogue #EL0014) in a total volume of 50 µL completed with water. The mixture was incubated for 20 cycles at 37 °C for 5 min and 20 °C for 5 min, followed by 80 °C for 20 min.

Five microliters of the resulting solution were used for TOP10 bacteria (Thermo Fisher; catalogue #C404003) transformation using prewarmed LB agar plates (Thermo Fisher; catalogue #22700-025) containing 100 µg/mL of ampicillin, in accordance with the instructions of the manufacturer. Single colonies were inoculated in LB broth (Thermo Fisher; catalogue #12780-052) with 50 µg/mL ampicillin and incubated at 37 °C overnight. Plasmid DNA was then collected with the PureYield Plasmid Miniprep System (Promega; catalogue #A1223), and its concentration was obtained using a NanoDrop device (Thermo Fisher). Sequences were verified by Sanger Sequencing (Genewiz, Leipzig, Germany).

Cancer cells at 70%–80% confluence were transfected with the Lipofectamine LTX/Plus transfection kit (Thermo Fisher; catalogue #15338100) or with the jetOPTIMUS kit (Westburg, Leusden, The Netherlands; catalogue #117-01). The first kit was used with 0.25 µg of each gRNA plasmid, for a total of 0.5 µg of DNA in 100 µL of OptiMEM, containing 0.5 µL of Plus and 2.25 µL of lipofectamine LTX, with incubation times of 15 and 30 min, respectively. The second kit was used with 0.5 µg of each gRNA plasmid, for a total of 1 µg of DNA, with 1 µL of reagent in 200 µL of buffer for each well in a 6-well plate. Cells were selected with puromycin (1 µg/mL)-containing medium for 48–72 h or FACS-sorted for mCherry fluorescence 48 h after transfection on a Becton Dickinson FACSAriaIII system.

Appendix A.3 Cox7b Overexpression

The human untagged *COX7B* cDNA ORF Clone in expression vector pCMV3 (Bio-Connect; catalogue #HG20762-UT) was used to overexpress Cox7b in MDA-MB-231 cancer cells. Cells at 70–80% confluence were transfected with 10 µg of the plasmid and Lipofectamine 3000 (Thermo Fisher; catalogue #L3000001) in a 10 cm dish, allowed to recover the next day in fresh DMEM containing glutaMAX and 4.5 g/L glucose (Thermo Fisher; catalogue #61965026) supplemented with 10% FBS, and selected with hygromycin (400 µg/mL)-containing medium for 10 days. Medium was renewed every 3–4 days. Colonies were individually picked, expanded, and tested by western blotting for the expression of Cox7b.

Appendix A.4 Cell Migration and Invasion

Invasion was assessed by coating the inserts with 250 µg/mL of Matrigel (Corning, Tewksbury, MA, USA; #356231) for 2 h at 37 °C, and migration without Matrigel coating. Fifty thousand cancer cells were seeded in the upper chamber of each transwell in 500 µL of serum-free culture medium, while the lower chamber contained FBS 1% (general migration/invasion) or confluent nonmalignant astrocytes, hepatocytes, or bronchial cells, which were used as attractants. Cancer cells were allowed to migrate/invade for 24 h at 37 °C in a 5% CO_2 humidified atmosphere. At the end of the assay, cells were fixed with 4% PFA in PBS for 10 min, rinsed three times with PBS, and immobile cells (upper compartment of the insert) were wiped away. Mobile cells were stained with DAPI for 30 min, rinsed three times with PBS, and imaged at 5x on an AxioVert microscope equipped with an AxioCam-MRc camera (Zeiss). Two images were taken per well, thus covering the upper and lower halves. Nuclei were counted using QuPath software version 0.1.2. with the Positive Cell Detection analysis tool.

Appendix A.5 Seahorse Oximetry

Basal, maximal, and ATP-linked oxygen consumption rates (OCRs) were quantified using the XF Cell Mito Stress Test Kit (Agilent) on a Seahorse XF96 bioenergetics analyzer (Agilent). Briefly, 10,000 cells were seeded in XF96 culture plates 16 h before the experiments in DMEM, containing glutaMAX and 4.5 g/L glucose (Thermo Fisher; catalogue #61965026) supplemented with 10% FBS. On the day of analysis, the culture medium was replaced by DMEM containing 10 mM glucose, 2 mM glutamine, 1.85 g/L NaCl, and 3 mg/L phenol red, pH 7.4. Cells were further incubated for 1 h in a CO_2-free incubator before analysis. Sequentially, basal OCR was acquired without treatment, ATP-linked OCR after the addition of 1 µM of ATP synthase inhibitor oligomycin, maximal OCR after mitochondrial potential disruption using 1 µM of ionophore carbonyl cyanide-4-(trifluoromethoxy)phenylhydrazone (FCCP), and non-mitochondrial OCR after the addition of 0.5 µM of Complex I inhibitor rotenone together with 0.5 µM of Complex III inhibitor antimycin A.

Mitochondrial fuel dependency was determined using the Fuel Flex test kit (Agilent) with either 2 µM of mitochondrial pyruvate carrier (MPC) inhibitor UK5099, 3 µM of glutaminase inhibitor BPTES, or 4 µM of carnitine palmitoyltransferase-1 (CPT-1) inhibitor etomoxir, to challenge oxidative glucose metabolism, glutaminolysis, and lipolysis, respectively.

Mitochondrial OCRs (mtOCRs) were calculated by subtracting non-mitochondrial OCRs from the corresponding basal, maximal, and ATP-linked OCRs. Respiration used for ATP production is the difference between basal OCR and OCR in the presence of ATP-synthase inhibitor oligomycin. All data were normalized by the total protein content.

References

1. Weiss, F.; Lauffenburger, D.; Friedl, P. Towards targeting of shared mechanisms of cancer metastasis and therapy resistance. *Nat. Rev. Cancer* **2022**, *22*, 157–173. [CrossRef] [PubMed]
2. Seoane, J.; De Mattos-Arruda, L. Brain metastasis: New opportunities to tackle therapeutic resistance. *Mol. Oncol.* **2014**, *8*, 1120–1131. [CrossRef] [PubMed]
3. Kuksis, M.; Gao, Y.; Tran, W.; Hoey, C.; Kiss, A.; Komorowski, A.S.; Dhaliwal, A.J.; Sahgal, A.; Das, S.; Chan, K.K.; et al. The incidence of brain metastases among patients with metastatic breast cancer: A systematic review and meta-analysis. *Neuro. Oncol.* **2021**, *23*, 894–904. [CrossRef] [PubMed]
4. Dent, R.; Trudeau, M.; Pritchard, K.I.; Hanna, W.M.; Kahn, H.K.; Sawka, C.A.; Lickley, L.A.; Rawlinson, E.; Sun, P.; Narod, S.A. Triple-negative breast cancer: Clinical features and patterns of recurrence. *Clin. Cancer. Res.* **2007**, *13*, 4429–4434. [CrossRef]
5. Hugo, H.S.; Cortes, J.; Cescon, D.W.; Im, S.; Md Yusof, M.; Gallardo, C.; Lipatov, O.; Barrios, C.H.; Perez-Garcia, J.; Iwata, H.; et al. KEYNOTE-355: Final results from a randomized, double-blind phase III study of first-line pembrolizumab + chemotherapy vs placebo + chemotherapy for metastatic TNBC. *Annals Oncol.* **2021**, *32* (Suppl. 5), S1283–S1346.
6. Gennari, A.; Stockler, M.; Puntoni, M.; Sormani, M.; Nanni, O.; Amadori, D.; Wilcken, N.; D'Amico, M.; DeCensi, A.; Bruzzi, P. Duration of chemotherapy for metastatic breast cancer: A systematic review and meta-analysis of randomized clinical trials. *J. Clin. Oncol.* **2011**, *29*, 2144–2149. [CrossRef]
7. Damsky, W.E.; Rosenbaum, L.E.; Bosenberg, M. Decoding melanoma metastasis. *Cancers* **2010**, *3*, 126–163. [CrossRef]

8. Blecker, D.; Abraham, S.; Furth, E.E.; Kochman, M.L. Melanoma in the gastrointestinal tract. *Am. J. Gastroenterol.* **1999**, *94*, 3427–3433. [CrossRef]
9. Tas, F. Metastatic behavior in melanoma: Timing, pattern, survival, and influencing factors. *J. Oncol.* **2012**, *2012*, 647684. [CrossRef]
10. Lin, N.U.; Claus, E.; Sohl, J.; Razzak, A.R.; Arnaout, A.; Winer, E.P. Sites of distant recurrence and clinical outcomes in patients with metastatic triple-negative breast cancer: High incidence of central nervous system metastases. *Cancer* **2008**, *113*, 2638–2645. [CrossRef]
11. Jin, J.; Gao, Y.; Zhang, J.; Wang, L.; Wang, B.; Cao, J.; Shao, Z.; Wang, Z. Incidence, pattern and prognosis of brain metastases in patients with metastatic triple negative breast cancer. *BMC Cancer* **2018**, *18*, 446. [CrossRef]
12. Patrawala, L.; Calhoun, T.; Schneider-Broussard, R.; Li, H.; Bhatia, B.; Tang, S.; Reilly, J.G.; Chandra, D.; Zhou, J.; Claypool, K.; et al. Highly purified CD44+ prostate cancer cells from xenograft human tumors are enriched in tumorigenic and metastatic progenitor cells. *Oncogene* **2006**, *25*, 1696–1708. [CrossRef] [PubMed]
13. Capeloa, T.; Krzystyniak, J.; d'Hose, D.; Canas Rodriguez, A.; Payen, V.L.; Zampieri, L.X.; Van de Velde, J.A.; Benyahia, Z.; Pranzini, E.; Vazeille, T.; et al. MitoQ inhibits human breast cancer cell migration, invasion and clonogenicity. *Cancers* **2022**, *14*, 1516. [CrossRef] [PubMed]
14. Paget, S. The distribution of secondary growths in cancer of the breast. *Cancer Metastasis Rev.* **1889**, *8*, 98–101. [CrossRef]
15. Ribelles, N.; Santonja, A.; Pajares, B.; Llacer, C.; Alba, E. The seed and soil hypothesis revisited: Current state of knowledge of inherited genes on prognosis in breast cancer. *Cancer Treat. Rev.* **2014**, *40*, 293–299. [CrossRef] [PubMed]
16. Jang, A.; Hill, R.P. An examination of the effects of hypoxia, acidosis, and glucose starvation on the expression of metastasis-associated genes in murine tumor cells. *Clin. Exp. Metastasis* **1997**, *15*, 469–483. [CrossRef]
17. Vaupel, P. The role of hypoxia-induced factors in tumor progression. *Oncologist* **2004**, *9* (Suppl. 5), 10–17. [CrossRef]
18. Lunt, S.J.; Chaudary, N.; Hill, R.P. The tumor microenvironment and metastatic disease. *Clin. Exp. Metastasis* **2009**, *26*, 19–34. [CrossRef]
19. Gilkes, D.M.; Semenza, G.L.; Wirtz, D. Hypoxia and the extracellular matrix: Drivers of tumour metastasis. *Nat. Rev. Cancer* **2014**, *14*, 430–439. [CrossRef]
20. Rankin, E.B.; Giaccia, A.J. Hypoxic control of metastasis. *Science* **2016**, *352*, 175–180. [CrossRef]
21. Payen, V.L.; Porporato, P.E.; Baselet, B.; Sonveaux, P. Metabolic changes associated with tumor metastasis, part 1: Tumor pH, glycolysis and the pentose phosphate pathway. *Cell. Mol. Life Sci.* **2016**, *73*, 1333–1348. [CrossRef] [PubMed]
22. Porporato, P.E.; Payen, V.L.; Baselet, B.; Sonveaux, P. Metabolic changes associated with tumor metastasis, part 2: Mitochondria, lipid and amino acid metabolism. *Cell. Mol. Life Sci.* **2016**, *73*, 1349–1363. [CrossRef] [PubMed]
23. DeClerck, K.; Elble, R.C. The role of hypoxia and acidosis in promoting metastasis and resistance to chemotherapy. *Front. Biosci.* **2010**, *15*, 213–225. [CrossRef] [PubMed]
24. Pietila, M.; Ivaska, J.; Mani, S.A. Whom to blame for metastasis, the epithelial-mesenchymal transition or the tumor microenvironment? *Cancer Lett.* **2016**, *380*, 359–368. [CrossRef]
25. Klein, C.A. Selection and adaptation during metastatic cancer progression. *Nature* **2013**, *501*, 365–372. [CrossRef]
26. Gupta, G.P.; Massague, J. Cancer metastasis: Building a framework. *Cell* **2006**, *127*, 679–695. [CrossRef]
27. Kaplan, R.N.; Riba, R.D.; Zacharoulis, S.; Bramley, A.H.; Vincent, L.; Costa, C.; MacDonald, D.D.; Jin, D.K.; Shido, K.; Kerns, S.A.; et al. VEGFR1-positive haematopoietic bone marrow progenitors initiate the pre-metastatic niche. *Nature* **2005**, *438*, 820–827. [CrossRef]
28. Peinado, H.; Zhang, H.; Matei, I.R.; Costa-Silva, B.; Hoshino, A.; Rodrigues, G.; Psaila, B.; Kaplan, R.N.; Bromberg, J.F.; Kang, Y.; et al. Pre-metastatic niches: Organ-specific homes for metastases. *Nat. Rev. Cancer* **2017**, *17*, 302–317. [CrossRef]
29. Laubli, H.; Borsig, L. Selectins promote tumor metastasis. *Semin. Cancer Biol.* **2010**, *20*, 169–177. [CrossRef]
30. Sevenich, L.; Bowman, R.L.; Mason, S.D.; Quail, D.F.; Rapaport, F.; Elie, B.T.; Brogi, E.; Brastianos, P.K.; Hahn, W.C.; Holsinger, L.J.; et al. Analysis of tumour- and stroma-supplied proteolytic networks reveals a brain-metastasis-promoting role for cathepsin S. *Nat. Cell Biol.* **2014**, *16*, 876–888. [CrossRef]
31. Porporato, P.E.; Payen, V.L.; Perez-Escuredo, J.; De Saedeleer, C.J.; Danhier, P.; Copetti, T.; Dhup, S.; Tardy, M.; Vazeille, T.; Bouzin, C.; et al. A mitochondrial switch promotes tumor metastasis. *Cell Rep.* **2014**, *8*, 754–766. [CrossRef]
32. Capeloa, T.; Krzystyniak, J.; Canas Rodriguez, A.; Payen, V.L.; Zampieri, L.X.; Pranzini, E.; Derouane, F.; Vazeille, T.; Bouzin, C.; Duhoux, F.P.; et al. MitoQ prevents human breast cancer recurrence and lung metastasis in mice. *Cancers* **2022**, *14*, 1488. [CrossRef] [PubMed]
33. Ishikawa, K.; Takenaga, K.; Akimoto, M.; Koshikawa, N.; Yamaguchi, A.; Imanishi, H.; Nakada, K.; Honma, Y.; Hayashi, J. ROS-generating mitochondrial DNA mutations can regulate tumor cell metastasis. *Science* **2008**, *320*, 661–664. [CrossRef] [PubMed]
34. Yoneda, T.; Williams, P.J.; Hiraga, T.; Niewolna, M.; Nishimura, R. A bone-seeking clone exhibits different biological properties from the MDA-MB-231 parental human breast cancer cells and a brain-seeking clone in vivo and in vitro. *J. Bone Miner. Res.* **2001**, *16*, 1486–1495. [CrossRef] [PubMed]
35. Patel, J.B.; Appaiah, H.N.; Burnett, R.M.; Bhat-Nakshatri, P.; Wang, G.; Mehta, R.; Badve, S.; Thomson, M.J.; Hammond, S.; Steeg, P.; et al. Control of EVI-1 oncogene expression in metastatic breast cancer cells through microRNA miR-22. *Oncogene* **2011**, *30*, 1290–1301. [CrossRef] [PubMed]

36. Burnett, R.M.; Craven, K.E.; Krishnamurthy, P.; Goswami, C.P.; Badve, S.; Crooks, P.; Mathews, W.P.; Bhat-Nakshatri, P.; Nakshatri, H. Organ-specific adaptive signaling pathway activation in metastatic breast cancer cells. *Oncotarget* **2015**, *6*, 12682–12696. [CrossRef]
37. Ran, F.A.; Hsu, P.D.; Wright, J.; Agarwala, V.; Scott, D.A.; Zhang, F. Genome engineering using the CRISPR-Cas9 system. *Nat. Protoc.* **2013**, *8*, 2281–2308. [CrossRef]
38. Piret, J.P.; Vankoningsloo, S.; Mejia, J.; Noel, F.; Boilan, E.; Lambinon, F.; Zouboulis, C.C.; Masereel, B.; Lucas, S.; Saout, C.; et al. Differential toxicity of copper (II) oxide nanoparticles of similar hydrodynamic diameter on human differentiated intestinal Caco-2 cell monolayers is correlated in part to copper release and shape. *Nanotoxicology* **2012**, *6*, 789–803. [CrossRef]
39. Grasso, D.; Medeiros, H.C.D.; Zampieri, L.X.; Bol, V.; Danhier, P.; van Gisbergen, M.W.; Bouzin, C.; Brusa, D.; Gregoire, V.; Smeets, H.; et al. Fitter mitochondria are associated with radioresistance in human head and neck SQD9 cancer cells. *Front. Pharmacol.* **2020**, *11*, 263. [CrossRef]
40. Li, H.; Durbin, R. Fast and accurate short read alignment with Burrows-Wheeler transform. *Bioinformatics* **2009**, *25*, 1754–1760. [CrossRef]
41. Van Hee, V.F.; Perez-Escuredo, J.; Cacace, A.; Copetti, T.; Sonveaux, P. Lactate does not activate NF-kappaB in oxidative tumor cells. *Front. Pharmacol.* **2015**, *6*, 228. [CrossRef]
42. Bankhead, P.; Loughrey, M.B.; Fernandez, J.A.; Dombrowski, Y.; McArt, D.G.; Dunne, P.D.; McQuaid, S.; Gray, R.T.; Murray, L.J.; Coleman, H.G.; et al. QuPath: Open source software for digital pathology image analysis. *Sci. Rep.* **2017**, *7*, 16878. [CrossRef] [PubMed]
43. Gyorffy, B. Survival analysis across the entire transcriptome identifies biomarkers with the highest prognostic power in breast cancer. *Comput. Struct. Biotechnol. J.* **2021**, *19*, 4101–4109. [CrossRef] [PubMed]
44. Vaz, F.M.; Fouchier, S.W.; Ofman, R.; Sommer, M.; Wanders, R.J. Molecular and biochemical characterization of rat gamma-trimethylaminobutyraldehyde dehydrogenase and evidence for the involvement of human aldehyde dehydrogenase 9 in carnitine biosynthesis. *J. Biol. Chem.* **2000**, *275*, 7390–7394. [CrossRef] [PubMed]
45. Zhao, D.; McCaffery, P.; Ivins, K.J.; Neve, R.L.; Hogan, P.; Chin, W.W.; Drager, U.C. Molecular identification of a major retinoic-acid-synthesizing enzyme, a retinaldehyde-specific dehydrogenase. *Eur. J. Biochem.* **1996**, *240*, 15–22. [CrossRef]
46. Schmidt, C.; Sciacovelli, M.; Frezza, C. Fumarate hydratase in cancer: A multifaceted tumour suppressor. *Semin. Cell. Dev. Biol.* **2020**, *98*, 15–25. [CrossRef]
47. Zhu, J.; Vinothkumar, K.R.; Hirst, J. Structure of mammalian respiratory complex I. *Nature* **2016**, *536*, 354–358. [CrossRef]
48. Kadenbach, B.; Huttemann, M. The subunit composition and function of mammalian cytochrome c oxidase. *Mitochondrion* **2015**, *24*, 64–76. [CrossRef]
49. Tsukihara, T.; Aoyama, H.; Yamashita, E.; Tomizaki, T.; Yamaguchi, H.; Shinzawa-Itoh, K.; Nakashima, R.; Yaono, R.; Yoshikawa, S. The whole structure of the 13-subunit oxidized cytochrome c oxidase at 2.8 A. *Science* **1996**, *272*, 1136–1144. [CrossRef]
50. Nakhjavani, M.; Samarasinghe, R.M.; Shigdar, S. Triple-negative breast cancer brain metastasis: An update on druggable targets, current clinical trials, and future treatment options. *Drug Discov. Today* **2022**, *27*, 1298–1314. [CrossRef]
51. Kadenbach, B.; Jarausch, J.; Hartmann, R.; Merle, P. Separation of mammalian cytochrome c oxidase into 13 polypeptides by a sodium dodecyl sulfate-gel electrophoretic procedure. *Anal. Biochem.* **1983**, *129*, 517–521. [CrossRef]
52. Kuhn-Nentwig, L.; Kadenbach, B. Immunological identification of four different polypeptides in 'subunit VII' of mammalian cytochrome c oxidase. *FEBS Lett.* **1984**, *172*, 189–192. [CrossRef]
53. Cunatova, K.; Reguera, D.P.; Houstek, J.; Mracek, T.; Pecina, P. Role of cytochrome c oxidase nuclear-encoded subunits in health and disease. *Physiol. Res.* **2020**, *69*, 947–965. [CrossRef] [PubMed]
54. Indrieri, A.; van Rahden, V.A.; Tiranti, V.; Morleo, M.; Iaconis, D.; Tammaro, R.; D'Amato, I.; Conte, I.; Maystadt, I.; Demuth, S.; et al. Mutations in COX7B cause microphthalmia with linear skin lesions, an unconventional mitochondrial disease. *Am. J. Hum. Genet.* **2012**, *91*, 942–949. [CrossRef] [PubMed]
55. Jolly, M.K.; Ware, K.E.; Gilja, S.; Somarelli, J.A.; Levine, H. EMT and MET: Necessary or permissive for metastasis? *Mol. Oncol.* **2017**, *11*, 755–769. [CrossRef] [PubMed]
56. Perez-Escuredo, J.; Van Hee, V.F.; Sboarina, M.; Falces, J.; Payen, V.L.; Pellerin, L.; Sonveaux, P. Monocarboxylate transporters in the brain and in cancer. *Biochim. Biophys. Acta.* **2016**, *1863*, 2481–2497. [CrossRef]
57. Mashimo, T.; Pichumani, K.; Vemireddy, V.; Hatanpaa, K.J.; Singh, D.K.; Sirasanagandla, S.; Nannepaga, S.; Piccirillo, S.G.; Kovacs, Z.; Foong, C.; et al. Acetate is a bioenergetic substrate for human glioblastoma and brain metastases. *Cell* **2014**, *159*, 1603–1614. [CrossRef]
58. Bergers, G.; Fendt, S.M. The metabolism of cancer cells during metastasis. *Nat. Rev. Cancer* **2021**, *21*, 162–180. [CrossRef]
59. Martin, A.M.; Cagney, D.N.; Catalano, P.J.; Warren, L.E.; Bellon, J.R.; Punglia, R.S.; Claus, E.B.; Lee, E.Q.; Wen, P.Y.; Haas-Kogan, D.A.; et al. Brain metastases in newly diagnosed breast cancer: A population-based study. *JAMA Oncol.* **2017**, *3*, 1069–1077. [CrossRef]
60. O'Reilly, D.; Sendi, M.A.; Kelly, C.M. Overview of recent advances in metastatic triple negative breast cancer. *World J. Clin. Oncol.* **2021**, *12*, 164–182. [CrossRef]
61. Wang, C.; Luo, D. The metabolic adaptation mechanism of metastatic organotropism. *Exp. Hematol. Oncol* **2021**, *10*, 30. [CrossRef] [PubMed]

62. Tanaka, N.; Katayama, S.; Reddy, A.; Nishimura, K.; Niwa, N.; Hongo, H.; Ogihara, K.; Kosaka, T.; Mizuno, R.; Kikuchi, E.; et al. Single-cell RNA-seq analysis reveals the platinum resistance gene COX7B and the surrogate marker CD63. *Cancer Med.* **2018**, *7*, 6193–6204. [CrossRef] [PubMed]
63. Cong, L.; Ran, F.A.; Cox, D.; Lin, S.; Barretto, R.; Habib, N.; Hsu, P.D.; Wu, X.; Jiang, W.; Marraffini, L.A.; et al. Multiplex genome engineering using CRISPR/Cas systems. *Science* **2013**, *339*, 819–823. [CrossRef] [PubMed]
64. Chu, V.T.; Weber, T.; Wefers, B.; Wurst, W.; Sander, S.; Rajewsky, K.; Kuhn, R. Increasing the efficiency of homology-directed repair for CRISPR-Cas9-induced precise gene editing in mammalian cells. *Nat. Biotechnol.* **2015**, *33*, 543–548. [CrossRef]
65. Sanjana, N.E.; Shalem, O.; Zhang, F. Improved vectors and genome-wide libraries for CRISPR screening. *Nat. Methods* **2014**, *11*, 783–784. [CrossRef]
66. Engler, C.; Kandzia, R.; Marillonnet, S. A one pot, one step, precision cloning method with high throughput capability. *PLoS ONE* **2008**, *3*, e3647. [CrossRef]

Table S1. Short tandem repeat profiles.

STRs	MDA-MB-231	231-BR	231-BR-2
D8S1179	13, 13	13, 13	13, 13
D21S11	30, 33.2	30, 33.2	30, 33.2
D7S820	8, 9	8, 8	8, 8
CSF1PO	12, 13	12, 13	12, 13
D3S1358	16, 16	16, 16	16, 16
TH01	7, 9.3	7, 9.3	7, 9.3
D13S317	13, 13	13, 13	13, 13
D16S539	12, 12	12, 12	12, 12
D2S1338	20, 21	20, 21	20, 21
D19S433	11, 14	11, 14	11, 14
vWA	15, 18	15, 16	15, 18
TPOX	8, 9	8, 9	8, 9
D18S51	11, 16	11, 15, 16	16, 16
AMEL	X, X	X, X	X, X
D5S818	12, 12	12, 12	12, 12
FGA	22, 23	22, 23	22, 23

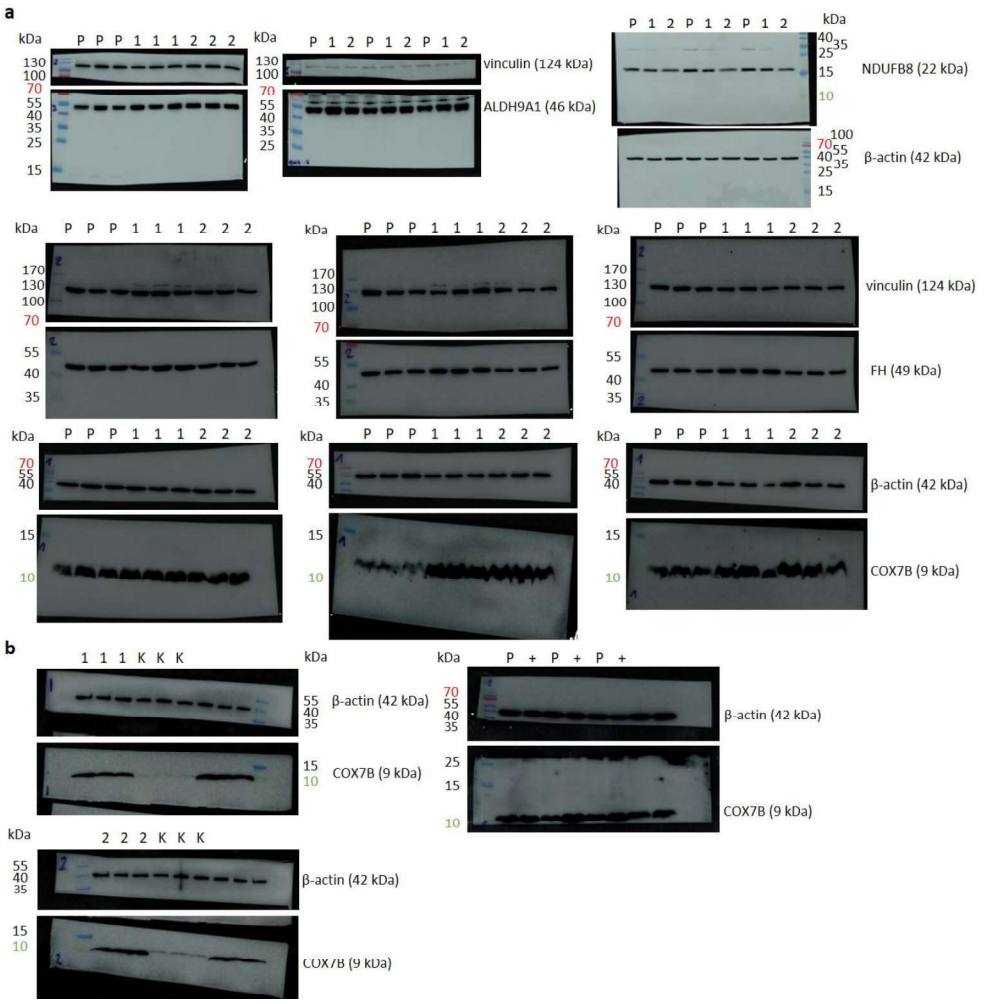


Figure S1. Uncropped western blot images. (**a**, **b**) Shown are whole western blot membranes corresponding to (**a**) Figure 3a-d, and (**b**) Figure S2. Note that, in order to be able to show molecular ladders, the membranes are shown at the longest exposure time (often overexposed), which does not always correspond to the acquisition time on an ECL imager 600. Abbreviations: P, parental; 1, 231-BR; 2, 231-BR-2; K, KO cells for *COX7B*; +, cells overexpressing COX7b.

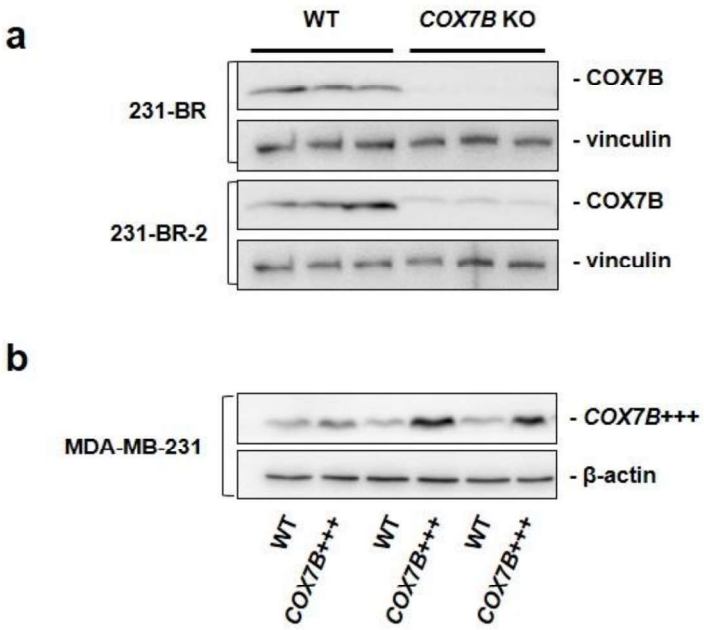


Figure S2. Validation of *COX7B* silencing and overexpression. (**a**) *COX7B* was silenced in 231-BR and 231-BR-2 brain-seeking variants using a CRISPR-Cas9 strategy. Shown are western blots reporting in triplicate on COX7b expression. Vinculin served as a loading control. (**b**) COX7b was overexpressed in parental MDA-MB-231 cells using a pCMV3 vector. Shown are western blots reporting in triplicate on COX7b expression. β-actin served as a loading control.

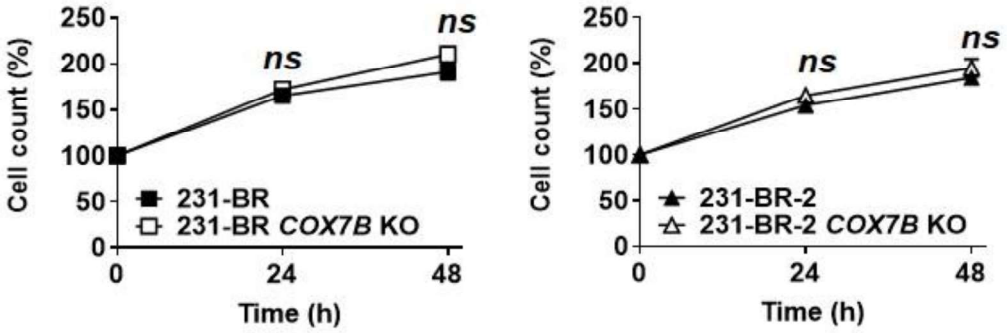


Figure S3. *COX7B* silencing does not alter brain-seeking variant cell numbers *in vitro*. 231-BR and 231-BR-2 cells were either wild-type or silenced for *COX7B* using a CRISPR-Cas9 strategy. Graphs show cell count (%) over time on a SpectraMax i3 spectrophotometer equipped with a MiniMax imaging cytometer, after seeding 5,000 cells per well in a 96-wells plate (n = 3-4). Data are shown as means ± SEM. *ns*: $p > 0.05$ compared to MDA-MB-231 cells; using two-way ANOVA with Dunnett's post hoc test.

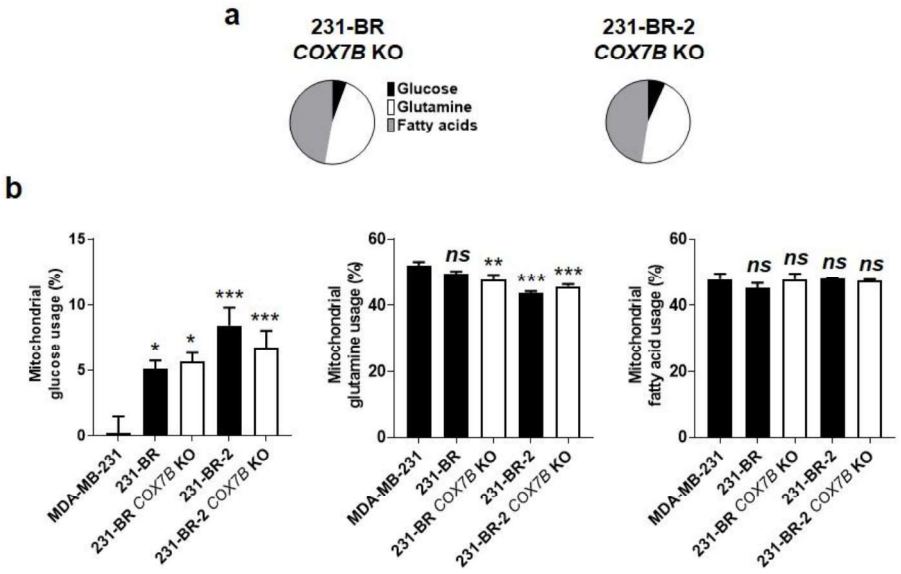


Figure S4. *COX7B* silencing does not alter the metabolic plasticity of brain-seeking variant cells. (**a, b**) 231-BR and 231-BR-2 cells were either wild-type or silenced for *COX7B* using a CRISPR-Cas9 strategy. (**a**) Mitochondrial fuel usage of *COX7B*-deficient 231-BR (left, n = 7-14) and *COX7B*-deficient 231-BR-2 (right, n = 12-16) cancer cells was determined using the Fuel Flex test kit (Agilent) on a Seahorse XF96 bioenergetics analyzer. Data are presented as pie graphs. (**b**) Mitochondrial fuel usage of parental MDA-MB-231 cells, 231-BR cells expressing or not expressing Cox7b and 231-BR-2 cells expressing or not expressing COX7b. Column graphs show mitochondrial glucose (left; n = 7-15), glutamine (middle; n = 12-16) and fatty acid (right; n = 14-16) usage, where total fuel (glucose + glutamine + fatty acids) usage = 100% for each cell line. Data are shown as means ± SEM. * $p < 0.05$, ** $p < 0.01$, *** $p < 0.005$, *ns*: $p > 0.05$ compared to MDA-MB-231 cells; using one-way ANOVA with Dunnett's post hoc test.

IV. DISCUSSION

1. The need for brain protection

The brain is a sensitive tissue orchestrating basic as well as advanced functions of our body and mind. Metastatic cancer invasion of this organ rapidly translates in severe neurological defects and short-term death, impacting both patient quality of life and overall survival. It is one of patients' most dreaded cancer cell localization.

Brain metastases are the most frequent intracranial malignancy, since their incidence is higher than primary brain tumors (Patchell 2003, Maher 2009, Valiente 2018, Achrol 2019). Even when neoplasms arise in other organs than the brain, brain colonization is a feared outcome. Brain metastases are associated with a poor prognosis, as patient survival with untreated brain metastases is less than two months (Markesbery 1978) and is around 8 to 14 months upon treatment (Sperduto 2013, Niikura 2014, Shen 2015, Darlix 2019). The incidence of brain metastases is around 20% for all cancers, originating mainly from lung cancer, breast cancer and melanoma (Nayak 2012, Sacks 2020). As detailed in section 4.5.3, brain incidence has been increasing in the last decades due to better imaging techniques and increased survival rates of patients, granting more time for metastatic progenitor cells to colonize such a complex metastatic site. Another possible cause promoting brain metastasis is the use of drugs with low BBB penetrance to treat tumors, which may exert a selective pressure, hindering tumor growth at the primary site and other metastatic sites while selecting for a brain-penetrating phenotype (Olson 2013). Since other metastatic areas are better reached by systemic therapies, it is crucial to develop therapies to prevent cancer cell colonization of the brain. For now, local resection, radiation therapies and systemic therapies are used, but with limited efficiencies and harsh adverse effects (Valiente 2018, Achrol 2019). For instance, stereotactic radiation therapy yields less neurocognitive deterioration compared to whole-brain radiation therapy that grants less recurrence, and patients are thus faced with either higher recurrence rates or a more apparent neurocognitive decline (Chang 2009). Designing pharmacological agents that can efficiently penetrate the brain and/or that can trigger a transient opening of the BBB is one of the strategies

explored. Developing new modalities to increase drug availability in the brain is a possible solution; however, toxic substances in the brain may prove to have worse secondary effects than in the rest of the body. The brain is indeed designed to be impenetrable for a reason: ensuring its role of protecting the delicate neural cells that it contains. Concerns regarding neuronal toxicity associated with BBB disruption are also paralleled with the potential initiation of new brain lesions by easier access for circulating cancer cells. An alternate solution would be to target cancer cells while they are still in the bloodstream, circumventing the need for penetrable agents. Others, however, argue that brain metastases are exposed to therapeutic drugs due to BBB leakiness, and that protection from chemotherapy-induced cytotoxicity by brain cells (such as astrocytes) is the main limitation to treatments (McWilliams 2005, Langley 2011).

It may prove particularly difficult to implement a therapeutic strategy targeting cancer cell interactions with brain cells (like astrocytes and neurons) or the neuronal phenotype of cancer cells (such as the glutamate-driven NMDAR signaling dependency [Zeng 2019]) while sparing astrocytes and neurons of the patient. It can be speculated that inhibiting neuronal properties that are hijacked by brain metastatic cancer cells would elicit neurotoxicity, and thus result in dramatic adverse effects (Ikonomidou 2002). In my opinion, it is of utmost importance to avoid toxicity to neural cells to prevent neurological defects and preserve patients' quality of life.

Systemic therapies (including endocrine therapy, anti-HER2 therapy and chemotherapy) against breast cancer brain metastases usually follow breast cancer treatment and can help to prolong survival, but essentially in patients with luminal and HER2+ tumors (Niwinska 2010b). However, the importance of targeting metastases differently than the primary tumor is underlined by the reported fact that metastatic tumors often have distinct mutational profiles as compared with primary tumors, even if they still share key driver and passenger mutations with the original tumor (Turajlic 2016). This is further underlined by the work of Niikura *et al.* (Niikura 2012) reporting the loss of HER2 expression in metastatic sites of primary HER2+ breast cancers. In line with this study, brain metastases have been reported to display altered ER/PR and HER2 status compared to primary breast tumors (Kaidar-

Person 2018, Sperduto 2020). Furthermore, brain metastatic cells of different primary tumors were shown to transcriptionally regroup together, as compared to their primary tumors of origin and other metastatic sites, further advocating for the acquisition of new characteristics for metastatic development in the brain (Park 2011, see section 5.2.3). Precision medicine aiming to analyze metastases aside from the patient primary tumor should be implemented and can be achieved, for example, by integrating liquid biopsies to collect CTCs, metastatic progenitor cells, exosomes, etc. To provide dedicated targeted therapies for brain metastases, one must gain a deeper understanding of metastatic organotropism.

2. Achievements

At the start of my thesis, previous work of our team (Porporato 2014) had unraveled the fact that metabolism could modulate and even drive metastasis. In the context of the seed-and-soil hypothesis (Paget 1889), I aimed to identify possible metabolic drivers of metastatic tropism. More specifically, I studied the brain tropism of TNBC cells as a model, using MDA-MB-231 and its two independently generated brain-trophic variants 231-BR and 231-BR-2. Through *in vitro* and *in vivo* experiments, we showed that COX7b drives metastatic homing of these TNBC cells to the brain of mice (Blackman 2022).

First, we assessed the metabolic properties of breast cancer cells showing brain-targeting (variants) or unspecific (parental) metastatic behaviors. We observed that mitochondrial respiration and mtDNA abundance were increased in both brain-seeking cancer cells. In parallel, we noticed that they displayed enlarged or more abundant mitochondria. These findings indicated that our model brain variants had gained a more oxidative phenotype.

Second, we uncovered that the COX7b subunit of the fourth complex (CIV) of the ETC, called cytochrome c oxidase (COX), was overexpressed in both brain-seeking variant cell lines. The mitochondrial localization of this shared metabolic driver of brain tropism is in line with previous observations of mitochondrial changes occurring in brain-trophic variants. We demonstrated the importance of COX7b, the expression of which modulated brain tropism and the oxidative phenotype of TNBC cells (**Figure**

18). Silencing *COX7B* using a CRISPR-Cas9 strategy hindered the *in vitro* migration of TNBC cells towards astrocytes, but not towards the other cell types (immortalized bronchial cells and hepatocytes) that we used as controls. Conversely, the overexpression of COX7b was sufficient to trigger brain tropism of parental (pan-metastatic) TNBC cells. As increased or decreased astrocyte-targeted migration in our experiments could be biased by variation in general migration, we also assessed cancer cell migration towards FBS and other cell lines than astrocytes, which was not significantly affected by *COX7B* silencing or overexpression, meaning that the observed effect was specific for astrocytes and not caused by a modulation of general migration mechanisms. The importance of OXPHOS in brain tropism was further illustrated by the observation that *COX7B* silencing reduced OXPHOS in brain-seeking variants, whereas COX7b overexpression increased OXPHOS in parental cells.

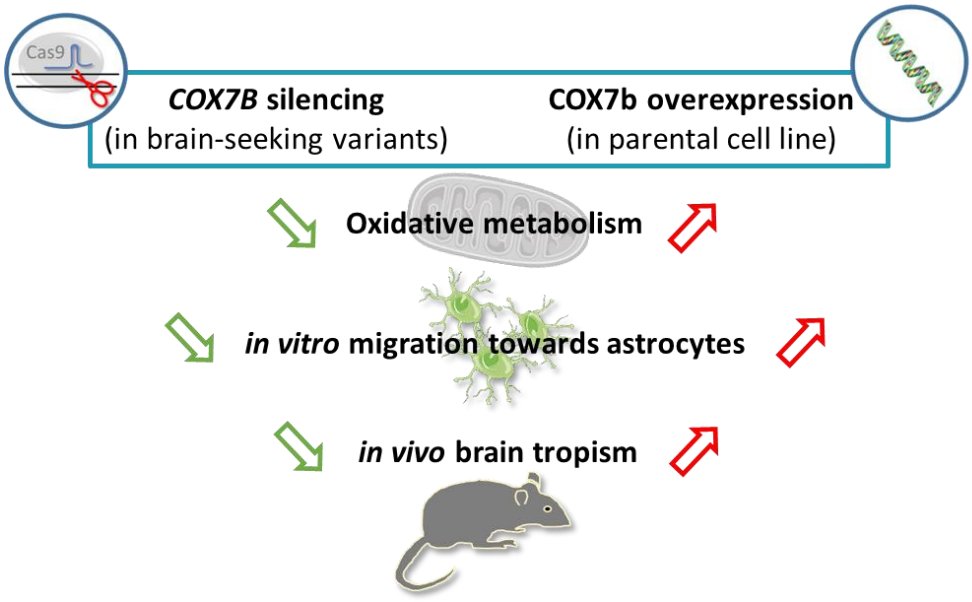


Figure 18. Graphical representation of the results obtained regarding the identification of COX7b as a driver of metastatic brain tropism. *COX7B* silencing and overexpression have opposite effects on oxidative metabolism, *in vitro* migration towards astrocytes and *in vivo* brain tropism (Blackman 2022).

Importantly, *in vitro* data demonstrating a cause-effect relationship between COX7b expression and the brain tropism of TNBC cells were successfully translated *in vivo.* Indeed, *COX7B* silencing abolished brain metastasis in mice: mice injected with *COX7B*-KO brain-trophic cancer cells were preserved from brain colonization, whereas mice injected with unmodified brain-trophic cancer cells were typically loaded with brain metastases. Metastatic development was experimentally followed by the *in vivo* acquisition of bioluminescence signals, and validated by immunohistochemistry. Moreover, we further showed that COX7b overexpression in parental cells promoted brain colonization. Therefore, not only did *COX7B* silencing block cancer cell tropism to the brain, but its overexpression conversely promoted the brain homing of pan-metastatic cells. Even if the mechanism is currently unknown, our results demonstrate that COX7b is a driver of brain metastasis. We hypothesize that COX7b could be functioning as a shared metabolic sensor for brain-specific chemoattractants in our human TNBC cell models (**Figure 19**).

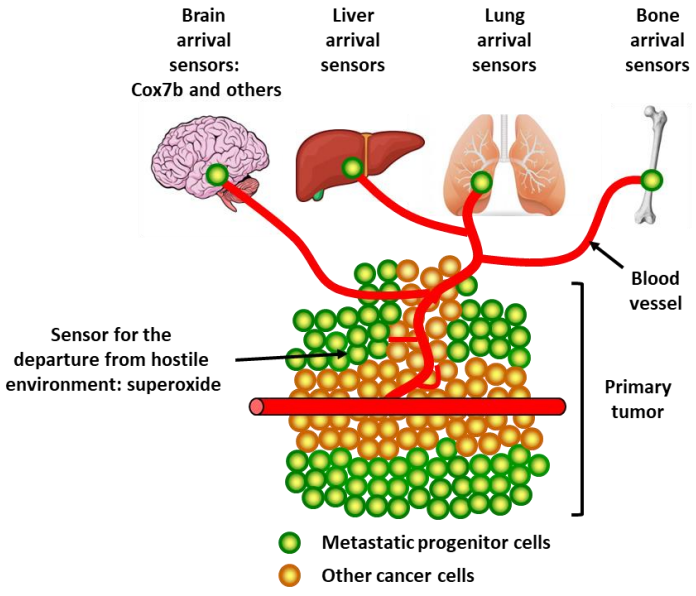


Figure 19. COX7b as a metabolic sensor for brain tropism. Metastatic progenitor cells are selected in a hostile environment and employ sensors to leave the primary tumor. Organs secrete different soluble molecules that metastatic progenitor cells could sense as chemoattractants through specific sensors driving organotropism.

Finally, COX7b was shown to be associated with worse prognosis in patients. We analyzed publicly available clinical data, which revealed that a high *COX7B* expression in primary tumors correlated with decreased overall patient survival in breast and lung cancers, and renal clear cell carcinoma. We reported on patient survival since we found no adequate parameters to obtain clinical data specifically on brain metastasis. At the time of this work, databases do not include 'brain metastasis free survival' or data on brain metastases and primary tumor to evaluate COX7b expression in both types of lesions. Because metastasis is associated with cancer cell dedifferentiation (EMT and the acquisition of stem cell traits) in primary tumors but redifferentiation in metastatic lesions (MET and the loss of stem cell traits), one also has to consider the possibility that high COX7b expression in metastatic progenitor cells could be lost in established brain metastases. Keeping an organ-sorting sensor after homing could, indeed, be unnecessary.

In our *in vitro* experiments, astrocytes were used as surrogates for the brain microenvironment. One may question the use of a single cell type to represent a whole tissue. However, astrocytes have repeatedly been used as such in the literature (Lin 2010, Sartorius 2015, Chen 2016, Kaverina 2017). Furthermore, Park *et al.* (Park 2011) had shown that the patterns of transcriptome reprogramming of MDA-MB-231 cancer cells in the brain were remarkably similar, although lower in magnitude, to the reprogramming occurring with astrocytes co-cultures (and not with fibroblasts), demonstrating that astrocytes are representative of the brain microenvironment. We used both human and mouse astrocytes to account for the human origin of the cancer cell lines and the fact that the brain-specific variants were selected in mice (Yoneda 2001, Patel 2011, Burnett 2015). Our results were highly similar in both cases, indicating that the sensed factor(s) is (are) commonly produced by mouse and human astrocytes.

For *in vivo* experiments, we decided to engineer cell lines with simultaneous luciferase and GFP expression in order to enable the measurement of bioluminescence signals in the whole brain and to perform immunohistochemistry on brain sections. This was to ensure a proper detection of brain metastases and to circumvent the limitations of each technique by using the other. Indeed,

bioluminescence measurements may fail to detect smaller and deeper lesions, whereas immunohistochemistry does not encompass the whole tissue. With this approach employing both strategies, we aimed to diminish the magnitude of errors that would arise with the use of only one of the techniques. It is worth noting that 231-BR cells were shown to form micrometastases, which play a role in relapse (Heyn 2006), thus supporting the importance of detecting both macro and micrometastases. The *COX7B*-KO cancer cell-receiving mouse that had a very slight indication of brain metastasis may be explained by an escape from the knockdown resulting in the development of a metastatic lesion. This hypothesis can be tested by single cell analysis of GFP+ cells from the brain of mice injected with wild-type and *COX7B*-KO cells. Metastatic growth was interrupted after the same time period of 4 weeks for all mice, to ensure consistency across the different experiments. Therefore, one cannot exclude that metastasis-free brains may develop metastatic lesions over a longer period of time. Difficult to implement for the experiments involving brain variants due to the rapid metastatic growth, the question, however, remains whether a longer time lapse may reveal an even higher effect of overexpressing COX7b in the parental cells.

3. Limitations and strengths of the study

Our study faced several limitations inherent to the cell lines and techniques that we used.

In vitro assays for metastasis are useful tools but limited, since they do not recapitulate all the complex properties of the host organ, such as anatomical barriers, full stromal determinants and the immune system. However, our scope here was to establish a proof of principle of the existence of a metabolic sensor for brain homing, not to identify BBB crossing molecules or the involvement of the immune system. These considerations should be addressed in follow-up studies. In particular, our *in vivo* assays, similarly to many other studies in the field, were conducted using immunocompromised mice. Although necessary for the successful growth of human cancer cell lines, immunodeficient mice do not recapitulate the full host/patient situation, since they lack an intact immune system. To address a

potential role of immunity in brain-selective metastasis, COX7b could be overexpressed in murine (breast) cancer cell lines injected to syngeneic mice monitored as previously done.

Focusing on mitochondria, we have yet to explore dynamic mitochondrial changes, like morphology and subcellular localization. To adapt to cellular stresses and needs, mitochondria undergo continuous changes in morphology through the processes of fusion and fission. Mitochondrial shape dynamics are governed by dynamin-related protein family, mainly dynamin-related protein 1 (DRP1) for fission and mitofusins (MFN) and optic atrophy 1 (Opa1) for fusion (reviewed in Yang 2022). Fused mitochondrial networks are characterized by enhanced OXPHOS capacity and protection from degradation, while fragmented mitochondria are optimal for recycling and trafficking, including for their distribution to the cell periphery for membrane protrusions (reviewed in Boulton 2022). Dysregulated dynamin-related proteins and alteration of mitochondrial shape dynamics have been linked to metabolism, ROS production, tumor growth, migration, metastasis and patient outcomes (Wu 2022, Xie 2022, Boulton 2022), rationalizing the emergence of strategies aiming at mitochondrial dynamics (Yin 2021). Next experiments should include the assessment of the expression and phosphorylation status of fission/fusion proteins, as well as their recruitment to mitochondria and the quantification of fission/fusion dynamics with reliable imaging techniques.

Our *in vivo* assays were performed by directly injecting cancer cells into the circulation, thus bypassing the initial steps of the metastatic cascade. Our experimental design was indeed purposely intended to study the final steps of metastasis and, more specifically, metastatic progenitor cell homing and engraftment into the brain.

We chose to work with 231-BR and 231-BR-2 brain-seeking variant cell lines. In a brain metastasis cell line panel (Valiente 2020), they indeed best represented brain metastasis, as other brain-seeking variant models were less specific or used with intracarotid or intracranial injections, as opposed to intracardiac (left ventricle) injections allowing cells to indiscriminately access to all mouse organs. The use of

cell models generated independently in two different laboratories gave us the opportunity to identify features that are shared by both cell lines. They nevertheless originate from the same parental MDA-MB-231 cell line. Therefore, our experimental design technically only used one TNBC model. Since we did not yet attempt to validate our findings in other (breast) cancer cell lines, at this stage we cannot draw conclusions for TNBC in general, for other breast cancer subtypes, and for cancer as a whole. However, our investigation involved a comparison of brain metastatic and parental cells, as well as with other organ-specific metastatic cells (for the microarray analyzed). We further used mRNA data sets from cancer patients to support our findings. The abovementioned limitations should be addressed in future studies. In particular, additional experiments overexpressing or downregulating COX7b expression in other (breast) cancer cell lines are now required. However useful, cell lines much less accurately represent the complex heterogeneity of neoplasms, especially when clonal expansion was needed to propagate generated COX7b overexpressing cells. To circumvent loss of heterogeneity, we used several clones that were pooled together for experiments. It is important to note that the model cell lines were profiled twice using STR profiling in the course of this work, which is not always performed and showcased in studies. It was indeed crucial in my opinion to ensure the correct identification of the cell lines employed, as cell lines are sometimes misidentified or cross-contaminated (Lacroix 2008).

4. Role of / targeting COX7B

The gene of interest uncovered in this work, *COX7B*, is a rather unexpected one. It is a X-linked nuclear-encoded transmembrane subunit of the terminal ETC complex (CIV) transiting electron from reduced cytochrome c to molecular oxygen (thus forming water) (Kadenbach 2015). The multimeric enzyme named ‘COX’ is located in the IMM and is composed of 13 subunits, with mitochondrial-encoded catalytic core subunits COX1, COX2 and COX3 surrounded by 10 nuclear-encoded subunits. The short (80 amino acids) non-catalytic COX7b subunit has very few references in the literature, being merely known to be assembled at the last stages of COX constitution (Hermann 2005), during which it associates with catalytic subunits COX1, COX2 and COX3 by interacting with COX4 and COX6a/c (Tsukihara 1996).

COX7b stabilizes COX assembly and positively modulates COX activity (Indrieri 2012). In cancer cells, high COX7b expression has been associated with platinum resistance (Tanaka 2018). Conversely, when inactivated in humans, COX7b causes microphthalmia with linear skin lesions syndrome (MLS), a neurodevelopmental disorder presenting typical eye and skin defects as well as other neurodevelopmental features, including microcephaly and facial dysmorphisms (Indrieri 2012). How COX7b is regulated in mammalian cells remains unknown. A better characterization of the protein is therefore essential for understanding its role in physiological cellular functions and in cancer-related behaviors. Our work showing that *COX7B* silencing impedes OXPHOS while COX7b overexpression triggers OXPHOS is in accordance with the role of COX7b in COX assembly and activity. It may also be involved in the formation of the respirasome, which, to my knowledge, has not yet been addressed in the literature. The exact mechanisms behind increased brain colonization upon COX7b overexpression, and the opposite upon silencing, remain unexplained. Even if COX7b is ubiquitously expressed, phenotypic manifestations associated with mutated COX7B (MLS) mainly affect the CNS (Indrieri 2012), which suggests a more specific function of COX7b in the brain.

The effects of overexpressing or silencing *COX7B* in our cancer cell models are worth further investigation. It would allow to explore the role of COX7b by addressing remaining questions: whether the number of mitochondria is affected, whether their morphology is changed, whether their functions are altered, whether metabolic substrate preference is modulated, whether (and which) signaling pathways are induced or suppressed, whether other subunits are overexpressed to compensate for COX7b absence. Ideally, these questions should be answered for a functional analysis of COX7B. Deeper analyses of the genetically manipulated cells could be performed: electron microscopy, measurements of the enzymatic activity of ETC complexes, metabolic dependency experiments, PAMgene assays measuring the activity of kinases and phosphatases, RNAseq to pinpoint changes in mRNA expression and, thus, the biological processes related to *COX7B* overexpression and silencing.

According to the seed and soil theory (Paget 1889), metastasis is a complex phenomenon that depends on the seed (the metastatic progenitor cell), the soil (the microenvironment of the organ of destination, which may be modified by tumoral preconditioning in a premetastatic niche [Kaplan 2005, Peinado 2017]), and interactions between the two. When it comes to the seed and soil hypothesis, research has mainly focused on the seed (*i.e.*, the properties of the metastatic cancer cells) (Liu 2017), but less attention has been given to the soil counterpart and to the interactions between the two. Further investigation should address the soil-derived factors that attract metastatic progenitor cells and the sensors that recognize these factors. Indeed, metastatic progenitor cells need soluble molecules produced by host cells as chemoattractants, and sensor systems to inform them when they have reached a preferred location. Even though the precise mechanisms through which COX7b drives brain tropism in our model remain elusive, its role as a sensor is supported by the fact that *COX7B* silencing selectively hindered *in vitro* migration towards astrocytes, while its overexpression selectively promoted *in vitro* migration towards astrocytes (cause-effect relationship).

Regarding the premetastatic niche, using conditioned medium from distinct cell cultures may not adequately represent the tumor microenvironment *in vivo*, since cells in the primary tumor can also secrete factors to modify distant regions in the body. As such, astrocyte-conditioned medium did not recapitulate the data obtained with astrocytes seeded at the bottom well in migration experiments (data not shown), which suggests an active interplay between cancer cells and astrocytes. In my opinion, the establishment of a chemoattractant gradient necessitating active astrocytes may be a key for brain organotropism. Alternatively or in addition, chemoattractant(s) sensed by COX7b may have a relatively short half-life in conditioned medium at room temperature.

As shown in studies regarding PMNs, factors secreted by cancer cells in primary tumors can modulate the activities of resident cells (section 1.6). Therefore, the interplay between cancer cells and distant organs should be further investigated. In our system, factors could be secreted (since there was no direct cell-cell contacts in the *in vitro* migration settings) by cancer cells to modulate the activities of astrocytes;

in return, astrocytes secreted factors to attract cancer cells. An additional experiment that could be conducted is to condition astrocytes with cancer cell medium, then test preconditioned astrocyte-conditioned medium in transwells.

A main question that arises when considering COX7b as a metabolic sensor is inquiring to which factor it is sensitive. Additional experiments are required to explore factors produced as chemoattractants in this context. TCA cycle intermediates are potential candidates, since OXPHOS activity is increased when COX7b is highly expressed. One of the follow-up experiments to start exploring this question would be to analyze the medium of migration experiments before cells have been in (distant) contact and after the allocated incubation period used for migration. In such an approach, however, factors from the cancer cells and from astrocytes would be mixed. It can nevertheless already pinpoint some potential effectors of the intercommunication between cancer cells and astrocytes. An alternative would be to compare, directly *in vivo*, the metabolic activities of parental *versus* brain-seeking cells that would be implanted in the brain. Technologies at the state of the art, such as laser sampling on tissue slices coupled to HPLC-MS/MS, could potentially help to identify differences in the use of local resources.

A noteworthy aspect of future research on COX7b is that such a small subunit (80 amino acids) has such a great impact on the metabolic and metastatic behaviors of cancer cells. Another paper has shown the involvement of this small subunit on a bigger phenomenon, reporting that high COX7b expression in primary tumors is involved in cisplatin resistance (Tanaka 2018). We cannot exclude for COX7b to have a role in addition of being a sensor. For example, since in our experiments cancer cells were injected in the bloodstream, COX7b could have a role in cell survival in the circulation. The use of liquid blood biopsies would allow to address this question, taking into account that all CTCs are not metastatic progenitor cells, and that all metastatic progenitor cells do not mandatorily have a same destination. Also, we cannot exclude at this stage that, in addition of being a sensor, COX7b would enable a specific metabolism promoting survival in the brain. Coculture experiments with astrocytes and our genetically manipulated or parental cancer cells

should be conducted to address whether COX7b expression promotes survival and growth in the presence of astrocytes.

Our choice to focus on breast cancer brain metastasis was also intended for the possible identification of a suitable target for the prevention of this life-threatening outcome. Speculating on how to integrate COX7b in the clinical context, one must admit that this protein is, unfortunately, difficult to target pharmaceutically, as this subunit does not exhibit enzymatic activity and is embedded in CIV inside mitochondria. Targeting a structure is difficult to implement, but future improvements of gene therapy might help to make COX7b targetable. A better understanding of its role may further help to find other actors implicated in its effects and easier to target. To unveil potential targetable candidates, further investigation to uncover upstream regulators and/or downstream effectors of COX7b responsible for brain metastasis is required.

We do not exclude – rather, we expect – the existence of COX7b-unrelated sensors and effectors that would control the brain tropism of cancer cells in general. The reason why we focused on COX7b in TNBC cells resided in the fact that the other analyzed proteins of interest did not show increased expression in both variants, and we therefore considered that they were not worth investigating in priority. Additional work using the strategy established here should help to identify other proteins of interest for brain tropism in other cancer cell models, which we hope will be more easily targetable (such as enzymes or transporters). Taking in consideration all cancer types that can metastasize in the brain, we believe that (1) COX7b could be shared as a brain sensor by different types of cancers, but (2) that other metabolic sensors would also exist, driving brain tropism in one or several cancer types, including MDA-MB-231-unrelated breast cancers. A similar situation is predictable for the tropism to other secondary organs.

5. Metabolomic experiments

A particularly relevant follow-up of this work would be to perform metabolomics on the cells of interest. This approach would allow to compare metabolite levels in *COX7B*-KO and COX7b-overexpressing cells with those in wild-type parental and

brain-specific cell lines in order to identify the effects of COX7b on the metabolic behavior of cells. It would help to uncover the function of COX7b and to potentially identify other targets related to brain homing. Changes in the metabolites consumed and produced by the brain-trophic variants as compared to parental cells would also enable us to identify new targets.

6. Other proteins of interest

To discover other potential drivers of brain tropism, we started to explore other targets. Indeed, in parallel to this work, a RNAseq has been performed comparing not only the 231-BR variant but also the 231-BR-2 variant with parental MDA-MB-231 cells. The strength of the microarray used for our first set of genes of interest was because it included data of other metastatic sites. However, only one brain-specific variant was included. Our new microarray allowed the combination of the two independently developed brain variants to pinpoint interesting targets upregulated (or downregulated) in both cell lines. The genes of interest that we identified imply that both variant cell lines similarly modulated their expression, underscoring their potential relevance and warranting further investigation. In addition, a PAMgene assay has been performed with our two brain-trophic variants along with the parental cells. This assay detects changes in the phosphorylation state of proteins, allowing not to look at the expression nor at the production of kinases and phosphatases, but rather directly at their (de)phosphorylating activity. The combination of both microarrays (RNA expression and phosphorylation pattern) identified several new genes of interest to be studied, which will be disclosed in future publications of my team.

Moreover, during my doctoral research, I observed that some stemness-related genes were upregulated in brain-seeking variants. Indeed, *SOX2*, *c-Myc* and *KLF4* were found to be upregulated at both the mRNA and protein levels in both brain-seeking variants (**Figure 20**). Since stemness has already been associated with a higher metastatic potential, better cell survival and a more aggressive phenotype (Zhao 2017, Peitzsch 2017, Shen 2021), we primarily left these factors aside to primarily focus on the discovery of metabolic sensor COX7b. However, our

observations confirmed what had been observed in other studies where brain metastasis had been linked to stemness. Indeed, data from the literature indicate that brain metastatic cells are related to CSC markers nestin (Sihto 2011), CD133 (Sihto 2011, Witzel 2016), CD44 (Okuda 2013, Witzel 2016), and stemness factor KLF4 (Okuda 2013). I believe that stemness is a true driver of brain metastasis in a sense that it procures cancer cells with a metabolic plasticity most probably particularly required in the very divergent surroundings encountered in the brain microenvironment as compared to other organs. Potential targets are also mentioned in section 6 and in the review of Wang *et al.* (Wang 2021): FABP7, ACSS2, FASN, GDH, FBP2, ABAT, etc. All these trails and additional research with the strategy developed in this work should lead to discover new potential targets to better prevent brain colonization.

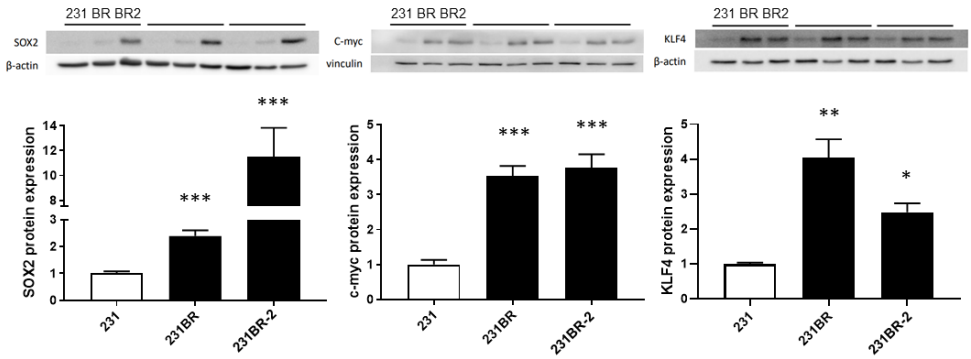


Figure 20. The expression of stemness markers SOX2, c-myc and KLF4 is increased in brain-seeking variants compared to wild-type MDA-MB-231 cells. Protein levels of SOX2, c-myc (N=3, n=9) and KLF4 (N=1, n=3) in brain-specific variants 231-BR and 231-BR-2 as well as parental cell line MDA-MB-231. Representative images of western blots are shown.

7. Proof-of-concept for metabolic drivers of metastatic tropism / for the use of our strategy with other tissue-specific metastases

Metabolic rewiring has now been widely accepted as a hallmark of cancer (Ward & Thompson 2012), but its involvement in metastasis and in metastatic organotropism is a new field of investigation (section 2.13). COX7B has proven that metabolic

elements, even a very small one, can bear responsibilities beyond energy production, and impact metastatic tropism. This proof-on-concept regarding metabolic drivers of metastatic organotropism is, in my opinion, a major finding that fulfills our primary aim. A rationale to apply the knowledge from one model to other cancer cell types with a same tissue-specific homing is supported by the idea that organ-specific metastases from different primary cancer types may display common characteristics and develop common metabolic properties in order to adapt to the same distant metabolic microenvironment (Paget 1889, Mashimo 2014, Gao 2019). For example, proteins driving the brain tropism of breast cancer cells may also drive the brain tropism of melanoma or lung cancer cells. More generally, our data underline the potential of the strategy established in this work. The strength of this strategy is the fact that we did not limit ourselves to the analysis of RNAseq data to identify genes of interest. We validated our findings not only by knocking-out the gene of interest in our brain variants but also by overexpressing it in parental cells, and evaluated the effects both *in vitro* and *in vivo*. The same approach can be applied for other tissue-homing locations, since other organs of destination would most probably reveal other proteins of interest.

8. Preventing (brain)-specific metastasis

In line with the famous quote ‘prevention is better than cure’, it would be more advantageous to prevent than to treat metastasis (*i.e.*, to circumvent the issue before patients are faced with problematic metastases). In this aim, further investigations are needed to prevent seed dissemination to distant organs, including (1) managing the primary tumor or the primary tumor microenvironment (since harsh environmental clues force primary cancer cells to adapt and to acquire new characteristics, encompassing metastatic abilities), (2) protecting patients at risk (by *ea.* finding biomarkers to identify cancer-bearing patients more at risk of developing metastasis in a given organ, which would then help to adapt the therapeutic protocol), and (3) blocking the dissemination route by therapeutically targeting cancer cells while they are in circulation. Blocking tissue-specific metastasis could be achieved by identifying the mechanisms underlying the intercommunication/interplay occurring between cancer cells and distant organ cells,

and targeting chemoattractants, metabolic sensors and homing mechanisms involved in tissue-specific colonization. Interfering with metabolic sensing is an innovative and promising anticancer strategy to target metastasis.

Anticancer approaches include agents targeting metastatic dissemination, like the promising results obtained with the use of MitoQ to target mtROS for the prevention of metastases (Capeloa 2022a/b/c). An attractive strategy would be to combine targeting the ‘departure sensor’ of metastatic cells (superoxide) with targeting their arrival (COX7b) for synergistic effects: the second approach could eradicate the cells who would escape the first one (**Figure 19**).

It is worth noting that other (external) factors than the seed and the soil may play a pivotal role in cancer metastasis and may shed new light on the matter, which should be integrated for a comprehensive understanding of the classic seed and soil hypothesis. For example, primary tumor removal by surgical resection, commensal microbiota, and dietary molecules may modulate the tumor microenvironment and metastasis development (detailed in Liu 2017), which advocates for external factors to be taken into consideration for more comprehensive therapeutic strategies.

Discussion

V. GENERAL CONCLUSION

My PhD thesis work shows for the first time that COX7b, a non-catalytic subunit of ETC Complex IV, is an important promoter of brain colonization in TNBC. COX7b expression was increased in brain-trophic human model cell lines. Moreover, COX7b silencing effectively reduced brain colonization of brain-trophic variant cells and its overexpression was sufficient to increase the brain metastasis incidence of parental TNBC cells. These effects demonstrate that COX7b drives brain tropism in our model TNBC cell line and, more importantly, open the quest for metabolic drivers of metastatic organotropism and the potential identification of innovative anticancer treatments.

General Conclusion

VI. PERSONAL CONTRIBUTIONS

Meetings & Awards

Belgium Association for Cancer Research (BACR) Annual Meeting 2018 (Poster; Liège, 27-01-2018)

IREC PhD Day 2019 (Poster; Brussels, 08-03-2019)

Brain Metastasis Research Symposium (Poster; Vienna, Austria; 28-06-2019)

ISCaM 6th Annual Meeting (Talk; Braga, Portugal; 18-10-2019), ISCaM Award 2019 (Travel grant)

Télévie's Research Seminar 2020 (Poster; Brussels; 29-01-2020)

BACR Annual Meeting 2020 (Poster; Brussels; 07-02-2020; EACR 2nd Poster Award)

IREC PhD Day 2020 (Talk, Brussels, 18-12-2020)

ISCaM 9th Annual Meeting (Talk; Turin, Italy; 02-07-2022), ISCaM Award 2022 (Travel grant)

Publications

Blackman, M. C. N. M., Capeloa, T., Rondeau, J. D., Zampieri, L. X., Benyahia, Z., Van de Velde, J. A., Fransolet, M., Daskalopoulos, E. P., Michiels, C., Beauloye, C., & Sonveaux, P. (2022). Mitochondrial Protein Cox7b Is a Metabolic Sensor Driving Brain-Specific Metastasis of Human Breast Cancer Cells. *Cancers*, *14*(18), 4371.

Payen, V. L., Porporato, P. E., Danhier, P., Vazeille, T., Blackman, M. C. N. M., May, B. H., Niebes, P., & Sonveaux, P. (2017). (+)-Catechin in a 1:2 Complex with Lysine Inhibits Cancer Cell Migration and Metastatic Take in Mice. *Frontiers in pharmacology*, *8*, 869.

Benyahia, Z., Blackman, M. C. N. M., Hamelin, L., Zampieri, L. X., Capeloa, T., Bedin, M. L., Vazeille, T., Schakman, O., & Sonveaux, P. (2021). In Vitro and In Vivo Characterization of MCT1 Inhibitor AZD3965 Confirms Preclinical Safety Compatible with Breast Cancer Treatment. *Cancers*, *13*(3), 569.

Vilela, J. M. V., Dolmans, M. M., Maruhashi, E., Blackman, M. C. N. M., Sonveaux, P., Miranda-Vilela, A. L., & Amorim, C. A. (2020). Evidence of metabolic activity during low-temperature ovarian tissue preservation in different media. *Journal of assisted reproduction and genetics*, *37*(10), 2477–2486.

Capelôa, T., Benyahia, Z., Zampieri, L. X., Blackman, M. C. N. M., & Sonveaux, P. (2020). Metabolic and non-metabolic pathways that control cancer resistance to anthracyclines. *Seminars in cell & developmental biology*, *98*, 181–191.

Cancer stem cell metabolism (publication in preparation).

Patent

Sonveaux P, Blackman MCNM, Bedin M, Rondeau JD, Capeloa T, Kienlen-Campard P, Van de Velde J. Stem cells with brain tropism. Priority date: 24 Aug 2022. Filling number: EP22191920

VII. REFERENCES

Abbott NJ. Evidence for bulk flow of brain interstitial fluid: significance for physiology and pathology. *Neurochem Int* 2004; 45: 545-552.

Abbott NJ, Ronnback L, Hansson E. Astrocyte-endothelial interactions at the blood-brain barrier. *Nat Rev Neurosci* 2006; 7: 41-53.

Aceto N, Bardia A, Miyamoto DT, Donaldson MC, Wittner BS, Spencer JA *et al*. Circulating tumor cell clusters are oligoclonal precursors of breast cancer metastasis. *Cell* 2014; 158: 1110-1122.

Acheampong T, Kehm RD, Terry MB, Argov EL, Tehranifar P. Incidence trends of breast cancer molecular subtypes by age and race/ethnicity in the US from 2010 to 2016. *JAMA Netw Open* 2020; 3: e2013226.

Achrol AS, Rennert RC, Anders C, Soffietti R, Ahluwalia MS, Nayak L *et al*. Brain metastases. *Nat Rev Dis Primers* 2019; 5: 5.

Ahluwalia MS, Vogelbaum MV, Chao ST, Mehta MM. Brain metastasis and treatment. *F1000Prime Rep* 2014; 6: 114.

Ahn CS, Metallo CM. Mitochondria as biosynthetic factories for cancer proliferation. *Cancer Metab* 2015; 3: 1.

Ahn SG, Kim SJ, Kim C, Jeong J. Molecular classification of triple-negative breast cancer. *J Breast Cancer* 2016; 19: 223-230.

Aigner S, Sthoeger ZM, Fogel M, Weber E, Zarn J, Ruppert M *et al*. CD24, a mucin-type glycoprotein, is a ligand for P-selectin on human tumor cells. *Blood* 1997; 89: 3385-3395.

Aizawa F, Nishinaka T, Yamashita T, Nakamoto K, Koyama Y, Kasuya F *et al*. Astrocytes release polyunsaturated fatty acids by lipopolysaccharide stimuli. *Biol Pharm Bull* 2016; 39: 1100-1106.

Al-Hajj M, Wicha MS, Benito-Hernandez A, Morrison SJ, Clarke MF. Prospective identification of tumorigenic breast cancer cells. *Proc Natl Acad Sci U S A* 2003; 100: 3983-3988.

Almuhaideb A, Papathanasiou N, Bomanji J. 18F-FDG PET/CT imaging in oncology. *Ann Saudi Med* 2011; 31: 3-13.

Alvero AB, Montagna MK, Holmberg JC, Craveiro V, Brown D, Mor G. Targeting the mitochondria activates two independent cell death pathways in ovarian cancer stem cells. *Mol Cancer Ther* 2011; 10: 1385-1393.

Ananieva EA, Wilkinson AC. Branched-chain amino acid metabolism in cancer. *Curr Opin Clin Nutr Metab Care* 2018; 21: 64-70.

Avraham HK, Jiang S, Fu Y, Nakshatri H, Ovadia H, Avraham S. Angiopoietin-2 mediates blood-brain barrier impairment and colonization of triple-negative breast cancer cells in brain. *J Pathol* 2014; 232: 369-381.

Azevedo AS, Follain G, Patthabhiraman S, Harlepp S, Goetz JG. Metastasis of circulating tumor cells: favorable soil or suitable biomechanics, or both? *Cell Adh Migr* 2015; 9: 345-356.

Azevedo FA, Carvalho LR, Grinberg LT, Farfel JM, Ferretti RE, Leite RE *et al*. Equal numbers of neuronal and nonneuronal cells make the human brain an isometrically scaled-up primate brain. *J Comp Neurol* 2009; 513: 532-541.

Bahmad HF, Cheaito K, Chalhoub RM, Hadadeh O, Monzer A, Ballout F *et al*. Sphere-

formation assay: three-dimensional in vitro culturing of prostate cancer stem/progenitor sphere-forming cells. *Front Oncol* 2018; 8: 347.

Banyard J, Bielenberg DR. The role of EMT and MET in cancer dissemination. *Connect Tissue Res* 2015; 56: 403-413.

Barcena C, Mayoral P, Quiros PM. Mitohormesis, an antiaging paradigm. *Int Rev Cell Mol Biol* 2018; 340: 35-77.

Bareche Y, Venet D, Ignatiadis M, Aftimos P, Piccart M, Rothe F *et al*. Unravelling triple-negative breast cancer molecular heterogeneity using an integrative multiomic analysis. *Ann Oncol* 2018; 29: 895-902.

Barok M, Joensuu H, Isola J. Trastuzumab emtansine: mechanisms of action and drug resistance. *Breast Cancer Res* 2014; 16: 209.

Bartkowiak K, Koch C, Gartner S, Andreas A, Gorges TM, Pantel K. In vitro modeling of reoxygenation effects on mRNA and protein levels in hypoxic tumor cells upon entry into the bloodstream. *Cells* 2020; 9.

Bastiaansen JA, Cheng T, Mishkovsky M, Duarte JM, Comment A, Gruetter R. In vivo enzymatic activity of acetylCoA synthetase in skeletal muscle revealed by (13)C turnover from hyperpolarized [1-(13)C]acetate to [1-(13)C]acetylcarnitine. *Biochim Biophys Acta* 2013; 1830: 4171-4178.

Bastien RR, Rodriguez-Lescure A, Ebbert MT, Prat A, Munarriz B, Rowe L *et al*. PAM50 breast cancer subtyping by RT-qPCR and concordance with standard clinical molecular markers. *BMC Med Genomics* 2012; 5: 44.

Batchuluun B, Pinkosky SL, Steinberg GR. Lipogenesis inhibitors: therapeutic opportunities and challenges. *Nat Rev Drug Discov* 2022; 21: 283-305.

Bauer DE, Hatzivassiliou G, Zhao F, Andreadis C, Thompson CB. ATP citrate lyase is an important component of cell growth and transformation. *Oncogene* 2005; 24: 6314-6322.

Begley DJ, Brightman MW. Structural and functional aspects of the blood-brain barrier. *Prog Drug Res* 2003; 61: 39-78.

Benatti P, Peluso G, Nicolai R, Calvani M. Polyunsaturated fatty acids: biochemical, nutritional and epigenetic properties. *J Am Coll Nutr* 2004; 23: 281-302.

Bendell JC, Domchek SM, Burstein HJ, Harris L, Younger J, Kuter I *et al*. Central nervous system metastases in women who receive trastuzumab-based therapy for metastatic breast carcinoma. *Cancer* 2003; 97: 2972-2977.

Berndtsson M, Hagg M, Panaretakis T, Havelka AM, Shoshan MC, Linder S. Acute apoptosis by cisplatin requires induction of reactive oxygen species but is not associated with damage to nuclear DNA. *Int J Cancer* 2007; 120: 175-180.

Bertucci F, Finetti P, Cervera N, Esterni B, Hermitte F, Viens P *et al*. How basal are triple-negative breast cancers? *Int J Cancer* 2008; 123: 236-240.

Birsoy K, Possemato R, Lorbeer FK, Bayraktar EC, Thiru P, Yucel B *et al*. Metabolic determinants of cancer cell sensitivity to glucose limitation and biguanides. *Nature* 2014; 508: 108-112.

Blackman M, Capeloa T, Rondeau JD, Zampieri LX, Benyahia Z, Van de Velde JA *et al*. Mitochondrial protein cox7b is a metabolic sensor driving brain-specific metastasis of human breast cancer cells. *Cancers (Basel)* 2022; 14.

Blecker D, Abraham S, Furth EE, Kochman ML. Melanoma in the gastrointestinal tract. *Am J Gastroenterol* 1999; 94: 3427-3433.

References

Bochev P, Klisarova A, Kaprelyan A, Chaushev B, Dancheva Z. Brain metastases detectability of routine whole body (18)F-FDG PET and low dose CT scanning in 2502 asymptomatic patients with solid extracranial tumors. *Hell J Nucl Med* 2012; 15: 125-129.

Boire A, Brastianos PK, Garzia L, Valiente M. Brain metastasis. *Nat Rev Cancer* 2020; 20: 4-11.

Bonanni B, Puntoni M, Cazzaniga M, Pruneri G, Serrano D, Guerrieri-Gonzaga A *et al*. Dual effect of metformin on breast cancer proliferation in a randomized presurgical trial. *J Clin Oncol* 2012; 30: 2593-2600.

Bonnet S, Archer SL, Allalunis-Turner J, Haromy A, Beaulieu C, Thompson R *et al*. A mitochondria-K+ channel axis is suppressed in cancer and its normalization promotes apoptosis and inhibits cancer growth. *Cancer Cell* 2007; 11: 37-51.

Boogerd W, Vos VW, Hart AA, Baris G. Brain metastases in breast cancer; natural history, prognostic factors and outcome. *J Neurooncol* 1993; 15: 165-174.

Bos PD, Zhang XH, Nadal C, Shu W, Gomis RR, Nguyen DX *et al*. Genes that mediate breast cancer metastasis to the brain. *Nature* 2009; 459: 1005-1009.

Boulton DP, Caino MC. Mitochondrial fission and fusion in tumor progression to metastasis. *Front Cell Dev Biol* 2022; 10: 849962.

Brasnjevic I, Steinbusch HW, Schmitz C, Martinez-Martinez P, European NanoBioPharmaceutics Research I. Delivery of peptide and protein drugs over the blood-brain barrier. *Prog Neurobiol* 2009; 87: 212-251.

Bray F, Ferlay J, Soerjomataram I, Siegel RL, Torre LA, Jemal A. Global cancer statistics 2018: GLOBOCAN estimates of incidence and mortality worldwide for 36 cancers in 185 countries. *CA Cancer J Clin* 2018; 68: 394-424.

Brierley JDG, M. K.; Wittekind C. *TNM classification of malignant tumours*, 8th edn: Chichester, 2017.

Brightman MW. Ultrastructure of brain endothelium. In: Bradbury MWB (ed). *Physiology and pharmacology of the blood-brain barrier*. Springer-Verlag: Berlin Heidelberg, 1992, pp 1-22.

Brightman MW, Reese TS. Junctions between intimately apposed cell membranes in the vertebrate brain. *J Cell Biol* 1969; 40: 648-677.

Brinker T, Stopa E, Morrison J, Klinge P. A new look at cerebrospinal fluid circulation. *Fluids Barriers CNS* 2014; 11: 10.

Broadfield LA, Pane AA, Talebi A, Swinnen JV, Fendt SM. Lipid metabolism in cancer: New perspectives and emerging mechanisms. *Dev Cell* 2021; 56: 1363-1393.

Brown PD, Ballman KV, Cerhan JH, Anderson SK, Carrero XW, Whitton AC *et al*. Postoperative stereotactic radiosurgery compared with whole brain radiotherapy for resected metastatic brain disease (NCCTG N107C/CEC.3): a multicentre, randomised, controlled, phase 3 trial. *Lancet Oncol* 2017; 18: 1049-1060.

Brufsky AM, Mayer M, Rugo HS, Kaufman PA, Tan-Chiu E, Tripathy D *et al*. Central nervous system metastases in patients with HER2-positive metastatic breast cancer: incidence, treatment, and survival in patients from registHER. *Clin Cancer Res* 2011; 17: 4834-4843.

Brunelle JK, Bell EL, Quesada NM, Vercauteren K, Tiranti V, Zeviani M *et al*. Oxygen sensing requires mitochondrial ROS but not oxidative phosphorylation. *Cell Metab* 2005; 1: 409-414.

References

Burdick MM, Chu JT, Godar S, Sackstein R. HCELL is the major E- and L-selectin ligand expressed on LS174T colon carcinoma cells. *J Biol Chem* 2006; 281: 13899-13905.

Burnett RM, Craven KE, Krishnamurthy P, Goswami CP, Badve S, Crooks P *et al*. Organ-specific adaptive signaling pathway activation in metastatic breast cancer cells. *Oncotarget* 2015; 6: 12682-12696.

Burstein MD, Tsimelzon A, Poage GM, Covington KR, Contreras A, Fuqua SA *et al*. Comprehensive genomic analysis identifies novel subtypes and targets of triple-negative breast cancer. *Clin Cancer Res* 2015; 21: 1688-1698.

Cailleau R, Olive M, Cruciger QV. Long-term human breast carcinoma cell lines of metastatic origin: preliminary characterization. *In Vitro* 1978; 14: 911-915.

Capeloa T, Krzystyniak J, d'Hose D, Canas Rodriguez A, Payen VL, Zampieri LX *et al*. MitoQ inhibits human breast cancer cell migration, invasion and clonogenicity. *Cancers (Basel)* 2022a; 14.

Capeloa T, Krzystyniak J, Rodriguez AC, Payen VL, Zampieri LX, Pranzini E *et al*. MitoQ prevents human breast cancer recurrence and lung metastasis in mice. *Cancers (Basel)* 2022b; 14.

Capeloa T, Van de Velde JA, d'Hose D, Lipari SG, Derouane F, Hamelin L *et al*. Inhibition of mitochondrial redox signaling with MitoQ prevents metastasis of human pancreatic cancer in mice. *Cancers (Basel)* 2022c; 14: 4918.

Carbonell WS, Ansorge O, Sibson N, Muschel R. The vascular basement membrane as "soil" in brain metastasis. *PLoS One* 2009; 4: e5857.

Cardoso F, Senkus E, Costa A, Papadopoulos E, Aapro M, Andre F *et al*. 4th ESO-ESMO international consensus guidelines for advanced breast cancer (ABC 4)dagger. *Ann Oncol* 2018; 29: 1634-1657.

Carvalho R, Paredes J, Ribeiro AS. Impact of breast cancer cells secretome on the brain metastatic niche remodeling. *Semin Cancer Biol* 2020; 60: 294-301.

Chajes V, Cambot M, Moreau K, Lenoir GM, Joulin V. Acetyl-CoA carboxylase alpha is essential to breast cancer cell survival. *Cancer Res* 2006; 66: 5287-5294.

Chambers AF, Groom AC, MacDonald IC. Dissemination and growth of cancer cells in metastatic sites. *Nat Rev Cancer* 2002; 2: 563-572.

Chang EL, Wefel JS, Hess KR, Allen PK, Lang FF, Kornguth DG *et al*. Neurocognition in patients with brain metastases treated with radiosurgery or radiosurgery plus whole-brain irradiation: a randomised controlled trial. *Lancet Oncol* 2009; 10: 1037-1044.

Chatterjee K, Carman-Esparza CM, Munson JM. Methods to measure, model and manipulate fluid flow in brain. *J Neurosci Methods* 2020; 333: 108541.

Chavez KJ, Garimella SV, Lipkowitz S. Triple negative breast cancer cell lines: one tool in the search for better treatment of triple negative breast cancer. *Breast Dis* 2010; 32: 35-48.

Cheang MC, Chia SK, Voduc D, Gao D, Leung S, Snider J *et al*. Ki67 index, HER2 status, and prognosis of patients with luminal B breast cancer. *J Natl Cancer Inst* 2009; 101: 736-750.

Chen EI, Hewel J, Krueger JS, Tiraby C, Weber MR, Kralli A *et al*. Adaptation of energy metabolism in breast cancer brain metastases. *Cancer Res* 2007; 67: 1472-1486.

Chen J, Lee HJ, Wu X, Huo L, Kim SJ, Xu L *et al*. Gain of glucose-independent growth upon metastasis of breast cancer cells to the brain. *Cancer Res* 2015; 75: 554-565.

Chen LB. Mitochondrial membrane potential in living cells. *Annu Rev Cell Biol* 1988; 4: 155-

181.

Chen Q, Boire A, Jin X, Valiente M, Er EE, Lopez-Soto A *et al*. Carcinoma-astrocyte gap junctions promote brain metastasis by cGAMP transfer. *Nature* 2016; 533: 493-498.

Chen W. Clinical applications of PET in brain tumors. *J Nucl Med* 2007; 48: 1468-1481.

Chen W, Hoffmann AD, Liu H, Liu X. Organotropism: new insights into molecular mechanisms of breast cancer metastasis. *NPJ Precis Oncol* 2018; 2: 4.

Christofk HR, Vander Heiden MG, Harris MH, Ramanathan A, Gerszten RE, Wei R *et al*. The M2 splice isoform of pyruvate kinase is important for cancer metabolism and tumour growth. *Nature* 2008; 452: 230-233.

Chu DJ, Yao DE, Zhuang YF, Hong Y, Zhu XC, Fang ZR *et al*. Azithromycin enhances the favorable results of paclitaxel and cisplatin in patients with advanced non-small cell lung cancer. *Genet Mol Res* 2014; 13: 2796-2805.

Clark AG, Vignjevic DM. Modes of cancer cell invasion and the role of the microenvironment. *Curr Opin Cell Biol* 2015; 36: 13-22.

Comerford SA, Huang Z, Du X, Wang Y, Cai L, Witkiewicz AK *et al*. Acetate dependence of tumors. *Cell* 2014; 159: 1591-1602.

Conrad C, Gotte M, Schlomann U, Roessler M, Pagenstecher A, Anderson P *et al*. ADAM8 expression in breast cancer derived brain metastases: Functional implications on MMP-9 expression and transendothelial migration in breast cancer cells. *Int J Cancer* 2018; 142: 779-791.

Conte P, Schneeweiss A, Loibl S, Mamounas EP, von Minckwitz G, Mano MS *et al*. Patient-reported outcomes from KATHERINE: A phase 3 study of adjuvant trastuzumab emtansine versus trastuzumab in patients with residual invasive disease after neoadjuvant therapy for human epidermal growth factor receptor 2-positive breast cancer. *Cancer* 2020; 126: 3132-3139.

Corbet C, Pinto A, Martherus R, Santiago de Jesus JP, Polet F, Feron O. Acidosis drives the reprogramming of fatty acid metabolism in cancer cells through changes in mitochondrial and histone acetylation. *Cell Metab* 2016; 24: 311-323.

Cordero A, Kanojia D, Miska J, Panek WK, Xiao A, Han Y *et al*. FABP7 is a key metabolic regulator in HER2+ breast cancer brain metastasis. *Oncogene* 2019; 38: 6445-6460.

Cortes J, Cescon DW, Rugo HS, Nowecki Z, Im SA, Yusof MM *et al*. Pembrolizumab plus chemotherapy versus placebo plus chemotherapy for previously untreated locally recurrent inoperable or metastatic triple-negative breast cancer (KEYNOTE-355): a randomised, placebo-controlled, double-blind, phase 3 clinical trial. *Lancet* 2020; 396: 1817-1828.

Cortes J, Kim SB, Chung WP, Im SA, Park YH, Hegg R *et al*. Trastuzumab deruxtecan versus trastuzumab emtansine for breast cancer. *N Engl J Med* 2022; 386: 1143-1154.Costa-Silva B, Aiello NM, Ocean AJ, Singh S, Zhang H, Thakur BK *et al*. Pancreatic cancer exosomes initiate pre-metastatic niche formation in the liver. *Nat Cell Biol* 2015; 17: 816-826.

Crivellari D, Pagani O, Veronesi A, Lombardi D, Nole F, Thurlimann B *et al*. High incidence of central nervous system involvement in patients with metastatic or locally advanced breast cancer treated with epirubicin and docetaxel. *Ann Oncol* 2001; 12: 353-356.

Cunatova K, Reguera DP, Houstek J, Mracek T, Pecina P. Role of cytochrome c oxidase nuclear-encoded subunits in health and disease. *Physiol Res* 2020; 69: 947-965.

Curigliano G, Mueller V, Borges V, Hamilton E, Hurvitz S, Loi S *et al*. Tucatinib versus placebo added to trastuzumab and capecitabine for patients with pretreated HER2+ metastatic

breast cancer with and without brain metastases (HER2CLIMB): final overall survival analysis. *Ann Oncol* 2022; 33: 321-329.

Daikhin Y, Yudkoff M. Compartmentation of brain glutamate metabolism in neurons and glia. *J Nutr* 2000; 130: 1026S-1031S.

Dalvi S.; On NN, h.; Pogorzelec, M.; Miller, D. W.; Hatch, G. M. The blood brain barrier — regulation of fatty acid and drug transport. In: Heinbockel T (ed). *Neurochemistry*. InTechOpen: London, 2014, pp 1-33.

Damsky WE, Rosenbaum LE, Bosenberg M. Decoding melanoma metastasis. *Cancers (Basel)* 2010; 3: 126-163.

Danbolt NC. Glutamate uptake. *Prog Neurobiol* 2001; 65: 1-105.

Dang L, White DW, Gross S, Bennett BD, Bittinger MA, Driggers EM *et al*. Cancer-associated IDH1 mutations produce 2-hydroxyglutarate. *Nature* 2009; 462: 739-744.

Darlix A, Louvel G, Fraisse J, Jacot W, Brain E, Debled M *et al*. Impact of breast cancer molecular subtypes on the incidence, kinetics and prognosis of central nervous system metastases in a large multicentre real-life cohort. *Br J Cancer* 2019; 121: 991-1000.

Davidson SM, Papagiannakopoulos T, Olenchock BA, Heyman JE, Keibler MA, Luengo A *et al*. Environment impacts the metabolic dependencies of Ras-driven non-small cell lung cancer. *Cell Metab* 2016; 23: 517-528.

Dawood S, Broglio K, Esteva FJ, Ibrahim NK, Kau SW, Islam R *et al*. Defining prognosis for women with breast cancer and CNS metastases by HER2 status. *Ann Oncol* 2008; 19: 1242-1248.

de la Cruz-Lopez KG, Castro-Munoz LJ, Reyes-Hernandez DO, Garcia-Carranca A, Manzo-Merino J. Lactate in the regulation of tumor microenvironment and therapeutic approaches. *Front Oncol* 2019; 9: 1143.

De Luca A, Fiorillo M, Peiris-Pages M, Ozsvari B, Smith DL, Sanchez-Alvarez R *et al*. Mitochondrial biogenesis is required for the anchorage-independent survival and propagation of stem-like cancer cells. *Oncotarget* 2015; 6: 14777-14795.

De Piano M, Manuelli V, Zadra G, Otte J, Edqvist PD, Ponten F *et al*. Lipogenic signalling modulates prostate cancer cell adhesion and migration via modification of Rho GTPases. *Oncogene* 2020; 39: 3666-3679.

de Ronde JJ, Hannemann J, Halfwerk H, Mulder L, Straver ME, Vrancken Peeters MJ *et al*. Concordance of clinical and molecular breast cancer subtyping in the context of preoperative chemotherapy response. *Breast Cancer Res Treat* 2010; 119: 119-126.

Dean M, Hamon Y, Chimini G. The human ATP-binding cassette (ABC) transporter superfamily. *J Lipid Res* 2001; 42: 1007-1017.

DeBerardinis RJ, Chandel NS. Fundamentals of cancer metabolism. *Sci Adv* 2016; 2: e1600200.

DeBerardinis RJ, Cheng T. Q's next: the diverse functions of glutamine in metabolism, cell biology and cancer. *Oncogene* 2010; 29: 313-324.

DeBerardinis RJ, Mancuso A, Daikhin E, Nissim I, Yudkoff M, Wehrli S *et al*. Beyond aerobic glycolysis: transformed cells can engage in glutamine metabolism that exceeds the requirement for protein and nucleotide synthesis. *Proc Natl Acad Sci U S A* 2007; 104: 19345-19350.

DeClerck K, Elble RC. The role of hypoxia and acidosis in promoting metastasis and resistance to chemotherapy. *Front Biosci (Landmark Ed)* 2010; 15: 213-225.

Degli Esposti M, Chouaia B, Comandatore F, Crotti E, Sassera D, Lievens PM *et al*. Evolution

of mitochondria reconstructed from the energy metabolism of living bacteria. *PLoS One* 2014; 9: e96566.

DeNicola GM, Cantley LC. Cancer's fuel choice: new flavors for a picky eater. *Mol Cell* 2015; 60: 514-523.

DeNicola GM, Chen PH, Mullarky E, Sudderth JA, Hu Z, Wu D *et al*. NRF2 regulates serine biosynthesis in non-small cell lung cancer. *Nat Genet* 2015; 47: 1475-1481.

DeNicola GM, Karreth FA, Humpton TJ, Gopinathan A, Wei C, Frese K *et al*. Oncogene-induced Nrf2 transcription promotes ROS detoxification and tumorigenesis. *Nature* 2011; 475: 106-109.

Denisenko TV, Gorbunova AS, Zhivotovsky B. Mitochondrial involvement in migration, invasion and metastasis. *Front Cell Dev Biol* 2019; 7: 355.

Dent R, Trudeau M, Pritchard KI, Hanna WM, Kahn HK, Sawka CA *et al*. Triple-negative breast cancer: clinical features and patterns of recurrence. *Clin Cancer Res* 2007; 13: 4429-4434.

Derouane F, Punie K, Duhoux FP. Systemic treatment landscape and algorithm for hormone-receptor positive, HER2 negative advanced breast cancer. *Belg J Med Oncol* 2021; 15: 20-33.

DeVito NCG, M. D.; Caplain, J.; Rajagopal, S.; Popowich, D.; Orkin, B. A.; Grimm, E.; Tsichlis, P. N., Martell, R. E.; Saif, W. M. A pilot study evaluating the safety and impact of pretreatment with metformin on colorectal cancer stem cells (CCSC) in patients undergoing resection. *J Clin Oncol* 2014; 32: e14581-e14581.

Dewaele M, Maes H, Agostinis P. ROS-mediated mechanisms of autophagy stimulation and their relevance in cancer therapy. *Autophagy* 2010; 6: 838-854.

Dias K, Dvorkin-Gheva A, Hallett RM, Wu Y, Hassell J, Pond GR *et al*. Claudin-low breast cancer; clinical & pathological characteristics. *PLoS One* 2017; 12: e0168669.

Diehn M, Cho RW, Lobo NA, Kalisky T, Dorie MJ, Kulp AN *et al*. Association of reactive oxygen species levels and radioresistance in cancer stem cells. *Nature* 2009; 458: 780-783.

Dieras V, Miles D, Verma S, Pegram M, Welslau M, Baselga J *et al*. Trastuzumab emtansine versus capecitabine plus lapatinib in patients with previously treated HER2-positive advanced breast cancer (EMILIA): a descriptive analysis of final overall survival results from a randomised, open-label, phase 3 trial. *Lancet Oncol* 2017; 18: 732-742.

Dimitroff CJ, Descheny L, Trujillo N, Kim R, Nguyen V, Huang W *et al*. Identification of leukocyte E-selectin ligands, P-selectin glycoprotein ligand-1 and E-selectin ligand-1, on human metastatic prostate tumor cells. *Cancer Res* 2005; 65: 5750-5760.

DiStefano A, Yong Yap Y, Hortobagyi GN, Blumenschein GR. The natural history of breast cancer patients with brain metastases. *Cancer* 1979; 44: 1913-1918.

Dolman D, Drndarski S, Abbott NJ, Rattray M. Induction of aquaporin 1 but not aquaporin 4 messenger RNA in rat primary brain microvessel endothelial cells in culture. *J Neurochem* 2005; 93: 825-833.

Dong LF, Kovarova J, Bajzikova M, Bezawork-Geleta A, Svec D, Endaya B *et al*. Horizontal transfer of whole mitochondria restores tumorigenic potential in mitochondrial DNA-deficient cancer cells. *Elife* 2017; 6.

Dou J, Gu N. Emerging strategies for the identification and targeting of cancer stem cells. *Tumour Biol* 2010; 31: 243-253.

Dupuy F, Tabaries S, Andrzejewski S, Dong Z, Blagih J, Annis MG *et al*. PDK1-dependent

metabolic reprogramming dictates metastatic potential in breast cancer. *Cell Metab* 2015; 22: 577-589.

Eichler AF, Chung E, Kodack DP, Loeffler JS, Fukumura D, Jain RK. The biology of brain metastases-translation to new therapies. *Nat Rev Clin Oncol* 2011; 8: 344-356.

El Waly B, Macchi M, Cayre M, Durbec P. Oligodendrogenesis in the normal and pathological central nervous system. *Front Neurosci* 2014; 8: 145.

Erler JT, Bennewith KL, Cox TR, Lang G, Bird D, Koong A *et al*. Hypoxia-induced lysyl oxidase is a critical mediator of bone marrow cell recruitment to form the premetastatic niche. *Cancer Cell* 2009; 15: 35-44.

Erpenbeck L, Schon MP. Deadly allies: the fatal interplay between platelets and metastasizing cancer cells. *Blood* 2010; 115: 3427-3436.

Ewing J. *Neoplastic diseases: a treatise on tumours*, 3rd edn. W. B. Saunders Co. Ltd.: Philadelphia and London, 1928.

Fan J, Cai B, Zeng M, Hao Y, Giancotti FG, Fu BM. Integrin β4 signaling promotes mammary tumor cell adhesion to brain microvascular endothelium by inducing ErbB2-mediated secretion of VEGF. *Ann Biomed Eng* 2011; 39(8): 2223-2241.

Fan J, Ye J, Kamphorst JJ, Shlomi T, Thompson CB, Rabinowitz JD. Quantitative flux analysis reveals folate-dependent NADPH production. *Nature* 2014; 510: 298-302.

Fares J, Cordero A, Kanojia D, Lesniak MS. The network of cytokines in brain metastases. *Cancers (Basel)* 2021; 13.

Fendt SM, Bell EL, Keibler MA, Olenchock BA, Mayers JR, Wasylenko TM *et al*. Reductive glutamine metabolism is a function of the alpha-ketoglutarate to citrate ratio in cells. *Nat Commun* 2013; 4: 2236.

Feng L, Hatten ME, Heintz N. Brain lipid-binding protein (BLBP): a novel signaling system in the developing mammalian CNS. *Neuron* 1994; 12: 895-908.

Ferlay J, Colombet M, Soerjomataram I, Dyba T, Randi G, Bettio M *et al*. Cancer incidence and mortality patterns in Europe: estimates for 40 countries and 25 major cancers in 2018. *Eur J Cancer* 2018; 103: 356-387.

Ferraro GB, Ali A, Luengo A, Kodack DP, Deik A, Abbott KL *et al*. Fatty acid synthesis is required for breast cancer brain metastasis. *Nat Cancer* 2021; 2: 414-428.

Fhu CW, Ali A. Fatty acid synthase: an emerging target in cancer. *Molecules* 2020; 25.

Fidler IJ. Metastasis: quantitative analysis of distribution and fate of tumor emboli labeled with 125 I-5-iodo-2'-deoxyuridine. *J Natl Cancer Inst* 1970; 45: 773-782.

Fidler IJ. The pathogenesis of cancer metastasis: the 'seed and soil' hypothesis revisited. *Nat Rev Cancer* 2003; 3: 453-458.

Fidler IJ. The role of the organ microenvironment in brain metastasis. *Semin Cancer Biol* 2011; 21: 107-112.

Fidler IJ, Nicolson GL. Organ selectivity for implantation survival and growth of B16 melanoma variant tumor lines. *J Natl Cancer Inst* 1976; 57: 1199-1202.

Figley CR, Stroman PW. The role(s) of astrocytes and astrocyte activity in neurometabolism, neurovascular coupling, and the production of functional neuroimaging signals. *Eur J Neurosci* 2011; 33: 577-588.

Fiorillo M, Lamb R, Tanowitz HB, Mutti L, Krstic-Demonacos M, Cappello AR *et al*. Repurposing atovaquone: targeting mitochondrial complex III and OXPHOS to eradicate cancer stem cells. *Oncotarget* 2016; 7: 34084-34099.

Fiorillo M, Toth F, Brindisi M, Sotgia F, Lisanti MP. Deferiprone (DFP) targets cancer stem cell (CSC) propagation by inhibiting mitochondrial metabolism and inducing ROS production. *Cells* 2020; 9.

Fiorillo M, Toth F, Sotgia F, Lisanti MP. Doxycycline, Azithromycin and Vitamin C (DAV): a potent combination therapy for targeting mitochondria and eradicating cancer stem cells (CSCs). *Aging (Albany NY)* 2019; 11: 2202-2216.

Fischer GM, Jalali A, Kircher DA, Lee WC, McQuade JL, Haydu LE *et al*. Molecular profiling reveals unique immune and metabolic features of melanoma brain metastases. *Cancer Discov* 2019; 9: 628-645.

Flavin R, Peluso S, Nguyen PL, Loda M. Fatty acid synthase as a potential therapeutic target in cancer. *Future Oncol* 2010; 6: 551-562.

Fong MY, Zhou W, Liu L, Alontaga AY, Chandra M, Ashby J *et al*. Breast-cancer-secreted miR-122 reprograms glucose metabolism in premetastatic niche to promote metastasis. *Nat Cell Biol* 2015; 17: 183-194.

Fougner C, Bergholtz H, Kuiper R, Norum JH, Sorlie T. Claudin-low-like mouse mammary tumors show distinct transcriptomic patterns uncoupled from genomic drivers. *Breast Cancer Res* 2019; 21: 85.

Fougner C, Bergholtz H, Norum JH, Sorlie T. Re-definition of claudin-low as a breast cancer phenotype. *Nat Commun* 2020; 11: 1787.

Freedland SJ, Moul JW. Prostate specific antigen recurrence after definitive therapy. *J Urol* 2007; 177: 1985-1991.

Frezza C. Mitochondrial metabolites: undercover signalling molecules. *Interface Focus* 2017; 7: 20160100.

Fulda S, Galluzzi L, Kroemer G. Targeting mitochondria for cancer therapy. *Nat Rev Drug Discov* 2010; 9: 447-464.

Fulford LG, Reis-Filho JS, Ryder K, Jones C, Gillett CE, Hanby A *et al*. Basal-like grade III invasive ductal carcinoma of the breast: patterns of metastasis and long-term survival. *Breast Cancer Res* 2007; 9: R4.

Galluzzi L, Baehrecke EH, Ballabio A, Boya P, Bravo-San Pedro JM, Cecconi F *et al*. Molecular definitions of autophagy and related processes. *EMBO J* 2017; 36: 1811-1836.

Gammon L, Biddle A, Heywood HK, Johannessen AC, Mackenzie IC. Sub-sets of cancer stem cells differ intrinsically in their patterns of oxygen metabolism. *PLoS One* 2013; 8: e62493.

Gao Y, Bado I, Wang H, Zhang W, Rosen JM, Zhang XH. Metastasis organotropism: redefining the congenial soil. *Dev Cell* 2019; 49: 375-391.

Garrido-Castro AC, Lin NU, Polyak K. Insights into molecular classifications of triple-negative breast cancer: improving patient selection for treatment. *Cancer Discov* 2019; 9: 176-198.

Gaude E, Frezza C. Defects in mitochondrial metabolism and cancer. *Cancer Metab* 2014; 2: 10.

Geenen JJJ, Linn SC, Beijnen JH, Schellens JHM. PARP inhibitors in the treatment of triple-negative breast cancer. *Clin Pharmacokinet* 2018; 57: 427-437.

Geng Y, Yeh K, Takatani T, King MR. Three to tango: MUC1 as a ligand for both E-selectin and ICAM-1 in the breast cancer metastatic cascade. *Front Oncol* 2012; 2: 76.

Gennari A, Andre F, Barrios CH, Cortes J, de Azambuja E, DeMichele A *et al*. ESMO Clinical

Practice Guideline for the diagnosis, staging and treatment of patients with metastatic breast cancer. *Ann Oncol* 2021; 32: 1475-1495.

Genre L, Roche H, Varela L, Kanoun D, Ouali M, Filleron T *et al*. External validation of a published nomogram for prediction of brain metastasis in patients with extra-cerebral metastatic breast cancer and risk regression analysis. *Eur J Cancer* 2017; 72: 200-209.

German NJ, Yoon H, Yusuf RZ, Murphy JP, Finley LW, Laurent G *et al*. PHD3 loss in cancer enables metabolic reliance on fatty acid oxidation via deactivation of ACC2. *Mol Cell* 2016; 63: 1006-1020.

Gilkes DM, Semenza GL, Wirtz D. Hypoxia and the extracellular matrix: drivers of tumour metastasis. *Nat Rev Cancer* 2014; 14: 430-439.

Ginestier C, Hur MH, Charafe-Jauffret E, Monville F, Dutcher J, Brown M *et al*. ALDH1 is a marker of normal and malignant human mammary stem cells and a predictor of poor clinical outcome. *Cell Stem Cell* 2007; 1: 555-567.

Giuliano AE, Connolly JL, Edge SB, Mittendorf EA, Rugo HS, Solin LJ *et al*. Breast Cancer-Major changes in the American Joint Committee on Cancer eighth edition cancer staging manual. *CA Cancer J Clin* 2017; 67: 290-303.

Gjedde A, Crone C. Induction processes in blood-brain transfer of ketone bodies during starvation. *Am J Physiol* 1975; 229: 1165-1169.

Gloor SM, Wachtel M, Bolliger MF, Ishihara H, Landmann R, Frei K. Molecular and cellular permeability control at the blood-brain barrier. *Brain Res Brain Res Rev* 2001; 36: 258-264.

Goldhirsch A, Winer EP, Coates AS, Gelber RD, Piccart-Gebhart M, Thurlimann B *et al*. Personalizing the treatment of women with early breast cancer: highlights of the St Gallen International Expert Consensus on the Primary Therapy of Early Breast Cancer 2013. *Ann Oncol* 2013; 24: 2206-2223.

Goodwin ML, Gladden LB, Nijsten MW, Jones KB. Lactate and cancer: revisiting the warburg effect in an era of lactate shuttling. *Front Nutr* 2014; 1: 27.

Gorrini C, Harris IS, Mak TW. Modulation of oxidative stress as an anticancer strategy. *Nat Rev Drug Discov* 2013; 12: 931-947.

Goubran HA, Stakiw J, Radosevic M, Burnouf T. Platelets effects on tumor growth. *Semin Oncol* 2014; 41: 359-369.

Gout S, Morin C, Houle F, Huot J. Death receptor-3, a new E-Selectin counter-receptor that confers migration and survival advantages to colon carcinoma cells by triggering p38 and ERK MAPK activation. *Cancer Res* 2006; 66: 9117-9124.

Grimes DR, Fletcher AG, Partridge M. Oxygen consumption dynamics in steady-state tumour models. *R Soc Open Sci* 2014a; 1: 140080.

Grimes DR, Kelly C, Bloch K, Partridge M. A method for estimating the oxygen consumption rate in multicellular tumour spheroids. *J R Soc Interface* 2014b; 11: 20131124.

Griss T, Vincent EE, Egnatchik R, Chen J, Ma EH, Faubert B *et al*. Metformin antagonizes cancer cell proliferation by suppressing mitochondrial-dependent biosynthesis. *PLoS Biol* 2015; 13: e1002309.

Grosse-Wilde A, Fouquier d'Herouel A, McIntosh E, Ertaylan G, Skupin A, Kuestner RE *et al*. Stemness of the hybrid epithelial/mesenchymal state in breast cancer and Its association with poor survival. *PLoS One* 2015; 10: e0126522.

Gruetter R, Novotny EJ, Boulware SD, Rothman DL, Mason GF, Shulman GI *et al*. Direct

measurement of brain glucose concentrations in humans by 13C NMR spectroscopy. *Proc Natl Acad Sci U S A* 1992; 89: 1109-1112.

Gunasinghe NP, Wells A, Thompson EW, Hugo HJ. Mesenchymal-epithelial transition (MET) as a mechanism for metastatic colonisation in breast cancer. *Cancer Metastasis Rev* 2012; 31: 469-478.

Hadad S, Iwamoto T, Jordan L, Purdie C, Bray S, Baker L *et al*. Evidence for biological effects of metformin in operable breast cancer: a pre-operative, window-of-opportunity, randomized trial. *Breast Cancer Res Treat* 2011; 128: 783-794.

Hadnagy A, Gaboury L, Beaulieu R, Balicki D. SP analysis may be used to identify cancer stem cell populations. *Exp Cell Res* 2006; 312: 3701-3710.

Han JJ, Kim TM, Jeon YK, Kim MK, Khwarg SI, Kim CW *et al*. Long-term outcomes of first-line treatment with doxycycline in patients with previously untreated ocular adnexal marginal zone B cell lymphoma. *Ann Hematol* 2015; 94: 575-581.

Hanahan D, Weinberg RA. The hallmarks of cancer. *Cell* 2000; 100: 57-70.

Hanahan D, Weinberg RA. Hallmarks of cancer: the next generation. *Cell* 2011; 144: 646-674.

Harbeck N, Penault-Llorca F, Cortes J, Gnant M, Houssami N, Poortmans P *et al*. Breast cancer. *Nat Rev Dis Primers* 2019; 5: 66.

Harrell JC, Pfefferle AD, Zalles N, Prat A, Fan C, Khramtsov A *et al*. Endothelial-like properties of claudin-low breast cancer cells promote tumor vascular permeability and metastasis. *Clin Exp Metastasis* 2014; 31: 33-45.

Harrell JC, Prat A, Parker JS, Fan C, He X, Carey L *et al*. Genomic analysis identifies unique signatures predictive of brain, lung, and liver relapse. *Breast Cancer Res Treat* 2012; 132: 523-535.

Haseloff RF, Blasig IE, Bauer HC, Bauer H. In search of the astrocytic factor(s) modulating blood-brain barrier functions in brain capillary endothelial cells in vitro. *Cell Mol Neurobiol* 2005; 25: 25-39.

Hatzivassiliou G, Zhao F, Bauer DE, Andreadis C, Shaw AN, Dhanak D *et al*. ATP citrate lyase inhibition can suppress tumor cell growth. *Cancer Cell* 2005; 8: 311-321.

Haunerland NH, Spener F. Fatty acid-binding proteins--insights from genetic manipulations. *Prog Lipid Res* 2004; 43: 328-349.

Hawkins BT, Davis TP. The blood-brain barrier/neurovascular unit in health and disease. *Pharmacol Rev* 2005; 57: 173-185.

Hayasaka H, Yoshida J, Kuroda Y, Nishiguchi A, Matsusaki M, Kishimoto K *et al*. CXCL12 promotes CCR7 ligand-mediated breast cancer cell invasion and migration toward lymphatic vessels. *Cancer Sci* 2022; 113: 1338-1351.

Heeke AL, Tan AR. Checkpoint inhibitor therapy for metastatic triple-negative breast cancer. *Cancer Metastasis Rev* 2021; 40: 537-547.

Herrmann JM, Funes S. Biogenesis of cytochrome oxidase-sophisticated assembly lines in the mitochondrial inner membrane. *Gene* 2005; 354: 43-52.

Herschkowitz JI, Simin K, Weigman VJ, Mikaelian I, Usary J, Hu Z *et al*. Identification of conserved gene expression features between murine mammary carcinoma models and human breast tumors. *Genome Biol* 2007; 8: R76.

Hines SL, Vallow LA, Tan WW, McNeil RB, Perez EA, Jain A. Clinical outcomes after a diagnosis of brain metastases in patients with estrogen- and/or human epidermal growth factor receptor 2-positive versus triple-negative breast cancer. *Ann Oncol* 2008; 19: 1561-1565.

Hiratsuka S, Goel S, Kamoun WS, Maru Y, Fukumura D, Duda DG *et al*. Endothelial focal adhesion kinase mediates cancer cell homing to discrete regions of the lungs via E-selectin up-regulation. *Proc Natl Acad Sci U S A* 2011; 108: 3725-3730.

Hirsch HA, Iliopoulos D, Tsichlis PN, Struhl K. Metformin selectively targets cancer stem cells, and acts together with chemotherapy to block tumor growth and prolong remission. *Cancer Res* 2009; 69: 7507-7511.

Hollingsworth MA, Swanson BJ. Mucins in cancer: protection and control of the cell surface. *Nat Rev Cancer* 2004; 4: 45-60.

Hoshino A, Costa-Silva B, Shen TL, Rodrigues G, Hashimoto A, Tesic Mark M *et al*. Tumour exosome integrins determine organotropic metastasis. *Nature* 2015; 527: 329-335.

Houten SM, Wanders RJ. A general introduction to the biochemistry of mitochondrial fatty acid beta-oxidation. *J Inherit Metab Dis* 2010; 33: 469-477.

Hsu CC, Tseng LM, Lee HC. Role of mitochondrial dysfunction in cancer progression. *Exp Biol Med (Maywood)* 2016; 241: 1281-1295.

Hsu JL, Hsieh Y, Tu C, O'Connor D, Nick HS, Silverman DN. Catalytic properties of human manganese superoxide dismutase. *J Biol Chem* 1996; 271: 17687-17691.

Hu L, Zhang J, Zhu H, Min J, Feng Y, Zhang H. Biological characteristics of a specific brain metastatic cell line derived from human lung adenocarcinoma. *Med Oncol* 2010; 27: 708-714.

Huang M, Myers CR, Wang Y, You M. Mitochondria as a novel target for cancer chemoprevention: emergence of mitochondrial-targeting agents. *Cancer Prev Res (Phila)* 2021; 14: 285-306.

Huber JD, Egleton RD, Davis TP. Molecular physiology and pathophysiology of tight junctions in the blood-brain barrier. *Trends Neurosci* 2001; 24: 719-725.

Hudson BG, Reeders ST, Tryggvason K. Type IV collagen: structure, gene organization, and role in human diseases. Molecular basis of Goodpasture and Alport syndromes and diffuse leiomyomatosis. *J Biol Chem* 1993; 268: 26033-26036.

Icard P, Wu Z, Fournel L, Coquerel A, Lincet H, Alifano M. ATP citrate lyase: a central metabolic enzyme in cancer. *Cancer Lett* 2020; 471: 125-134.

Ikonomidou C, Turski L. Why did NMDA receptor antagonists fail clinical trials for stroke and traumatic brain injury? *Lancet Neurol* 2002; 1: 383-386.

Iliff JJ, Wang M, Liao Y, Plogg BA, Peng W, Gundersen GA *et al*. A paravascular pathway facilitates CSF flow through the brain parenchyma and the clearance of interstitial solutes, including amyloid beta. *Sci Transl Med* 2012; 4: 147ra111.

Indrieri A, van Rahden VA, Tiranti V, Morleo M, Iaconis D, Tammaro R *et al*. Mutations in COX7B cause microphthalmia with linear skin lesions, an unconventional mitochondrial disease. *Am J Hum Genet* 2012; 91: 942-949.

Ishikawa K, Takenaga K, Akimoto M, Koshikawa N, Yamaguchi A, Imanishi H *et al*. ROS-generating mitochondrial DNA mutations can regulate tumor cell metastasis. *Science* 2008; 320: 661-664.

Ishiwata K, Kubota K, Murakami M, Kubota R, Sasaki T, Ishii S *et al*. Re-evaluation of amino acid PET studies: can the protein synthesis rates in brain and tumor tissues be measured in vivo? *J Nucl Med* 1993a; 34: 1936-1943.

Ishiwata K, Tsurumi Y, Kameyama M, Sato K, Iwata R, Takahashi T *et al*. Brain tumor accumulation and plasma pharmacokinetic parameters of 2'-deoxy-5-18F-fluorouridine. *Ann Nucl Med* 1993b; 7: 199-205.

Jain M, Ngoy S, Sheth SA, Swanson RA, Rhee EP, Liao R *et al*. A systematic survey of lipids across mouse tissues. *Am J Physiol Endocrinol Metab* 2014; 306: E854-868.

Jain RK, Munn LL, Fukumura D. Dissecting tumour pathophysiology using intravital microscopy. *Nat Rev Cancer* 2002; 2: 266-276.

Jang A, Hill RP. An examination of the effects of hypoxia, acidosis, and glucose starvation on the expression of metastasis-associated genes in murine tumor cells. *Clin Exp Metastasis* 1997; 15: 469-483.

Janku F, LoRusso P, Mansfield AS, Nanda R, Spira A, Wang T *et al*. First-in-human evaluation of the novel mitochondrial complex I inhibitor ASP4132 for treatment of cancer. *Invest New Drugs* 2021; 39: 1348-1356.

Janzer A, German NJ, Gonzalez-Herrera KN, Asara JM, Haigis MC, Struhl K. Metformin and phenformin deplete tricarboxylic acid cycle and glycolytic intermediates during cell transformation and NTPs in cancer stem cells. *Proc Natl Acad Sci U S A* 2014; 111: 10574-10579.

Janzer RC, Raff MC. Astrocytes induce blood-brain barrier properties in endothelial cells. *Nature* 1987; 325: 253-257.

Jeon SM, Chandel NS, Hay N. AMPK regulates NADPH homeostasis to promote tumour cell survival during energy stress. *Nature* 2012; 485: 661-665.

Jiang YZ, Ma D, Suo C, Shi J, Xue M, Hu X *et al*. Genomic and transcriptomic landscape of triple-negative breast cancers: subtypes and treatment strategies. *Cancer Cell* 2019; 35: 428-440 e425.

Jin J, Gao Y, Zhang J, Wang L, Wang B, Cao J *et al*. Incidence, pattern and prognosis of brain metastases in patients with metastatic triple negative breast cancer. *BMC Cancer* 2018; 18: 446.

Jin X, Demere Z, Nair K, Ali A, Ferraro GB, Natoli T *et al*. A metastasis map of human cancer cell lines. *Nature* 2020; 588: 331-336.

Jin Y, Desta Z, Stearns V, Ward B, Ho H, Lee KH *et al*. CYP2D6 genotype, antidepressant use, and tamoxifen metabolism during adjuvant breast cancer treatment. *J Natl Cancer Inst* 2005; 97: 30-39.

Jolly MK, Ware KE, Gilja S, Somarelli JA, Levine H. EMT and MET: necessary or permissive for metastasis? *Mol Oncol* 2017; 11: 755-769.

Joyce JA, Pollard JW. Microenvironmental regulation of metastasis. *Nat Rev Cancer* 2009; 9: 239-252.

Jung J, Kang E, Gwak JM, Seo AN, Park SY, Lee AS *et al*. Association between basal-like phenotype and BRCA1/2 germline mutations in Korean breast cancer patients. *Curr Oncol* 2016; 23: 298-303.

Jung JW, Park SB, Lee SJ, Seo MS, Trosko JE, Kang KS. Metformin represses self-renewal of the human breast carcinoma stem cells via inhibition of estrogen receptor-mediated OCT4 expression. *PLoS One* 2011; 6: e28068.

Jung SY, Rosenzweig M, Sereika SM, Linkov F, Brufsky A, Weissfeld JL. Factors associated with mortality after breast cancer metastasis. *Cancer Causes Control* 2012; 23: 103-112.

Kadenbach B, Huttemann M. The subunit composition and function of mammalian cytochrome c oxidase. *Mitochondrion* 2015; 24: 64-76.

Kaelin WG, Jr., Ratcliffe PJ. Oxygen sensing by metazoans: the central role of the HIF hydroxylase pathway. *Mol Cell* 2008; 30: 393-402.

Kaidar-Person O, Meattini I, Jain P, Bult P, Simone N, Kindts I *et al*. Discrepancies between biomarkers of primary breast cancer and subsequent brain metastases: an international multicenter study. *Breast Cancer Res Treat* 2018; 167: 479-483.

Kang SA, Hasan N, Mann AP, Zheng W, Zhao L, Morris L *et al*. Blocking the adhesion cascade at the premetastatic niche for prevention of breast cancer metastasis. *Mol Ther* 2015; 23: 1044-1054.

Kannagi R. Carbohydrate-mediated cell adhesion involved in hematogenous metastasis of cancer. *Glycoconj J* 1997; 14: 577-584.

Kaplan RN, Riba RD, Zacharoulis S, Bramley AH, Vincent L, Costa C *et al*. VEGFR1-positive haematopoietic bone marrow progenitors initiate the pre-metastatic niche. *Nature* 2005; 438: 820-827.

Katz R, Hamilton JA, Pownall HJ, Deckelbaum RJ, Hillard CJ, Leboeuf RC *et al*. Brain uptake and utilization of fatty acids, lipids & lipoproteins: recommendations for future research. *J Mol Neurosci* 2007; 33: 146-150.

Kaverina N, Borovjagin AV, Kadagidze Z, Baryshnikov A, Baryshnikova M, Malin D *et al*. Astrocytes promote progression of breast cancer metastases to the brain via a KISS1-mediated autophagy. *Autophagy* 2017; 13: 1905-1923.

Keller KE, Doctor ZM, Dwyer ZW, Lee YS. SAICAR induces protein kinase activity of PKM2 that is necessary for sustained proliferative signaling of cancer cells. *Mol Cell* 2014; 53: 700-709.

Keller KE, Tan IS, Lee YS. SAICAR stimulates pyruvate kinase isoform M2 and promotes cancer cell survival in glucose-limited conditions. *Science* 2012; 338: 1069-1072.

Kennecke H, Yerushalmi R, Woods R, Cheang MC, Voduc D, Speers CH *et al*. Metastatic behavior of breast cancer subtypes. *J Clin Oncol* 2010; 28: 3271-3277.

Kennedy KM, Scarbrough PM, Ribeiro A, Richardson R, Yuan H, Sonveaux P *et al*. Catabolism of exogenous lactate reveals it as a legitimate metabolic substrate in breast cancer. *PLoS One* 2013; 8: e75154.

Kenny PA, Lee GY, Myers CA, Neve RM, Semeiks JR, Spellman PT *et al*. The morphologies of breast cancer cell lines in three-dimensional assays correlate with their profiles of gene expression. *Mol Oncol* 2007; 1: 84-96.

Kessenbrock K, Plaks V, Werb Z. Matrix metalloproteinases: regulators of the tumor microenvironment. *Cell* 2010; 141: 52-67.

Kienast Y, von Baumgarten L, Fuhrmann M, Klinkert WE, Goldbrunner R, Herms J *et al*. Real-time imaging reveals the single steps of brain metastasis formation. *Nat Med* 2010; 16: 116-122.

Kim SJ, Kim JS, Park ES, Lee JS, Lin Q, Langley RR *et al*. Astrocytes upregulate survival genes in tumor cells and induce protection from chemotherapy. *Neoplasia* 2011; 13: 286-298.

Kim YJ, Varki A. Perspectives on the significance of altered glycosylation of glycoproteins in cancer. *Glycoconj J* 1997; 14: 569-576.

Kirikae M, Diksic M, Yamamoto YL. Quantitative measurements of regional glucose utilization and rate of valine incorporation into proteins by double-tracer autoradiography in the rat brain tumor model. *J Cereb Blood Flow Metab* 1989; 9: 87-95.

Kirsch DG, Loeffler JS. Brain metastases in patients with breast cancer: new horizons. *Clin Breast Cancer* 2005; 6: 115-124.

Kitajima K, Nakamoto Y, Okizuka H, Onishi Y, Senda M, Suganuma N *et al*. Accuracy of

whole-body FDG-PET/CT for detecting brain metastases from non-central nervous system tumors. *Ann Nucl Med* 2008; 22: 595-602.

Klein A, Olendrowitz C, Schmutzler R, Hampl J, Schlag PM, Maass N *et al*. Identification of brain- and bone-specific breast cancer metastasis genes. *Cancer Lett* 2009; 276: 212-220.

Klein EA, Thompson IM, Jr., Tangen CM, Crowley JJ, Lucia MS, Goodman PJ *et al*. Vitamin E and the risk of prostate cancer: the Selenium and Vitamin E Cancer Prevention Trial (SELECT). *JAMA* 2011; 306: 1549-1556.

Klos KJ, O'Neill BP. Brain metastases. *Neurologist* 2004; 10: 31-46.

Klotz R, Thomas A, Teng T, Han SM, Iriondo O, Li L *et al*. Circulating tumor cells exhibit metastatic tropism and reveal brain metastasis drivers. *Cancer Discov* 2020; 10: 86-103.

Knowles SE, Jarrett IG, Filsell OH, Ballard FJ. Production and utilization of acetate in mammals. *Biochem J* 1974; 142: 401-411.

Kuksis M, Gao Y, Tran W, Hoey C, Kiss A, Komorowski AS *et al*. The incidence of brain metastases among patients with metastatic breast cancer: a systematic review and meta-analysis. *Neuro Oncol* 2021; 23: 894-904.

Kumar S, Nandi A, Singh S, Regulapati R, Li N, Tobias JW *et al*. Dll1(+) quiescent tumor stem cells drive chemoresistance in breast cancer through NF-kappaB survival pathway. *Nat Commun* 2021; 12: 432.

Labelle M, Hynes RO. The initial hours of metastasis: the importance of cooperative host-tumor cell interactions during hematogenous dissemination. *Cancer Discov* 2012; 2: 1091-1099.

Lacroix M. Persistent use of "false" cell lines. *Int J Cancer* 2008; 122: 1-4.

Ladanyi A, Mukherjee A, Kenny HA, Johnson A, Mitra AK, Sundaresan S *et al*. Adipocyte-induced CD36 expression drives ovarian cancer progression and metastasis. *Oncogene* 2018; 37: 2285-2301.

Lai CH, Kuo KH. The critical component to establish in vitro BBB model: pericyte. *Brain Res Brain Res Rev* 2005; 50: 258-265.

Lamb R, Harrison H, Hulit J, Smith DL, Lisanti MP, Sotgia F. Mitochondria as new therapeutic targets for eradicating cancer stem cells: quantitative proteomics and functional validation via MCT1/2 inhibition. *Oncotarget* 2014; 5: 11029-11037.

Lamb R, Ozsvari B, Lisanti CL, Tanowitz HB, Howell A, Martinez-Outschoorn UE *et al*. Antibiotics that target mitochondria effectively eradicate cancer stem cells, across multiple tumor types: treating cancer like an infectious disease. *Oncotarget* 2015; 6: 4569-4584.

Lambert AW, Pattabiraman DR, Weinberg RA. Emerging biological principles of metastasis. *Cell* 2017; 168: 670-691.

Langley RR, Fidler IJ. The seed and soil hypothesis revisited--the role of tumor-stroma interactions in metastasis to different organs. *Int J Cancer* 2011; 128: 2527-2535.

Laubli H, Borsig L. Selectins promote tumor metastasis. *Semin Cancer Biol* 2010; 20: 169-177.

Laubli H, Spanaus KS, Borsig L. Selectin-mediated activation of endothelial cells induces expression of CCL5 and promotes metastasis through recruitment of monocytes. *Blood* 2009; 114: 4583-4591.

LeBleu VS, O'Connell JT, Gonzalez Herrera KN, Wikman H, Pantel K, Haigis MC *et al*. PGC-

1alpha mediates mitochondrial biogenesis and oxidative phosphorylation in cancer cells to promote metastasis. *Nat Cell Biol* 2014; 16: 992-1003, 1001-1015.

Lee BC, Lee TH, Avraham S, Avraham HK. Involvement of the chemokine receptor CXCR4 and its ligand stromal cell-derived factor 1alpha in breast cancer cell migration through human brain microvascular endothelial cells. *Mol Cancer Res* 2004; 2: 327-338.

Lee HJ, Li CF, Ruan D, He J, Montal ED, Lorenz S *et al*. Non-proteolytic ubiquitination of hexokinase 2 by HectH9 controls tumor metabolism and cancer stem cell expansion. *Nat Commun* 2019; 10: 2625.

Lee HT, Xue J, Chou PC, Zhou A, Yang P, Conrad CA *et al*. Stat3 orchestrates interaction between endothelial and tumor cells and inhibition of Stat3 suppresses brain metastasis of breast cancer cells. *Oncotarget* 2015; 6: 10016-10029.

Lee P, Chandel NS, Simon MC. Cellular adaptation to hypoxia through hypoxia inducible factors and beyond. *Nat Rev Mol Cell Biol* 2020; 21: 268-283.

Lee YT. Breast carcinoma: pattern of metastasis at autopsy. *J Surg Oncol* 1983; 23: 175-180.

Lehmann BD, Bauer JA, Chen X, Sanders ME, Chakravarthy AB, Shyr Y *et al*. Identification of human triple-negative breast cancer subtypes and preclinical models for selection of targeted therapies. *J Clin Invest* 2011; 121: 2750-2767.

Lehmann BD, Jovanovic B, Chen X, Estrada MV, Johnson KN, Shyr Y *et al*. Refinement of triple-negative breast cancer molecular subtypes: implications for neoadjuvant chemotherapy selection. *PLoS One* 2016; 11: e0157368.

Lei Y, Han H, Yuan F, Javeed A, Zhao Y. The brain interstitial system: anatomy, modeling, in vivo measurement, and applications. *Prog Neurobiol* 2017; 157: 230-246.

Lewerenz J, Hewett SJ, Huang Y, Lambros M, Gout PW, Kalivas PW *et al*. The cystine/glutamate antiporter system x(c)(-) in health and disease: from molecular mechanisms to novel therapeutic opportunities. *Antioxid Redox Signal* 2013; 18: 522-555.

Lewis CA, Parker SJ, Fiske BP, McCloskey D, Gui DY, Green CR *et al*. Tracing compartmentalized NADPH metabolism in the cytosol and mitochondria of mammalian cells. *Mol Cell* 2014; 55: 253-263.

Ley K, Laudanna C, Cybulsky MI, Nourshargh S. Getting to the site of inflammation: the leukocyte adhesion cascade updated. *Nat Rev Immunol* 2007; 7: 678-689.

Li B, Wang C, Zhang Y, Zhao XY, Huang B, Wu PF *et al*. Elevated PLGF contributes to small-cell lung cancer brain metastasis. *Oncogene* 2013; 32: 2952-2962.

Li J, Cheng JX. Direct visualization of de novo lipogenesis in single living cells. *Sci Rep* 2014; 4: 6807.

Li W, Ma H, Zhang J, Zhu L, Wang C, Yang Y. Unraveling the roles of CD44/CD24 and ALDH1 as cancer stem cell markers in tumorigenesis and metastasis. *Sci Rep* 2017; 7: 13856.

Li W, Ma H, Zhang J, Zhu L, Wang C, Yang Y. Author Correction: unraveling the roles of CD44/CD24 and ALDH1 as cancer stem cell markers in tumorigenesis and metastasis. *Sci Rep* 2018; 8: 4276.

Li Y, Rogoff HA, Keates S, Gao Y, Murikipudi S, Mikule K *et al*. Suppression of cancer relapse and metastasis by inhibiting cancer stemness. *Proc Natl Acad Sci U S A* 2015; 112: 1839-1844.

Lieberman BP, Ploessl K, Wang L, Qu W, Zha Z, Wise DR *et al*. PET imaging of glutaminolysis in tumors by 18F-(2S,4R)4-fluoroglutamine. *J Nucl Med* 2011; 52: 1947-1955.

Lim E, Vaillant F, Wu D, Forrest NC, Pal B, Hart AH *et al*. Aberrant luminal progenitors as the

candidate target population for basal tumor development in BRCA1 mutation carriers. *Nat Med* 2009; 15: 907-913.

Lin BR, Chang CC, Chen LR, Wu MH, Wang MY, Kuo IH *et al*. Cysteine-rich 61 (CCN1) enhances chemotactic migration, transendothelial cell migration, and intravasation by concomitantly up-regulating chemokine receptor 1 and 2. *Mol Cancer Res* 2007; 5: 1111-1123.

Lin M, Jin Y, Jin J, Wang B, Hu X, Zhang J. A risk stratification model for predicting brain metastasis and brain screening benefit in patients with metastatic triple-negative breast cancer. *Cancer Med* 2020; 9: 8540-8551.

Lin NU, Bellon JR, Winer EP. CNS metastases in breast cancer. *J Clin Oncol* 2004; 22: 3608-3617.

Lin NU, Claus E, Sohl J, Razzak AR, Arnaout A, Winer EP. Sites of distant recurrence and clinical outcomes in patients with metastatic triple-negative breast cancer: high incidence of central nervous system metastases. *Cancer* 2008; 113: 2638-2645.

Lin Q, Balasubramanian K, Fan D, Kim SJ, Guo L, Wang H *et al*. Reactive astrocytes protect melanoma cells from chemotherapy by sequestering intracellular calcium through gap junction communication channels. *Neoplasia* 2010; 12: 748-754.

Lippoldt A, Kniesel U, Liebner S, Kalbacher H, Kirsch T, Wolburg H *et al*. Structural alterations of tight junctions are associated with loss of polarity in stroke-prone spontaneously hypertensive rat blood-brain barrier endothelial cells. *Brain Res* 2000; 885: 251-261.

Liu H, Kato Y, Erzinger SA, Kiriakova GM, Qian Y, Palmieri D *et al*. The role of MMP-1 in breast cancer growth and metastasis to the brain in a xenograft model. *BMC Cancer* 2012; 12: 583.

Liu H, Zang C, Fenner MH, Possinger K, Elstner E. PPARgamma ligands and ATRA inhibit the invasion of human breast cancer cells in vitro. *Breast Cancer Res Treat* 2003; 79: 63-74.

Liu JJ, Green P, John Mann J, Rapoport SI, Sublette ME. Pathways of polyunsaturated fatty acid utilization: implications for brain function in neuropsychiatric health and disease. *Brain Res* 2015; 1597: 220-246.

Liu Q, Zhang H, Jiang X, Qian C, Liu Z, Luo D. Factors involved in cancer metastasis: a better understanding to "seed and soil" hypothesis. *Mol Cancer* 2017; 16: 176.

Liu YR, Jiang YZ, Xu XE, Yu KD, Jin X, Hu X *et al*. Comprehensive transcriptome analysis identifies novel molecular subtypes and subtype-specific RNAs of triple-negative breast cancer. *Breast Cancer Res* 2016; 18: 33.

Locasale JW. Serine, glycine and one-carbon units: cancer metabolism in full circle. *Nat Rev Cancer* 2013; 13: 572-583.

Locasale JW, Grassian AR, Melman T, Lyssiotis CA, Mattaini KR, Bass AJ *et al*. Phosphoglycerate dehydrogenase diverts glycolytic flux and contributes to oncogenesis. *Nat Genet* 2011; 43: 869-874.

Lockman PR, Mittapalli RK, Taskar KS, Rudraraju V, Gril B, Bohn KA *et al*. Heterogeneous blood-tumor barrier permeability determines drug efficacy in experimental brain metastases of breast cancer. *Clin Cancer Res* 2010; 16: 5664-5678.

Lord CJ, Ashworth A. BRCAness revisited. *Nat Rev Cancer* 2016; 16: 110-120.

Lorger M, Felding-Habermann B. Capturing changes in the brain microenvironment during initial steps of breast cancer brain metastasis. *Am J Pathol* 2010; 176: 2958-2971.

Lorger M, Krueger JS, O'Neal M, Staflin K, Felding-Habermann B. Activation of tumor cell

integrin alphavbeta3 controls angiogenesis and metastatic growth in the brain. *Proc Natl Acad Sci U S A* 2009; 106: 10666-10671.

Lu SC. Glutathione synthesis. *Biochim Biophys Acta* 2013; 1830: 3143-3153.

Lu W, Kang Y. Epithelial-mesenchymal plasticity in cancer progression and metastasis. *Dev Cell* 2019; 49: 361-374.

Lu Y, Chen L, Li L, Cao Y. Exosomes derived from brain metastatic breast cancer cells destroy the blood-brain barrier by carrying lncRNA GS1-600G8.5. *Biomed Res Int* 2020; 2020: 7461727.

Lunt SJ, Chaudary N, Hill RP. The tumor microenvironment and metastatic disease. *Clin Exp Metastasis* 2009; 26: 19-34.

Lunt SY, Vander Heiden MG. Aerobic glycolysis: meeting the metabolic requirements of cell proliferation. *Annu Rev Cell Dev Biol* 2011; 27: 441-464.

Maan M, Peters JM, Dutta M, Patterson AD. Lipid metabolism and lipophagy in cancer. *Biochem Biophys Res Commun* 2018; 504: 582-589.

Mackey JR, Pienkowski T, Crown J, Sadeghi S, Martin M, Chan A *et al*. Long-term outcomes after adjuvant treatment of sequential versus combination docetaxel with doxorubicin and cyclophosphamide in node-positive breast cancer: BCIRG-005 randomized trial. *Ann Oncol* 2016; 27: 1041-1047.

Maddocks OD, Berkers CR, Mason SM, Zheng L, Blyth K, Gottlieb E *et al*. Serine starvation induces stress and p53-dependent metabolic remodelling in cancer cells. *Nature* 2013; 493: 542-546.

Magdoom KN, Brown A, Rey J, Mareci TH, King MA, Sarntinoranont M. MRI of whole rat brain perivascular network reveals role for ventricles in brain waste clearance. *Sci Rep* 2019; 9: 11480.

Mahajan A, Ahmed S, McAleer MF, Weinberg JS, Li J, Brown P *et al*. Post-operative stereotactic radiosurgery versus observation for completely resected brain metastases: a single-centre, randomised, controlled, phase 3 trial. *Lancet Oncol* 2017; 18: 1040-1048.

Maher EA, Marin-Valencia I, Bachoo RM, Mashimo T, Raisanen J, Hatanpaa KJ *et al*. Metabolism of [U-13 C]glucose in human brain tumors in vivo. *NMR Biomed* 2012; 25: 1234-1244.

Maher EA, Mietz J, Arteaga CL, DePinho RA, Mohla S. Brain metastasis: opportunities in basic and translational research. *Cancer Res* 2009; 69: 6015-6020.

Makki J. Diversity of breast carcinoma: histological subtypes and clinical relevance. *Clin Med Insights Pathol* 2015; 8: 23-31.

Malin D, Strekalova E, Petrovic V, Deal AM, Al Ahmad A, Adamo B *et al*. AlphaB-crystallin: a novel regulator of breast cancer metastasis to the brain. *Clin Cancer Res* 2014; 20: 56-67.

Manohar K, Bhattacharya A, Mittal BR. Low positive yield from routine inclusion of the brain in whole-body 18F-FDG PET/CT imaging for noncerebral malignancies: results from a large population study. *Nucl Med Commun* 2013; 34: 540-543.

Margulis L. Symbiotic theory of the origin of eukaryotic organelles; criteria for proof. *Symp Soc Exp Biol* 1975: 21-38.

Marino G, Pietrocola F, Eisenberg T, Kong Y, Malik SA, Andryushkova A *et al*. Regulation of autophagy by cytosolic acetyl-coenzyme A. *Mol Cell* 2014; 53: 710-725.

Markesbery WR, Brooks WH, Gupta GD, Young AB. Treatment for patients with cerebral

metastases. *Arch Neurol* 1978; 35: 754-756.

Marra A, Trapani D, Viale G, Criscitiello C, Curigliano G. Practical classification of triple-negative breast cancer: intratumoral heterogeneity, mechanisms of drug resistance, and novel therapies. *NPJ Breast Cancer* 2020; 6: 54.

Mashima T, Seimiya H, Tsuruo T. De novo fatty-acid synthesis and related pathways as molecular targets for cancer therapy. *Br J Cancer* 2009; 100: 1369-1372.

Mashimo T, Pichumani K, Vemireddy V, Hatanpaa KJ, Singh DK, Sirasanagandla S *et al*. Acetate is a bioenergetic substrate for human glioblastoma and brain metastases. *Cell* 2014; 159: 1603-1614.

Mazurek S. Pyruvate kinase type M2: a key regulator of the metabolic budget system in tumor cells. *Int J Biochem Cell Biol* 2011; 43: 969-980.

McCommis KS, Finck BN. Mitochondrial pyruvate transport: a historical perspective and future research directions. *Biochem J* 2015; 466: 443-454.

McEver RP. Selectin-carbohydrate interactions during inflammation and metastasis. *Glycoconj J* 1997; 14: 585-591.

McGowan PM, Simedrea C, Ribot EJ, Foster PJ, Palmieri D, Steeg PS *et al*. Notch1 inhibition alters the CD44hi/CD24lo population and reduces the formation of brain metastases from breast cancer. *Mol Cancer Res* 2011; 9: 834-844.

McKee MJ, Keith K, Deal AM, Garrett AL, Wheless AA, Green RL *et al*. A multidisciplinary breast cancer brain metastases clinic: the University of North Carolina experience. *Oncologist* 2016; 21: 16-20.

McWilliams RR, Rao RD, Brown PD, Link MJ, Buckner JC. Treatment options for brain metastases from melanoma. *Expert Rev Anticancer Ther* 2005; 5: 809-820.

Melone MAB, Valentino A, Margarucci S, Galderisi U, Giordano A, Peluso G. The carnitine system and cancer metabolic plasticity. *Cell Death Dis* 2018; 9: 228.

Mendes O, Kim HT, Lungu G, Stoica G. MMP2 role in breast cancer brain metastasis development and its regulation by TIMP2 and ERK1/2. *Clin Exp Metastasis* 2007; 24: 341-351.

Mendes O, Kim HT, Stoica G. Expression of MMP2, MMP9 and MMP3 in breast cancer brain metastasis in a rat model. *Clin Exp Metastasis* 2005; 22: 237-246.

Menendez JA, Lupu R. Fatty acid synthase and the lipogenic phenotype in cancer pathogenesis. *Nat Rev Cancer* 2007; 7: 763-777.

Metallo CM, Gameiro PA, Bell EL, Mattaini KR, Yang J, Hiller K *et al*. Reductive glutamine metabolism by IDH1 mediates lipogenesis under hypoxia. *Nature* 2011; 481: 380-384.

Migita T, Narita T, Nomura K, Miyagi E, Inazuka F, Matsuura M *et al*. ATP citrate lyase: activation and therapeutic implications in non-small cell lung cancer. *Cancer Res* 2008; 68: 8547-8554.

Miles FL, Pruitt FL, van Golen KL, Cooper CR. Stepping out of the flow: capillary extravasation in cancer metastasis. *Clin Exp Metastasis* 2008; 25: 305-324.

Milgraum LZ, Witters LA, Pasternack GR, Kuhajda FP. Enzymes of the fatty acid synthesis pathway are highly expressed in in situ breast carcinoma. *Clin Cancer Res* 1997; 3: 2115-2120.

Minn AJ, Gupta GP, Siegel PM, Bos PD, Shu W, Giri DD *et al*. Genes that mediate breast cancer metastasis to lung. *Nature* 2005; 436: 518-524.

Mitchell P. Coupling of phosphorylation to electron and hydrogen transfer by a chemi-osmotic type of mechanism. *Nature* 1961; 191: 144-148.

Modi S, Saura C, Yamashita T, Park YH, Kim SB, Tamura K *et al*. Trastuzumab deruxtecan in previously treated HER2-positive breast cancer. *N Engl J Med* 2020; 382: 610-621.

Mohiuddin SS, Khattar D. Biochemistry, ammonia. *StatPearls*. StatPearls Publishing: Treasure Island (FL), 2022.

Momeny M, Saunus JM, Marturana F, McCart Reed AE, Black D, Sala G *et al*. Heregulin-HER3-HER2 signaling promotes matrix metalloproteinase-dependent blood-brain-barrier transendothelial migration of human breast cancer cell lines. *Oncotarget* 2015; 6: 3932-3946.

Morel AP, Ginestier C, Pommier RM, Cabaud O, Ruiz E, Wicinski J *et al*. A stemness-related ZEB1-MSRB3 axis governs cellular pliancy and breast cancer genome stability. *Nat Med* 2017; 23: 568-578.

Morra A, Jung AY, Behrens S, Keeman R, Ahearn TU, Anton-Culver H *et al*. Breast cancer risk factors and survival by tumor subtype: pooled analyses from the Breast Cancer Association consortium. *Cancer Epidemiol Biomarkers Prev* 2021; 30: 623-642.

Mullen AR, Hu Z, Shi X, Jiang L, Boroughs LK, Kovacs Z *et al*. Oxidation of alpha-ketoglutarate is required for reductive carboxylation in cancer cells with mitochondrial defects. *Cell Rep* 2014; 7: 1679-1690.

Mullen AR, Wheaton WW, Jin ES, Chen PH, Sullivan LB, Cheng T *et al*. Reductive carboxylation supports growth in tumour cells with defective mitochondria. *Nature* 2011; 481: 385-388.

Muller A, Homey B, Soto H, Ge N, Catron D, Buchanan ME *et al*. Involvement of chemokine receptors in breast cancer metastasis. *Nature* 2001; 410: 50-56.

Murakami T, Nishiyama T, Shirotani T, Shinohara Y, Kan M, Ishii K *et al*. Identification of two enhancer elements in the gene encoding the type 1 glucose transporter from the mouse which are responsive to serum, growth factor, and oncogenes. *J Biol Chem* 1992; 267: 9300-9306.

Murphy MP. How mitochondria produce reactive oxygen species. *Biochem J* 2009; 417: 1-13.

Nam DH, Jeon HM, Kim S, Kim MH, Lee YJ, Lee MS *et al*. Activation of notch signaling in a xenograft model of brain metastasis. *Clin Cancer Res* 2008; 14: 4059-4066.

Nath A, Chan C. Genetic alterations in fatty acid transport and metabolism genes are associated with metastatic progression and poor prognosis of human cancers. *Sci Rep* 2016; 6: 18669.

Neman J, Termini J, Wilczynski S, Vaidehi N, Choy C, Kowolik CM *et al*. Human breast cancer metastases to the brain display GABAergic properties in the neural niche. *Proc Natl Acad Sci U S A* 2014; 111: 984-989.

Ngo B, Kim E, Osorio-Vasquez V, Doll S, Bustraan S, Liang RJ *et al*. Limited environmental serine and glycine confer brain metastasis sensitivity to PHGDH inhibition. *Cancer Discov* 2020; 10: 1352-1373.

Nguyen DX, Bos PD, Massague J. Metastasis: from dissemination to organ-specific colonization. *Nat Rev Cancer* 2009; 9: 274-284.

Nicholls DF, S. *Bioenergetics*, 3rd edn. Academic Press: San Diego, 2002.

Nielsen S, Smith BL, Christensen EI, Agre P. Distribution of the aquaporin CHIP in secretory and resorptive epithelia and capillary endothelia. *Proc Natl Acad Sci U S A* 1993; 90: 7275-7279.

Nielsen TO, Hsu FD, Jensen K, Cheang M, Karaca G, Hu Z *et al*. Immunohistochemical and clinical characterization of the basal-like subtype of invasive breast carcinoma. *Clin*

Cancer Res 2004; 10: 5367-5374.

Nieman KM, Kenny HA, Penicka CV, Ladanyi A, Buell-Gutbrod R, Zillhardt MR *et al*. Adipocytes promote ovarian cancer metastasis and provide energy for rapid tumor growth. *Nat Med* 2011; 17: 1498-1503.

Nieto MA, Huang RY, Jackson RA, Thiery JP. EMT: 2016. *Cell* 2016; 166: 21-45.

Niikura N, Hayashi N, Masuda N, Takashima S, Nakamura R, Watanabe K *et al*. Treatment outcomes and prognostic factors for patients with brain metastases from breast cancer of each subtype: a multicenter retrospective analysis. *Breast Cancer Res Treat* 2014; 147: 103-112.

Niikura N, Liu J, Hayashi N, Mittendorf EA, Gong Y, Palla SL *et al*. Loss of human epidermal growth factor receptor 2 (HER2) expression in metastatic sites of HER2-overexpressing primary breast tumors. *J Clin Oncol* 2012; 30: 593-599.

Nilsson R, Jain M, Madhusudhan N, Sheppard NG, Strittmatter L, Kampf C *et al*. Metabolic enzyme expression highlights a key role for MTHFD2 and the mitochondrial folate pathway in cancer. *Nat Commun* 2014; 5: 3128.

Niraula S, Dowling RJ, Ennis M, Chang MC, Done SJ, Hood N *et al*. Metformin in early breast cancer: a prospective window of opportunity neoadjuvant study. *Breast Cancer Res Treat* 2012; 135: 821-830.

Niwinska A, Murawska M, Pogoda K. Breast cancer brain metastases: differences in survival depending on biological subtype, RPA RTOG prognostic class and systemic treatment after whole-brain radiotherapy (WBRT). *Ann Oncol* 2010; 21: 942-948.

Nybo L, Secher NH. Cerebral perturbations provoked by prolonged exercise. *Prog Neurobiol* 2004; 72: 223-261.

O'Brien JS, Sampson EL. Lipid composition of the normal human brain: gray matter, white matter, and myelin. *J Lipid Res* 1965; 6: 537-544.

Obenauf AC, Massague J. Surviving at a distance: organ-specific metastasis. *Trends Cancer* 2015; 1: 76-91.

Okajima T, Fukumoto S, Ito H, Kiso M, Hirabayashi Y, Urano T *et al*. Molecular cloning of brain-specific GD1alpha synthase (ST6GalNAc V) containing CAG/Glutamine repeats. *J Biol Chem* 1999; 274: 30557-30562.

Olive PL, Vikse C, Trotter MJ. Measurement of oxygen diffusion distance in tumor cubes using a fluorescent hypoxia probe. *Int J Radiat Oncol Biol Phys* 1992; 22: 397-402.

Olson EM, Abdel-Rasoul M, Maly J, Wu CS, Lin NU, Shapiro CL. Incidence and risk of central nervous system metastases as site of first recurrence in patients with HER2-positive breast cancer treated with adjuvant trastuzumab. *Ann Oncol* 2013; 24: 1526-1533.

Ott M, Robertson JD, Gogvadze V, Zhivotovsky B, Orrenius S. Cytochrome c release from mitochondria proceeds by a two-step process. *Proc Natl Acad Sci U S A* 2002; 99: 1259-1263.

Owen OE, Kalhan SC, Hanson RW. The key role of anaplerosis and cataplerosis for citric acid cycle function. *J Biol Chem* 2002; 277: 30409-30412.

Ozsvari B, Bonuccelli G, Sanchez-Alvarez R, Foster R, Sotgia F, Lisanti MP. Targeting flavin-containing enzymes eliminates cancer stem cells (CSCs), by inhibiting mitochondrial respiration: Vitamin B2 (Riboflavin) in cancer therapy. *Aging (Albany NY)* 2017; 9: 2610-2628.

Ozsvari B, Sotgia F, Lisanti MP. First-in-class candidate therapeutics that target mitochondria and effectively prevent cancer cell metastasis: mitoriboscins and TPP compounds.

Aging (Albany NY) 2020; 12: 10162-10179.

Paget S. The distribution of secondary growths in cancer of the breast. 1889. *Cancer Metastasis Rev* 1989; 8: 98-101.

Pai K, Baliga P, Shrestha BL. E-cadherin expression: a diagnostic utility for differentiating breast carcinomas with ductal and lobular morphologies. *J Clin Diagn Res* 2013; 7: 840-844.

Palumbo JS, Talmage KE, Massari JV, La Jeunesse CM, Flick MJ, Kombrinck KW *et al*. Tumor cell-associated tissue factor and circulating hemostatic factors cooperate to increase metastatic potential through natural killer cell-dependent and-independent mechanisms. *Blood* 2007; 110: 133-141.

Pan J, Fan Z, Wang Z, Dai Q, Xiang Z, Yuan F *et al*. CD36 mediates palmitate acid-induced metastasis of gastric cancer via AKT/GSK-3beta/beta-catenin pathway. *J Exp Clin Cancer Res* 2019; 38: 52.

Papandreou I, Cairns RA, Fontana L, Lim AL, Denko NC. HIF-1 mediates adaptation to hypoxia by actively downregulating mitochondrial oxygen consumption. *Cell Metab* 2006; 3: 187-197.

Park ES, Kim SJ, Kim SW, Yoon SL, Leem SH, Kim SB *et al*. Cross-species hybridization of microarrays for studying tumor transcriptome of brain metastasis. *Proc Natl Acad Sci U S A* 2011; 108: 17456-17461.

Park JH, Vithayathil S, Kumar S, Sung PL, Dobrolecki LE, Putluri V *et al*. Fatty acid oxidation-driven Src links mitochondrial energy reprogramming and oncogenic properties in triple-negative breast cancer. *Cell Rep* 2016; 14: 2154-2165.

Parker JS, Mullins M, Cheang MC, Leung S, Voduc D, Vickery T *et al*. Supervised risk predictor of breast cancer based on intrinsic subtypes. *J Clin Oncol* 2009; 27: 1160-1167.

Pascual G, Avgustinova A, Mejetta S, Martin M, Castellanos A, Attolini CS *et al*. Targeting metastasis-initiating cells through the fatty acid receptor CD36. *Nature* 2017; 541: 41-45.

Pascual G, Dominguez D, Benitah SA. The contributions of cancer cell metabolism to metastasis. *Dis Model Mech* 2018; 11.

Patchell RA. The management of brain metastases. *Cancer Treat Rev* 2003; 29: 533-540.

Patel JB, Appaiah HN, Burnett RM, Bhat-Nakshatri P, Wang G, Mehta R *et al*. Control of EVI-1 oncogene expression in metastatic breast cancer cells through microRNA miR-22. *Oncogene* 2011; 30: 1290-1301.

Patrawala L, Calhoun T, Schneider-Broussard R, Li H, Bhatia B, Tang S *et al*. Highly purified CD44+ prostate cancer cells from xenograft human tumors are enriched in tumorigenic and metastatic progenitor cells. *Oncogene* 2006; 25: 1696-1708.

Pavlova NN, Thompson CB. The emerging hallmarks of cancer metabolism. *Cell Metab* 2016; 23: 27-47.

Pavlova NN, Zhu J, Thompson CB. The hallmarks of cancer metabolism: Still emerging. *Cell Metab* 2022; 34: 355-377.

Payen VL, Brisson L, Dewhirst MW, Sonveaux P. Common responses of tumors and wounds to hypoxia. *Cancer J* 2015; 21: 75-87.

Payen VL, Porporato PE, Baselet B, Sonveaux P. Metabolic changes associated with tumor metastasis, part 1: tumor pH, glycolysis and the pentose phosphate pathway. *Cell Mol Life Sci* 2016; 73: 1333-1348.

Payen VL, Zampieri LX, Porporato PE, Sonveaux P. Pro- and antitumor effects of mitochondrial reactive oxygen species. *Cancer Metastasis Rev* 2019; 38: 189-203.

Peddi PF, Ellis MJ, Ma C. Molecular basis of triple negative breast cancer and implications for therapy. *Int J Breast Cancer* 2012; 2012: 217185.

Pedrosa R, Mustafa DA, Soffietti R, Kros JM. Breast cancer brain metastasis: molecular mechanisms and directions for treatment. *Neuro Oncol* 2018; 20: 1439-1449.

Peinado H, Zhang H, Matei IR, Costa-Silva B, Hoshino A, Rodrigues G *et al*. Pre-metastatic niches: organ-specific homes for metastases. *Nat Rev Cancer* 2017; 17: 302-317.

Peitzsch C, Tyutyunnykova A, Pantel K, Dubrovska A. Cancer stem cells: the root of tumor recurrence and metastases. *Semin Cancer Biol* 2017; 44: 10-24.

Pelvig DP, Pakkenberg H, Stark AK, Pakkenberg B. Neocortical glial cell numbers in human brains. *Neurobiol Aging* 2008; 29: 1754-1762.

Perou CM, Sorlie T, Eisen MB, van de Rijn M, Jeffrey SS, Rees CA *et al*. Molecular portraits of human breast tumours. *Nature* 2000; 406: 747-752.

Pestalozzi BC, Holmes E, de Azambuja E, Metzger-Filho O, Hogge L, Scullion M *et al*. CNS relapses in patients with HER2-positive early breast cancer who have and have not received adjuvant trastuzumab: a retrospective substudy of the HERA trial (BIG 1-01). *Lancet Oncol* 2013; 14: 244-248.

Petty MA, Lo EH. Junctional complexes of the blood-brain barrier: permeability changes in neuroinflammation. *Prog Neurobiol* 2002; 68: 311-323.

Phillips TM, McBride WH, Pajonk F. The response of CD24(-/low)/CD44+ breast cancer-initiating cells to radiation. *J Natl Cancer Inst* 2006; 98: 1777-1785.

Pierre K, Pellerin L. Monocarboxylate transporters in the central nervous system: distribution, regulation and function. *J Neurochem* 2005; 94: 1-14.

Pietila M, Ivaska J, Mani SA. Whom to blame for metastasis, the epithelial-mesenchymal transition or the tumor microenvironment? *Cancer Lett* 2016; 380: 359-368.

Piomelli D, Astarita G, Rapaka R. A neuroscientist's guide to lipidomics. *Nat Rev Neurosci* 2007; 8: 743-754.

Piskounova E, Agathocleous M, Murphy MM, Hu Z, Huddlestun SE, Zhao Z *et al*. Oxidative stress inhibits distant metastasis by human melanoma cells. *Nature* 2015; 527: 186-191.

Pommier RM, Sanlaville A, Tonon L, Kielbassa J, Thomas E, Ferrari A *et al*. Comprehensive characterization of claudin-low breast tumors reflects the impact of the cell-of-origin on cancer evolution. *Nat Commun* 2020; 11: 3431.

Porporato PE, Filigheddu N, Pedro JMB, Kroemer G, Galluzzi L. Mitochondrial metabolism and cancer. *Cell Res* 2018; 28: 265-280.

Porporato PE, Payen VL, Baselet B, Sonveaux P. Metabolic changes associated with tumor metastasis, part 2: mitochondria, lipid and amino acid metabolism. *Cell Mol Life Sci* 2016; 73: 1349-1363.

Porporato PE, Payen VL, Perez-Escuredo J, De Saedeleer CJ, Danhier P, Copetti T *et al*. A mitochondrial switch promotes tumor metastasis. *Cell Rep* 2014; 8: 754-766.

Possemato R, Marks KM, Shaul YD, Pacold ME, Kim D, Birsoy K *et al*. Functional genomics reveal that the serine synthesis pathway is essential in breast cancer. *Nature* 2011; 476: 346-350.

Prat A, Parker JS, Karginova O, Fan C, Livasy C, Herschkowitz JI *et al*. Phenotypic and molecular characterization of the claudin-low intrinsic subtype of breast cancer. *Breast*

Cancer Res 2010; 12: R68.

Prat, A. & Perou, C. M. Deconstructing the molecular portraits of breast cancer. *Mol. Oncol.* **5**, 5–23 (2011)

Priego N, Zhu L, Monteiro C, Mulders M, Wasilewski D, Bindeman W *et al*. STAT3 labels a subpopulation of reactive astrocytes required for brain metastasis. *Nat Med* 2018; 24: 1024-1035.

Priego N, Zhu L, Monteiro C, Mulders M, Wasilewski D, Bindeman W *et al*. Author Correction: STAT3 labels a subpopulation of reactive astrocytes required for brain metastasis. *Nat Med* 2018; 24: 1481.

Qian B, Deng Y, Im JH, Muschel RJ, Zou Y, Li J *et al*. A distinct macrophage population mediates metastatic breast cancer cell extravasation, establishment and growth. *PLoS One* 2009; 4: e6562.

Quigley MR, Fukui O, Chew B, Bhatia S, Karlovits S. The shifting landscape of metastatic breast cancer to the CNS. *Neurosurg Rev* 2013; 36: 377-382.

Ramakrishna R, Rostomily R. Seed, soil, and beyond: the basic biology of brain metastasis. *Surg Neurol Int* 2013; 4: S256-264.

Rankin EB, Giaccia AJ. Hypoxic control of metastasis. *Science* 2016; 352: 175-180.

Rattan R, Ali Fehmi R, Munkarah A. Metformin: an emerging new therapeutic option for targeting cancer stem cells and metastasis. *J Oncol* 2012; 2012: 928127.

Redzic Z. Molecular biology of the blood-brain and the blood-cerebrospinal fluid barriers: similarities and differences. *Fluids Barriers CNS* 2011; 8: 3.

Reymond N, d'Agua BB, Ridley AJ. Crossing the endothelial barrier during metastasis. *Nat Rev Cancer* 2013; 13: 858-870.

Ricoult SJ, Yecies JL, Ben-Sahra I, Manning BD. Oncogenic PI3K and K-Ras stimulate de novo lipid synthesis through mTORC1 and SREBP. *Oncogene* 2016; 35: 1250-1260.

Ristow M. Unraveling the truth about antioxidants: mitohormesis explains ROS-induced health benefits. *Nat Med* 2014; 20: 709-711.

Roberts E. Failure of GABAergic inhibition: a key to local and global seizures. *Adv Neurol* 1986; 44: 319-341.

Rodriguez PL, Jiang S, Fu Y, Avraham S, Avraham HK. The proinflammatory peptide substance P promotes blood-brain barrier breaching by breast cancer cells through changes in microvascular endothelial cell tight junctions. *Int J Cancer* 2014; 134: 1034-1044.

Rosai J. *Rosai and Ackerman's Surgical Pathology*, Tenth ed. Elsevier: Lyon, France, 2011.

Rostami R, Mittal S, Rostami P, Tavassoli F, Jabbari B. Brain metastasis in breast cancer: a comprehensive literature review. *J Neurooncol* 2016; 127: 407-414.

Roussos ET, Condeelis JS, Patsialou A. Chemotaxis in cancer. *Nat Rev Cancer* 2011; 11: 573-587.

Rubin LL, Hall DE, Porter S, Barbu K, Cannon C, Horner HC *et al*. A cell culture model of the blood-brain barrier. *J Cell Biol* 1991; 115: 1725-1735.

Rugo HS, Rumble RB, Macrae E, Barton DL, Connolly HK, Dickler MN *et al*. Endocrine therapy for hormone receptor-positive metastatic breast cancer: American Society of Clinical Oncology guideline. *J Clin Oncol* 2016; 34: 3069-3103.

Ruscetti M, Quach B, Dadashian EL, Mulholland DJ, Wu H. Tracking and functional characterization of epithelial-mesenchymal transition and mesenchymal tumor cells

during prostate cancer metastasis. *Cancer Res* 2015; 75: 2749-2759.

Rycaj K, Tang DG. Cell-of-origin of cancer versus cancer stem cells: assays and interpretations. *Cancer Res* 2015; 75: 4003-4011.

Sabatier R, Finetti P, Guille A, Adelaide J, Chaffanet M, Viens P *et al*. Claudin-low breast cancers: clinical, pathological, molecular and prognostic characterization. *Mol Cancer* 2014; 13: 228.

Sabharwal SS, Schumacker PT. Mitochondrial ROS in cancer: initiators, amplifiers or an Achilles' heel? *Nat Rev Cancer* 2014; 14: 709-721.

Sacks P, Rahman M. Epidemiology of brain metastases. *Neurosurg Clin N Am* 2020; 31: 481-488.

Salzillo TC, Hu J, Nguyen L, Whiting N, Lee J, Weygand J *et al*. Interrogating metabolism in brain cancer. *Magn Reson Imaging Clin N Am* 2016; 24: 687-703.

Santana-Codina N, Marce-Grau A, Muixi L, Nieva C, Marro M, Sebastian D *et al*. GRP94 Is involved in the lipid phenotype of brain metastatic cells. *Int J Mol Sci* 2019; 20.

Santidrian AF, Matsuno-Yagi A, Ritland M, Seo BB, LeBoeuf SE, Gay LJ *et al*. Mitochondrial complex I activity and NAD+/NADH balance regulate breast cancer progression. *J Clin Invest* 2013; 123: 1068-1081.

Sartorius CA, Hanna CT, Gril B, Cruz H, Serkova NJ, Huber KM *et al*. Estrogen promotes the brain metastatic colonization of triple negative breast cancer cells via an astrocyte-mediated paracrine mechanism. *Oncogene* 2016; 35: 2881-2892.

Sassi N, Mattarei A, Azzolini M, Bernardi P, Szabo I, Paradisi C *et al*. Mitochondria-targeted resveratrol derivatives act as cytotoxic pro-oxidants. *Curr Pharm Des* 2014; 20: 172-179.

Savagner P. Epithelial-mesenchymal transitions: from cell plasticity to concept elasticity. *Curr Top Dev Biol* 2015; 112: 273-300.

Sayin VI, Ibrahim MX, Larsson E, Nilsson JA, Lindahl P, Bergo MO. Antioxidants accelerate lung cancer progression in mice. *Sci Transl Med* 2014; 6: 221ra215.

Schafer ZT, Grassian AR, Song L, Jiang Z, Gerhart-Hines Z, Irie HY *et al*. Antioxidant and oncogene rescue of metabolic defects caused by loss of matrix attachment. *Nature* 2009; 461: 109-113.

Schild T, Low V, Blenis J, Gomes AP. Unique metabolic adaptations dictate distal organ-specific metastatic colonization. *Cancer Cell* 2018; 33: 347-354.

Schmid P, Adams S, Rugo HS, Schneeweiss A, Barrios CH, Iwata H *et al*. Atezolizumab and Nab-paclitaxel in advanced triple-negative breast cancer. *N Engl J Med* 2018; 379: 2108-2121.

Schmid P, Salgado R, Park YH, Munoz-Couselo E, Kim SB, Sohn J *et al*. Pembrolizumab plus chemotherapy as neoadjuvant treatment of high-risk, early-stage triple-negative breast cancer: results from the phase 1b open-label, multicohort KEYNOTE-173 study. *Ann Oncol* 2020; 31: 569-581.

Schug ZT, Peck B, Jones DT, Zhang Q, Grosskurth S, Alam IS *et al*. Acetyl-CoA synthetase 2 promotes acetate utilization and maintains cancer cell growth under metabolic stress. *Cancer Cell* 2015; 27: 57-71.

Sciacovelli M, Frezza C. Oncometabolites: unconventional triggers of oncogenic signalling cascades. *Free Radic Biol Med* 2016; 100: 175-181.

Sciacovelli M, Goncalves E, Johnson TI, Zecchini VR, da Costa AS, Gaude E *et al*. Fumarate is an epigenetic modifier that elicits epithelial-to-mesenchymal transition. *Nature* 2016;

537: 544-547.

Sciacovelli M, Goncalves E, Johnson TI, Zecchini VR, da Costa AS, Gaude E *et al*. Corrigendum: fumarate is an epigenetic modifier that elicits epithelial-to-mesenchymal transition. *Nature* 2016; 540: 150.

Selivanov VA, Votyakova TV, Pivtoraiko VN, Zeak J, Sukhomlin T, Trucco M *et al*. Reactive oxygen species production by forward and reverse electron fluxes in the mitochondrial respiratory chain. *PLoS Comput Biol* 2011; 7: e1001115.

Semenza GL. Hypoxia-inducible factors in physiology and medicine. *Cell* 2012; 148: 399-408.

Sena LA, Chandel NS. Physiological roles of mitochondrial reactive oxygen species. *Mol Cell* 2012; 48: 158-167.

Sevenich L, Bowman RL, Mason SD, Quail DF, Rapaport F, Elie BT *et al*. Analysis of tumour- and stroma-supplied proteolytic networks reveals a brain-metastasis-promoting role for cathepsin S. *Nat Cell Biol* 2014; 16: 876-888.

Sharma DS, M.; Gupta, R.; Kumar, V.; Kumar, V.; Reshma, R. Intervention on lactate in cancer: a promising approach for the development of cancer therapeutics. *Advances in cancer biology - metastasis*, vol. 5. Elsevier BV: Amsterdam, 2022, p 100058.

Shen YA, Chen CC, Chen BJ, Wu YT, Juan JR, Chen LY *et al*. Potential therapies targeting metabolic pathways in cancer stem Cells. *Cells* 2021; 10.

Shestov AA, Emir UE, Kumar A, Henry PG, Seaquist ER, Oz G. Simultaneous measurement of glucose transport and utilization in the human brain. *Am J Physiol Endocrinol Metab* 2011; 301: E1040-1049.

Shetty AK, Zanirati G. The interstitial system of the brain in health and disease. *Aging Dis* 2020; 11: 200-211.

Shukla SK, Purohit V, Mehla K, Gunda V, Chaika NV, Vernucci E *et al*. MUC1 and HIF-1alpha signaling crosstalk induces anabolic glucose metabolism to impart Gemcitabine resistance to pancreatic cancer. *Cancer Cell* 2017; 32: 392.

Siegel RL, Miller KD, Jemal A. Cancer statistics, 2016. *CA Cancer J Clin* 2016; 66: 7-30.

Siegel RL, Miller KD, Jemal A. Cancer statistics, 2017. *CA Cancer J Clin* 2017; 67: 7-30.

Sierra A, Price JE, Garcia-Ramirez M, Mendez O, Lopez L, Fabra A. Astrocyte-derived cytokines contribute to the metastatic brain specificity of breast cancer cells. *Lab Invest* 1997; 77: 357-368.

Sihto H, Lundin J, Lundin M, Lehtimaki T, Ristimaki A, Holli K *et al*. Breast cancer biological subtypes and protein expression predict for the preferential distant metastasis sites: a nationwide cohort study. *Breast Cancer Res* 2011; 13: R87.

Singh M, Bakhshinyan D, Venugopal C, Singh SK. Preclinical modeling and therapeutic avenues for cancer metastasis to the central nervous system. *Front Oncol* 2017; 7: 220.

Singhai R, Patil VW, Jaiswal SR, Patil SD, Tayade MB, Patil AV. E-Cadherin as a diagnostic biomarker in breast cancer. *N Am J Med Sci* 2011; 3: 227-233.

Sinn HP, Kreipe H. A Brief Overview of the WHO Classification of Breast Tumors, 4th Edition, Focusing on Issues and Updates from the 3rd Edition. *Breast Care (Basel)* 2013; 8: 149-154.

Smallbone K, Gatenby RA, Gillies RJ, Maini PK, Gavaghan DJ. Metabolic changes during carcinogenesis: potential impact on invasiveness. *J Theor Biol* 2007; 244: 703-713.

Smid M, Wang Y, Zhang Y, Sieuwerts AM, Yu J, Klijn JG *et al*. Subtypes of breast cancer show preferential site of relapse. *Cancer Res* 2008; 68: 3108-3114.

Sofroniew MV, Vinters HV. Astrocytes: biology and pathology. *Acta Neuropathol* 2010; 119: 7-35.

Sonveaux P, Vegran F, Schroeder T, Wergin MC, Verrax J, Rabbani ZN *et al*. Targeting lactate-fueled respiration selectively kills hypoxic tumor cells in mice. *J Clin Invest* 2008; 118: 3930-3942.

Sorg BS, Hardee ME, Agarwal N, Moeller BJ, Dewhirst MW. Spectral imaging facilitates visualization and measurements of unstable and abnormal microvascular oxygen transport in tumors. *J Biomed Opt* 2008; 13: 014026.

Soto MS, Serres S, Anthony DC, Sibson NR. Functional role of endothelial adhesion molecules in the early stages of brain metastasis. *Neuro Oncol* 2014; 16: 540-551.

Sottnik JL, Lori JC, Rose BJ, Thamm DH. Glycolysis inhibition by 2-deoxy-D-glucose reverts the metastatic phenotype in vitro and in vivo. *Clin Exp Metastasis* 2011; 28: 865-875.

Sperduto PW, Kased N, Roberge D, Chao ST, Shanley R, Luo X *et al*. The effect of tumor subtype on the time from primary diagnosis to development of brain metastases and survival in patients with breast cancer. *J Neurooncol* 2013; 112: 467-472.

Sperduto PW, Mesko S, Li J, Cagney D, Aizer A, Lin NU *et al*. Estrogen/progesterone receptor and HER2 discordance between primary tumor and brain metastases in breast cancer and its effect on treatment and survival. *Neuro Oncol* 2020; 22: 1359-1367.

Spinelli JB, Yoon H, Ringel AE, Jeanfavre S, Clish CB, Haigis MC. Metabolic recycling of ammonia via glutamate dehydrogenase supports breast cancer biomass. *Science* 2017; 358: 941-946.

St-Pierre J, Drori S, Uldry M, Silvaggi JM, Rhee J, Jager S *et al*. Suppression of reactive oxygen species and neurodegeneration by the PGC-1 transcriptional coactivators. *Cell* 2006; 127: 397-408.

Stark AM, Anuszkiewicz B, Mentlein R, Yoneda T, Mehdorn HM, Held-Feindt J. Differential expression of matrix metalloproteinases in brain- and bone-seeking clones of metastatic MDA-MB-231 breast cancer cells. *J Neurooncol* 2007; 81: 39-48.

Stassart RM, Mobius W, Nave KA, Edgar JM. The axon-myelin unit in development and degenerative disease. *Front Neurosci* 2018; 12: 467.

Steeg PS. Targeting metastasis. *Nat Rev Cancer* 2016; 16: 201-218.

Stock D, Leslie AG, Walker JE. Molecular architecture of the rotary motor in ATP synthase. *Science* 1999; 286: 1700-1705.

Stricker T, Arteaga CL. Drug-resistant brain metastases: a role for pharmacology, tumor evolution, and too-late therapy. *Cancer Discov* 2015; 5: 1124-1126.

Stricker T, Arteaga CL. Correction: drug-resistant brain metastases: a role for pharmacology, tumor evolution, and too-late therapy. *Cancer Discov* 2019; 9: 302.

Suarez-Rivero JM, Pastor-Maldonado CJ, Povea-Cabello S, Alvarez-Cordoba M, Villalon-Garcia I, Talaveron-Rey M *et al*. Mitochondria and antibiotics: for good or for evil? *Biomolecules* 2021; 11.

Sullivan LB, Chandel NS. Mitochondrial reactive oxygen species and cancer. *Cancer Metab* 2014; 2: 17.

Sung H, Ferlay J, Siegel RL, Laversanne M, Soerjomataram I, Jemal A *et al*. Global Cancer Statistics 2020: GLOBOCAN estimates of incidence and mortality worldwide for 36 cancers in 185 countries. *CA Cancer J Clin* 2021; 71: 209-249.

Svensson RU, Parker SJ, Eichner LJ, Kolar MJ, Wallace M, Brun SN *et al*. Inhibition of acetyl-CoA carboxylase suppresses fatty acid synthesis and tumor growth of non-small-cell

lung cancer in preclinical models. *Nat Med* 2016; 22: 1108-1119.

Takahashi K, Yamanaka S. Induction of pluripotent stem cells from mouse embryonic and adult fibroblast cultures by defined factors. *Cell* 2006; 126: 663-676.

Tan AS, Baty JW, Dong LF, Bezawork-Geleta A, Endaya B, Goodwin J *et al*. Mitochondrial genome acquisition restores respiratory function and tumorigenic potential of cancer cells without mitochondrial DNA. *Cell Metab* 2015; 21: 81-94.

Tanaka N, Katayama S, Reddy A, Nishimura K, Niwa N, Hongo H *et al*. Single-cell RNA-seq analysis reveals the platinum resistance gene COX7B and the surrogate marker CD63. *Cancer Med* 2018; 7: 6193-6204.

Tannock IF. Oxygen diffusion and the distribution of cellular radiosensitivity in tumours. *Br J Radiol* 1972; 45: 515-524.

Tas F. Metastatic behavior in melanoma: timing, pattern, survival, and influencing factors. *J Oncol* 2012; 2012: 647684.

Tasdogan A, Faubert B, Ramesh V, Ubellacker JM, Shen B, Solmonson A *et al*. Metabolic heterogeneity confers differences in melanoma metastatic potential. *Nature* 2020; 577: 115-120.

Taube JH, Herschkowitz JI, Komurov K, Zhou AY, Gupta S, Yang J *et al*. Core epithelial-to-mesenchymal transition interactome gene-expression signature is associated with claudin-low and metaplastic breast cancer subtypes. *Proc Natl Acad Sci U S A* 2010; 107: 15449-15454.

Termini J, Neman J, Jandial R. Role of the neural niche in brain metastatic cancer. *Cancer Res* 2014; 74: 4011-4015.

Thomlinson RH, Gray LH. The histological structure of some human lung cancers and the possible implications for radiotherapy. *Br J Cancer* 1955; 9: 539-549.

Thorne RG, Nicholson C. In vivo diffusion analysis with quantum dots and dextrans predicts the width of brain extracellular space. *Proc Natl Acad Sci U S A* 2006; 103: 5567-5572.

Tibbetts AS, Appling DR. Compartmentalization of mammalian folate-mediated one-carbon metabolism. *Annu Rev Nutr* 2010; 30: 57-81.

Tilkorn DJ, Hauser J, Ring A, Goertz O, Stricker I, Steinau HU *et al*. Leiomyosarcoma of intravascular origin--a rare tumor entity: clinical pathological study of twelve cases. *World J Surg Oncol* 2010; 8: 103.

Tomasetti C, Vogelstein B. Cancer etiology. Variation in cancer risk among tissues can be explained by the number of stem cell divisions. *Science* 2015; 347: 78-81.

Tominaga N, Kosaka N, Ono M, Katsuda T, Yoshioka Y, Tamura K *et al*. Brain metastatic cancer cells release microRNA-181c-containing extracellular vesicles capable of destructing blood-brain barrier. *Nat Commun* 2015; 6: 6716.

Touil Y, Igoudjil W, Corvaisier M, Dessein AF, Vandomme J, Monte D *et al*. Colon cancer cells escape 5FU chemotherapy-induced cell death by entering stemness and quiescence associated with the c-Yes/YAP axis. *Clin Cancer Res* 2014; 20: 837-846.

Townsend DM, He L, Hutchens S, Garrett TE, Pazoles CJ, Tew KD. NOV-002, a glutathione disulfide mimetic, as a modulator of cellular redox balance. *Cancer Res* 2008; 68: 2870-2877.

Tsukada Y, Fouad A, Pickren JW, Lane WW. Central nervous system metastasis from breast carcinoma. Autopsy study. *Cancer* 1983; 52: 2349-2354.

Tsukihara T, Aoyama H, Yamashita E, Tomizaki T, Yamaguchi H, Shinzawa-Itoh K *et al*. The whole structure of the 13-subunit oxidized cytochrome c oxidase at 2.8 A. *Science*

1996; 272: 1136-1144.

Turajlic S, Swanton C. Metastasis as an evolutionary process. *Science* 2016; 352: 169-175.

Turner N, Tutt A, Ashworth A. Hallmarks of 'BRCAness' in sporadic cancers. *Nat Rev Cancer* 2004; 4: 814-819.

Turner NC, Reis-Filho JS. Basal-like breast cancer and the BRCA1 phenotype. *Oncogene* 2006; 25: 5846-5853.

Valiente M, Ahluwalia MS, Boire A, Brastianos PK, Goldberg SB, Lee EQ *et al*. The evolving landscape of brain metastasis. *Trends Cancer* 2018; 4: 176-196.

Valiente M, Obenauf AC, Jin X, Chen Q, Zhang XH, Lee DJ *et al*. Serpins promote cancer cell survival and vascular co-option in brain metastasis. *Cell* 2014; 156: 1002-1016.

Valiente M, Van Swearingen AED, Anders CK, Bairoch A, Boire A, Bos PD *et al*. Brain metastasis cell lines panel: a public resource of organotropic cell lines. *Cancer Res* 2020; 80: 4314-4323.

Van Hee VF, Labar D, Dehon G, Grasso D, Gregoire V, Muccioli GG *et al*. Radiosynthesis and validation of (+/-)-[18F]-3-fluoro-2-hydroxypropionate ([18F]-FLac) as a PET tracer of lactate to monitor MCT1-dependent lactate uptake in tumors. *Oncotarget* 2017; 8: 24415-24428.

Vander Heiden MG, Cantley LC, Thompson CB. Understanding the Warburg effect: the metabolic requirements of cell proliferation. *Science* 2009; 324: 1029-1033.

Vanharanta S, Massague J. Origins of metastatic traits. *Cancer Cell* 2013; 24: 410-421.

Vannucci SJ, Maher F, Simpson IA. Glucose transporter proteins in brain: delivery of glucose to neurons and glia. *Glia* 1997; 21: 2-21.

Vaupel P. The role of hypoxia-induced factors in tumor progression. *Oncologist* 2004; 9 Suppl 5: 10-17.

Venneti S, Dunphy MP, Zhang H, Pitter KL, Zanzonico P, Campos C *et al*. Glutamine-based PET imaging facilitates enhanced metabolic evaluation of gliomas in vivo. *Sci Transl Med* 2015; 7: 274ra217.

Vestweber D. Regulation of endothelial cell contacts during leukocyte extravasation. *Curr Opin Cell Biol* 2002; 14: 587-593.

Voduc KD, Cheang MC, Tyldesley S, Gelmon K, Nielsen TO, Kennecke H. Breast cancer subtypes and the risk of local and regional relapse. *J Clin Oncol* 2010; 28: 1684-1691.

Vyas S, Zaganjor E, Haigis MC. Mitochondria and cancer. *Cell* 2016; 166: 555-566.

Wallace DC. Mitochondria and cancer. *Nat Rev Cancer* 2012; 12: 685-698.

Wang C, Guo K, Gao D, Kang X, Jiang K, Li Y *et al*. Identification of transaldolase as a novel serum biomarker for hepatocellular carcinoma metastasis using xenografted mouse model and clinic samples. *Cancer Lett* 2011; 313: 154-166.

Wang C, Luo D. The metabolic adaptation mechanism of metastatic organotropism. *Exp Hematol Oncol* 2021; 10: 30.

Wang DY, Jiang Z, Ben-David Y, Woodgett JR, Zacksenhaus E. Molecular stratification within triple-negative breast cancer subtypes. *Sci Rep* 2019; 9: 19107.

Wang H, Mei Y, Luo C, Huang Q, Wang Z, Lu GM *et al*. Single-cell analyses reveal mechanisms of cancer stem cell maintenance and epithelial-mesenchymal transition in recurrent bladder cancer. *Clin Cancer Res* 2021; 27: 6265-6278.

Wang L, Cossette SM, Rarick KR, Gershan J, Dwinell MB, Harder DR *et al*. Astrocytes directly influence tumor cell invasion and metastasis in vivo. *PLoS One* 2013; 8: e80933.

Wang Y, Ye F, Liang Y, Yang Q. Breast cancer brain metastasis: insight into molecular mechanisms and therapeutic strategies. *Br J Cancer* 2021; 125: 1056-1067.

Waniewski RA, Martin DL. Preferential utilization of acetate by astrocytes is attributable to transport. *J Neurosci* 1998; 18: 5225-5233.

Warburg O. The metabolism of carcinoma cells. *Cancer res* 1925; 9: 149-163.

Warburg O. On the origin of cancer cells. *Science* 1956; 123: 309-314.

Ward PS, Thompson CB. Metabolic reprogramming: a cancer hallmark even Warburg did not anticipate. *Cancer Cell* 2012; 21: 297-308.

Weinberg SE, Chandel NS. Targeting mitochondria metabolism for cancer therapy. *Nat Chem Biol* 2015; 11: 9-15.

Weiss N, Miller F, Cazaubon S, Couraud PO. The blood-brain barrier in brain homeostasis and neurological diseases. *Biochim Biophys Acta* 2009; 1788: 842-857.

Wellen KE, Hatzivassiliou G, Sachdeva UM, Bui TV, Cross JR, Thompson CB. ATP-citrate lyase links cellular metabolism to histone acetylation. *Science* 2009; 324: 1076-1080.

Wen J, Min X, Shen M, Hua Q, Han Y, Zhao L *et al*. ACLY facilitates colon cancer cell metastasis by CTNNB1. *J Exp Clin Cancer Res* 2019; 38: 401.

Westcott JM, Prechtl AM, Maine EA, Dang TT, Esparza MA, Sun H *et al*. An epigenetically distinct breast cancer cell subpopulation promotes collective invasion. *J Clin Invest* 2015; 125: 1927-1943.

Wheaton WW, Weinberg SE, Hamanaka RB, Soberanes S, Sullivan LB, Anso E *et al*. Metformin inhibits mitochondrial complex I of cancer cells to reduce tumorigenesis. *Elife* 2014; 3: e02242.

Wilhelm I, Molnar J, Fazakas C, Hasko J, Krizbai IA. Role of the blood-brain barrier in the formation of brain metastases. *Int J Mol Sci* 2013; 14: 1383-1411.

Wise DR, Ward PS, Shay JE, Cross JR, Gruber JJ, Sachdeva UM *et al*. Hypoxia promotes isocitrate dehydrogenase-dependent carboxylation of alpha-ketoglutarate to citrate to support cell growth and viability. *Proc Natl Acad Sci U S A* 2011; 108: 19611-19616.

Witzel I, Oliveira-Ferrer L, Pantel K, Muller V, Wikman H. Breast cancer brain metastases: biology and new clinical perspectives. *Breast Cancer Res* 2016; 18: 8.

Wolak DJ, Thorne RG. Diffusion of macromolecules in the brain: implications for drug delivery. *Mol Pharm* 2013; 10: 1492-1504.

Wong TZ, van der Westhuizen GJ, Coleman RE. Positron emission tomography imaging of brain tumors. *Neuroimaging Clin N Am* 2002; 12: 615-626.

Wrobel JK, Toborek M. Blood-brain barrier remodeling during brain metastasis formation. *Mol Med* 2016; 22: 32-40.

Wu D, Yang Y, Hou Y, Zhao Z, Liang N, Yuan P *et al*. Increased mitochondrial fission drives the reprogramming of fatty acid metabolism in hepatocellular carcinoma cells through suppression of Sirtuin 1. *Cancer Commun (Lond)* 2022; 42: 37-55.

Wu G, Fang YZ, Yang S, Lupton JR, Turner ND. Glutathione metabolism and its implications for health. *J Nutr* 2004; 134: 489-492.

Wu K, Fukuda K, Xing F, Zhang Y, Sharma S, Liu Y *et al*. Roles of the cyclooxygenase 2 matrix metalloproteinase 1 pathway in brain metastasis of breast cancer. *J Biol Chem* 2015; 290: 9842-9854.

Wu Q, Li J, Zhu S, Wu J, Chen C, Liu Q *et al*. Breast cancer subtypes predict the preferential site of distant metastases: a SEER based study. *Oncotarget* 2017; 8: 27990-27996.

Wu R, Racker E. Regulatory mechanisms in carbohydrate metabolism. IV. Pasteur effect and Crabtree effect in ascites tumor cells. *J Biol Chem* 1959; 234: 1036-1041.

Wyss MT, Magistretti PJ, Buck A, Weber B. Labeled acetate as a marker of astrocytic metabolism. *J Cereb Blood Flow Metab* 2011; 31: 1668-1674.

Xie C, Wang FY, Sang Y, Chen B, Huang JH, He FJ *et al*. Mitochondrial micropeptide STMP1 enhances mitochondrial fission to promote tumor metastasis. *Cancer Res* 2022; 82: 2431-2443.

Xie TX, Huang FJ, Aldape KD, Kang SH, Liu M, Gershenwald JE *et al*. Activation of stat3 in human melanoma promotes brain metastasis. *Cancer Res* 2006; 66: 3188-3196.

Xie XP, Laks DR, Sun D, Ganbold M, Wang Z, Pedraza AM *et al*. Quiescent human glioblastoma cancer stem cells drive tumor initiation, expansion, and recurrence following chemotherapy. *Dev Cell* 2022; 57: 32-46 e38.

Xing F, Kobayashi A, Okuda H, Watabe M, Pai SK, Pandey PR *et al*. Reactive astrocytes promote the metastatic growth of breast cancer stem-like cells by activating Notch signalling in brain. *EMBO Mol Med* 2013; 5: 384-396.

Xu J, Rodriguez D, Petitclerc E, Kim JJ, Hangai M, Moon YS *et al*. Proteolytic exposure of a cryptic site within collagen type IV is required for angiogenesis and tumor growth in vivo. *J Cell Biol* 2001; 154: 1069-1079.

Xu X, Zur Hausen A, Coy JF, Lochelt M. Transketolase-like protein 1 (TKTL1) is required for rapid cell growth and full viability of human tumor cells. *Int J Cancer* 2009; 124: 1330-1337.

Yang L, Venneti S, Nagrath D. Glutaminolysis: a hallmark of cancer metabolism. *Annu Rev Biomed Eng* 2017; 19: 163-194.

Yang Y, Estrada EY, Thompson JF, Liu W, Rosenberg GA. Matrix metalloproteinase-mediated disruption of tight junction proteins in cerebral vessels is reversed by synthetic matrix metalloproteinase inhibitor in focal ischemia in rat. *J Cereb Blood Flow Metab* 2007; 27: 697-709.

Yang Z, Wang L, Yang C, Pu S, Guo Z, Wu Q *et al*. Mitochondrial membrane remodeling. *Front Bioeng Biotechnol* 2021; 9: 786806.

Ye J, Fan J, Venneti S, Wan YW, Pawel BR, Zhang J *et al*. Serine catabolism regulates mitochondrial redox control during hypoxia. *Cancer Discov* 2014; 4: 1406-1417.

Yeh CT, Su CL, Huang CY, Lin JK, Lee WH, Chang PM *et al*. A preclinical evaluation of antimycin a as a potential antilung cancer stem cell agent. *Evid Based Complement Alternat Med* 2013; 2013: 910451.

Yetkin-Arik B, Vogels IMC, Nowak-Sliwinska P, Weiss A, Houtkooper RH, Van Noorden CJF *et al*. The role of glycolysis and mitochondrial respiration in the formation and functioning of endothelial tip cells during angiogenesis. *Sci Rep* 2019; 9: 12608.

Yin CF, Chang YW, Huang HC, Juan HF. Targeting protein interaction networks in mitochondrial dynamics for cancer therapy. *Drug Discov Today* 2022; 27: 1077-1087.

Yin L, Duan JJ, Bian XW, Yu SC. Triple-negative breast cancer molecular subtyping and treatment progress. *Breast Cancer Res* 2020; 22: 61.

Yoneda T, Williams PJ, Hiraga T, Niewolna M, Nishimura R. A bone-seeking clone exhibits different biological properties from the MDA-MB-231 parental human breast cancer cells and a brain-seeking clone in vivo and in vitro. *J Bone Miner Res* 2001; 16: 1486-1495.

Yoo HC, Park SJ, Nam M, Kang J, Kim K, Yeo JH *et al*. A Variant of SLC1A5 is a mitochondrial

glutamine transporter for metabolic reprogramming in cancer cells. *Cell Metab* 2020; 31: 267-283.

Yudkoff M. Brain metabolism of branched-chain amino acids. *Glia* 1997; 21: 92-98.

Yudkoff M, Nissim I, Daikhin Y, Lin ZP, Nelson D, Pleasure D *et al*. Brain glutamate metabolism: neuronal-astroglial relationships. *Dev Neurosci* 1993; 15: 343-350.

Yun J, Finkel T. Mitohormesis. *Cell Metab* 2014; 19: 757-766.

Zamzami N, Marchetti P, Castedo M, Decaudin D, Macho A, Hirsch T *et al*. Sequential reduction of mitochondrial transmembrane potential and generation of reactive oxygen species in early programmed cell death. *J Exp Med* 1995; 182: 367-377.

Zarse K, Schmeisser S, Groth M, Priebe S, Beuster G, Kuhlow D *et al*. Impaired insulin/IGF1 signaling extends life span by promoting mitochondrial L-proline catabolism to induce a transient ROS signal. *Cell Metab* 2012; 15: 451-465.

Zeng Q, Michael IP, Zhang P, Saghafinia S, Knott G, Jiao W *et al*. Synaptic proximity enables NMDAR signalling to promote brain metastasis. *Nature* 2019; 573: 526-531.

Zhang L, Zhang S, Yao J, Lowery FJ, Zhang Q, Huang WC *et al.* Microenvironment-induced PTEN loss by exosomal microRNA primes brain metastasis outgrowth. *Nature* 2015; 527: 100-104.

Zhang X, Powell K, Li L. Breast cancer stem cells: biomarkers, identification and isolation methods, regulating mechanisms, cellular origin, and beyond. *Cancers (Basel)* 2020; 12.

Zhao RZ, Jiang S, Zhang L, Yu ZB. Mitochondrial electron transport chain, ROS generation and uncoupling (review). *Int J Mol Med* 2019; 44: 3-15.

Zhao W, Li Y, Zhang X. Stemness-related markers in cancer. *Cancer Transl Med* 2017; 3: 87-95.

Zheng Y, Miyamoto DT, Wittner BS, Sullivan JP, Aceto N, Jordan NV *et al*. Expression of beta-globin by cancer cells promotes cell survival during blood-borne dissemination. *Nat Commun* 2017; 8: 14344.

Zhou W, Fong MY, Min Y, Somlo G, Liu L, Palomares MR *et al*. Cancer-secreted miR-105 destroys vascular endothelial barriers to promote metastasis. *Cancer Cell* 2014; 25: 501-515.

Zhou Y, Danbolt NC. GABA and glutamate transporters in brain. *Front Endocrinol (Lausanne)* 2013; 4: 165.

Zhu A, Lee D, Shim H. Metabolic positron emission tomography imaging in cancer detection and therapy response. *Semin Oncol* 2011; 38: 55-69.

Zielke HR, Zielke CL, Baab PJ. Direct measurement of oxidative metabolism in the living brain by microdialysis: a review. *J Neurochem* 2009; 109 Suppl 1: 24-29.

Zielonka J, Joseph J, Sikora A, Hardy M, Ouari O, Vasquez-Vivar J *et al*. Mitochondria-targeted triphenylphosphonium-based compounds: syntheses, mechanisms of action, and therapeutic and diagnostic applications. *Chem Rev* 2017; 117: 10043-10120.

Zimorski V, Ku C, Martin WF, Gould SB. Endosymbiotic theory for organelle origins. *Curr Opin Microbiol* 2014; 22: 38-48.

Zong WX, Rabinowitz JD, White E. Mitochondria and cancer. *Mol Cell* 2016; 61: 667-676.

Zou Y, Watters A, Cheng N, Perry CE, Xu K, Alicea GM *et al*. Polyunsaturated fatty acids from astrocytes activate PPARgamma signaling in cancer cells to promote brain metastasis. *Cancer Discov* 2019; 9: 1720-1735.

The Private Defense of this thesis was held on December 21st, 2022.

The Public Defense of this thesis was held on March 13th, 2023.

Printed in Louvain-la-Neuve in March 2023.